

SLOPE INSTABILITY ON THE JORDANIAN HIGHWAYS

By:

SAFWAN KHALIL SAKET

Thesis submitted to the University of London
for the degree of Doctor of Philosophy in
Engineering Geology.

October, 1974.

Engineering Geology Division,
Imperial College of Science and
Technology,
London S.W.7.

ABSTRACT

The research is directed towards the investigation of existing engineering geological problems on three main highways in Jordan and seven major landslides were selected to be studied in detail. Different types of movement mechanism, such as circular and translational failures, rockfalls, creep and mud-flows are present. The movements are of an active type occurring yearly after periods of heavy rainfall resulting in damage and traffic delays.

Most of the Jordanian highways lie within a sequence composed of marly clayey material forming the Lower part of the Upper Cretaceous and many sections of these highways are located within an old landslide area activated recently by construction.

In order to fully understand these problems an intensive field and laboratory testing programme was devised; representative disturbed and undisturbed samples were tested to establish the shear strength parameters of these clays. Field exploratory drilling, resistivity sounding and seismic refraction studies were also used to explore the subsurface geology and to detect ground water levels. Geological maps checked by aerial photographs were prepared, and the main topographic features of the displacement recorded.

The use of effective stress methods of stability

analysis is used for the first time in Jordan for the purpose of this study. The stability methods of Bishop (1953) in terms of effective stresses were used for the circular type landslides, and the methods by Fellenius (1926) and Janbu (1957) were used for the translation type failures. These methods are believed to be the most reliable and appropriate to be used for application to long term stability problems of natural slopes. Residual strength parameters were used for stability analysis of failures on pre-existing slip surfaces.

The main conclusion arising from this study is that all the landslides investigated on the Jordanian highways lie within the same sequence of the Lower part of the Cenomanian clays. These clays are found to be of montmorillonite, illite, and kaolinite type of medium to high plasticity and low shearing strength. Slopes steeper than 12° and 14° in such materials in northern and southern Jordan respectively are considered unstable.

	<u>Page</u>
4.2	General investigation of the route. 120
4.2.1	General field investigations 120
4.2.2	General laboratory investigations 132
4.3	Detailed investigation of landslide V. 144
4.3.1	Geology and hydrogeology 144
4.3.2	Engineering geology of the landslide 152
4.3.2.1	General description of landslide V 152
4.3.2.2	Field investigations of landslide V 162
4.3.2.3	Laboratory investigations 166
4.3.2.4	Slope stability analyses 171
4.3.2.5	Remedial measures 174
4.3.2.6	Conclusions 177
4.4	Detailed investigation of landslide VI. 181
4.4.1	Geology and hydrogeology 181
4.4.2	Engineering geology of the landslide 185
4.4.2.1	General description of landslide VI 185
4.4.2.2	Field investigations of landslide VI 189
4.4.2.3	Laboratory investigations 193
4.4.2.4	Slope stability analyses 195
4.4.2.5	Remedial measures 200
4.4.2.6	Conclusions 202
4.5	The Amman Slide VII (Ras-El-Ain). 204
4.5.1	Introduction 204
4.5.2	Geology 204
4.5.3	Topographic features 207
4.5.4	Failure mechanism 207
4.5.5	Main causes of the slope failure 214
4.5.6	Stabilization measures 214

	<u>Page</u>
Chapter 5	
	<u>DETAILED INVESTIGATIONS OF LANDSLIDES</u>
	<u>ALONG THE SWEILEH-JARASH ROAD</u>
	(landslides I, II, III and IV)
	216
5.1	Introduction. 216
5.2	General description of the route. 216
5.3	Detailed investigation of landslide III. 233
5.3.1	Geography and geomorphology 233
5.3.2	Geology of the study area 233
	- stratigraphy 235
	- structure 236
5.3.3	Climate and hydrology 237
5.3.4	Engineering geology of the landslide 240
	5.3.4.1 Recognition and general description of landslide III 240
	5.3.4.2 Field investigations 248
	5.3.4.3 Laboratory investigations 251
	5.3.4.4 Slope stability analysis 264
	5.3.4.5 Remedial measures 270
	5.3.4.6 Conclusions 270
5.4	Detailed investigation of landslide IV. 273
5.4.1	Geology and hydrology 273
5.4.2	General description of landslide IV 279
5.4.3	Field investigations 281
5.4.4	Laboratory investigations 284
5.4.5	Slope stability analysis 288
5.4.6	Remedial measures 293
5.4.7	Conclusions 295
5.5	Detailed investigation of landslide I 297
5.5.1	Geology and hydrology 297
5.5.2	General description of landslide I 301
5.5.3	Laboratory investigations 303
5.5.4	Slope stability analysis 305
5.5.5	Remedial measures 307
5.5.6	Conclusions 310

	<u>Page</u>
5.6 Detailed investigation of landslide II	313
5.6.1 Geology and hydrogeology	313
5.6.2 General description of landslide II	318
5.6.3 Field investigations	319
5.6.4 Laboratory investigations	323
5.6.5 Slope stability analysis	328
5.6.6 Remedial measures	332
5.6.7 Conclusions	334
Chapter 6 <u>SLOPE STABILITY ON MA'AN-AQABA ROAD</u> <u>(RAS-EN-NAQAB ESCARPMENT).</u>	337
6.1 Introduction.	337
6.2 Geography and geomorphology.	339
6.3 Geology of the study area.	341
6.3.1 Stratigraphy	341
6.3.2 Structure	347
6.4 Hydrology and hydrogeology.	348
6.5 Field investigation and survey.	350
6.6 Laboratory investigations.	359
6.7 Summary and conclusions.	369
Chapter 7 <u>RECOMMENDATIONS AND CONCLUSIONS</u>	379
Acknowledgements	385
Appendix A	386
Appendix B	399
Appendix C	405
Bibliography	424

LIST OF FIGURES

<u>Fig.</u> <u>No.</u>		<u>Page</u>
1.1	Main types of translational landslides.	32
1.2	Main types of rotational landslides.	35
1.3	Main types of flows.	40
1.4	Main types of falls.	40
1.5	Typical slump type subsidence.	40
2.1	Geological map of central part of Jordan involving the study areas of Sweileh-Jarash road and Naur-Adasiye road.	56
2.2	Isopachous maps of the Kurnub Group.	59
2.3	Isopachous maps of the Ajlun Group.	65
2.4	The structural pattern of East Jordan.	70
2.5	Distribution of main soil types in Jordan.	73
2.6	Distribution of Mediterranean Bioclimatic stages in Jordan.	75
2.7	Distribution of Rainfall in Jordan.	77
3.1	Diagram of the seismograph.	93
3.2	Diagram of the open drive tube sampler.	95
3.3	Diagram of the maximum water absorption equipment.	100
3.4	Diagram of the Differential Thermal Analysis apparatus.	101
3.5	Typical stress-strain curves for normally and over-consolidated clays tested under drained conditions.	110
3.6	Cross-section showing the principal forces in the circular arc.	112
3.7	Janbu's curves for values of (f_0) for different d/L values.	117
3.8	Cross-section showing the principal forces in the non-circular failure surfaces.	117
4.1	Monthly rainfall relationship for the period (1962-1972) at Naur station.	122
4.2	Geological map of the study area along the Naur-Adasiye road.	123

<u>Fig. No.</u>	<u>Page</u>
4.3 Plasticity and activity charts showing values for the analysed samples taken from the study areas of landslides V and VI.	135
4.4 Grainsize distribution curves of representative samples taken from landslides V and VI.	136
4.5 Maximum water absorption curves of the representative samples taken from landslides V and VI.	137
4.6 Correlation (comparison) of the Differential Thermal Analysis of the representative samples taken from landslides V and VI.	138
4.7 Correlation (comparison) of the X-ray diffraction curves for the oriented mount specimens taken from landslides V and VI.	141
4.8 Stereographic projection-contour diagram of joints at the crest of landslide V following the movements of 1969 and 1971.	148
4.9 Map of landslide V (1969) showing the main features of the movement.	153
4.10 Map of landslide V (1971) showing the main features of the movement, location of boreholes and geophysical surveys.	156
4.11 Cross-sections showing the evolution (history) of movements of landslide V.	158
4.12 Principal sketches of the proposed evolution (history) of movements of landslide V.	160
4.13 Schematic block diagram showing the main features of the study area V.	161
4.14 A lithological cross-section of the site of landslide V based on interpretation of exploratory drilling and geophysical surveys.	164
4.15 Typical curves obtained from triaxial compression test and multi-reversal shear tests on specimens taken from landslide V.	169
4.16 Cross-section of landslide V (before sliding), with the results of the stability analysis.	173
4.17 Cross-section of landslide V (after sliding), with the results of the stability analysis.	175
4.18 Recommended remedial measures for landslide V.	176

<u>Fig. No.</u>		<u>Page</u>
4.19	Schematic geological cross-section of Wadi Umariye showing the location of landslide VI.	182
4.20	Map of landslide VI showing the main features of the movement, location of boreholes, geophysical surveys and simplified geology.	186
4.21	Cross-sections of landslide VI showing the evolution (history) of movements in the area.	188
4.22	A lithological cross-section of the site of landslide VI based on interpretation of the exploratory drilling and geophysical surveys.	190
4.23	A lithological log of borehole I in the vicinity of landslide VI.	192
4.24	Typical curves obtained from multi-reversal shear tests on samples taken from landslide VI.	196
4.25	Cross-section of landslide VI (before sliding of 1964), with the results of the stability analysis.	197
4.26	Cross-section of landslide VI (after sliding) with the results of stability analysis.	199
4.27	Recommended remedial measures for landslide VI.	201
4.28	Schematic plan view of the study area of landslide VII.	208
4.29	Schematic block diagram of the study area VII illustrating the sliding and the major joints.	209
4.30	Geometry of the block on inclined plane.	210
4.31	Conditions for sliding and toppling of a block on an inclined plane.	211
4.32	Cross-section of the landslide VII, showing the major joints.	213
5.1	Major structural elements and simplified geology in relation to location of landslides I, II, III & IV.	218
5.2	Stratigraphic columnar sections measured between Sweileh and Jarash and north Jarash.	219
5.3	Cross-section showing the unfavourable orientation of joints near observation point 4.	223
5.4	Stereographic projection-contour diagram of joints near observation point 4.	224

<u>Fig.</u> <u>No.</u>		<u>Page</u>
5.5	Cross-section showing the unfavourable stratification along CD section of the highway.	227
5.6	Geological map of landslide area III.	234
5.7	Monthly rainfall relationship for period (1962-1972) at Jarash, Sweileh and Rumman stations along Sweileh-Jarash road.	239
5.8	Map of landslide III showing the main features of the movement, location of boreholes and geophysical surveys.	241
5.9	Principal sketches of the proposed history (evolution) of movements of the study area III.	247
5.10	A lithological cross-section of the site of landslide III based on interpretation of the exploratory drilling and geophysical surveys.	252
5.11	Plasticity chart showing values for the analysed samples taken from the study areas of landslides I, II, III and IV.	254
5.12	Activity chart showing values for the analysed samples taken from the study areas of landslides I, II, III and IV.	254
5.13	Typical curves obtained from consolidated undrained triaxial compression tests on samples taken from landslide III.	256
5.14	Typical curves obtained from multi-reversal shear tests on samples taken from landslide III.	256
5.15	Correlation (comparison) of the D.T.A. Curves of the representative samples taken along the Sweileh-Jarash road.	258
5.16	Correlation (comparison) of the X-ray diffraction curves for the oriented mount specimens taken along the Sweileh-Jarash road.	262
5.17	Cross-section of landslide III (before sliding), with the results of the stability analysis.	267
5.18	Cross section (1) of landslide III (after sliding), with the results of the stability analysis and proposed remedial measures.	267
5.19	Cross-section (2) of landslide III after sliding with the results of the stability analysis.	269

<u>Fig.</u> <u>No.</u>		<u>Page</u>
5.20	Cross-section (3) along landslide III after sliding with the results of the stability analysis.	269
5.21	Geological map of landslide IV.	274
5.22	Map of landslide IV showing the main features of the movement, location of boreholes and geophysical surveys.	275
5.23	Schematic diagram and cross-section of landslide IV.	282
5.24	A lithological cross-section of the site of landslide IV based on interpretation of the exploratory drilling and geophysical surveys.	285
5.25	Typical curves obtained from multi-reversal shear tests and drained triaxial compression tests on samples taken from landslide IV.	289
5.26	Cross-section of landslide IV (after sliding) with the stability analysis.	291
5.27	Results of the stability analysis of landslide IV.	292
5.28	Recommended remedial measures for landslide IV.	294
5.29	Geological map of landslide area I.	298
5.30	Cross-section and plan showing the main features of landslide I.	299
5.31	Typical curves obtained from drained triaxial compression tests on samples taken from landslide I.	306
5.32	Cross-section along landslide I (after sliding) with the stability analysis.	308
5.33	Recommended remedial measures for landslide I.	309
5.34	Map of landslide II showing the main features of the movement, location of the boreholes and geophysical surveys.	314
5.35	Lithological logs of the exploratory boreholes in the vicinity of landslide II.	322
5.36	A lithological cross-section based on interpretation of the exploratory drilling and geophysical surveys.	324
5.37	Typical curves obtained from triaxial compression tests and multi-reversal shear tests on specimens taken from landslide II.	327
5.38	Cross-sections of landslide II (before sliding and after sliding) with the results of the stability analysis.	330

<u>Fig. No.</u>	<u>Page</u>
5.39 Recommended remedial measures for landslide II.	333
6.1 Location map of the proposed realignment sections at Ras-En-Naqab escarpment.	338
6.2 Contour map of Ras-En-Naqab section showing the existing alignment.	340
6.2.1 Geological map and cross-section showing the main tectonic and landslides along the proposed alignment.	
6.2.2 Location of boreholes, trial pits, joint surveying areas and observation points along the proposed alignment.	
6.3 Measured columnar section at Ras-En-Naqab escarpment.	345
6.4 Exploratory boreholes lithology in correlation with the drilling time and core recovery percentage.	351
6.5 Lithology of the trial pits along the proposed alignment.	353
6.6 Stereographic projection-contour diagram of joints measured in the surveying area (1).	355
6.7 Stereographic projection-contour diagram of joints measured in the surveying area (2).	357
6.8 Stereographic projection-contour diagram of joints measured in the surveying area (3).	358
6.9 Plasticity chart showing values of representative materials along the proposed alignment.	362
6.10 Activity chart showing values for the representative materials along the proposed alignment.	362
6.11 Maximum water absorption of the samples representative of the materials along the proposed alignment.	364
6.12 Typical grading curves of samples representative of the materials along the proposed alignment.	365
6.13 Proctor compaction test curves and summary of the results.	366
6.14 Correlation (comparison) of the D.T.A. of the representative samples along the proposed alignment.	368

LIST OF TABLES

<u>Table No.</u>	<u>Page</u>
1.1 Classification of landslides proposed by D.J. Varnes (1958).	26
1.2 Classification of landslides proposed by Hutchinson (1968).	28
1.3 Classification of mass movements in Jordan proposed by the author.	30
2.1 Correlation of the litho-stratigraphic units recognised in East Jordan.	54
2.2 Correlation of the litho-stratigraphic units recognised in the study area.	60
3.1 Comparison of analyses of circular and non-circular landslides using Janbu's, Fellenius' and Bishop's methods.	118
4.1 Representative peaks and temperatures obtained from the D.T.A. curves of the samples taken from landslides V and VI.	139
4.2 The X-ray diffraction results of representative samples taken from landslides V and VI.	142
4.3 Chemical analyses of representative samples taken from landslides V and VI.	143
4.4 The precipitation record for the month and year of landslide V.	151
4.5 The range of resistivities and velocities of the materials in the vicinity of landslide V.	165
4.6 A summary of the principal soil index results of the analyses performed on representative samples taken from landslide V.	166
4.7 A summary of the analyses results performed on samples taken from borehole I in the vicinity of landslide V.	170
4.8 Chemical analyses of water samples taken from two springs in the vicinity of landslide V.	170
4.9 A summary of the principal soil index results of the analyses performed on representative samples taken from landslide VI.	193
5.1 The precipitation record for the month and year of the failure of landslide III.	238

<u>Table No.</u>		<u>Page</u>
5.2	The average resistivities and velocities of the materials in the vicinity of landslide III.	250
5.3	A summary of the principal soil index results of the analyses performed on representative samples taken from the study areas.	253
5.4	A summary of the D.T.A. of representative samples taken from the study areas	258
5.5	Representative peaks and temperatures obtained from the D.T.A. curves of the samples taken from the study areas.	259
5.6	Chemical analyses of representative samples taken from the study areas.	263
5.7	Summary of the X-ray diffraction analyses and Cation Exchange capacities of representative samples taken from the study areas.	264
5.8	X-ray diffraction of whole-rock specimens taken from the study areas.	264
5.9	The precipitation record for the month and year of landslide IV.	277
5.10	Chemical analyses of water samples taken from two springs in the vicinity of landslide IV.	278
5.11	The range of resistivities and velocities of the materials in the vicinity of landslide IV.	284
5.12	A summary of the principal soil index results of the analyses performed on representative samples taken from landslide IV.	286
5.13	The precipitation record for the month and year of landslide I.	301
5.14	A summary of the principal soil index results of the analyses performed on representative samples taken from landslide I.	303
5.15	The precipitation record for the month and year of landslide II.	318
5.16	The range of seismic velocities and resistivities of the materials in the vicinity of landslide II.	323
5.17	A summary of the principal classification results of the analyses performed on representative samples taken from landslide II.	325

<u>Table No.</u>		<u>Page</u>
6.1	The distribution of monthly precipitation at Ras-En-Naqab station.	348
6.2	The characteristic statistics of annual precipitation at Ras-En-Naqab.	349
6.3	A summary of the principal soil index results of the analyses performed on representative samples along the proposed alignment.	360
6.4	Chemical analysis of two representative samples along the proposed alignment.	369

LIST OF PLATES

<u>Plate</u> <u>No.</u>		<u>Page</u>
1.1	Slabslide with internal toppling of a limestone along a bedding plane-geologic plane of weakness.	34
1.2	Block flow into the underlying soft clay.	34
1.3	Rockfall due to the erosion of the underlying soft clay.	41
1.4	Earthfall due to erosion by the river.	41
4.1	General view of landslide V - 1971 (looking down the slope). The sliding material near the toe is covering the lower road (observation point 1).	125
4.2	The main features of the movement of landslide V - 1971 (the main scarp) (observation point 5).	125
4.3	A mudflow consisting of brown silty clay, yellowish clay and marl (observation point 6).	127
4.4	A mudflow, consisting of yellowish marl and clay (observation point 7).	127
4.5	A mudflow consisting of yellowish marl and green clay; trees have recently been planted (observation point 8).	129
4.6	Marly limestone underlain by marl and clay. Notice loose blocks of limestone adjacent to the pavement (observation point 11).	129
4.7	Showing two blocks separated from the parent rock owing to the erosion and undercutting of the underlying soft clay and marl.	130
4.8	Showing sets of continuous downward movement of rock masses along pre-existing joint surfaces. Block 1 failed. The final collapse of the blocks B2, B3, and B4 will take place in the same manner along pre-existing joint surfaces J2, J3 and J4.	130
4.9	Active landslide. The pavement is pushed up at the toe of the movement while the upper part shows displacement. Notice loose blocks adjacent to the pavement (observation point 12).	131
4.10	Active landslide. The upper part shows block creeping and probable toppling failure mode (observation point 12).	131
4.11	The main features of landslide VI. The main scarp and the moved road (observation point 13).	133

<u>Plate</u> <u>No.</u>		<u>Page</u>
4.12	Sets of continuous mass movements along pre-existing failure surfaces (joints). Mass 1 moved along joint 1. The final collapse of the moving mass 2 will occur after the lateral support is removed completely. Mass 1 shows intense jointing and disturbance while mass 2 is less disturbed (observation point 14).	133
4.13	General view of the study area of landslide V in 1969. Old landslides, faults and hummocky terrain.	145
4.14	Jointing and faulting of the strata at the crown of landslide V. The bedrock is marly limestone underlain by marl and clay.	147
4.15	Toppling and rockfall at the crown of landslide V.	147
4.16	Loose blocky appearance of the strata at the crown of landslide V. Rockfall and potential rockslips are the dominant mechanism at this site.	150
4.17	Shearing of the strata at the crown of landslide V.	150
4.18	A spring discharging from the bottom of the main scarp.	155
4.19	Flow of the material near the main scarp.	155
4.20	General view of landslide V (looking up the slope). The main scarp, left and right flanks, the upper and lower road.	157
4.21	General view of the study area of landslide VI.	183
4.22	General view of the study area of landslide VII.	205
4.23	The main features of landslide VII (the moved mass, the faults and the clay bands).	205
4.24)	Showing the old existing joint (A), the tension joint (B),	
4.25)	then the failure surface (C) and the slipped mass (D).	206
5.1	Landslide activated by the undercutting of the river near the Zerqa River bridge.	221
5.2	Earth and mudflow within the silty clayey materials along the Sweileh-Jarash road (observation point 14).	229
5.3	Earth fall along the Sweileh-Jarash road.	229
5.4	General view of the landslide III in 1969.	242
5.5	Landslide III in 1971.	245
5.6	Landslide III in 1971. Establishment of tension cracks at the crown of the landslide.	245

<u>Plate No.</u>	<u>Page</u>
5.7 The main features of the lower part of landslide IV including simplified geology.	276
5.8 The main features of the upper part of landslide IV.	276
5.9 Earth and mudflow at the crown of landslide IV. Notice cracking in the retaining wall.	280
5.10 Shifted and curved backward trees at the crown of landslide IV indicating the progressive nature of the movement.	280
5.11 Showing the moved highway after the movement of 1966, Landslide I.	300
5.12 Main features of the 1971 landslide, showing the moved irrigation canal at the main scarp of landslide I.	302
5.13 The main scarp of the 1971 movement, showing the moved gabion at the crown of the landslide I.	302
5.14 General view of landslide II, showing the original route of the highway and the diversion.	315
5.15 Jointing and weathering of the silty clay at the highway level in the backslope of landslide II.	317
5.16 General view of landslide II showing the main features of the movement.	320
5.17 Shearing of the upper gabion at the crown of landslide II.	320
5.18 Tilting of the lower gabion at the level of the Zerqa River - landslide II.	320
6.1 General view of the study area of the Ras-En-Naqab escarpment showing a hummocky terrain owing to the combined action of the tectonic, old landsliding and weathering.	342
6.2 General view of the study area, showing the approximate geology along the proposed alignment.	343
6.3 Exploratory pit shows the disturbed nature of the bedrock indicating the old movements in the area.	
6.4 The intensely jointed bedrock of the Upper Ajlun Formation (joint surveying area 1).	356
6.5 The upper part of the Lower Ajlun rock unit showing intense jointing and expected toppling (joint surveying area 2).	356
6.6 The intensely jointed Lower Ajlun rock unit (joint surveying area 3).	356

<u>Plate No.</u>		<u>Page</u>
6.7	Block flow within the Lower Ajlun Formation.	372
6.8	Block flow of the Middle Ajlun Formation underlain by the clay-marl unit of the Lower Ajlun Group.	372
6.9	Creep of the hard ledges of bedrock into the under- lying plastic clay of the marl-clay unit.	373
6.10	Old landslide within the marl-clay unit of the Lower Ajlun Group.	373

APPENDIX A

(List of Figures)

Fig. No.

- 4.1A Seismic refraction profiles SS_I, II, III in landslide area V.
- 4.2A Resistivity sounding profiles in landslide area V.
- 4.3A Seismic refraction profiles $SS_{I,II,III,IV}$ in landslide area VI.
- 5.1A Geologic map and location of landslides along the Sweileh-Jarash road.
- 5.2A Stereographic projection-contour diagram of joints in landslide area III.
- 5.3A Seismic refraction profiles SS_I, SS_{II} in landslide area III.
- 5.4A Resistivity sounding profiles in landslide area III.
- 5.5A Maximum water absorption curves of representative samples taken from the landslides I, II, III and IV.
- 5.6A Grainsize distribution curves of representative samples taken from landslides I, II, III and IV.
- 5.7A Resistivity sounding profiles in landslide area IV.
- 5.8A Seismic refraction profiles in landslide area IV.
- 5.9A Seismic refraction profiles in landslide area II.
- 5.10A Correlation of the resistivity sounding profiles in landslide area II.

APPENDIX B

(List of Tables)

Table No.

- 4.1B Annual precipitation for the period (1942 - 1972) at Naur station.
- 4.2B A summary of representative results of analyses performed on samples taken from landslides V and VI.
- 5.1B A summary of representative results of analyses performed on samples taken from landslides I and II.
- 5.2B A summary of representative results of analyses performed on samples taken from landslides III and IV.
- 6.1B A summary of representative results of analyses performed on samples taken along the proposed alignment of Ras-En-Naqab.
- 6.2B Detailed Differential Thermal Analyses of representative samples taken from the proposed realignment of Ras-En-Naqab escarpment.

APPENDIX C

(List of Tables)

- C.1 Detailed Differential Thermal Analysis of representative samples taken from the study area of Naur-Adasiye road.
- C.2 Detailed description of the proposed realignment of the Ras-En-Naqab escarpment.
- C.3 Detailed description of the measured columnar section at Ras-En-Naqab escarpment (on Fig. 6.3).
- C.4 Detailed description of the exploratory boreholes along the proposed realignment of Ras-En-Naqab escarpment.
- C.5 Trial pits' description along the proposed realignment of the Ras-En-Naqab escarpment.

CHAPTER ONE

GENERAL

1.1 INTRODUCTION

It is now widely recognised that slope stability analysis forms an integral part in the routing of highways. Stability analysis requires, inter alia, a knowledge of the shear strength parameters of representative soil samples and hence laboratory tests form an essential part of the investigations. In Jordan there has been a complete lack of engineering geological investigations undertaken prior to the construction of the highways. Although slope stability analyses have been made of isolated small areas in terms of total stresses (internal report of the Engineering Geology Division of the Natural Resources Authority) there is a total lack of detailed regional investigations of landslides, with accompanying stability analyses in terms of effective stresses.

In the first three parts of this thesis, the theoretical basis of study is outlined together with the method of approach and this is followed by a systematic account of the detailed surveys and investigations of existing major landslides on three major highways in Jordan. The surveys included details of the topography, geological investigations and detailed laboratory testing of representative samples obtained from the study areas. Slope stability analyses are given in terms of effective stresses for each of the landslides described using the widely accepted limit

design technique. Case histories of slope failures provide the best source of information on the reliability of theories of stability analysis. The factor of safety of the failed slope should be equal to unity if the shear strength parameters and other information used prove to be correct.

Some of the landslides described are what may be called first time slides (Skempton, 1970), whilst others are reactivated old landslides. It is important to note that many sections of the highways in Jordan have been routed over old landslide areas, and renewed instability has often arisen during the construction of the highways.

1.2 HISTORICAL BACKGROUND

Systematic geological studies in Jordan began in 1852 with the official report of the United States expedition to explore the Dead Sea and the River Jordan. The first publications dealing with the geology were by H. Larlet in 1869 and by E. Hull in 1886. However, no attempts at regional mapping were made.

The regional geology of Jordan was first presented by Burdon (1959) and was based on a geological map of the area east of the Wadi Araba-Jordan graben on a scale of 1:250,000 (Quennell, 1956). At about the same time an important contribution to the understanding of the regional stratigraphic relations was made by Wetzel and Morton (1959) in their comprehensive description of

the geology of Jordan. Geological research in Jordan started relatively late and was connected with various development projects which commenced in the last fifteen years, i.e. since 1959. Hydrogeology and pedology studies were undertaken by Wilson and Wozab (1954); Baker and Harza Engineering Co., 1955; Hunting Technical Services Ltd. (1956); MacDonald (1965); Rofe and Raffety (1963 and (1965), the hydrogeological project of the United Nations and the Central Water Authority as well as the Sandstone Aquifer project of East Jordan (Parker and Lloyd, 1966-69) Geological mapping, hydrological studies, and estimates of recharge were prepared by Sir Murdoch Macdonald and Partners in association with Hunting Technical Services and the Jordan Office for Geological and Engineering Services. Between 1961 and 1965 a German geological mission worked on the detailed geological investigations of Jordan and remapped the country on scales of 1:25,000 or 1:100,000 and published a geological map of Jordan on a scale of 1:250,000 (Bender, 1968).

The Jordanian Geological Survey and Bureau of Mines was first established in 1965, and in 1966 it was named "Natural Resources Authority". Until 1966 no engineering geological investigations of any kind had been undertaken despite the many problems of slope stability on the Jordanian highways. A first preliminary engineering geology report was prepared by the author in 1967, dealing with two small landslides in Amman and

one landslide on the Arda Road. In 1968, upon the advice of the author, an Engineering Geological Division was established and provided with appropriate field and laboratory equipment. This Division deals with site investigations and soil analysis. Stability analyses in isolated small areas have been made in terms of total stresses (Internal Engineering Geology Reports), but no stability analyses in terms of effective stresses have been made prior to this thesis.

1.3 CLASSIFICATION OF LANDSLIDES

The stability of natural slopes and cuts forms part of soil mechanics and engineering geology. Failure of any slope can be described as a landslide. In a typical landslide there is a downward and outward displacement of the forming materials with the crown part of the landslide moving downward and the toe part heaving upwards. Many classifications have been proposed for mass movements. Terzaghi's (1925) classification of landslides was based on the physical properties of materials involved. Sharp (1938) divided the mass movements with regard to the materials involved in the slide mass and to the rate and type of the movement in relation to the geomorphic cycle and climatic factors. D.J. Varnes (1958) proposed a classification which included the old classifications with modification and is used by the Landslide Committee of the Highway Research Board. This may be summarized in the following table:-

Type of Movement	Type of Materials				
	Bedrock			Soils	
Falls	Rockfall			Soilfall	
Slides	Few units	Rotational Slump	Planar Blockglide Rockslide	Planar Blockglide	Rotational Blockslump Failure by lateral spreading
	Many units			Debris slide	
Flows	ALL Unconsolidated				
	Dry	Rock fragments	Sand or silt	Mixed	Mostly plastic
		Rock fragments flow	sand run	loess flow	
Wet			Rapid earth flow	Debris avalanche	Mudflow
			sand or silt flow	Debris flow	
Complex	Combinations of materials or types of movement.				

Table 1.1

As can be seen from the above table, mass movements are divided into four major types; falls, slides, flows and complex landslides. These main divisions are related to the type of materials involved and to the shape of the movement. The falls and slides occur mainly within consolidated materials along circular arc or planar failure surfaces, whilst flows occur mainly within unconsolidated materials and may be either

slow or rapid. The complex type movements are combinations of the materials and compound shape of failures.

Zaruba (1969) proposed a classification of mass movements in Czechoslovakia which took into consideration regional geological conditions and was based on the following factors:-

- A) Slope movements of superficial deposits
 - a. creep of debris
 - b. sheet slides
 - c. earth flows
 - d. debris flows (liquification of sands)

- B) Slides in pelitic, unconsolidated or partly consolidated rocks (clays, marl, claystones, pelitic shales) developed:
 - a. on cylindrical surfaces
 - b. on predisposed surfaces, on ancient planes of separation
 - c. by squeezing out the soft underlying rocks

- C) Slope movement of solid rocks:
 - a. slides on predisposed surfaces (bedding, schistority, jointing, etc.)
 - b. long-term deformation of mountain slopes
 - c. rock falls.

D) Special kinds of slope movements (do not occur in Czechoslovakia):

- a. Solifluction
- b. slides in sensitive clays
- c. sub-aqueous slides.

As can be seen from the above classification of mass movement, Zaruba took into consideration the type of materials, climatic conditions and regional geology as main factors.

In England Hutchinson (1968) proposed a new classification which is essentially similar. Hutchinson's classification is summarized in the following table:

Creep	<ul style="list-style-type: none"> 1. Shallow, predominantly seasonal creep; mantle creep:- <ul style="list-style-type: none"> a. soil creep b. Talus creep 2. Deep-seated continuous creep; mass creep. 3. Progressive creep
Frozen Ground Phenomena	<ul style="list-style-type: none"> 4. Freeze-thaw movements <ul style="list-style-type: none"> a. combering and valley bulging b. solifluction sheets and lobes c. stone streams d. rock glaciers
Landslides	<ul style="list-style-type: none"> 5. Translational slides <ul style="list-style-type: none"> a. rock slides, block glides b. slab or flake slides c. detritus or debris slides

landslides	<ul style="list-style-type: none"> d. mudflows <ul style="list-style-type: none"> i) climatic mudflows ii) volcanic mudflows or lahars e. Bog flows, bog bursts f. flow failures <ul style="list-style-type: none"> i) loess flows ii) flow slides 6. Rotational slips <ul style="list-style-type: none"> a. single rotational slips b. multiple rotational slips <ul style="list-style-type: none"> i) in stiff fissured clays ii) in soft, extra-sensitive clays; clay flows, quick clays c. sensitive, or stepped rotational slips 7. falls <ul style="list-style-type: none"> a. stone and boulder falls b. rock and soil falls 8. sub-aqueous slides <ul style="list-style-type: none"> a. flow slides b. under-consolidated clay slides
------------	--

Table 1.2

Hutchinson took into consideration many factors of mass movement such as: (i) type of materials involved, (ii) the shape of the failure surface, (iii) depth of the slip surface, (iv) climatic conditions and the rate of the movement as the main factors of classification, where he divided the mass movement according to velocity into three main categories; creep, frozen ground phenomena and landslides.

For Jordan and for the purpose of engineering geology the most convenient and applicable classification is one which takes into consideration the following points:

- a) the shape of failure surface,
- b) the rate of movement, and
- c) simplicity and ease of recognition in the field.

This classification may be summarized as follows
(Classification of mass movement of slopes in Jordan):

Character of the Movement		Shape of the Failure
Creep	Creep ↑	No definite sliding surface
Translational	↑	<ul style="list-style-type: none"> a) slab slide (planar and shallow) b) block slide (planar and moderate to deep) c) debris slide (planar and moderate depth)
Rotational	LANDSLIDES ↓	<ul style="list-style-type: none"> a) single rotational <ul style="list-style-type: none"> i. circular ii. non-circular b) multiple rotational <ul style="list-style-type: none"> i. circular ii. non-circular
Flows		<ul style="list-style-type: none"> a) mudflow b) rockflow
Falls	↓	<ul style="list-style-type: none"> a) rockfall b) earthfall c) toppling

Table 1.3

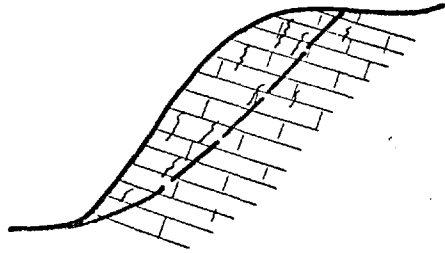
In terms of velocity of mass movements, they may be classified into two main categories:-

- I. Creep.
- II. Landslides.

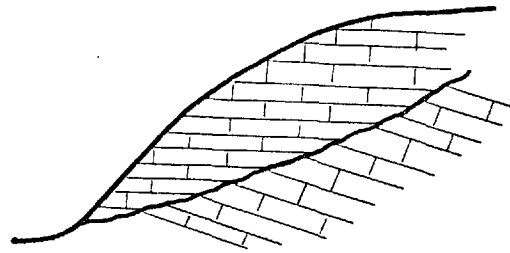
Creep is a continuous but slow movement with no definite slip surface. Creep is mainly seasonal in Jordan, which movements occur in the winter months only.

Landslide movement may be subdivided into four main divisions as shown in Table 1.3. Planar landslides (Fig. 1.1) are usually rapid movements with a planar shear surface following a geological plane of weakness. If the slope is to fail, it will fail along a geologic plane of weakness which is considered to be the least resistance in the mass. The planar type of mass movements occur mainly in heterogenous materials and rarely in homogeneous materials which should include structural distortion or pre-existing plane of weakness. This type of mass movement can be observed within the Upper Ajlun Group which is composed of intensely jointed limestones and dolomites interbedded with bands of marl and clay. These clay bands constituted the geological planes of weakness in the stratified strata; whilst the joints and faults act as discontinuous planes of weakness within the bedrock.

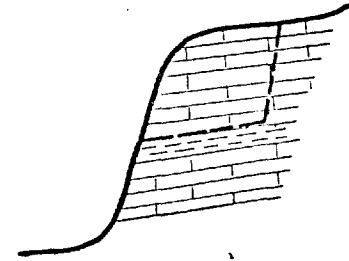
MAIN TYPES OF TRANSLATIONAL LANDSLIDES



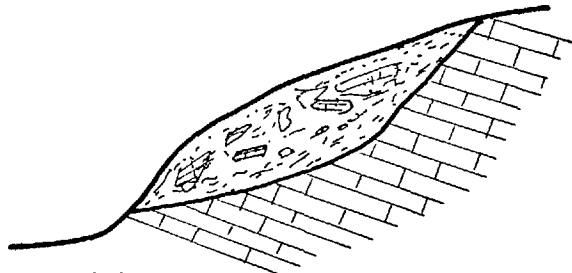
Block slide (Internal structure _ joints as planes of weakness)



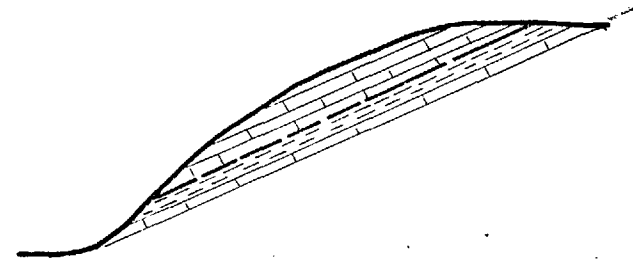
Block slide (Internal structure _ fault as plane of weakness)



Block slide (Lithologic contact _ as plane of weakness)



Debris slide (Weathering zone or old landslide)



Slab slide (Internal structure _ bedding planes as geologic planes of weakness)

Fig.(1.1)

A block slide is a typical planar type landslide which occurs rapidly and is bounded by one or more clear planes of weakness. The mass generally moves as one body without much distortion in the material. Amman slide VII is a typical example of a block slide. A slab slide also occurs rapidly and is formed by a planar geological stratification or schistosity. This type of mass movement is mainly shallow and can be observed in the side-cut slopes of the highways in Jordan (Plate 1.1).

Debris slides are mainly formed of weathered and decomposed materials. The movements of this type occur following periods of heavy rainfall and are accompanied by great amounts of distortion in the moved mass. In some cases this type of landslide forms a part of an old landslide. The Naur-Adasiye landslide V of 1971 is a typical debris slide formed on part of an old landslide of 1969 and consists of the disturbed zone of weathering with a shallow failure surface running almost parallel to the ground surface (Plate 4.20). Landslide VI is another typical debris slide occurring within a weathered zone along a pre-determined contact surface between the weathered materials and the intact bedrock (Fig. 4.22).

Rotational Slides (Fig. 1.2):

Fairly rapid deep-seated landslides occur mainly within the thick homogeneous marls and clays, on circular or non-



Plate 1.1 Slabslide with internal toppling of a limestone along a bedding plane - geologic plane of weakness.



Plate 1.2 Block flow into the underlying soft clay.

MAIN TYPES OF ROTATIONAL LANDSLIDES

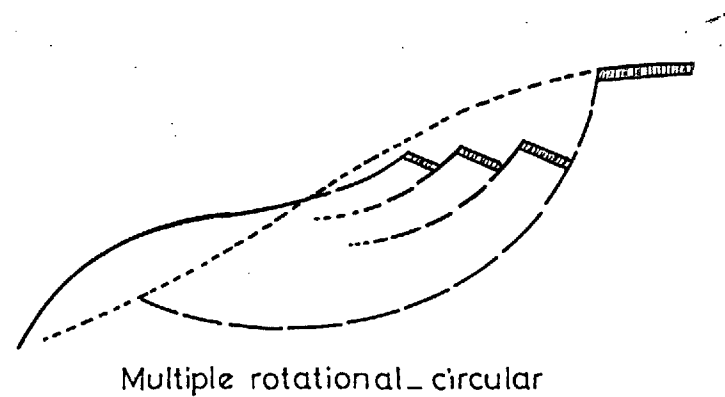
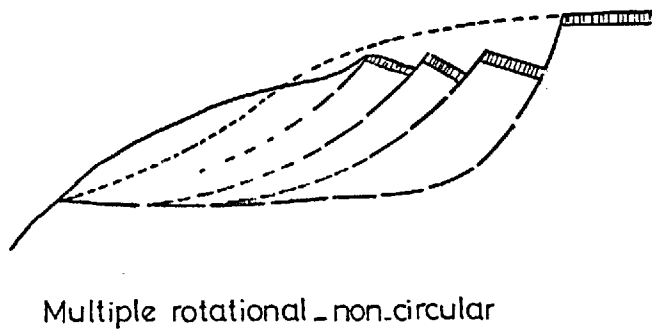
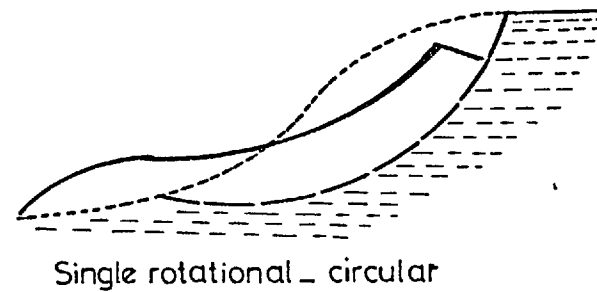
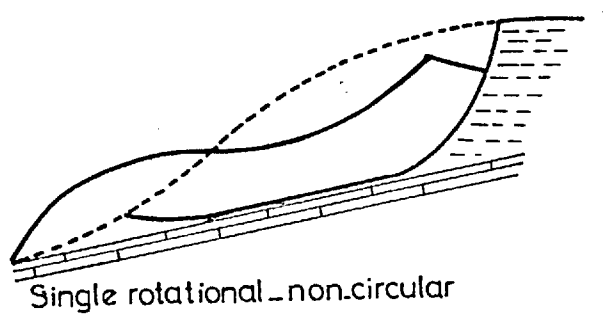


Fig.(1,2)

circular surfaces of rupture, showing slumping and back tilt of the strata at the crown part and heave at the toe part. This type of movement generally occurs without much structural distortion in the moved mass except for mudflows at the toe part.

According to the number of planes of weakness rotational landslides may be divided into:-

- a) single rotational, either
 - i) circular, or
 - ii) non-circular.

- b) multiple rotational, either
 - i) circular, or
 - ii) non-circular.

Circular single rotational slides occur on one concave failure surface within homogeneous clay materials thick enough to establish circular shape failure surface. The non-circular single rotational movements occur on one failure surface which is partly concave and partly planar owing to the presence of a hard stratum beneath the homogeneous clay material at a moderate depth. This type of movement is accompanied by more distortion of the moved mass but less than with typical planar movements.

Most of the landslides on the Jordanian highways are classified as single rotational circular and non-circular types, e.g. landslides I, II, IV and V are of circular rotational and III and VI are of non-circular single rotational type.

Multiple-rotational landslides occur on two or more failure surfaces where the clay material is fairly thick. This type of landslide moves as one monolithic body along one, common deep-seated failure surface, consisting of two or more sliding masses each occurring on separate minor slip surfaces which are probably established during or soon after the main mass movement has occurred. If the clay is thick enough, the common deep-seated failure surface would be concave and the movement should be called circular multiple rotational landslide. But if the clay is not thick enough to establish a deep-seated concave failure surface and is underlain by a rigid stratum at moderate depth, the common failure surface would be partly circular and partly non-circular, so this type of landslide is called a non-circular multiple rotational landslide (Fig. 1.2).

Flows (Fig. 1.3):

This is a landslide but without a visible failure surface. Flows are generally slow movements depending on the degree of saturation of the soil mass. They occur mainly in

soft weathered materials often mixed with rock fragments. Flows may be subdivided into: (i) earth flows, (ii) mudflows, and (iii) rock flows. Earth flows are a common type of movement which occur suddenly in softened weathered materials with a low moisture content and lead to less distortion in the moved material compared to mudflows, which are similar but associated with faster movements and accompanied by saturation and distortion of the materials. These types of movements are always observed at the toe part of each landslide and commonly occur within an old landslide area where the material has physically disintegrated (Plates 4.3, 4.4 and 4.5).

Block flows are a type of movement which occur in situations where jointed rigid strata are underlain by soft plastic material. After heavy rainfall the soft clay becomes saturated and turned into mudflow, the rigid overlying bedrock will participate in the movement of its base, and it will be torn into separate blocks moving within the flow material (Plate 1.2). The velocity of this type of movement can vary widely depending on the seasonal variation of rainfall and on the amount of rainfall percolating into the clay. Movements develop commonly in the winter and cease or slow down in summer.

Falls (Fig. 1.4):

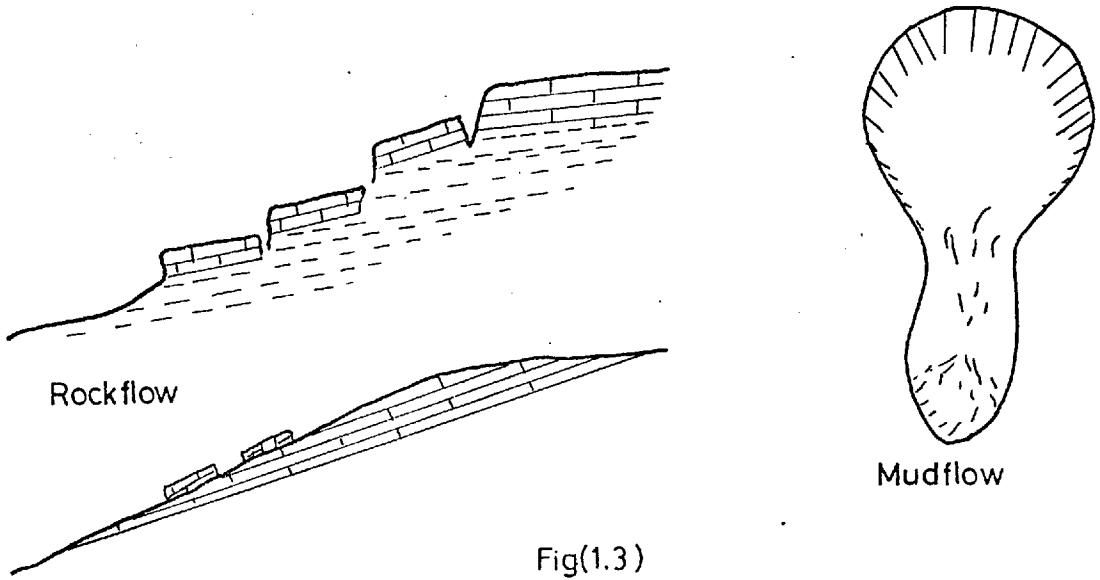
Falls are by definition the displacement of a mass of rock or soil in the air by free fall. This generally occurs very rapidly on steep slopes caused by river excursion, weathering or by tectonic and landslide movements, or by man-made cutting. This type of mass movement was observed at the crown of the landslides (Plate 4.15), and regionally within the Upper Ajlun Group at the contact between A2 and A3 where the erosion of the soft underlying marls allows the hard ledges of A3 to fall down (Plate 1.3). They are also observed along the river banks where the erosion by the river allows masses of earth and rock to fall freely into the river bed (Plate 1.4).

Subsidence is mainly slow, being caused by vertical mass movements associated with a decrease in volume of the soils underlying the superficial deposits. This decrease in volume may be caused by the following factors:-

1. decrease in porosity
2. leaching of the soluble binder between the particles
3. subsurface erosion or piping
4. undercutting or mining.

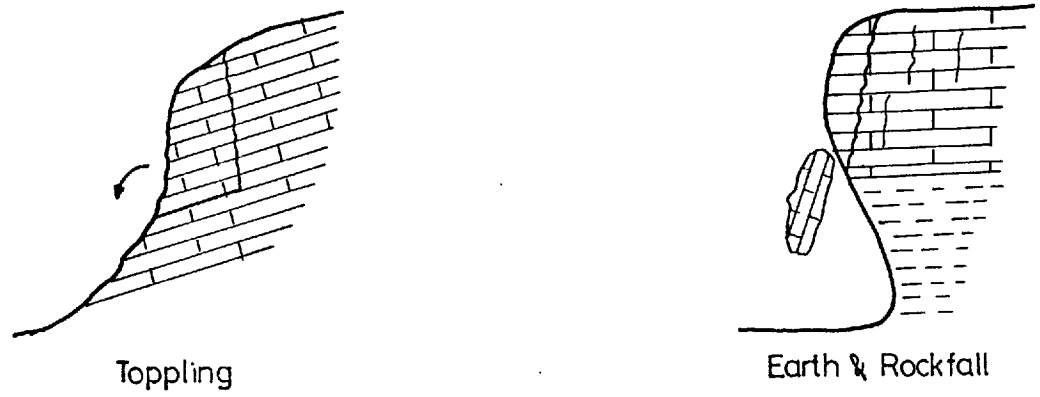
This type of subsidence can be observed in the phosphate mines and along the Jordanian highways as a limited settlement in the pavement. A slump type subsidence is of graben shape (Fig. 1.5),

FLOWS



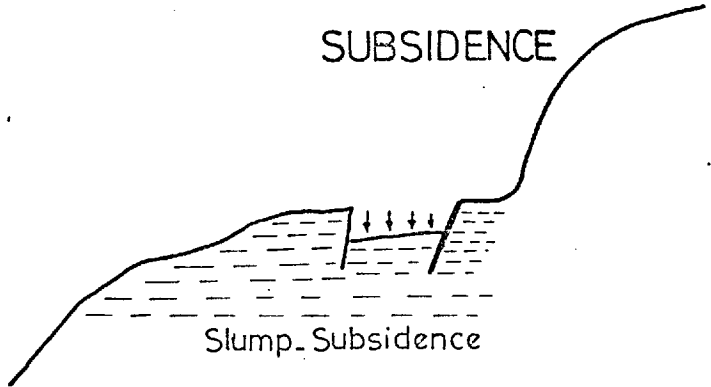
Fig(1.3)

FALLS



Fig(14)

SUBSIDENCE



Slump-Subsidence

Fig(1.5)



plate 1.3 Rockfall due to the erosion of the underlying soft clay.

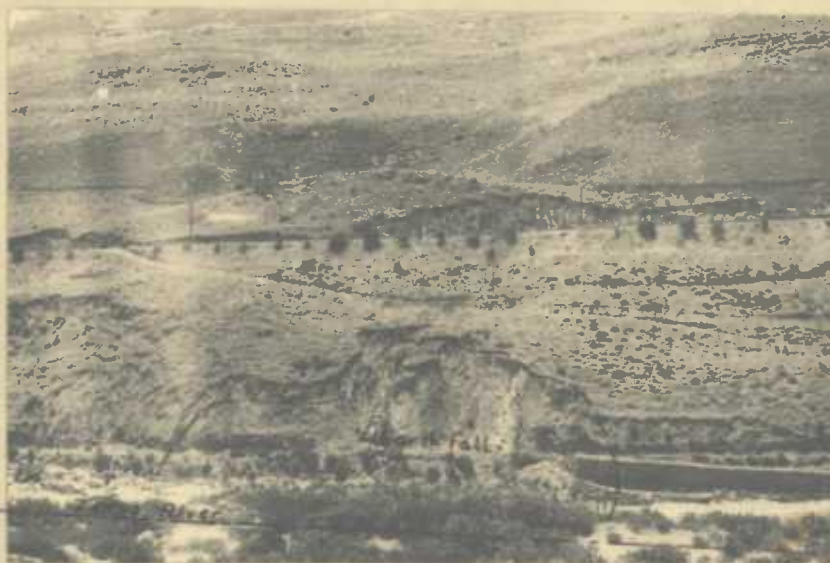


Plate 1.4 Earthfall due to erosion by the river.

which is probably caused by subsurface erosion or piping, or by high amount of leaching of the soluble salts from the soil which is as high as 7% in some Jordanian clays where this type of movement is observed.

As can be seen, all the proposed classifications of landslides have the same common names related to the same mechanism but every classification is applied to one region depending on the climatic conditions. Therefore the above mentioned classification is believed to be the most applicable for the Jordanian mass movements, and the definition of the terms is attained from the field recognition and observations. In summary one can say that mass movements may be classified on various bases, which are common in all classifications:-

1. the velocity of the movement (creep or landslide fall, flow, etc.).
2. natural or artificial origin.
3. history of the movement (new and old landslide).
4. form of the movement (circular, non-circular, complex).
5. depth of the failure surface (deep or shallow).
6. the number of moved masses (single or multiple).
7. the materials involved.

1.4 MAIN CAUSES OF THE LANDSLIDES

A landslide occurs when the disturbing forces exceed the resisting force. Primarily the driving forces are components of gravitational forces. The resisting forces are mainly a result of strength within the mass combined with components of gravitational forces that act in the proper direction.

The factors which produce an increase of the shearing stress and decrease of the resistance may be divided into external and internal respectively. The external forces which contribute to landslide movement are summarized as follows:-

I. Increase of the disturbing forces by loading the upper part (crown) of the slope by means of:-

- a. addition of load due to disposal of materials, etc.
- b. construction of embankment, buildings or bridge.
- c. weight of water enters the mass from precipitation or other means.

II. Decrease in the resisting forces caused by steepening or heightening of the slope by means of:-

- a. natural agencies such as erosion by river, stream, waves, weathering, etc.

- b. artificial agencies such as cuts at or near the toe part of the slope, removal of retaining structures, drawn down of reservoirs, etc.
- c. creation of new steep slopes owing to tectonic and landslide movements.

III. Shocks and vibrations may trigger off the stability of slopes, causing landslides. The vibration in soft rocks can cause a disturbance of the bond between the particles which causes a decrease in the cohesion or internal friction. In the hard rock, shocks and vibrations can lead to creation of planes of weakness contributing to instability.

The internal factors which contribute to landslide movements are summarized as follows:-

- I. Increase of pore water pressure affecting the shearing resistance by means of:-
 - a. the water soil body exerts upward forces. The higher the pore water pressure, the greater the part of the soil body carried by water, and when the pore water equals the normal pressure of the soils, the body floats. This in turn decreases the friction.

- b. The water penetrates into a soil body eliminating surface tension in fine-grained soils, thus reducing the cohesion and increasing the unit weight of the mass.
- c. The water also decreases the cohesion of the soil by means of reduction of the soil binder between the particles. A reduction of electrolyte concentration below 5 g/L can induce a critically sensitive clay and may flow spontaneously (R.S. Liebling).

Meyerhof (1957) noted that "artificial leaching reduced the remoulded shearing strength to such an extent that the clay becomes a viscous liquid."

- d. The moving ground water washes out fine sand and silt particles from the soil mass, forming cavities, thus weakening the soil mass.
- e. A sudden increase in pore water pressure can result in a sudden liquefaction of soil, where the water occupies the voids of the sand, prevents a rapid decrease of the porosity. During the time between the collapse of the structure and the reconsolidation under a new condition of equilibrium, the sediment has properties of a thick viscous liquid, which spreads laterally until its surface becomes almost

horizontal (Terzaghi, 1951). The spontaneous liquefaction may also be produced during a rapid rise or draw down of water table.

II. Changes in structure by means of:

- a. Fissuring of pre-consolidated clays due to the stress relaxation in a cut.
- b. Physical change by weathering of the materials decreases the cohesion.
- c. Shrinkage of clays in periods of drought creates cracks and planes of weakness. Thus the cohesion decreases and allows penetration by rainwater.

III. Physico-chemical reaction by means of:

- a. Hydration of clay minerals by absorption of water and decrease of cohesion at high water content.
- b. Base exchange has a great influence on physical properties of clays. Na or K bearing clays may be reasonably stable, whereas if these were replaced by Ca ions they can become extremely sensitive.

IV. Presence of rigid strata underlain by soft plastic materials dipping out of the slope.

- V. Presence of planes of weakness which act as stress concentrators.
- VI. Shape of the grain. Roundness of the grains decreases the friction of granular soils.
- VII. Disturbance of the internal structure of clays (sensitive clays) would reduce the shear strength.

If any landslide takes place, it will be caused by one or more of the above mentioned causes. The landslides on the Jordanian highways have probably been caused by one or more of the following:-

1. The presence of major tectonic and old landslide movements contributes to the structural distortion of the strata in the region and creates potentially critical conditions. The tectonic movements produced a stress relaxation in the strata adjoining the slopes and caused joints to open; rain water penetrates the joints and contributes to a high pore water pressure causing a decrease in shearing resistance and, as soon as it becomes equal to the average shearing stress on the potential surface of rupture, the slope fails.
2. Poor surface and subsurface drainage.
3. Abnormally high precipitation.
4. Bad siting of some sections of the highway through old landslide areas. These old landslides are reactivated either

by construction of high fill embankments on or near the crown of these landslides or improper excavation at the toe of these landslides which have triggered off the delicate balance of these areas by increasing the disturbing forces or decreasing the resistance forces.

5. Decrease of the resisting forces by stream erosion.
6. Improper steep-cut slopes along the highway.
7. Improperly constructed retaining walls, without drainage facilities, at or near the crown of the landslides have caused accumulation of rainwater behind these retaining structures, thus contributing to mudflows and larger movements.
8. Leakage from artificially created irrigation canals has caused softening of the materials, contributing to mudflows and landslides.
9. Absence of engineering geological investigations prior to the construction of the highway resulted in the incorrect selection of the highways' routes along unstable areas and also improperly designed slopes.

Following detailed investigations of a landslide and knowing the main causes contributing to the movement, it is

possible to select appropriate stabilizing and remedial measures. Generally, methods of stabilization in landslide areas may be summarized as follows:-

I. Reducing the main factors contributing to high shearing stress by means of:-

- 1) Excavation of loads at or near the crown of the landslides.
- 2) Flattening and benching the steep slopes.
- 3) Improving surface drainage.
- 4) Lining of artificial irrigation canals with clay to reduce leakage.
- 5) Lowering the ground water level by drainage.

II. Increasing the resisting forces of the soils by means of surface and subsurface drainage.

- 1) Diversion of the water.
- 2) Horizontal drainpipes.
- 3) Vertical pumping wells.
- 4) Drainage galleries.
- 5) Drainage blankets.
- 6) Stabilization benches.

III. Increasing the resisting forces by means of:-

- 1) Retaining walls.
- 2) Earth anchors.
- 3) Piles and sheeting.
- 4) Beams over the lower part of the landslide and beyond the toe.
- 5) Buttresses.
- 6) Grouting.
- 7) Freezing.
- 8) Densification of soils in situ by vibration and compaction.

CHAPTER TWO

REGIONAL GEOLOGY OF JORDAN

REGIONAL GEOLOGY OF JORDAN

2.1 INTRODUCTION

The Hashemite Kingdom of Jordan is situated between latitudes $29^{\circ}30'$ and $33^{\circ}N$ and longitudes 35° and 39° E. The Kingdom has a maximum length of approximately 380 Km and the maximum breadth is 400 Km, with a total area of about 96,500 Km². As stated in Section 1.2, the systematic geology of Jordan was first described by Burdon (1959) and geological maps of different scales have been prepared subsequently by many authors. In this chapter, a summary of the regional geology of Jordan is given together with a brief description of the stratigraphy and detailed description of the geological groups existing in the study areas of the landslides.

2.2 GEOLOGY

East Jordan lies across the northern rim of the Pre-Cambrian shield of crystalline basement rocks which extends under the Arabian peninsula and most of the African continent. Marine transgressions and regressions resulting from several epeirogenic movements of the shield have occurred ranging in age from Cambrian to early Tertiary. During these marine incursions, great thicknesses of sedimentary rocks accumulated.

During the Palaeozoic predominantly arenaceous, fluvial, estuarine, littoral and deltaic sediments accumulated

on a peneplained surface of Pre-Cambrian rocks. There is evidence that penecontemporaneous faulting took place during this period of Palaeozoic sedimentation (Lloyd, 1969).

Sedimentation resumed in Lower Triassic time but was restricted to north-western Jordan. At the end of the Triassic the seas regressed and the whole area was then subjected to sub-aerial erosion. During the Triassic phase of sedimentation a sequence of arenaceous, argillaceous and carbonate deposits accumulated.

Further marine sedimentation took place in the Middle Jurassic but was again restricted to north-western Jordan. During this period sandstones, clays and dolomitic limestones accumulated.

The most extensive Mesozoic marine transgression commenced with deposition of the Kurnub group in the Lower Cretaceous when a thick succession of sandstone with subsidiary clay and limestone accumulated. The sandy facies of the Kurnub group persists as the basal unit of the Cretaceous succession throughout the study area, but there is evidence that this zone is diachronous and becomes younger to the south-east (Bender, 1967). The sediments which overly the Kurnub group are, except in the south-east, mainly carbonates and consist of limestones, sandy

limestones and marls. Chert is common in the upper part of the succession. During the Upper Eocene the seas regressed and the youngest deposits of this phase of sedimentation are comprised of chalk of Upper Eocene age.

The extensive basalt lava flows of northern Jordan were extruded between Oligocene and Pleistocene times. This volcanic activity was contemporaneous with the start of the major earth movements which tilted the Mesozoic-Tertiary sediments towards the east-north east and faulted and folded them adjacent to the rift. Taphrogensis in the rift valley zone with associated disturbance in the adjacent area reached a maximum during the Pliocene-Pleistocene times. Localised lacustrine sedimentation occurred during the Upper Tertiary and Pleistocene. Late Quaternary fluvial gravels, lacustrine clays and weathering mantle blanket a large part of the study area.

2.2.1 Stratigraphy

The stratigraphic relationships of the various rock types existing in East Jordan are summarised in Table 2.1. Rocks range in age from Pre-Cambrian to Quaternary. However, only rocks of Cretaceous age are exposed in the study areas. Rocks of the Upper Kurnub and the Lower Ajlun groups are the

ERA	PERIOD	EPOCH	GROUP	FORMATION		NORTH-WEST	CENTRAL	SOUTH-WEST	SOUTH-EAST	
CAINOZOIC	Quaternary	Holocene	Fluviatile, lacustrine and eolian mantle rocks		M	M	M	M	M	
		Pleistocene		Jafr = Azraq	Ja Az		Az		Ja	
			Volcanics	Basalts	v			v		
	Tertiary	Pliocene		Sirhan = Dana	Si Da		Si		Da	Si
		Miocene	Volcanics	Basalts	v					
		Oligocene								
		Eocene			Wadi Shallala	B5	B5	B5		B5
		Paleocene	Belqa	Rijam	B4		B4	B4		B4
	Maestrichtian	Muwaqqar		B3	B3	B3	B3	B3		
	MESOZOIC	Upper Cretaceous	Campanian	Amman	B2	B2	B2	B2	B2	
Santonian			Wadi Gudran	B1	B1	B1	B1	B1		
Turonian			Wadi Sir A7	Fassua A	A7	A7	A7	A7	A7	
Cenomanian			Shuib A5,6		A5,6	A5,6	A5,6	A5,6		
			Hummar A4		A4	A4	A4	A4		
		Fuheis A3	A3	A3	A3	A3				
Naur A1,2		A1,2	A1,2	A1,2	A1,2	A1,2				
Lower Cretaceous		Albian	Kurnub	Subeihi	K2	K2	K2	K2	K2	
		Aptian		Aarda	K1	K1	K1	K1		
		Neocomian								
Jurassic		Zerqa	Azab	Z2	Z2					
Triassic	Main		Z1	Z1						
PALEOZOIC	Permian									
	Carboniferous			cb		Cb				
	Devonian									
	Silurian		Khreim	kh		?		kh		
	Ordovician						kh	kh		
	Cambrian		Disi	D	D	D	D	D		
PRECAMBRIAN	Late Precambrian		Saramuj	s	s ?	s	s	s		
	Early P		Basement Complex	Bc	Bc	Bc	Bc	Bc		

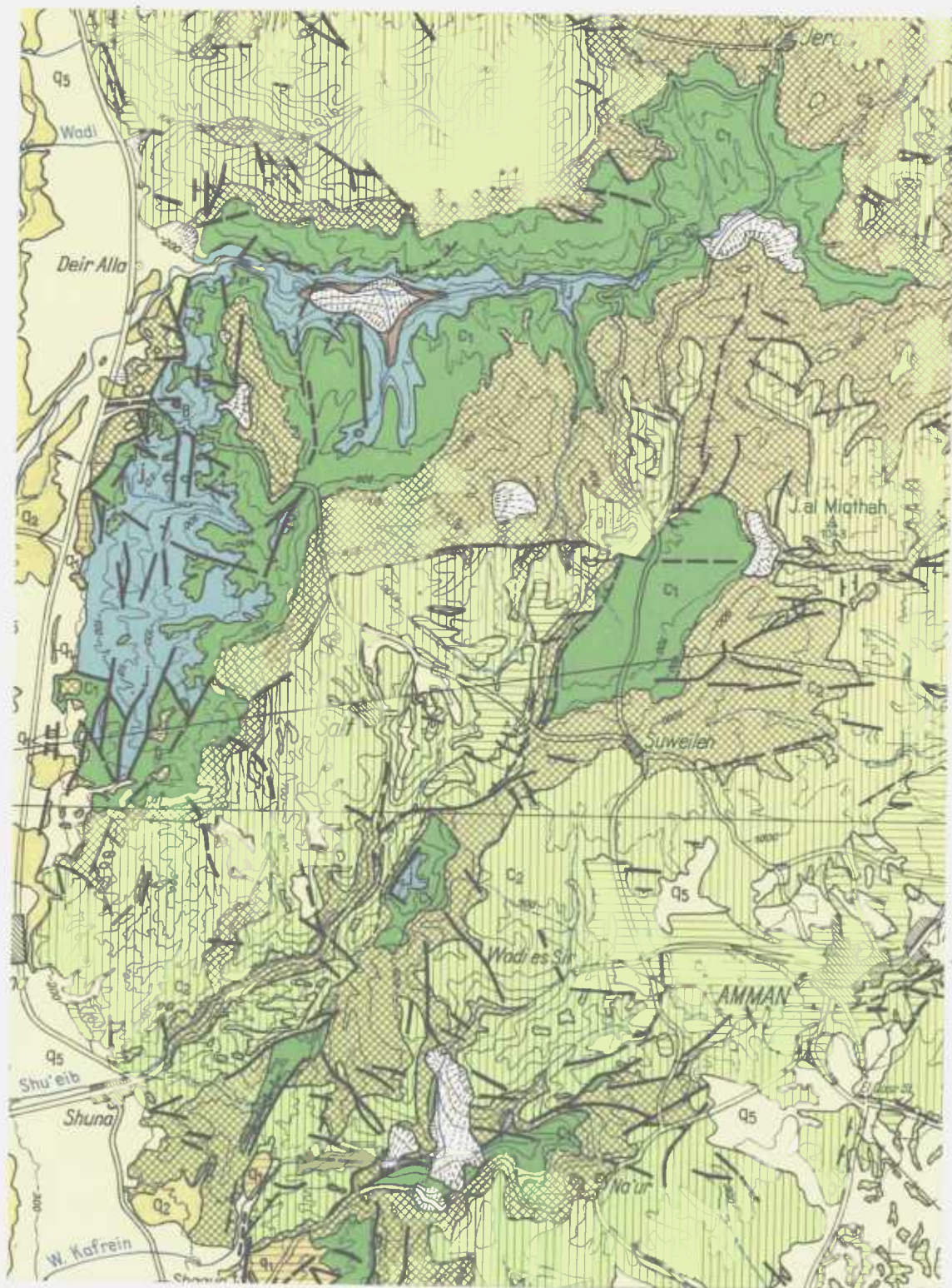
TABLE(2.1) - CORRELATION OF LITHO-STRATIGRAPHIC UNITS RECOGNISED IN EAST JORDAN

only ones exposed in the landslide areas, Fig. 2.1. These are described in detail, while for other rocks only brief descriptions are given.

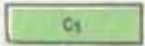
The Pre-Cambrian basement complex consists of granite, diorite, granodiorite and aplite granite. The Pre-Cambrian basement outcrops in the extreme south-western part of Jordan. Above the basement complex arenaceous sediments rest with angular unconformity on the granite rocks and reach a thickness of 1900 m. The sandstone sequence can be separated into approximately 1600m of older Palaeozoic age, succeeded by up to 300 m of sediments of Cretaceous age (Bender, 1969).

The Lower Palaeozoic succession can be divided into about 1000 m of sandstones of Cambrian to Middle Ordovician age, overlain conformably by 600-800 m of sandstones, siltstones and shales of Upper Ordovician to Upper Silurian age.

These Palaeozoic sediments are overlain unconformably by Mesozoic sediments. The lowest Mesozoic sediments consist of sandstones, shales, marls and dolomites. These are overlain by rocks of the Kurnub group of Lower Cretaceous age. The Kurnub group was first described by Shaw (1947). This group extends from the western side of Wadi Araba to the north coast of the Dead Sea and trends towards the east. These sediments



 Q5
Landslides, talus fans

 C1
Argillaceous sandstones, sandy dolomites, sandy limestones, locally limestones and marls, varicoloured sandstones, massive white sandstones

 J
Calcareous sandstones, sandstones, limestones, shales

 C2
Alternating limestones, marls and cherts, coquina, silicified limestones, phosphorites, locally crystalline and bituminous limestones

 C2
E of the graben : In the upper part chalky limestones, marls, cherts, in the SE sandy limestones; thickbedded limestones, dolomitic limestones, marls

 C2
Nodular limestones, clays and marls with gypsum, thickbedded limestones, locally dolomites

GEOLOGICAL MAP OF CENTRAL JORDAN
(involving the study areas)

2500 m

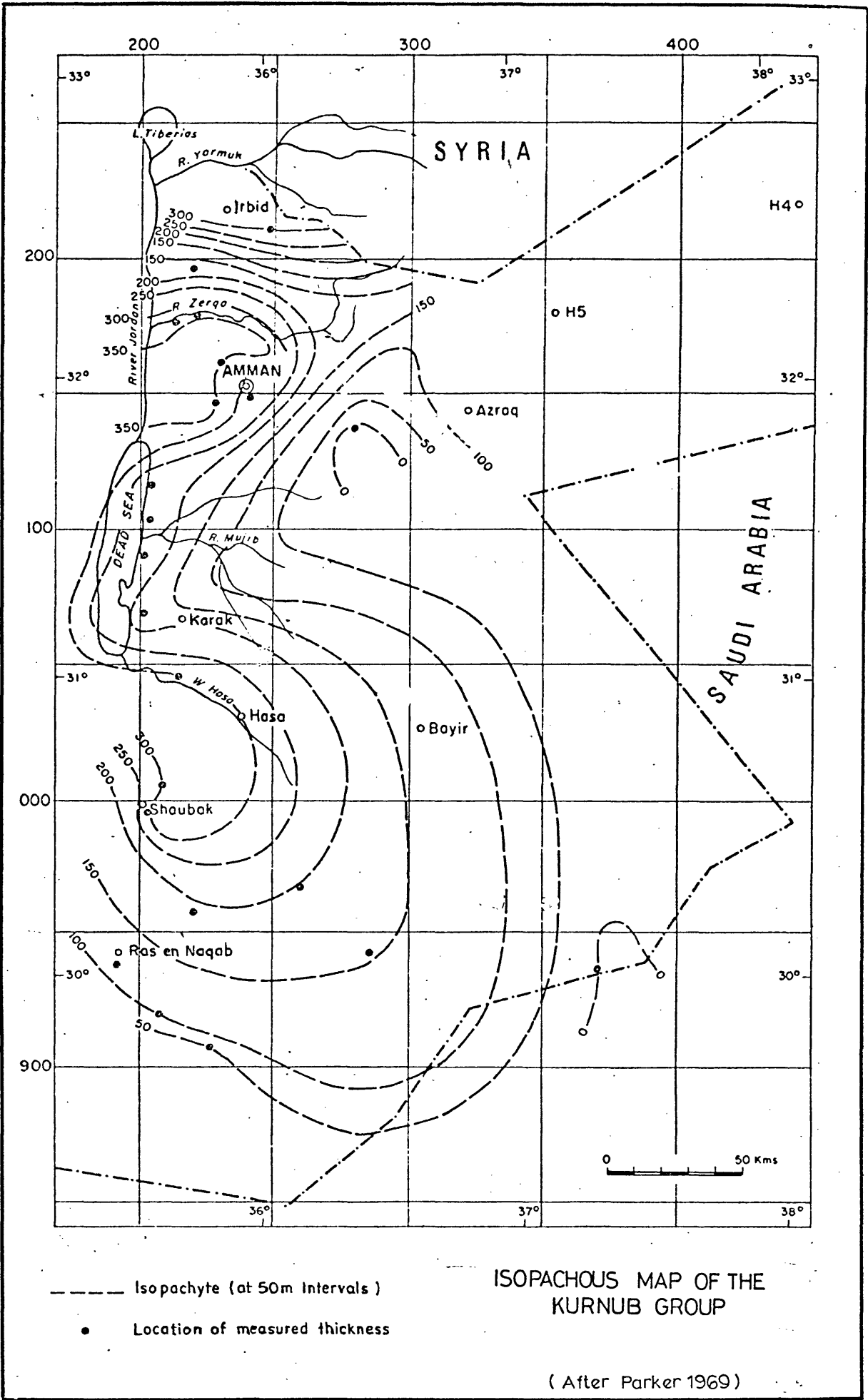
Fig.(21)

After F.Bender

overlie the Bathonian (e.g. Zerqa river, Wetzel and Morton, 1959) 10 to 20 Km further eastwards whilst southwards the Lower Cretaceous sediments unconformably overlie the Triassic. Along the eastern side of the Dead Sea the Wadi Araba to the south, these sediments overlie the Cambrian (Bender, 1965). From the south of the Wadi Araba towards the east along the Ras en-Naqab escarpment the Lower Cretaceous sediments are, from west to east, successively overlying younger Palaeozoic sediments, namely, Cambrian, Lower Ordovician, Upper Ordovician and Silurian (Bender, 1963). These sediments attain a thickness of about 180 m in the south-west of Jordan, but show a gradual decrease in thickness towards the east until they wedge out completely in south eastern Jordan. In northern Jordan the Lower Cretaceous overlies the Jurassic and starts with sandstones intercalated with conglomerates. These are overlain by alternations of silt or marl, coarse to medium grained sandstones with some clay and marl bands up to 140 m thick, yellowish, greenish marls and silty clays. The upper part of this succession consists mainly of vari-coloured sandstones alternating shales, marls, dolomites and calcareous sandstones. The upper contact of the Lower Cretaceous sediments is easily recognized by the lithological change from sandstones to nodular limestones, dolomites and marls. The lower part is predominantly composed of coarse sandstones, cross-bedded pebble bands, and

scattered quartz pebbles. Clay bands are prominent in the upper part only. The uppermost part is characterized by the sandstones with gypsum bands. The top of this group consists mainly of dark grey or green silty clays. In southern Jordan, between Ras-en-Naqab and the Hijaz railway, this sandy silty clay formation ranges up to Cenomanian age (Wiesman, 1966). In general this group consists of Carbonaceous sandstones in the northwest of Jordan and mainly clastic sediments in the south and east. At Ras-en-Naqab the uppermost part of this group is Albian in age, and Turonian at Wadi Araba. The topmost beds become younger from west to east (Bender, 1967). An isopach map (Fig. 2.2) shows that the Kurnub group reaches its maximum thickness west of Amman where the total thickness exceeds 350 m.

The Kurnub group is overlain by the Ajlun group of Upper Cretaceous age (Cenomanian to Turonian). The Ajlun group name was first used by Quennell (1951) for the sediments of the middle section of the Mesozoic succession (i.e. lower part of the Upper Cretaceous). The name Belqa was used for the upper part of the Upper Cretaceous. This name was first used by Sir Murdoch MacDonald and Partners (1965) where they divided the Ajlun group into seven subdivisions in the northwest and east of Jordan and three divisions in western central Jordan. (The correlation of the various lithostratigraphic units is shown in Table 2.2). The Engineering Geology Division of the



Fig(2.2)

Era	Period	Epoch	Quennel (1953) Group	Formation	German Geological Mission Classification (1961 - 1966)	M. MacDonald and Hunting (1965) Classification	Engineering Geological Classification (1971) (S. Saket & A. Tal)	United Nations Sandstone aquifer project classification (1969 - 70)	
Mesozoic	Upper Cretaceous	Campanian Santonian Turonian	Belqa	B ₂	Phosphorite and Silicified limestone unit	B ₂	Silicified limestone unit	Amman	
				B ₁	Massive limestone unit	B ₁	Sand-Marl Unit	Wadi-Ghudran	
		Cenomanian	Ajlun	Upper	Echinoid limestone unit	A ₇	Limestone-Marl Unit	Wadi Sir	Fossua
						A ₆			
						A ₅			
						A ₄			
				Lower	Nodular limestone Unit	A ₃	Marl-Clay Unit	Fuheis	
						A ₂			
		A ₁	Naur						
		Lower Cretaceous		Albian Aptian Neoconian	Kurnub	K	Vari-coloured sandstone unit	Sandstone unit	Subeih
Aarda									

TABLE 2.2

CORRELATION OF STRATIGRAPHIC NOMENCLATURE APPERTAINING TO THE STUDY AREA

N.R.A. (S. Saket and A. Tal, 1970) subdivided this group into two main lithological divisions.

The Ajlun group is generally carbonaceous in the central and northern parts of Jordan, but sandy in the south and southwest of Jordan. The Lower Ajlun group starts with the "marl-clay unit" (A1,2,3) which is well exposed and clearly recognized in the study areas of landslides along Sweileh-Jarash road, the Amman-Naur-Adassiye road, and in the Ras-en-Naqab escarpment area. The thickness of this formation decreases from northern and western Jordan (200-300 m) towards the south (about 86 m at Ras-en-Naqab area). Fig. 5.2 is a columnar and geomorphological section representing the Ajlun group in northern Jordan and Fig. 6.3 represents the situation in southern Jordan at the Ras-en-Naqab escarpment. This decrease in thickness is also accompanied by a relatively slight lithofacies change east and southeast of Ras-en-Naqab. The predominantly calcareous marl facies of the marl-clay unit is largely replaced by sandy clays and sandstones and the change in facies is accompanied by a decrease in thickness until it pinches out completely.

A detailed description of the "marl-clay unit" and its subdivisions is given by Sir Murdoch Macdonald and Partners (1965); this marl-clay formation corresponds to his A1, 2 and A3 subdivisions. The A1, 2 formation is well exposed in the western highlands of Jordan from Ajlun in the north to the east

of Ras-en-Naqab in the south. In the northern part of Jordan along the Amman-Sweileh Jarash highway A1 is mainly composed of clays and marls ranging in thickness from 50-120 m where A2 is composed of limestones and marly limestones between 100-150 m in thickness (Sir Murdoch Macdonald and Partners, 1965). The A1 formation thins towards the south and corresponds lithologically to the marly limestones of A2. The A3 formation also outcrops in the western highlands of Jordan. Wolfart (1959) described this formation in the north of Jordan at Irbid where there are 80 to 90 metres of marls, interbedded with marly limestones and limestones. Sir Murdoch Macdonald & Partners (1965) also described this formation in the northeast of Jordan where 70-80 metres of marls are intercalated with marly limestone which wedges out towards the southeast of Jordan, where it is replaced by a sandy facies. The A1, 2, 3 subdivisions are considered to be Cenomanian in age. As can be seen from the description of Sir Murdoch Macdonald and Partners, and Wolfart the formation is predominantly composed of marls and clays intercalated with marly limestones, limestones, nodular limestones, and dolomites. All the landslides on the Jordanian highways occur within this unit and it is the most critical geological formation from the engineering geology point of view.

Overlying the "marl-clay unit" is a limestone-marl unit which Sir Murdoch Macdonald & Partners (1965) renamed as subdivisions A4, A5, A6 and A7.

The A4 formation is clearly recognized in northern Jordan, while it pinches out southwards (Table 2.1). Masri (1963) recorded a thickness of 65 m at Sweileh and 40 m at Naur consisting of limestones and dolomitic limestones. North of Jarash city the formation consists of 40 m of dolomitic limestones and limestones and marly beds.

The A5, A6 formation outcrops in the western highlands of Jordan from Ajlun in the north to east of Ras-en-Naqab (south), and it occurs at a high elevation in the study areas of landslides. The A5, 6 formations are composed mainly of limestones and marls in approximately equal proportions. The total thickness of A5, 6 ranges from 60 m north of Jarash and 100 m at Naur (Masri, 1963). A5, 6 consists of 60 m of limestones, sandy limestones, marly limestones, marls and dolomitic limestones, with sandstones in the south at Ras-en-Naqab. It thins towards the southeast (Table 2.1).

A7 formation is exposed in the western highlands and consists of medium to thinly bedded limestones with chert nodules alternating with thin bands of cherts. This formation becomes sandy in the south and southwest and wedges out in the southeast of Jordan. Sir M. Macdonald & Partners recorded this formation in north Jordan, where it reaches 215 m in thickness.

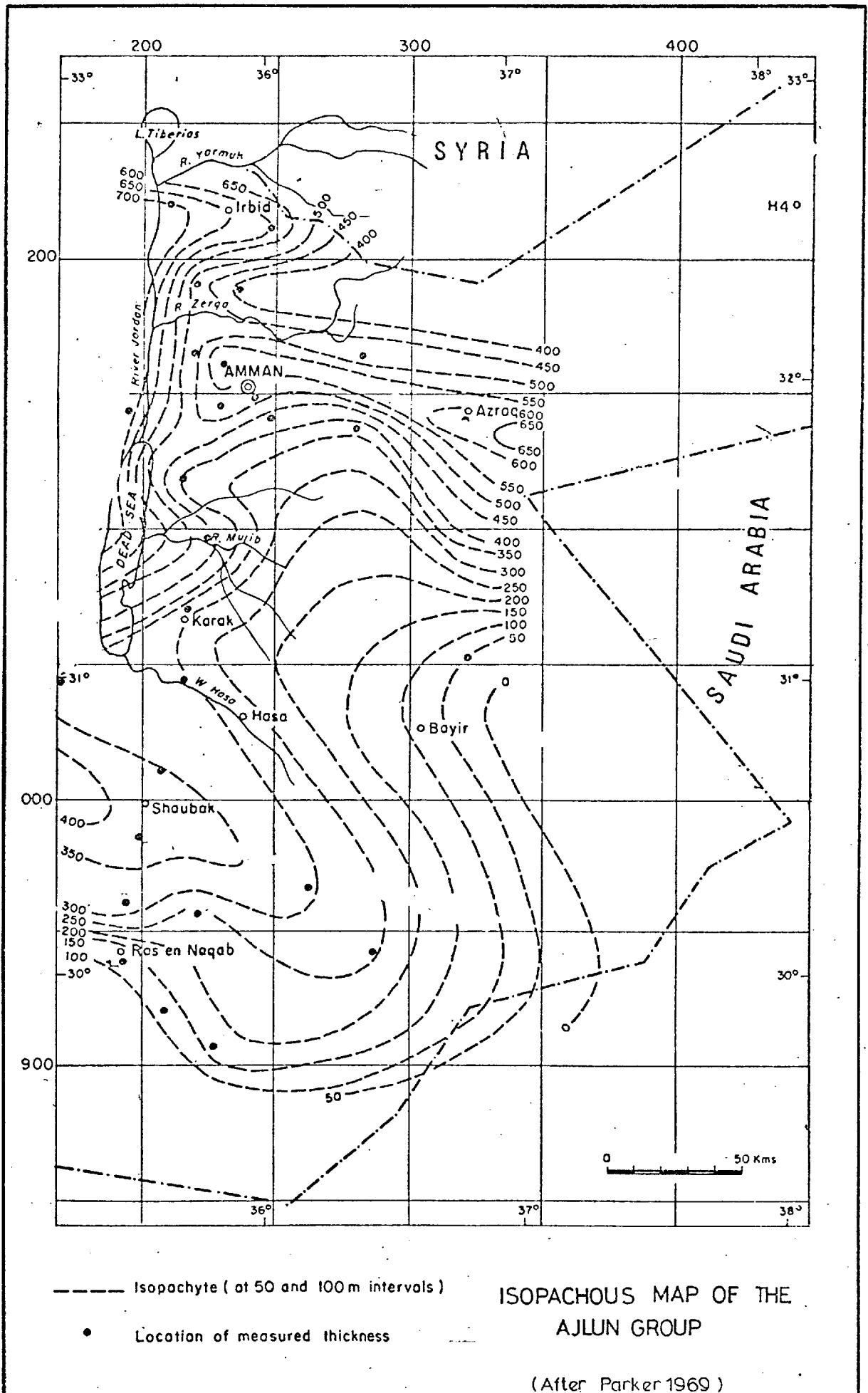
The A7 formation is about 35 m thick at Ras-en-Naqab where it consists of sand, cherty limestones and marls (Fig. 6.3). It pinches out in the southeast of Jordan.

Fig. 2.3 shows an isopach map for the Ajlun group of Jordan. This map shows that the maximum thickness of the group is about 650 m and occurs in the Irbid and Amman areas and thins towards the south of Jordan until it pinches out southeast of Ras-en-Naqab.

The Ajlun group is overlain by the Belqa group of the upper part of the Upper Cretaceous. The lower part of the Belqa group consists mainly of chalky marls, intercalated with marly limestones, while the upper part consists of silicified limestones, chalk, phosphorites interbedded with beds of chert (Santonian-Maestrichtian age).

2.2.2 Structure

The dominant structural features in northern Jordan are the northwest-southeast orientated monoclinial flexures (Amman-Zerqa flexure and Sweileh-Salt flexure). The Sweileh-Jarash road is located at the northern end of this flexure in the Salt block. These flexures are believed to be surface exposures of the existing deep seated faulting associated with



Fig(2.3)

taphrogenesis (Parker, 1968). Small scale folds are observed in the Lower Belqa group and are exposed from the north to the south of Jordan.

According to the dominant type of tectonic deformation, Jordan can be divided into five structural provinces (Bender, 1968):-

1. The Nubian-Arabian shield of southern Jordan.
2. The block-faulted area of eastern Jordan.
3. An area of up-warping, tilting and block faulting in northern Jordan, east of Jordan graben.
4. The Wadi Araba-Jordan graben.
5. An area of up-warping, anticlinorium development and block-faulting west of Jordan graben.

Southern Jordan is situated in the area where the Nubian-Arabian shield is submerging northwards and north-eastwards (De Sitter, 1962).

The extensive east Jordanian limestone plateau exhibits epeirogenetic flat undulations and is cut by several faults with small throws. The structures in the east Jordanian block-faulted areas can be grouped as follows:

a) NW-SE striking normal faults; narrow forst and graben blocks locally bordered by flexures of normal faults grading into flexures.

b) NNW-SSE trending faults with low throws.

Several of these faults intersect the north-westerly trending fault zones particularly in the area adjacent to the graben rim.

c) N to NNE-S to SSW (parallel to the graben) striking antithetic tilted blocks with narrow grabens. These structures, which are parallel to the graben, are rare and are restricted to the east Jordanian limestone plateau which is adjacent to the graben rim.

d) NE-SW striking narrow anticline; in south Jordan about 9 Km north-northwest of Ma'an. Heimbach (1962) described a steep anticlinal structure exposed NNW-SSE striking overthrust faults cutting the central part of the anticline.

e) E-W striking structural transversal elements; in the northern part of the east Jordan block-faulted area Ruef and Jeresat (1965) found three distinctive E-W striking fault zones; each of which was mapped for about 40 Km.

- f) Crypto-Volcanic structures; this type of structure is observed in the eastern area of east Jordanian limestone plateau which is tectonically undisturbed.

The block-faulted area of eastern Jordan gradually passes in a northerly direction into a structural province in which block-faulting occurs more frequently (Bender, 1968). It is assumed that the reason for this is the general increase in thickness in a northerly direction of sediments above the Pre-Cambrian. The tensional forces acting on the thin sedimentary cover above the Pre-Cambrian in the south led to the faulting, whilst the same forces produced block-faulting in the increasingly thicker sedimentary cover towards the north. The most characteristic example of this is the structure of Sweileh, which is a block tilted towards the southeast and extending in a NE-SW direction for over 12 Km. It culminates in a crystal zone of up to 4 Km in width before it is limited in the northwest by a steep NE-SW striking flexure. In the southern part of the flexure the Upper Cretaceous beds are vertical and are also locally overturned. In the central part of this structure, erosion has exposed the weakly cemented Lower Cretaceous sandstones, resulting in the Baqa'a depression.

The main faults and structures which dominate the

Wadi-Araba Jordan graben can be summarized as follows:

1. Commonly trending 180° (towards the north at an acute angle into the graben).
2. Commonly trending $15-25^{\circ}$ (towards the north at an acute angle out of the graben).
3. Often trending $80-100^{\circ}$ (transverse to the graben).
4. Often trending $5-15^{\circ}$ (approximately parallel to the graben).
5. Rarely trending $30-50^{\circ}$.

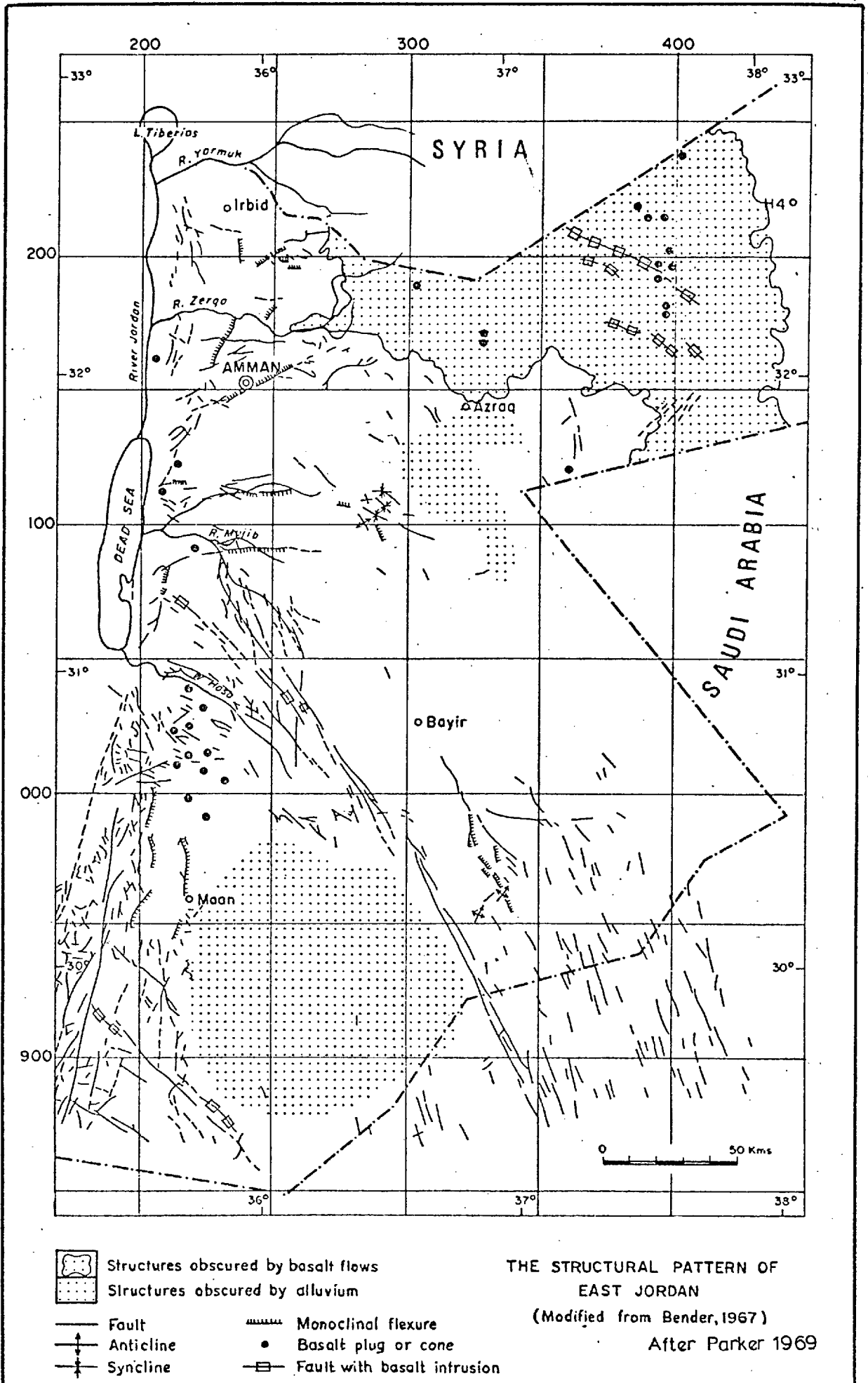
Fig. 2.4 shows the structural pattern of East Jordan.

2.2.3 Pedological soil types

The zonal or normal soils of East Jordan fall into three groups:

- I) Grey Desert soils, developed under arid climate.
- II) Yellow soils, developed under steppe conditions.
- III) Red and yellow Mediterranean soils, developed where the average annual rainfall exceeds 250 mm.

The yellow Mediterranean soils are intermediate between the yellow soils (steppe) and the true red Mediterranean soils.



Fig(2.4)

The Grey Desert soils cover some 50% of East Jordan. They are usually covered by lag-gravels or a desert-pavement of flint or basalt gravel. Lime concretions, leading to limestone crusts, commonly occur. They show a very weak soil development, and closely resemble the parent rock over which they have formed. Erosion removes the soil almost as soon as it forms. The Grey Desert soil is the normal soil in the regions where the average rainfall is less than 150 mm per annum.

The Yellow soils are related to the Brown soils but are more calcareous than typical Brown soils. They develop a compact impermeable surface layer. They are not deep, seldom exceeding 45 cm depth. They are found in the steppe region and in the foothills bordering the rift valley.

The red and yellow Mediterranean soils are confined to areas of higher rainfall; the yellow types form where there is an average annual rainfall of 250 to 350 mm, while the red soils form in areas with more than 350 mm precipitation. The yellow Mediterranean soils are prominent in a rather narrow belt between the cultivated highlands and the steppe area with yellow soils; they also occur on the slopes towards the rift valley and its tributaries. The red Mediterranean soil of East Jordan is higher in free CaCO_3 , as compared with somewhat

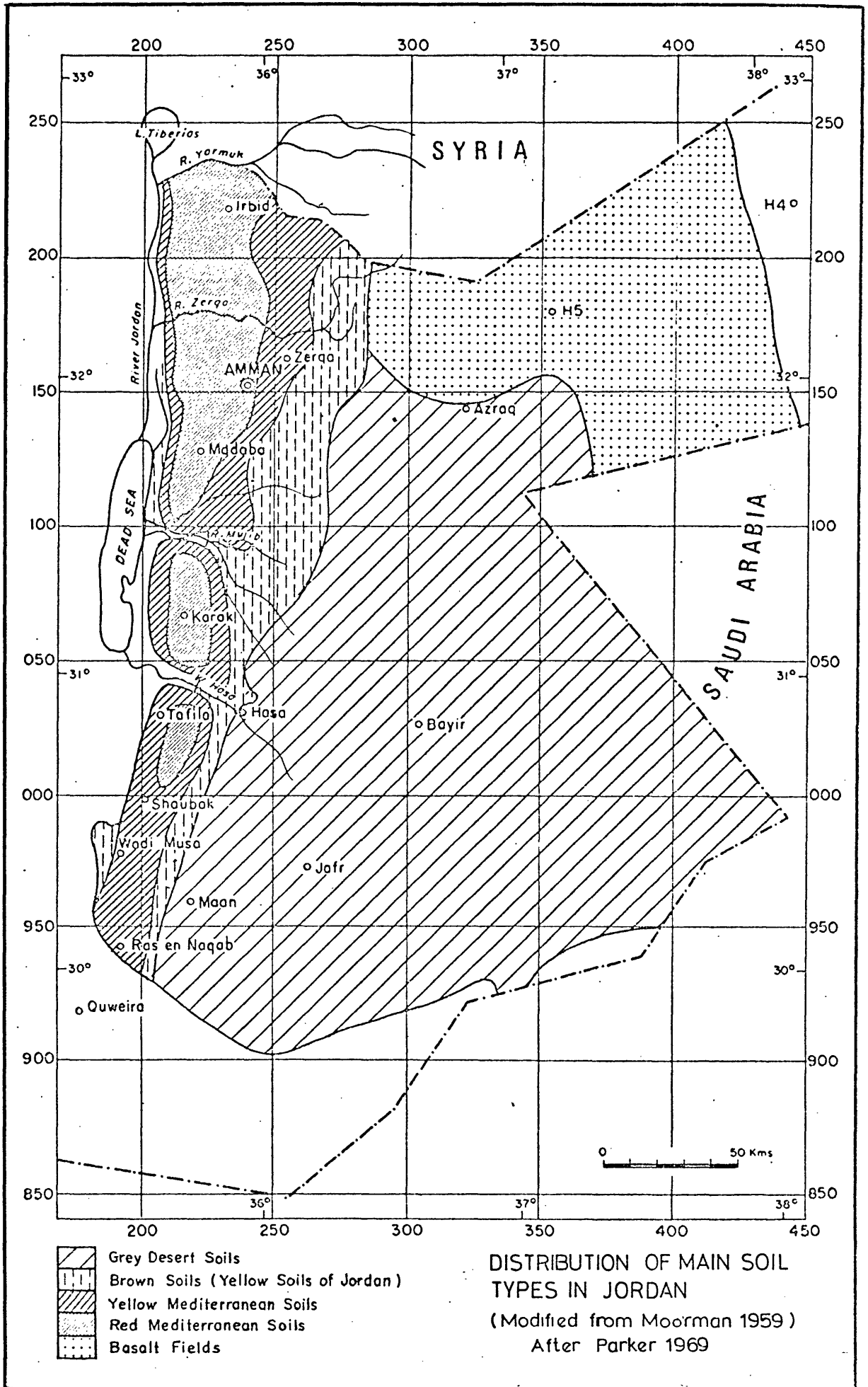
similar soils in the western part of the Mediterranean Basin. These red Mediterranean soils are predominant in the areas of higher rainfall. They are often quite deep, extending to 120 cm, and can hold much moisture; they are usually rich in potassium. The red-yellow Mediterranean soils are dominant in the study areas, where they are mainly clays and silty clays with a high percentage of CaCO_3 and are intermixed with rock fragments of limestones and dolomites ranging in size from gravels to boulders. In the northern part of the study areas (near Jarash city) these soils become more sandy.

The distribution of the major soil groups in Jordan is shown in Fig. 2.5.

2.3 CLIMATE

2.3.1 General

A Mediterranean climate prevails in the highlands from altitudes to a level 700 m higher than the valley floor, and in the mountain chains east of the Dead Sea and in the Wadi Araba as far south as Shoubak. This climate has, from April until October, a dry summer with an average maximum temperature of 38°C and from November until March having an average minimum temperature of 1° with an annual rainfall of more than 30 mm.



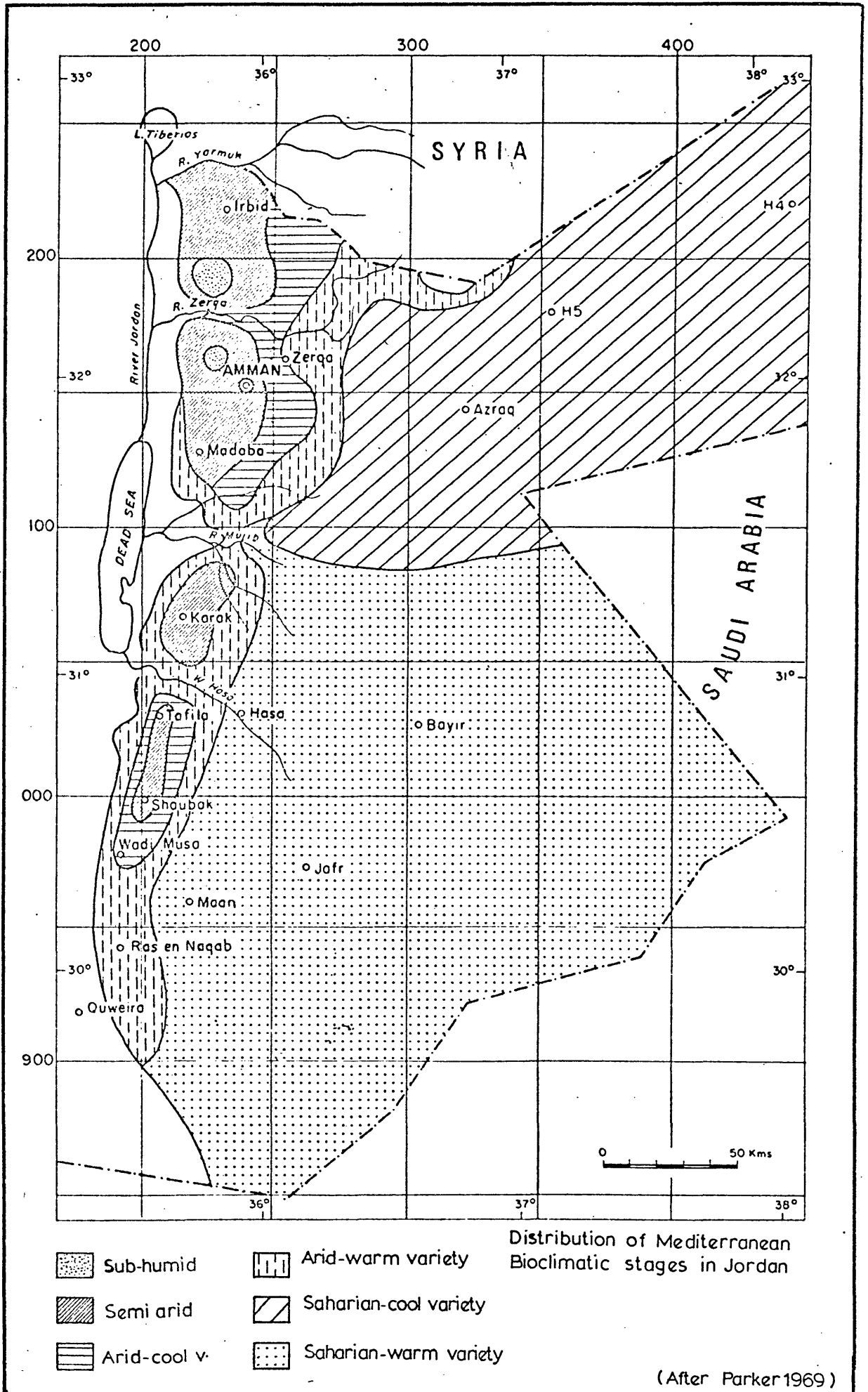
Fig(2.5)

East and south of the areas with a Mediterranean climate there is a wide transition zone to the arid climate which characterizes the desert areas of eastern and southern Jordan. In this semi-arid transition zone the average annual rainfall is between 30 to 50 mm. The areas east and south of the semi-arid zone, as well as the narrow area within the Wadi Araba, which extends northwards from the city of Aqaba (desert areas of Jordan), have an average annual rainfall of less than 50 mm.

Long (1957) subdivided the Mediterranean bioclimate as follows: (distribution is shown in Fig. 2.6).

Mediterranean Bioclimatic Stage	Average Rainfall (mm)	Average Temperature (January)C ^o	Average Max. Temp. (August) C ^o
Sub-humid stage	600	3 ^o	27-33
Semi-arid stage	300-600	3-7 ^o	-
Arid-cool stage	150-300	1-3 ^o	34-40
Arid-warm stage	200-300	3-7 ^o	34-40
Saharian-cool variety	25-150	1-3 ^o	36-42
Saharian-warm variety	25-150	3-8 ^o	36-42

The investigated landslide areas are located within a semi-arid and arid-cool variety, while the Ras-en-Naqab areas lies within the arid-warm variety (Fig. 2.6).



Fig(2.6)

2.3.2 Rainfall

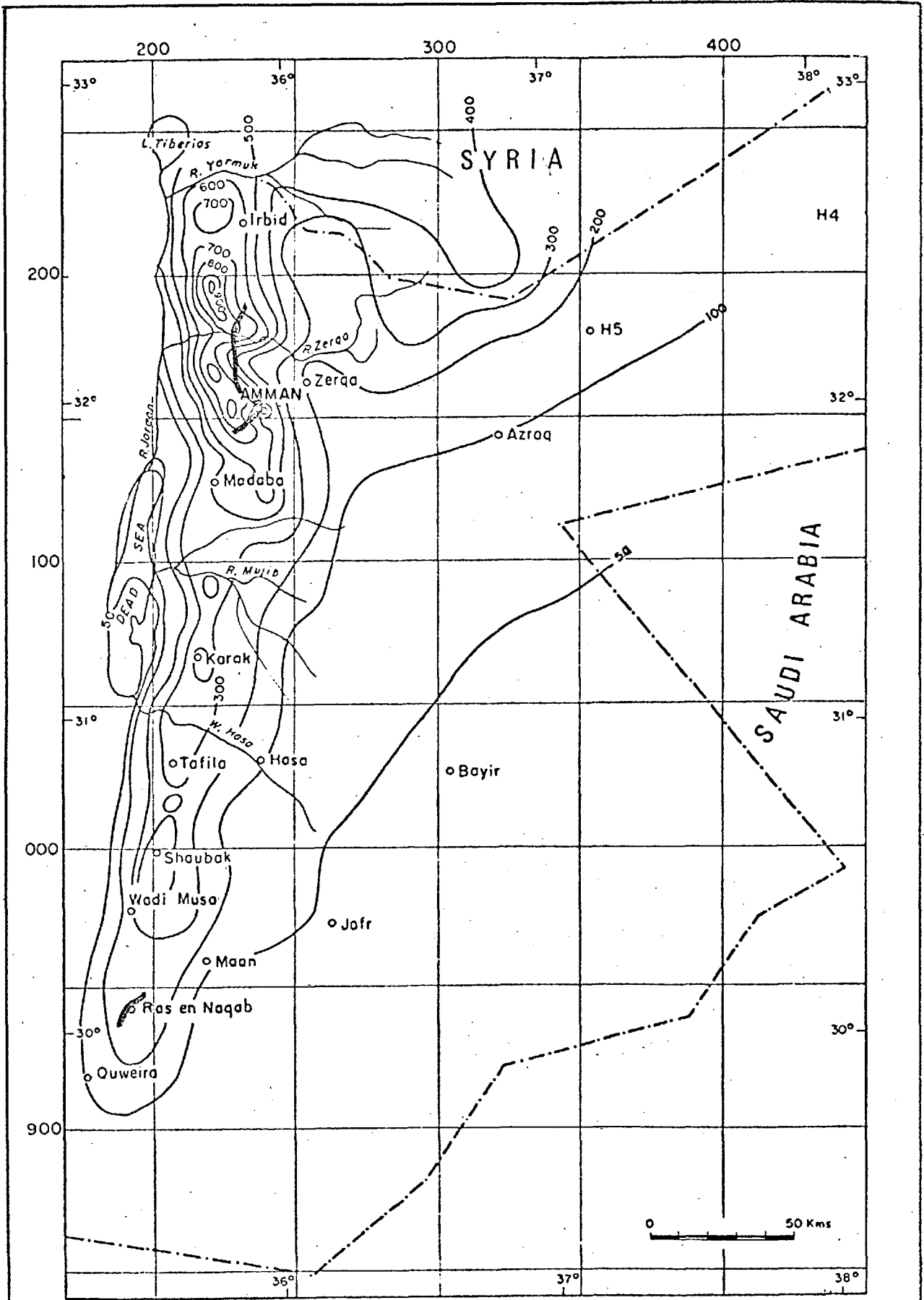
As previously stated, Jordan has an arid to semi-arid climate; warm and dry in summer, with a mild rainy winter. The Mediterranean-type climate prevails in the area.

The average annual rainfall in the main regions is as follows:-

Eastern highlands of Jordan River:	600-800 mm
Sweileh-Ajlun region:	600 mm
Amman area:	300 mm
Eastern and southern desert:	50 mm

The highest annual rainfalls recorded in the highlands of Jordan are 664 mm and 653 mm at Ajlun and Salt Stations, while the deep wadis which separate these mountains and the central plateau have a much lower rainfall. Rainfall is mainly concentrated in the months between October to May with most rain falling in the period from December to March. The eastern limit of the western highlands is characterized by 200 mm isohyets where the mean annual rainfall is less than 100 mm in the central plateau.

Fig. 2.7 shows that the average annual rainfall decreases rapidly westwards from the western highlands into the Jordan valley and eastward of these highlands to less than 100 mm in the Azraq area and less than 50 mm in the Bayer area.



DISTRIBUTION OF RAINFALL
(1966-67)

(After Parker 1969)

Fig(2.7)

South of the Dead Sea at Wadi Araba is less than 50 mm, while there is an increase to 400 mm near Lake Tiberias in North Jordan.

As can be seen from the isohyet map (Fig.2.7), the Sweileh-Jarash road, and the Naur-Adassiye road both lie within the high precipitation range of more than 400 mm, while the Ras-en-Naqab area lies in the region with very low annual precipitation of 100 mm.

The monthly rainfall varies very widely from year to year; Figs. 4.1, 5.7 and Table 6.1 show the monthly precipitation at three stations along the Naur-Adassiye road, Sweileh-Jarash road, and in the Ras-en-Naqab area.

According to Sir. M. Macdonald et al, 50% of the rainfall in the northern part of the western highlands falls in the periods of continuous rainfall of less than 12 hours. These storms comprise 80 percent periods of continuous rain. A rainfall of 35 mm in 20 minutes was recorded at Salt on 23rd November, 1968. This represents an intensity of 105 mm/hr and has been calculated to be a 50-year event; on the 11th March, 1966 36 mm of rainfall at Shoubak fell in 45 minutes and this storm was associated with a large flood which destroyed part of Ma'an city.

Relative humidities are of the order of 75% in the winter and 35% in the summer. In the Jordan valley the corresponding figures are 70% and 40% (D. Burden, 1959). Ionides and Blake (1939) gave the following average infiltration figures: the spring supply expressed as a percentage of the total rainfall is 7.4% for the northern region, 3.5% for the central region, and 5.1% for the southern region.

2.4 GROUND WATER HYDROLOGY

Precipitation in Jordan is restricted to the period between May and October and is insufficient to meet the great need for water throughout the country, so the groundwater is the most valuable natural resource. The rainwater penetrates through the intensely jointed bedrock and perches on the impermeable strata of clay and marl. Therefore the geology and structure controls the direction in which the percolated water will move underground through the aquifers. According to Quennell (1959) not more than 15% of the precipitation reaches and recharges the aquifers; for much of the country the recharge figures are of the order of 5 to 10%. Where the rainfall is less than 200 mm, it is probable that there is not much direct infiltration down to the permanent groundwater table.

The Kurnub, Ajlun and Belqa groups and the weathered zone of soils are mainly covering the study areas. The highly jointed Ajlun rocks have the largest aerial extent in the areas of landslides but the Belqa group has the largest aerial extent in the whole of Jordan. Groundwater occurs mainly in these jointed limestones and cherts and also in the lower sandstones. The recharge is restricted to the winter months.

As previously noted, most of the landslides are located within the A1, 2 formation of the Lower Ajlun group. This formation outcrops on the lower slopes of the rift escarpment and mainly in the deep incised wadis from near Wadi Zerqa southwards to the vicinity of Ras-en-Naqab (Parker, 1969). It is believed that no permanent groundwater exists within the landslide areas, but it is probable that the watertable rises very quickly during a heavy rainstorm, owing to the significant fracturing in the cap rock and the related structural deformation of these rocks, tending to rapid drawdown shortly after this period of rainfall. The springs in the study areas represent the visible discharge from the aquifers; they cease very soon after the winter season, indicating the limited extent of aquifers.

According to the hydrogeological classification the following formations are regarded as the best aquifers: B3, B2, A7 and the Lower Kurnub group.

Regionally the aquifers within the Ajlun group are also considered the most important, due to the presence of impervious layers such as marls and clays alternating with layers of highly jointed limestones and dolomites. The A7, A4 may be considered reasonably good aquifers and permeable to flow parallel to the strata, while A1, 2, A3 and A5, 6 are impervious aquicludes preventing further downward migration of the groundwater and forcing it to issue as surface springs. Most of the springs observed in the study areas are discharging either from these formations or through fault lines.

Owing to the presence of faults in the study areas it is probable that a vertical leakage of water through these faults from the considered aquifers within A1, 2 formation probably leads to recharge of the Kurnub sandstone aquifers. The lower part of the A1, 2 formation is mainly clayey and marly and it forms the confining layer which separates the aquifers within this formation from the aquifers within the Kurnub Group formation.

The lower part of the Kurnub Group is considered to be a good aquifer. In the southern part of Jordan, particularly in the study area, the rain is too light to produce any appreciable infiltration, no permanent groundwater body has been developed. Very small springs discharge temporarily

through fault lines. In the northern part of Jordan many springs are observed discharging from the Lower Kurnub Group, e.g. in Wadi Zerqa area and near Sweileh.

The B2 and B3 units of the Belqa Group are also considered to be good aquifers but aquicludes within this group are present. The Eocene, Palaeocene, Danian, Maestrichtian formations are considered to be aquicludes.

CHAPTER THREE

METHODOLOGY

INTRODUCTION

This chapter deals with the various types of both field and laboratory techniques applicable to the study of landslides and outlines the various slope stability analysis methods which have been used.

3.1 INVESTIGATION TECHNIQUES FOR LANDSLIDES

Before adequate remedial measures for a landslide can be prepared, there must first be a carefully planned field and laboratory investigation of the geological materials involved followed by an appropriate slope stability analysis. In general these investigations would proceed in the following broad stages:-

- 3.1.1 Application of field techniques.
- 3.1.2 Application of laboratory techniques.
- 3.1.3 Appraisal of the problems followed by stability analysis.

3.1.1 Field Techniques

Adequate field investigations of a landslide should reveal details of both surface and subsurface geological structure and the morphological history of the area. The required steps in a full field investigation may be summarized as follows:-

a. Topographic mapping:-

- i) topographic surveying,
- ii) aerial surveying.

b. Geological mapping:-

- i) regional small scale geological mapping,
- ii) regional landslide mapping,
- iii) local large scale geological mapping,
- iv) individual landslide mapping.

c. Observation, identification and recording:-

- i) photographs,
- ii) surface and subsurface displacements or movement indicators.

d. Exploratory drilling and excavation:-

- i) trial pits and trenches,
- ii) boreholes.

e. Geophysical surveys:-

- i) resistivity soundings,
- ii) seismic refraction survey.

d. Sampling:-

- i) disturbed,
- ii) undisturbed.

Each of these is described below.

a. Topographic mapping:

The first stage of the field investigations should be a topographical survey of the study area on scales of at least 1:1,000 or 1:5,000 or larger with two metre contour intervals. The main features of the movement should be shown, e.g. the main scarp, crown, toe and limiting flanks.

Cross sections through the landslide before and after movements should be prepared for comparison. The cross sections should be of sufficient length to include the area above and below the landslides.

Surveying makes it possible to determine the amount of movement and the limits of the displaced mass and is of great help in the geological investigations.

Aerial photographs provide a three-dimensional view of the landslide area, making it possible to determine the boundaries of the landslide and formulate ideas on the morphologic history of the slope. Comparison with older photographs is particularly useful.

On an aerial photograph the landslide appears as an irregularly undulating area with many minor scarps and depressions. The vegetative cover also acts as an indicator of movement; for example, the trees within the upper part of the landslide are tilted backward indicative of the recent sliding and the direction of the movement (Fig. 5.23, and Plate 5.10).

b. Geological mapping:

Detailed regional geological mapping of the study areas on a scale of 1:25,000 is necessary to illustrate the relation of landslide occurrence to geology. General features of the landslide should be plotted on the same map. Each study area should be mapped geologically on scales of 1:1,000 to 1:5,000 to show the relationship of the disturbed mass to the undisturbed surrounding area. This should be supplemented by individual mapping of each landslide in more detail on a scale of 1:1,000. These maps should show the main features of the movement, location of exploratory pits and boreholes and should be accompanied by geological cross sections including the undisturbed areas above and below the slide.

The regional geological mapping may help to establish regional factors that are contributing to instability.

c. Observation, identification and recording:

Regional observations and recognition of different

types of instability primarily require experience combined with a broad knowledge of the local and regional geology. Identification and classification of the problems of instability is related to type and causes; this again needs a broad knowledge of engineering geology combined with both soil and rock mechanics. Following the identification of the different problems it is essential to obtain a photographic record of the area, and to establish movement indicators to check for both horizontal and vertical movements. Joint separation surveying can also be useful as the joints are sensitive movement indicators.

d. Exploratory drilling:

The most commonly used methods for subsurface investigations of a landslide area are trial pits, trenches, auger borings and boreholes. The purpose of using these methods is to determine the geological, physical and mineralogical characteristics of the slipped mass and the underlying undisturbed strata as well as the location of the failure surface and observation of water table conditions. The first three methods are useful for shallow exploration and sampling where the bedrock is covered by a thin mantle of overburden. Trenches provide a continuous exposure of the ground and have an advantage of permitting visual examination of the undisturbed materials in situ. Trial pits also afford the most complete information of the ground penetrated. Pits of 1.5 x 1.5 m plan

size were excavated, the depth of these pits depending on the information required and on the type of materials involved; in the study areas the depth of these pits ranged from 0.5 to 3 m. Most of these were excavated manually but a few were carried out by machine excavators of the Ministry of Public Works. In the hand-dug pits the excavated materials are removed from the hole by buckets; the pits were dug at the rate of 1 metre depth/day.

Hand operated 4" to 12" diameter augers with helical and Iwan Auger blades were used at this stage of exploration. The depth of this type of boring is limited by the amount of the coarse fraction and boulders included in the excavated material

Rotary drilling is the most important and most useful method for exploratory investigations of landslides in rock materials. It serves a number of purposes:-

1. Provides core samples and soil samples for laboratory investigations.
2. Cores may be obtained for subsurface joint surveys in order to study the structural deformation of the strata. The relationship between the percentage of core recovery and drilling can provide useful qualitative information on the amount of structural distortion in the ground.

3. Location of the surface of rupture. The surface of rupture may be located by the following means:-
 - a. Observation (in the case of uniform lithology).
 - b. Fabric studies (in the case of uniform lithologies, the disturbance and the water content in argillaceous materials in the slipped mass is higher than in the part below the slide mass).
 - c. Water content determination: the water content in stiff clays increases near to the surface of rupture and decreases below it.
4. Determining the geological characteristics and the relative positions of the slipped mass and the underlying undisturbed strata.
5. The boreholes may also be used for the observation of groundwater conditions.

After detailed regional and local studies of landslide areas and the proposed routes of highways had indicated the importance of the study, the Ministry of Public Works approved the use of their drilling equipment for the study. The Ministry also gave a contractor* the opportunity to redesign the highway between Ramtha and Jerusalem. It was recommended that a seismic refraction survey be carried out and several boreholes

* Araby Consulting Engineering Office and Partners.

should be drilled.

The "Longyear" drill rig 24-Wolverine type of the Mineral Resources Division* was used in the exploratory stage. This rig was supplied with hydraulic feed, gives any of four feed speeds. The bit speeds range between 350-1500 rpm. The Ministry of Public Works equipment used was "Porta-drill" type consisting of a rotary drilling rig provided with single and double tube core barrels with diamond and carbide bits with hydraulic feed. This rig was capable of drilling to a depth of 300 m. The type of bit to be used was determined by the type of materials to be penetrated. The drill rig was provided with a winch for hoisting and lowering the drill rods, and a pump for circulating water to the bit. The pump had an associated water meter and pressure gauges. A few boreholes were drilled using air flush so that changes in water content with depth could be determined.

During the coring, minimum downward pressures of about 3 to 4 Kg/cm² in the clay layers and about 6-8 Kg/cm² in the limestones and convenient rotation speed of approximately 500 revolutions per minute were maintained. These parameters varied according to the bit used and the type of rock being penetrated. After completion of each drive, the rods and core barrel are withdrawn, care being taken to avoid any disturbance.

* Natural Resources Authority, Amman.

Typically only a small amount of flushed materials were obtained during the drilling due to the loss of circulation. Water to be used in the drilling process had to be brought to the site in private tanks.

Many difficulties were met during the drilling due to:-
(i) the inexperience of the drillers, (ii) structural disturbance of the strata, (iii) loss of circulation of water.

Drilling rate and percentage of core recovery were recorded during the drilling. Beside recording information on the character and composition of the materials present, information on the spacing and tightness of the joints and other structural details were noted.

Generally the recovered cores from the landslide mass were intensely broken as small fragments while the cores obtained from the underlying disturbed bedrock were slightly disturbed. The percentage of core recovery was between 0-50% from the displaced mass and between 80-100% from the underlying bedrock. Typical borehole logs are presented in Fig. 6.4.

e. Geophysical surveys:

Two geophysical methods were used in this stage of the field investigations: (i) resistivity sounding, and (ii) seismic refraction.

The resistivity method was used, and checked by drilling, to establish information concerning the subsurface structure of the study areas. In this study, carbon direct current resistivity instrument* was used with a Schlumberger configuration. The potential difference between two inner points and the current in the primary circuit were observed. The potential difference and the current were multiplied by a factor depending on electrode spacing to provide the resistivity of the materials encountered. The measurements were made in the usual manner with a fixed central point and progressive increasing of the electrode separation (Fig. 3.1). By carrying a large number of resistivity soundings at different distances it was possible to establish profiles of the study areas. The resistivity curves obtained were interpreted by utilizing two or three layers of master curves (Mooney, H.R. and Welzed, W.W., 1956). Owing to the amount of structural disturbance of the strata in the landslide areas, it was very difficult to always obtain a fair match, so interpretation between curves was used.

However, it was possible to differentiate between the layers in the light of their different electrical resistivities using some borehole control. It is worth mentioning that the resistivity in general changes considerably from place to place

* The equipment was used by I. Hasan and calculations by A. Rishesh (N.R.A.). Interpretations by the author.

according to electrical conductivity of the strata which depends on many significant factors such as the amount of water present, the manner of water distribution within the rock, the salinity of water, the amount of jointing in the strata, etc. The range of resistivities of the materials involved in the study areas were:-

<u>Mantle</u>	<u>Marl and Clay</u>	<u>Silty Clay</u>	<u>Sand and Silty Clay</u>	<u>Limestone</u>	<u>Sandstone</u>
4-34 Ω m	30-80 Ω m	48-60 Ω m	60-94 Ω m	> 90 Ω m	\approx 95 Ω m

a = electrode separation

C = current electrode

P = potential electrode

$$\text{Resistivity} = \left(2\pi a \frac{V}{I} \right) \Omega \text{ m}$$

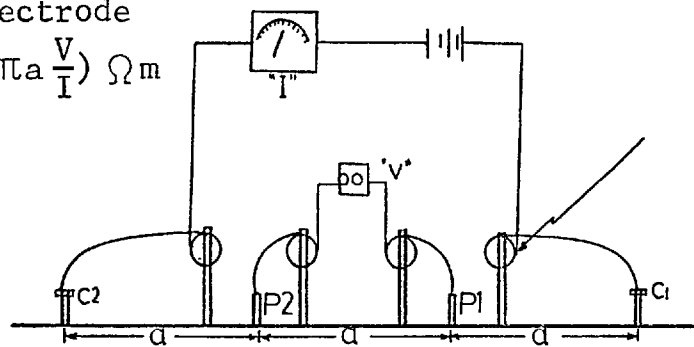


Figure 3.1

The seismic refraction method was applied in order to determine the depth of the horizontal and nearly horizontal formation boundaries. Generally this method would be used to:-

1. Determine the depth to the undisturbed strata.
2. Provide an estimate of the structure of the soil units overlying bedrocks.
3. Detect the thickness of the disturbed bedrock displaced.
4. Differentiate between the looser near-surface material of the underlying natural formation.

A seismograph which utilizes a blow of a sledge hammer on the ground was used as a source of seismic wave energy. Seismic wave travel time, from the striking point on the ground surface to the geophone (placed at a measured distance from the strike point) is recorded by a seismic timer and detected by series of small electric lights on the timer linked in a binary counting system. Travel times for the first arrivals were recorded along the profile using a 2 or 3 m hammer point spacing. The true velocities and depth of the refracting formations were determined from the variation of the travel time with distance. Owing to the amount of structural distortion of the strata involved in the landslide masses, scattered readings were obtained and interpretations were made for the best fit lines through these scattered readings. However, the undisturbed bedrock underlying the moved mass was clearly detected from the time-distance graphs. The method was found useful for landslide investigation correlating well with other field methods. The average velocities of the formations existing in the study areas were:-

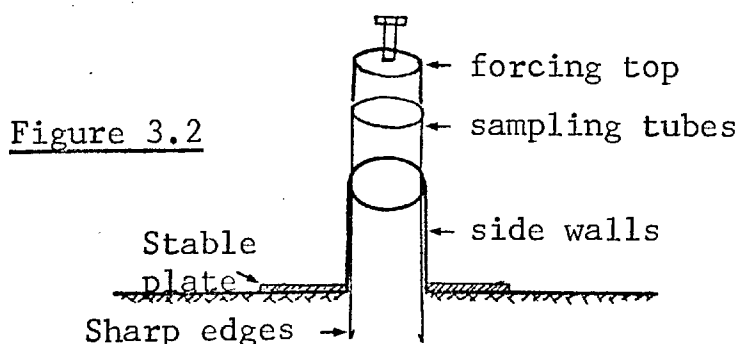
<u>Mantle</u>	<u>Clay and Marl</u>	<u>Silty Clay</u>	<u>Silty Sandy Clay</u>	<u>Limestone</u>	<u>Sandstone</u>
325-800 m/s	1000-2500 m/s	800-1200 m/s	≈2000 m/s.	3700-9000 m/s	≈2000 m/s

f. Sampling:

Following the exploratory drilling, samples were selected from the disturbed and undisturbed samples obtained from: (i) core drilling, (ii) auger boring, (iii) open drive tube samples, (iv) bulk block sampling from trenches and trial pits.

Core drilling and auger boring were the most useful for obtaining disturbed samples, but it was difficult and sometimes impossible to obtain undisturbed samples from the boreholes owing to the disturbed ground conditions.

The open drive tube sampling was successfully used for obtaining undisturbed samples close to ground surface at a depth of 0.5-3 m. The procedure adapted was to force the 4" x 6" thin walled tube with sharpened edges by loading or hammering carefully, without any rotation, very slowly into the soil followed by withdrawal and extruding the obtained sample from the tube. This tube was used with a plate and sidewall restraint so that it could be kept vertical (Fig. 3.2). Samples were waxed immediately after removal from the ground.



The hand cut block sampling was also used to obtain 10" x 10" x 10" samples from accessible excavation. A sample was excavated using trimming and cutting knives and then placed in a wooden or tin containers made to snugly fit the block sample. The block samples were also waxed immediately after removal from the ground.

3.1.2 Laboratory techniques

The physical, mechanical properties and chemical composition of the geological materials are the main factors influencing stability and their evaluation is essential for determining the remedial measures. A full laboratory testing programme was devised and performed on disturbed and undisturbed samples obtained from the study areas, to establish the engineering properties of the clays involved. The following tests were performed:-

1. Density and natural water content.
2. Specific gravity.
3. Grain size analysis.
4. Atterberg limits.
5. Maximum water absorption.
6. Total soluble salts.
7. Triaxial compression tests.
8. Direct shear tests.
9. Complete chemical analysis.
10. Differential diffraction analysis.

11. X-ray diffraction analysis.
12. Cation exchange capacities.

The above tests were carried out following the detailed procedures given in international standards such as ASTM, BSI, USBR and German standards. A summary of the main specifications of the various tests is presented here according to the standard used.

The density used in this study is the natural bulk density and moisture content as exists in the natural deposit. Bulk density is determined according to the Unified Soil Classification System* (U.S.C.S.) designation E24 which is similar to B.S. 1377, and it was also determined by obtaining undisturbed samples with a steel box of a known volume according to B.S. 1377. The specific gravity used in this study is the absolute specific gravity obtained by using the flask method. The value obtained is the highest for a given soil. Specific gravity was performed according to the U.S.C.S. D-10. The particle size analyses were made following the U.S.C.S. designation E-6 which is similar to the A.S.T.M. designation D.422-54T, and B.S. 1377, test 7. The principal difference is in sieve sizes used and the separation on the No. 4 instead of the No. 10 seive of the A.S.T.M. and 200 of B.S. sieves for the hydrometer

* The system (U.S.C.S.) was developed jointly by the U.S.S.R. and Corps of Engineers and Dept. of Army from a system proposed by Casagrande.

test, where the readings were made at time intervals of 1, 4, 19, 60, 7 hours 15 minutes and 24 hours 45 minutes.

The Atterberg limits were determined according to U.S.C.S. designation E.7 which is similar to the A.S.T.M. designation D.423-54T and B.S. 1377, tests 2; 3, 4. The principal difference is the seive size; no. 40 was used instead of the no. 36 of B.S. 1377. The results were plotted on the Casagrande plasticity chart.

The total soluble salts test was performed to determine the quantity of soluble salts in water present in the soil. This is a very important factor when considering the suitability of the soil for constructing embankments or in the arid regions when considering the type of cement to be used in constructing concrete structures in contact with the soil or when considering slope stability analysis. The amount of salt present in the soil affects very much the strength parameters, thus the stability analysis.

The method used for determining total soluble salts was that described in U.S.C.S. designation E.8 and outlined below.

An oven dried 200 g sample passing no. 4 seive is placed in a glass vessel with 2 litres of distilled water,

giving a soil to water ratio of 1:10. The suspension is agitated for a few minutes four or five times a day for at least 4 days. The mixture is then allowed to stand until the liquid becomes clear. 200 cc of the clear liquid is placed in a weighed evaporating dish and evaporated off until the solids' residue reaches a constant weight in an oven kept at 110°C. The weight of solids residue shall be determined. If the salt concentration is greater than 2000 ppm, a 1:50 soil to water ratio shall be used.

$$C = \frac{W \times 10^6}{V}, \quad \text{where } C = \text{soluble constituents in ppm.}$$

$$P = \frac{C - D}{10^4}, \quad W = \text{weight of residue in grams.}$$

$$V = \text{volume of filtrate in cm}^3.$$

P = percentage of soluble constituents by dry weight.

D = dilution of soil-water mixture if (1:5 D = 5).

In general, soluble salts are those which hydrate easily under atmospheric conditions, such as sulphates, chlorides and carbonates. The critical quantity is 0.5% of NaCl for sandy clay soils; if the chlorides content is below this limit, then there are no deleterious effects (H. Weinert and K. Klaus).

It is worth mentioning that the soluble salts are a common cause of the physical disintegration of rocks in arid

areas, causing failure of structures and leading to instability of compacted subgrade materials. The leaching of salts reduces the shear strength of the clay and can result in high sensitivity. Skempton and Northey have shown that leaching to reduce the salts concentration in the pore water by one-half can lead to the sensitivity being nearly doubled and as the liquid limit falls and the liquidity index increases. Some of the soils on the Jordanian highways show a very high soluble salts, rendering them susceptible to leaching and possible reduction of shear strength, thus leading to problems of instability.

The maximum water absorption test was performed according to the German Standards using the simplified German apparatus shown in Fig. 3.3.

The apparatus consists of a calibrated burette (A) and glass cone (B) provided with a filter stone (C) placed at the bottom of the cone and in touch with the top of the calibrated burette. This burette was filled completely with water without any air bubbles. An air-dried soil sample finer than 0.15 mm is placed in the glass cone above the filter stone in a pyramidal shape so that the largest area of the soil comes into contact with the water. Immediately after

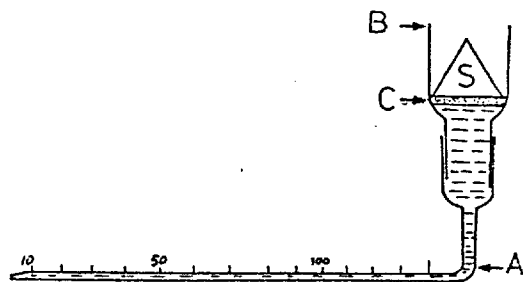


Figure 3.3

placing the sample the calibrated burette was read every two minutes until no more absorption took place. The last reading is the maximum water absorption of that material. The maximum water absorption gives some indication of the type and properties of the clay tested, e.g. montmorillonite comes to equilibrium at a higher water content than Na-montmorillonite. This of course would affect the stability of the soils. The maximum water absorption of the samples taken from the Jordanian highway is as high as 120%, which indicates the presence of montmorillonite type clays. Other types of clays absorb considerably less water.

The Differential Thermal Analysis* was performed on the representative samples by the standard DTA method which the temperature of the tested soil is measured relative to an adjacent inert material. The basic diagram of the apparatus is shown in Fig. 3.4, where T and S represent test and standard powder samples (≈ 0.5 g) enclosed in small adjacent cells in a sample holder placed in the hot zone of a wire wound furnace.

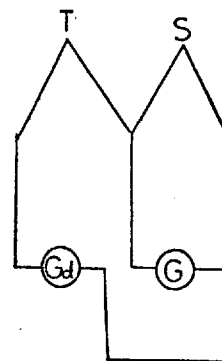


Figure 3.4

The standard sample is an inert powder which undergoes no phase change on heating. Each sample is provided with a thermocouple,

* This test was performed at the N.R.A. Laboratory.

the connection being as shown; Gs. records the temperature of the standard and Gd. the difference in temperature between test and standard samples. The equipment used has an automatic recorder of the differential temperature/temperature relationship ($\Delta T/T$). In clays it is known that every clay mineral has its own characteristic thermal properties. DTA should, whenever possible, be supplemented by X-ray diffraction analysis.

The X-ray diffraction analysis of representative clay samples was performed using a Phillips PW.1060 diffractometer provided with a linear recorder cobalt radiation (CoK α) with an Fe filter placed before the receiving slit to eliminate possible β radiation. A Kw generator was used to give intensity and a good peak to background ratio. The scanning speed was $1^\circ-2\theta/\text{min}$. Tests were performed on oriented $< 2\mu$ clay fractions in the following order:-

- a) Air dried specimens mounted on a ceramic disc were scanned from $2^\circ-34^\circ$ 2θ .
- b) The same oriented disc was subjected to glycerol and scanned from $2^\circ-20^\circ$ 2θ .
- c) The same disc was heated in a furnace first to 400°C and secondly to 550°C for a few hours and scanned in each case from $2^\circ-22^\circ$ 2θ .

Using these procedures it is possible to distinguish the different types of clay minerals present, following methods developed by Schultz (1964) and Shaw (1970).

Oriented specimens were prepared following the method proposed by Shaw (1972). The method involves filtering a clay suspension $< 2\mu$ under suction through a very fine 1.5" diameter and $\frac{1}{4}$ " thick ceramic disc to obtain a thin film of the minerals on the disc. The methods described fully by Schultz (1964) and Shaw (1971) were used for a semiquantitative analysis of the tested samples. The analyses showed that the dominant clay minerals were mixed layer illite-montmorillonite, illite, and kaolinite, with small amounts of quartz, calcite, gypsum and dolomite.

Cation exchange capacities were determined by Methylene Blue adsorption method*. C.E.C.s are expressed as meq/100 g and ranged between 26 and 43, which indicated a mixture of montmorillonite, illite and kaolinite; the cation exchange tests confirmed the D.T.A. and X-ray results. Complete chemical analyses^{**} were performed by using an atomic absorption, flame photometer, following the standard analytical chemistry methods according to A.S.T.M.

* C.E.C. Methylene Blue Absorption method by M.J. Nevins and D.J. Weinritt (1967).

** N.R.A. Laboratories Division.

Shear strength parameters were obtained by performing C.I.U. and C.I. . triaxial compression tests and fully drained direct shear tests*. The triaxial equipment used was 5 tonne and 10 tonne compression machines together with the Norwegian Geotechnical Institute triaxial equipment. These consolidated-undrained compression tests were performed on three or four specimens (3" x 1.5") taken from the same undisturbed sample. The specimens were consolidated under different cell pressures in the triaxial cells, which have held constant during the consolidation stage. When the consolidation was completed, the pore water pressure readings were started during the shearing stage until failure, so drainage was only permitted during the consolidation stage. A suitably slow rate of strain was used (1.0% per day) to avoid any build-up of differential pore water pressures.

The C.I.D. (consolidation isotropically drained) triaxial tests were performed on remoulded 3" x 1.5" specimens. Specimens were prepared and mounted in triaxial apparatus with drainage provided at both ends and side drains; a back pressure was used during the consolidation stage. From time and volume change readings in the consolidation stage, the coefficient of consolidation, (C_v), was calculated from:

* Following the standard procedure by Bishop and Henkel (1962).

$$C_v = \frac{\pi h^2}{100 t_{100}} \quad (\text{Bishop and Henkel, 1962}).$$

where t_{100} = time to full consolidation,

h = height of the sample.

$$\text{time of failure } t_f = \frac{20h^2}{\eta C_v} \quad \eta = \text{a factor depending on the drainage conditions at the sample boundaries.}$$

After determining t_f and knowing the properties of the clay material, it is possible to select an appropriate rate of strain. The rate of axial strain chosen such as to prevent any build-up of excess pore water pressures during the shearing stage. Since no p.w.p. exists, the effective stresses are equal to the applied stresses and the results of these tests were presented in the Mohr's diagram as a function of the effective stresses. The common tangent of the Mohr's circles determines the C' and ϕ' .

Direct shear box tests were performed using the standard 6 x 6 x 2.5 cm small shear box to determine both peak and residual drained shear strength parameters, C'_p and ϕ'_p , and ϕ'_r and C'_r for undisturbed samples obtained from the landslide areas. The peak strength parameters are defined as the maximum value of shearing resistance of the tested materials. The residual parameters were defined by reversing the shear box and reshearing the specimen until no further drop in shearing resistance was obtained (Skempton and Petley, 1968). This

test was also performed on remoulded specimens with pre-cut surfaces. Normally the test was performed on a series of three specimens prepared from the same sample and consolidated under different normal pressures over twelve hours to represent field conditions under the overburden, the shearing starts at a slow rate until failure. During the test a record is kept of the shearing resistance mobilized and the relative horizontal displacement occurring between the top and bottom halves of the sample. The rate of displacement selected was 0.000096 in/min which is slow enough to prevent the build-up of any excess pore water pressures in the failure zone. The test was performed with several reversals until no further drop in the shear strength was observed. Shear stresses versus displacement and maximum shear stress versus normal stress curves were drawn from which the peak and residual shear strength values were obtained.

3.1.3 Methods of Slope Stability Analysis

In order to delineate between areas suitable and unsuitable for further construction of highways, it is necessary to establish a complete idea of the field investigations and laboratory analyses. From a regional point of view it is necessary to develop a relation of a mechanism responsible and find out a common cause of the existing landslide problems. The

field observation and investigation showed that the lower part of the Ajlun Group is the one responsible for the existing problems and the most critical formation from the engineering geology point of view. All the areas with landslide problems were located within the Ajlun Group. The laboratory tests showed that the materials involved in the landslides have a common composition of clays of low shearing strength. Since the thickest clay formation exists within the Ajlun Group, it is probably the best example for the stability analyses of the existing natural slopes on the Jordanian highways with regard to both field investigation and laboratory testing. Therefore the study of stability analyses has concentrated on the clays of the lower part of this group. The movements on natural slopes within this group are of single-rotational circular and non-circular types.

Stability analyses constitute an important stage of investigations prior to the design of slopes for the selection of safe slope angles, and for the redesign of slopes where failures have occurred. The general procedure for analysing a slope is to collect full information concerning the slope (as described in Section 3.1.1), and calculate the shearing resistance and shearing stresses of the slope; thus the safety factor may be calculated by means of dividing the resisting

forces by the driving forces. This should satisfy the conditions for equilibrium of the mass. Peterson and Hultin (1916) were the first to assume circular failure surfaces for the purpose of analysis. The slip circle analysis in terms of total stresses was introduced by Fellenius (1920). Terzaghi (1925) was the first to introduce stability analysis in terms of effective stresses, where the shearing resistance of soil is equal to $S = C' + \tau' \tan \phi$. At that time it was not used in solving problems of long term stability.

In effective stress analysis the mobilized shear stress is expressed as:

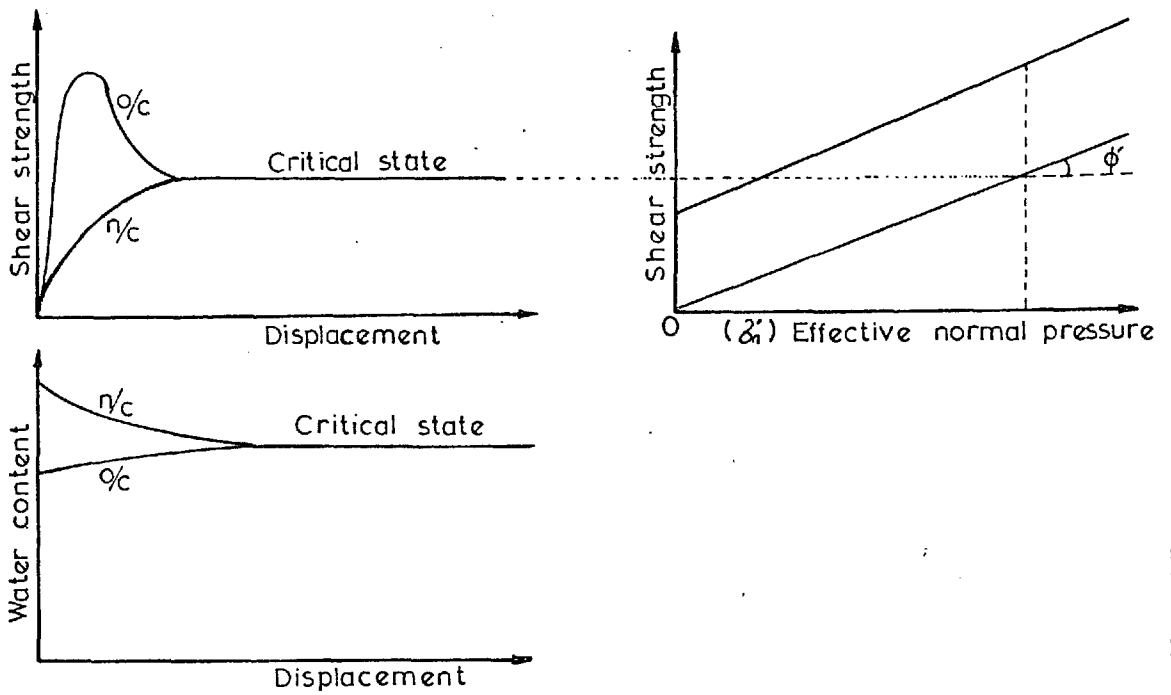
$$\sum \tau_m = \sum \frac{C'}{F} + \sum (\tau - u) \frac{\tan \phi}{F} \quad \tau' = \tau - u$$

$$F = \frac{C' + \sum (\tau - u) \tan \phi}{\tau}$$

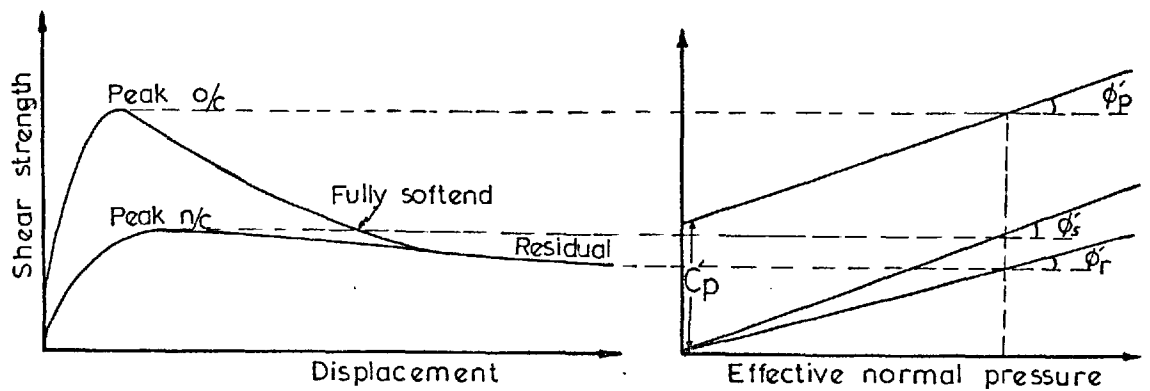
The factor of safety F , in the limit design method is defined as the ratio of the measured available strength of the soil as that required for limiting equilibrium. By definition where the slip occurs, the factor of safety is equal to unity, and the $\sum T = \sum S$. Slope stability studies have been made for slides of a rotational, translational or compound type. In all limit equilibrium analysis methods, a condition of incipient failure is postulated at all points along a continuous slip surface of known or assumed shape. These shapes could be planar or

circular or compound. The shape of the surface of rupture is dependent upon the pore water pressures and shear strength properties of the soils (Kenney, 1956). Therefore the shear strength parameters should be determined prior to any form of limit analysis to find the factor of safety. Shear strength parameters are usually classified into three types: (i) peak, (ii) residual, (iii) fully softened. Fig. 3.5 shows typical stress-strain curves for normally-consolidated and over-consolidated clays tested under drained conditions. The peak strength of a strained clay corresponds to the maximum resistance which could be offered by the material under a given effective pressure. After the peak strength has been reached, the shearing resistance decreases with increasing displacement. This process is called strain-softening which shows a further decrease in strength with larger displacements until it reaches the lower limit of resistance (residual strength). Most stiff clays exhibit a prominent fall in strength when passing from peak to residual as a result of both particle orientation and an increase in water content due to dilatancy within the shear zone (Skempton and Hutchinson, 1969). The peak strength of the normally-consolidated (remoulded) clay is in theory the limiting strength value of the stiff fissured clay which has undergone complete softening (Skempton, 1970).

Skempton also stated that when the strength has dropped to the fully softened value, there is probably no



Critical state in drained shear tests on clays
(Skempton 1970)



Shear characteristics of clays
(Skempton 1970)

Fig(3.5)

principal shear surface extending throughout the clay but there exists a complex of minor shears which have not linked together. Also the shear displacement required to reduce an over-consolidated clay to the fully softened state is very much greater than the displacement required to attain the peak, but it is large compared to that required to reach the residual strength of the clay; and he also stated that when moving from peak to residual, the cohesion intercept (C') disappears completely. During the process the angle of shearing resistance also decreases in some clays by 1° or 2° , but in others by 10° . In the Jordanian clays the decrease was very small, between 2° and 5° only. Skempton concluded that the fully softened value is a more realistic limit than the residual value for the ultimate drop in strength preceding a first-time slide in London clay. This was in agreement with the opinion previously expressed by Henkel (1956) and Skempton (1961) where they used the fully softened strength as the limiting value for non-fissured over-consolidated clays, because of the absence of softening due to the lack of any mechanism for progressive failure leading to post-peak strains. Therefore the use of peak strength in the non-fissured over-consolidated clays is the most adaptable.

Skempton (1970) listed the following points relating to the long-term stability of over-consolidated clays:

1. After a slide has taken place the strength on the slip surface is equal to the residual value. The residual strength is associated with strong re-orientation of the clay particles and is represented by an angle of shearing resistance ϕ'_r which is considerably smaller than the value of ϕ'_p at peak strength.
2. First-time slides in non-fissured clays correspond to strengths only slightly less than the peak.
3. First-time slides in fissured clays correspond to strengths well below the peak.
4. Some form of progressive failure must be operative to take the clay past the peak. This could be simply the result of a non-uniform ratio of stress to strength along the potential slip surface; but probably the fissures play an important role as stress concentrators and in leading to softening of the clay mass.

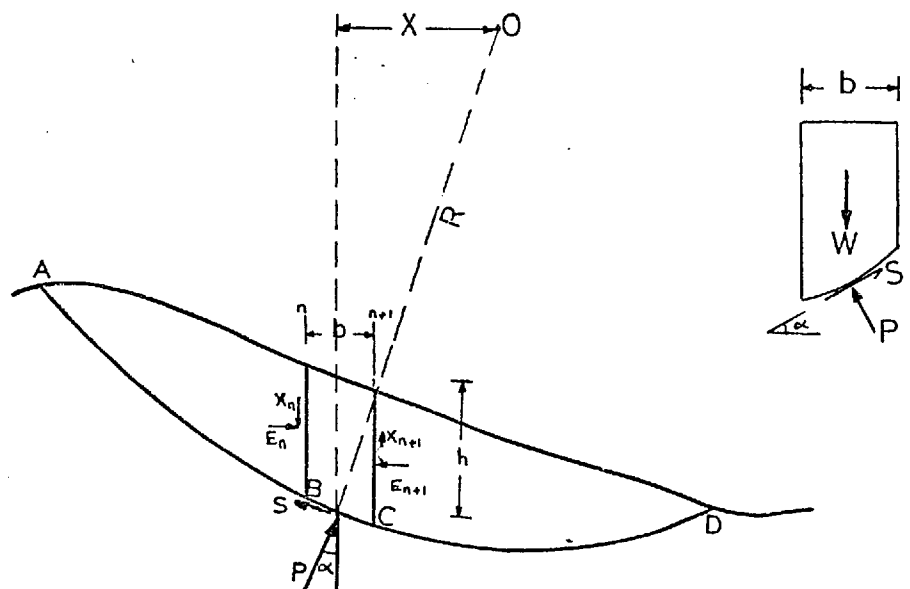


Figure 3.6 Forces in the circular arc (after Bishop, 1954).

5. The residual strength exists on pre-existing shear surfaces, whether these are the result of tectonic shearing or old landslides. Any subsequent movements on the existing slip surfaces will be controlled by the residual strength, no matter what type of clay is involved.

The methods of stability analysis used in this thesis are subdivided according to the shape of the failure surface: (1) circular slip surface, and (2) non-circular slip surface. The Bishop simplified method (1954) is the most frequently used for circular slip surfaces in terms of effective stresses. The Norwegian Geotechnical Institute has developed a graph and a tabulation scheme to be used jointly with this method in practical work. Bishop and Morgenstern (1960) have prepared a set of stability charts based on this method, and may also be used to obtain quick preliminary solutions to stability problems. The basic step in the Bishop approach is shown in Fig. 3.6. Forces S are found as with the Fellenius method, and are likewise summed to give a measure of the driving moment ($S = W_i \cdot \sin \alpha$). However, the forces P are found by applying a different rule; this rule provides for force equilibrium in the vertical direction, while ignoring the requirement of force equilibrium in the horizontal direction. This method also assumes, in effect, that the forces on the sides of any slide have no net component in the vertical direction. This method is mainly

derived by equating the moment about O of the weight of soil within ABCD with the moment of the shear forces acting on the slip surface. The normal effective forces $(P - ul) = P'$ on the base of the slice considered, is found by resolving vertically; and assuming that $X_n - X_{n+1} = 0$.

Using the nomenclature of Fig. 3.6, the factor of safety is defined as follows:-

$$F = \frac{1}{\sum W \sin \alpha} \cdot \sum \left[\left\{ c' b + (W - ub) \tan \phi' \right\} \cdot \frac{1}{m_\alpha} \right]$$

where $m_\alpha = \cos \alpha \left(1 - \frac{\tan \alpha \tan \phi'}{F} \right)$

Values of m_α can be read off a chart for any assumed value of F (Janbu et al, 1956; Terzaghi and Peck, 1967). This method is very rapid and can be carried out easily by hand or by computer (Little and Price, 1958).

Janbu (1957) extended the method of slices to non-circular slip surfaces (1954 and 1957). In this method the interslice forces were neglected for the moment, and resolving horizontally:-

$$\sum S \cos \alpha = \sum P \sin \alpha.$$

Using the nomenclature of Fig. 3.6 the factor of safety is expressed as:-

$$F = \frac{\sum S_1/\cos\alpha}{\sum W\tan\alpha} = \frac{\sum Sb/\cos^2\alpha}{\sum W\tan\alpha} \quad (1)$$

$$1 = \frac{b}{\cos\alpha}$$

$$P = W\cos\alpha$$

$$S = \frac{S}{F} \cdot 1$$

As in the conventional method, it is easily shown from force equilibrium slices, neglecting interslice forces:-

$$F = \frac{(C' + P\cos^2\alpha - u)\tan\phi'}{P \sin\alpha \cos\alpha} \quad (2)$$

where $P = W/b$. As $\cos^2\alpha = 1 - \sin^2\alpha$, by rearranging:-

$$F = \frac{C' + (P - u)\tan\phi'}{P\sin\alpha \cos\alpha} - \tan\alpha \tan\phi' \quad (3)$$

but also $F = \frac{S}{P\sin\alpha \cos\alpha}$

$$S = \frac{C' + (P - u)\tan\phi'}{1 + \tan\alpha \frac{\tan\phi'}{F}} \quad (4)$$

Substituting equation (4) in (1) and introducing factor f_o to take account of the effect of the interslice forces on F, we get, for the $C'\phi'$ case:-

$$F = f_o \frac{\sum [C' + (P - u)\tan\phi'] b \frac{\sec^2\alpha}{1 + \tan\alpha \frac{\tan\phi'}{F}}}{\sum W \tan\alpha}$$

This is the equation of Janbu's Routine Method, which is also suitable for hand calculation. Values of f_o for different d/L values have been derived by Janbu from the curve in Fig. 3.7.

A simpler but considerably less accurate method of analysis for circular slips is the Fellenius method (1926). The basic steps of this method of slices are outlined in Fig. 3.8. The forces P and S are set equal to the normal and tangential components of the weight W of the slice in question. The summation of S over all the slices provides a measure of the driving moment. Pore water forces across the base of the slices are subtracted from P to give the normal effective forces P'. The summation of P is taken as a measure of the frictional component of the resisting moment. The factor of safety is computed from the equation for moment equilibrium about the centre of the assumed failure circle. By following this procedure the individual slices are placed in force equilibrium in a direction normal to the arc at the base of the slice, but not in a direction tangential to this arc. The safety factor is then given by the expression:

$$F = \frac{1}{\sum W \sin \alpha} \sum \left[C'l + (W \cos \alpha - u_l) \tan \phi' \right]$$

$$P = W \cos \alpha, \quad S = W \sin \alpha \quad \text{and} \quad P' = W \cos \alpha - u_l.$$

Some comparisons of analyses of circular landslides at Northolt, Lodalen and Drammen, in natural slopes by both Bishop simplified and conventional methods, show that the Fellenius method may well under-estimate the factor of safety by over 20% (Bishop, 1954).

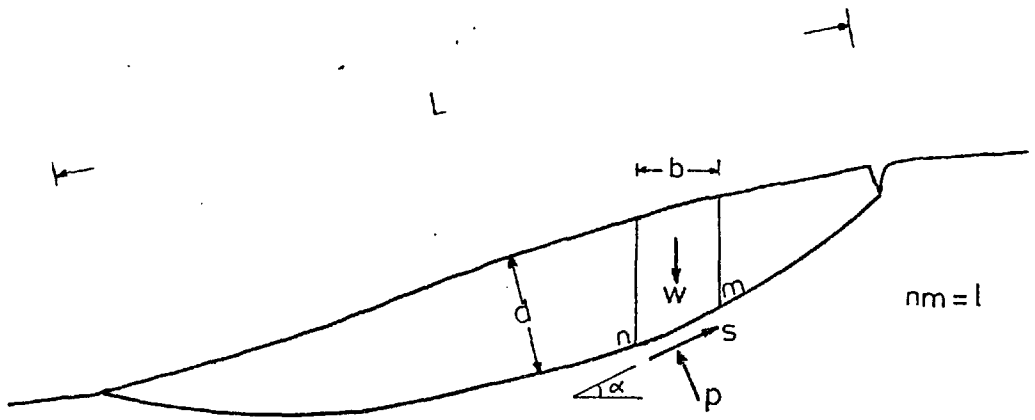
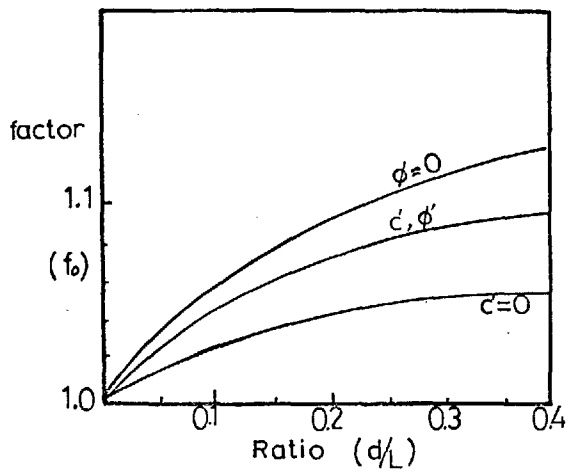


Fig.(3.8)- Forces in the non-circular surfaces
(Fellenius 1926)



Fig(3.7)- Values of f_0 for different d/L values
(Janbu 1957)

Another comparison of analysis of non-circular landslides at Walton's Wood, Guildford, Sudbury Hill, Folkestone Warren and Jarash road landslide III, in natural slopes, by both Fellenius and Janbu's methods shows that the safety factor of both methods is very close to each other and Fellenius method is more accurate where the slip surface is shallower (Table 3.1 and stability analysis of landslide III).

Experience indicates that Bishop's simplified method is accurate for circular-type landslides, whereas Fellenius and Janbu's methods are accurate, reliable and successfully used for non-circular landslides especially if a substantial portion of the slip surface is predominantly planar.

Landslide	Shape and cross section	Factor of Safety		
	Circular	Fellenius		Bishop
Northolt	d/L=0.14	0.94		1.0
Lodalen	0.20	0.79		1.0
Drammen	0.19	0.79		1.0
	Non-circular	Fellenius	Jambu	Morgenstern and Price
Walton's Wood	0.06	0.98	1.03	1.0
Guildford	0.09	0.97	1.00	1.0
Sudbury Hill	0.11	0.96	0.95	1.0
Folkestone Warren	0.17	0.92	0.97	1.0
Landslide III (Jarash Rd)	0.13	1.15	1.155	
	0.10	1.176	1.223	

Table 3.1

CHAPTER FOUR

DETAILED INVESTIGATIONS OF LANDSLIDES
ALONG AMMAN - NAUR-ADASIYE ROAD
(LANDSLIDES V, VI & VII)

4.1 INTRODUCTION

This chapter provides a brief description of the highway between Amman, Naur and Adasiye, field investigations at locations of areas of instability, together with details of laboratory tests and stability calculations.

The Naur-Adasiye road forms part of the main highway between Amman and Jerusalem. The planning and design of this highway was carried out in 1954, and was based on aerial photographs on a scale of 1:25,000 from Hunting Aerosurveys Ltd., 1953. Construction was completed in 1958, this having been supervised by U.S. Aid Highway Design Engineer - B.M. Parker - jointly with the Ministry of Public Works Engineers of Jordan. No engineering geological investigations were made prior to the commencement of construction.

For the purposes of the present study, intensive field investigations and laboratory testing were carried out, and stability analyses in terms of effective stress, using the methods proposed by Fellenius (1926) and Janbu (1957) for translational landslides, and Bishop's (1953) method for the circular-type failure, were carried out.

4.2 GENERAL INVESTIGATIONS OF THE ROUTE

4.2.1 General Field Investigations

The areas investigated are located in the northern part of Jordan, east of the Jordan Rift Valley, along the Amman-Jerusalem highway, between Km 20-25 to the southwest of the city of Amman.

The study area covers approximately 70 Km², where two major active landslides (landslides V and VI) and one rockslide in Amman itself were selected to be studied in detail. However, there are many other potentially unstable areas observed and these are on the map (Fig. 4.2).

The average altitude of the section of the highway investigated ranges between 550-650 m, with gentle topographical features and wide wadis. The lower parts of the mountains are covered with Pleistocene fans and mantle. The most important morphological and tectonic feature is the north-south trending Jordan Rift Valley with its Quaternary sediments. The formations close to the Rift Valley have been strongly faulted and intensely fractured by the formation of the graben.

Stratigraphically the rocks of the study area are representatives of the littoral, marine environment of the Tethys Geosyncline (Ruef, 1964).

The average annual precipitation (measured over a 20 years period) in the study area is 500 mm. This rainfall is usually concentrated in the period between November and April. The annual precipitation during the period between 1942 and 1973 is illustrated in Table 4.1B, and the monthly precipitation between the periods 1962 and 1972 is illustrated in Figure 4.1. There are no perennial flows in the wadis, the discharge is limited to the seasonal rainfall. The precipitation penetrates through the joints in the bedrock and perches on the subsurface clay horizons, therefore numerous springs can be observed between Naur and Adasiye. Most of them are dry in summer and this confirms the rather limited extent of the aquifers.

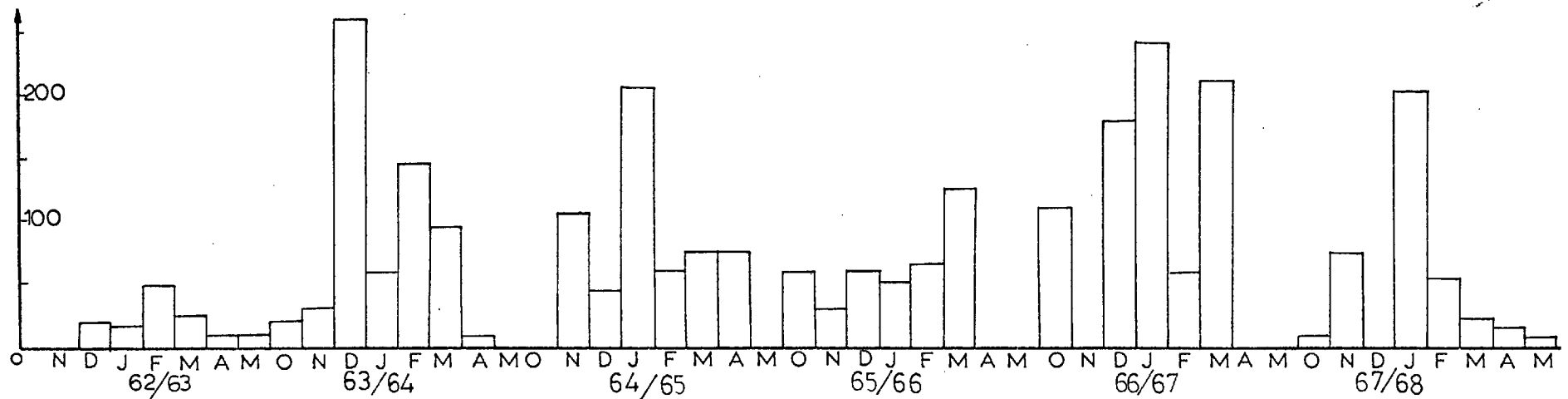
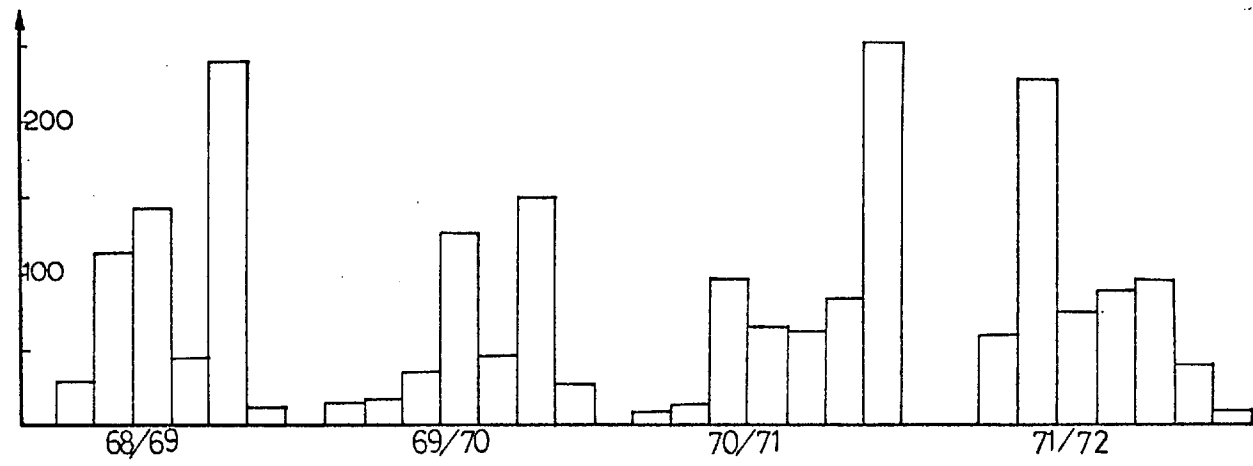
The drainage of the study area is mainly towards the west, and the wadis are tributaries of Wadi El-Kafrein.

After the first movement of landslide VI commenced in 1964, the Ministry of Public Works proposed a by-pass road (route 2, Fig. 4.2), due to the progressive nature of the movement. However, route 2 was also located on an active landslide area, and in 1969 landslide V occurred within the old landslide area as shown in Fig. 4.2.

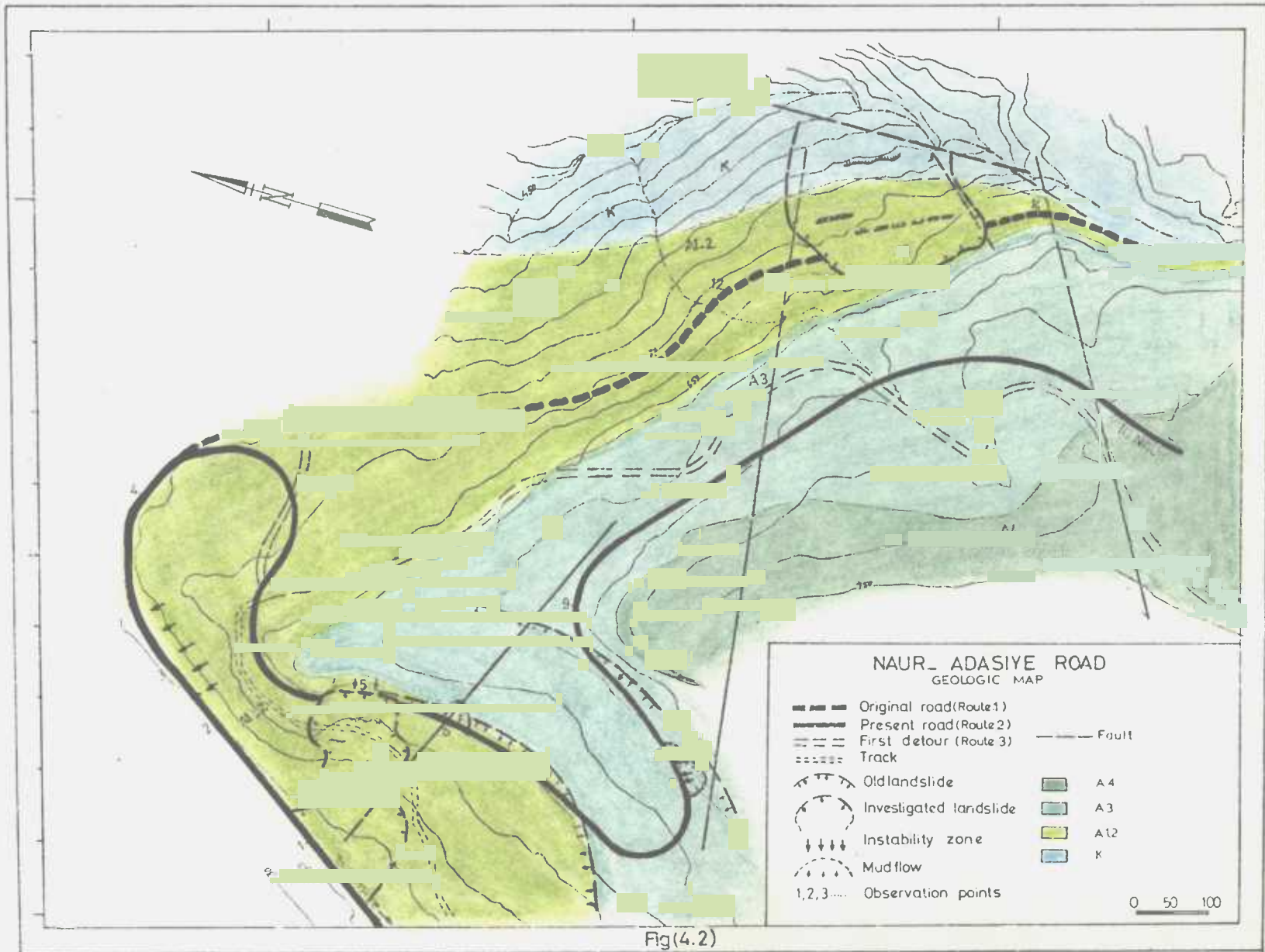
The rock units exposed in the study area are:-

- (a) Upper Kurnub Group (K2).

NAUR STATION
TEN YEARS ANNUAL PRECIPITATION



Fig(4.1)



Fig(4.2)

- (b) Clay-marl unit of the Lower Ajlun Group (A1,2, A3 and A4).

The main sedimentary formations crossed by this section of the highway are A1, 2. The Upper Kurnub Group in this area generally consists of varicoloured shaley sandstone and is silty and clayey in the upper part, but is generally coarse-grained in the lower part. The Lower Ajlun Group consists of white to yellow nodular marly limestones, with yellow to green marls and clays which are intensely jointed and weathered. The upper limestone is mainly white or cream and is finely crystalline with chert nodules.

The field observations and description of this section of the highway may be summarized as follows: (locations of the observation points are given in Fig. 4.2).

Observation point 1: The toe of the recent landslide V within an old landslide area. The main scarp of this landslide is located at the contact between A2 and A3 of the Lower Ajlun Group and affects the upper highway, while the toe of the landslide has over-ridden the lower highway with the sliding material (Plate 4.1).

Observation point 2; shows a nearly vertical side slope, composed of approximately 15 m of clay and marl overlain by intensely jointed limestone. This area is potentially unstable.



Plate 4.2 The main features of the movement of landslide V - 1971 (the main scarp), (Observation point 5.)



Plate 4.1 General view of landslide V - 1971 (looking down the slope). The sliding material near the toe is covering the lower road (observation point 1).

Observation point 3: shows a nearly vertical side slope consisting of highly jointed limestone underlain by marl and clay. Many small displacements and faults were observed in the back slope probably contributing to rockfalls.

The area between observation points (2) and (4) is potentially unstable owing to the well developed jointing in the upper strata and the presence of the underlying soft clay; many types of slope failure can be expected.

Observation point 5: the main scarp of the landslide V, Plate 4.2 . The back slope of this landslide is potentially unstable, rockfalls and toppling are expected.

Observation point 6: a mudflow consisting of brown silty clay, and yellow to green clay, with rock fragments, Plate 4.3 at a possible fault zone.

The area between observation points (6) and (7) shows subsidence and tilting in the pavement towards the west; this is probably due to the insufficient compaction of the embankment but may also be due to the progressive nature of the movements in the area.

Observation point 7: a mudflow. The material involved is mainly yellow marl and green clay. Trees have recently been planted at this site (Plate 4.4).



Plate 4.3 A mudflow consisting of brown silty clay, yellowish clay and marl (observation point 6).



Plate 4.4 A mudflow, consisting of yellowish marl and clay (observation point 7).

Observation point 8: a mudflow, composed of the same material as at observation point (7) (Plate 4.5). These two mudflows are located at the toe part of an old landslide area as shown in Fig. 4.2.

Observation point 9: a fault zone composed of intensely fractured marlstones and marly limestones. Rockfalls occur from time to time onto the highway. The highway between observation points (9) and (10) is mainly crossed by the limestone strata and no instability was observed.

Observation point 11: the right-hand back slope at this site is composed of 35 metres of clay overlain by intensely jointed marly limestone. Rockfalls are a dominant feature of this zone (Plate 4.6). Eighty metres ahead, the right back slope also consists of 7 m of soft clay overlain by highly fractured marly limestones. Two types of failure can be expected in this zone; (i) rockfalls due to the erosion of the underlying soft clay (Plate 4.7), and (ii) potential rockslips along pre-existing joint surfaces (Plate 4.8).

Observation point 12: landsliding in progress was observed. The pavement has been pushed up at the possible toe of the movement (Plates 4.9 and 4.10). The strata consist of 12.5 m of clay and marl overlain by marly limestone of the A3 formation.



Plate 4.5 A mudflow consisting of yellowish marl and green clay; trees have recently been planted (observation point 8).



Plate 4.6 Marly limestone underlain by marl and clay. Notice loose blocks of limestone adjacent to the pavement (observation point 11).



Plate 4.8 Shows sets of continuous downward movement of rock masses along pre-existing joint surfaces. Block 1 failed. The final collapse of the blocks 2, B3 and B4 will take place in the same manner along pre-existing joint surfaces J2, J3 and J4.



Plate 4.7 Shows two blocks separated from the parent rock owing to erosion and undercutting of the underlying soft clay and marl.



Plate 4.9 Active landslide. The pavement is pushed up at the toe of the movement while the upper part shows displacement. Notice loose blocks adjacent to the pavement (Observation Point 12).



Plate 4.10 Active landslide. The upper part shows block creeping and probable toppling failure mode (Observation Point 12).

Observation point 13: landslide VI (Section 4.4 and Plate 4.11).

The highway section between observation points (12) and (13) is potentially unstable. Many different types of instability were observed including cracking and subsidence in the pavement, mudflows, besides many progressive landslide movements. The average hillside cut slope is 75° .

Observation point 14: a highly sheared fault zone. A small landslide with rock slips in the back slope was observed (Plate 4.12).

In the light of the above observations, it can be seen that the area between observation points (5) and (9) and the area between observation points (11) and (14), slope failures are of a progressive nature. Two major landslides are located within the A1, A2 formation, each with a main scarp at the upper contact of A2 with A3. The rockfalls and rockslips were observed at the lower contact of A3 and A2.

4.2.2 General Laboratory Investigations

As part of the detailed slope stability studies, an intensive laboratory testing programme was devised and performed on both disturbed and undisturbed samples obtained from the two landslides V and VI, to determine the engineering properties of the clays involved. The strength parameters were used in the



Plate 4.11 The main features of landslide VI. The main scarp and the moved road (Observation Point 13).



Plate 4.12 Sets of continuous mass movements along pre-existing failure surface (joints). Mass 1 moved along Joint 1. The final collapse of the moving mass 2 will occur after the lateral support is removed completely. Mass 1 shows intense jointing and disturbance while mass 2 is less disturbed (Observation Point 14).

slope stability analysis. A summary of the test results is given in Table 4.2B.

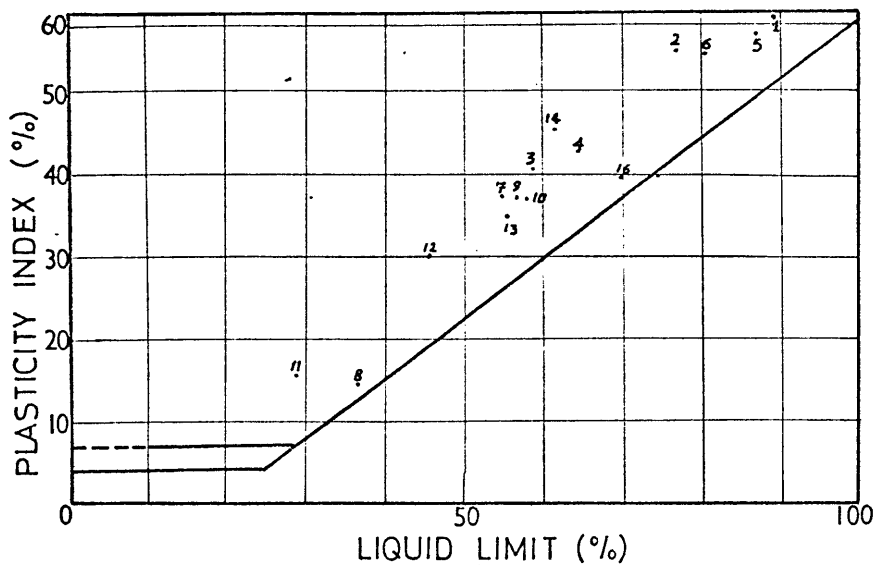
In order to compare the materials obtained from both sites, the test results were plotted on the same plasticity and activity charts, Fig. 4.3. These charts show that all the points lie above A-line and the clay has symbols CH and Cl, and is an inactive to normal clay. The samples obtained from landslide V have a slightly higher plasticity than the samples from landslide VI. The grainsize distribution curves show that the material obtained from landslide V contains a higher clay fraction than that of landslide VI and is mainly silty clay. The materials obtained from landslide VI are mainly sandy or silty clays, Fig. 4.4.

The maximum water absorption of the material obtained from landslide V is generally higher than that of landslide VI owing to the type and percentage of clay minerals in the samples (Fig. 4.5).

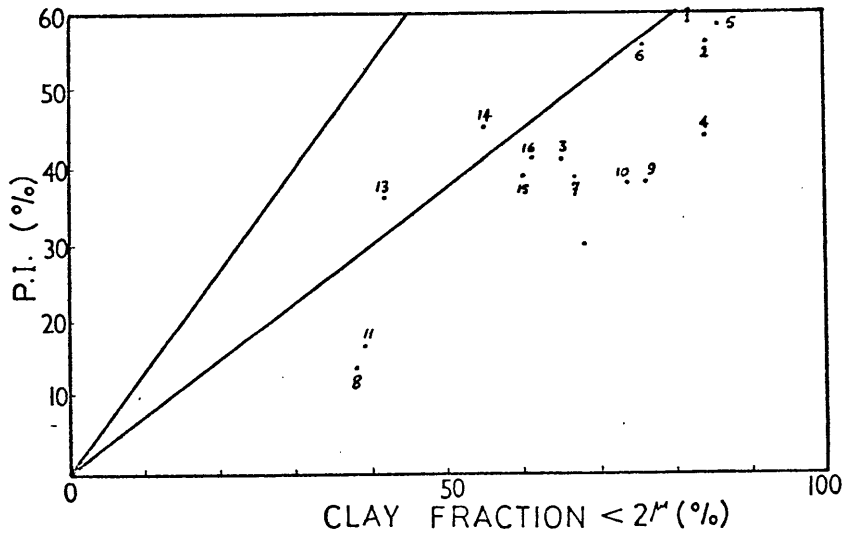
The mineralogical composition of representative clay samples obtained from the two landslide areas was studied by the Differential Thermal Analysis. The D.T.A. curves (Fig. 4.6) correlate very well and show that the samples 1, 2, 4, 5 and 6 from landslide V give very small peaks between 330 and 367

NAUR ADASIYE ROAD
PLASTICITY AND ACTIVITY CHARTS
OF REPRESENTATIVE SAMPLES
FROM LANDSLIDES V & VI

PLASTICITY CHART

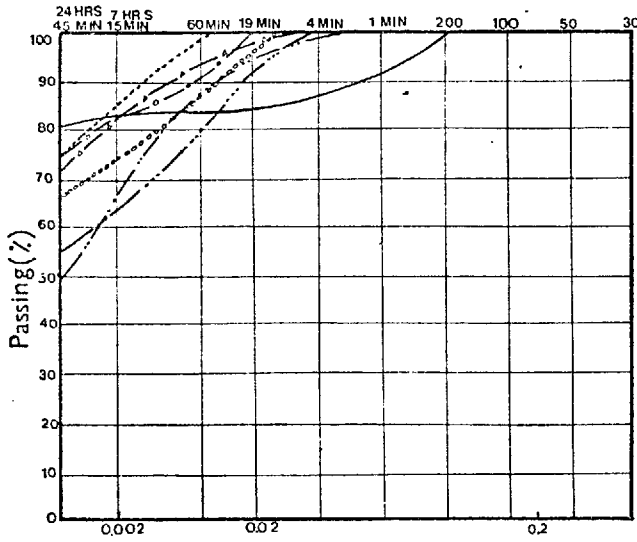


ACTIVITY CHART

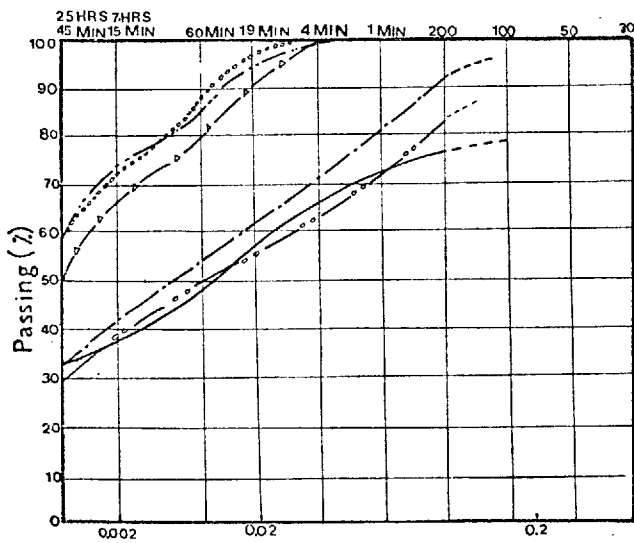


Samples: 1-7 Landslide V
8-16 Landslide VI

Fig(4.3)



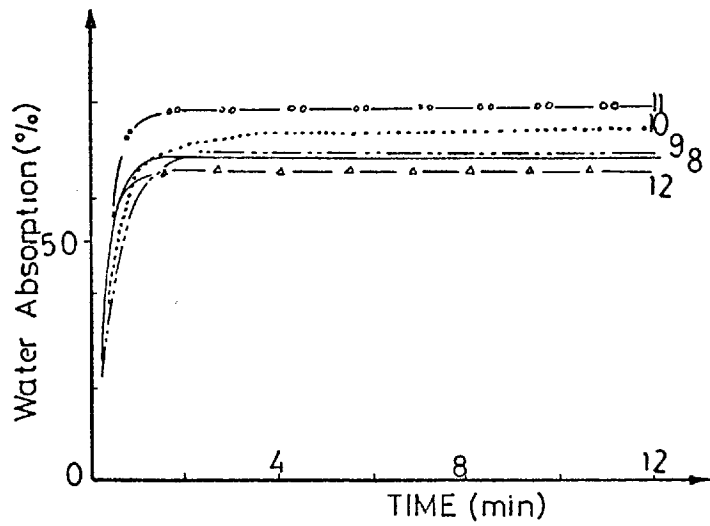
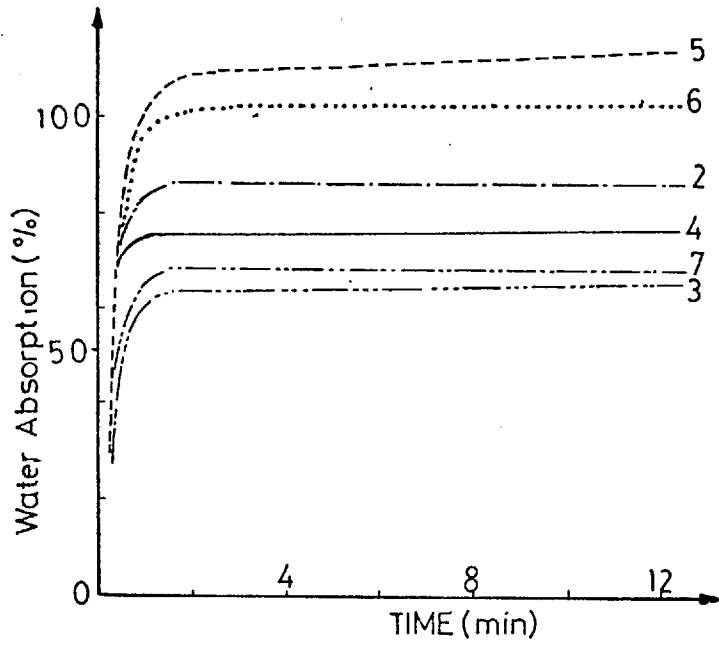
Sample	Symbol	Clay	Silt	Sand
1	—△—	82	18	—
2	—○—	84	16	—
3	—●—	65	35	—
4	—	84	16	—
5	—○—	86	14	—
6	76	24	—
7	—△—	67	33	—



Sample	Symbol	Clay	Silt	Sand
8	—	38	40	22
9	—○—	76	24	—
10	73	27	—
11	—○—	39	44	17
12	—△—	68	32	—
13	—○—	42	50	8

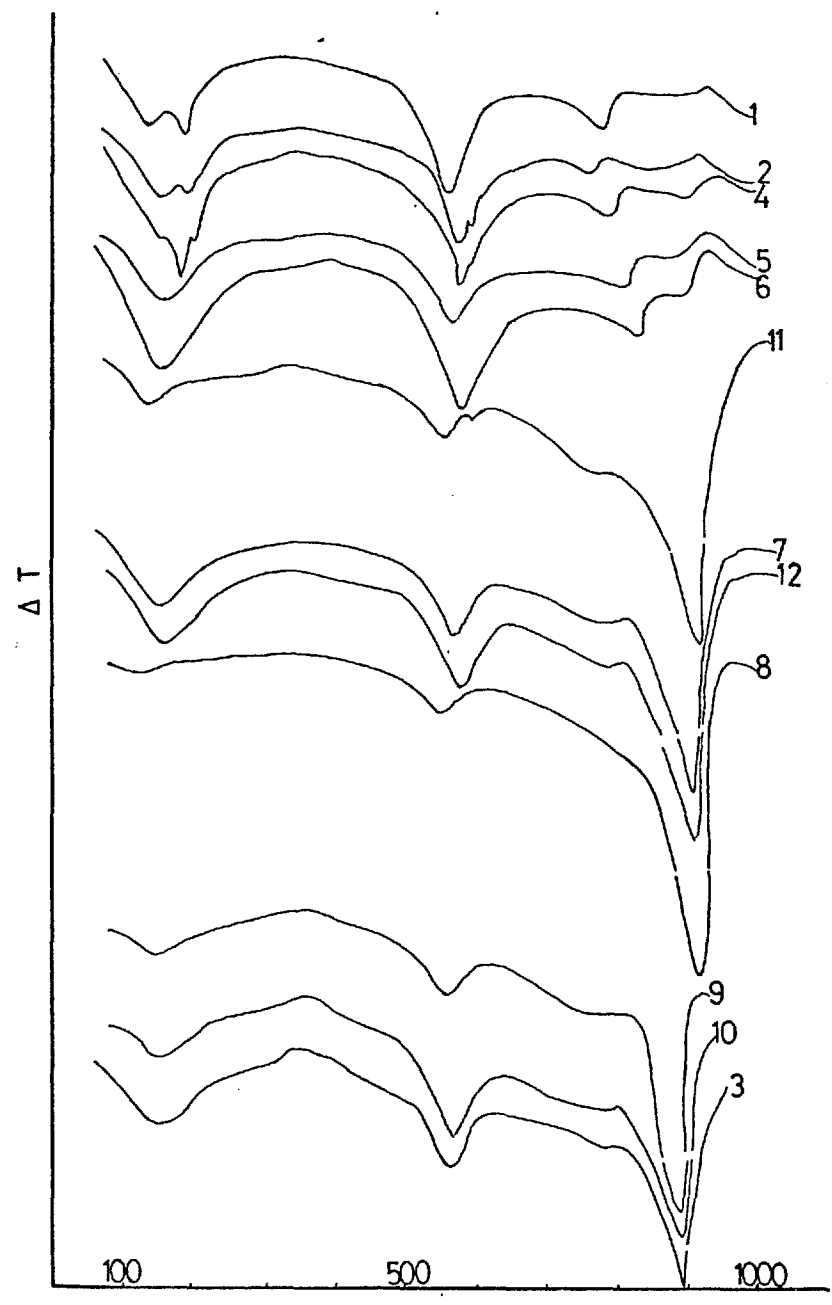
GRAINSIZE DISTRIBUTION
OF REPRESENTATIVE SAMPLES
FROM LANDSLIDES V & VI

Fig(4.4)



MAXIMUM WATER ABSORPTION OF REPRESENTATIVE SAMPLES FROM LANDSLIDES V(above) & VI (below) .

Fig(4.5)



CORRELATION OF THE D.T.A. OF THE REPRESENTATIVE SAMPLES FROM LANDSLIDE V(1-7) & LANDSLIDE VI(8-16)

Fig(4.6)

due to the burning of carbonates, which indicate that the material contains higher clay minerals and less carbonates, compared with the analysed samples from landslide VI. The clay consists mainly of mixed layer illite-montmorillonite, kaolinite, quartz, calcite with traces of organic impurities (a detailed mineralogical analysis is given in Appendix C.1.

The curves show the following peaks and temperatures:

Type of peak and temperature.	Explanation
Endo: 130 - 163	Evolution of absorbed H ₂ O.
Exo: 330 - 367	Burning of carbonate materials.
Endo: 552 - 576	Evolution of Hydroxyl H ₂ O.
Endo: 893 - 910	Evolution of CO ₂ .
> 910	May be a mixed layer of illite-montmorillonite.

Table 4.1

X-ray diffractometer traces for cavity mount specimens showed the following:

1. 18A⁰ broad peak indicating the presence of montmorillonite
2. A peak at C 10A⁰ indicating the presence of illite.
3. The third peak at about 7.10A⁰ is characteristic of kaolinite with a second basal reflection at 3.56A⁰.
4. Reflection at about 3.02A⁰ indicates the presence of calcite; the dolomite shows also a strong basal reflection in the region between 2.91 and 2.88A⁰. Small amounts of

accessory feldspars are indicated by the same peaks at 3.22\AA , 3.42\AA , and 3.78\AA .

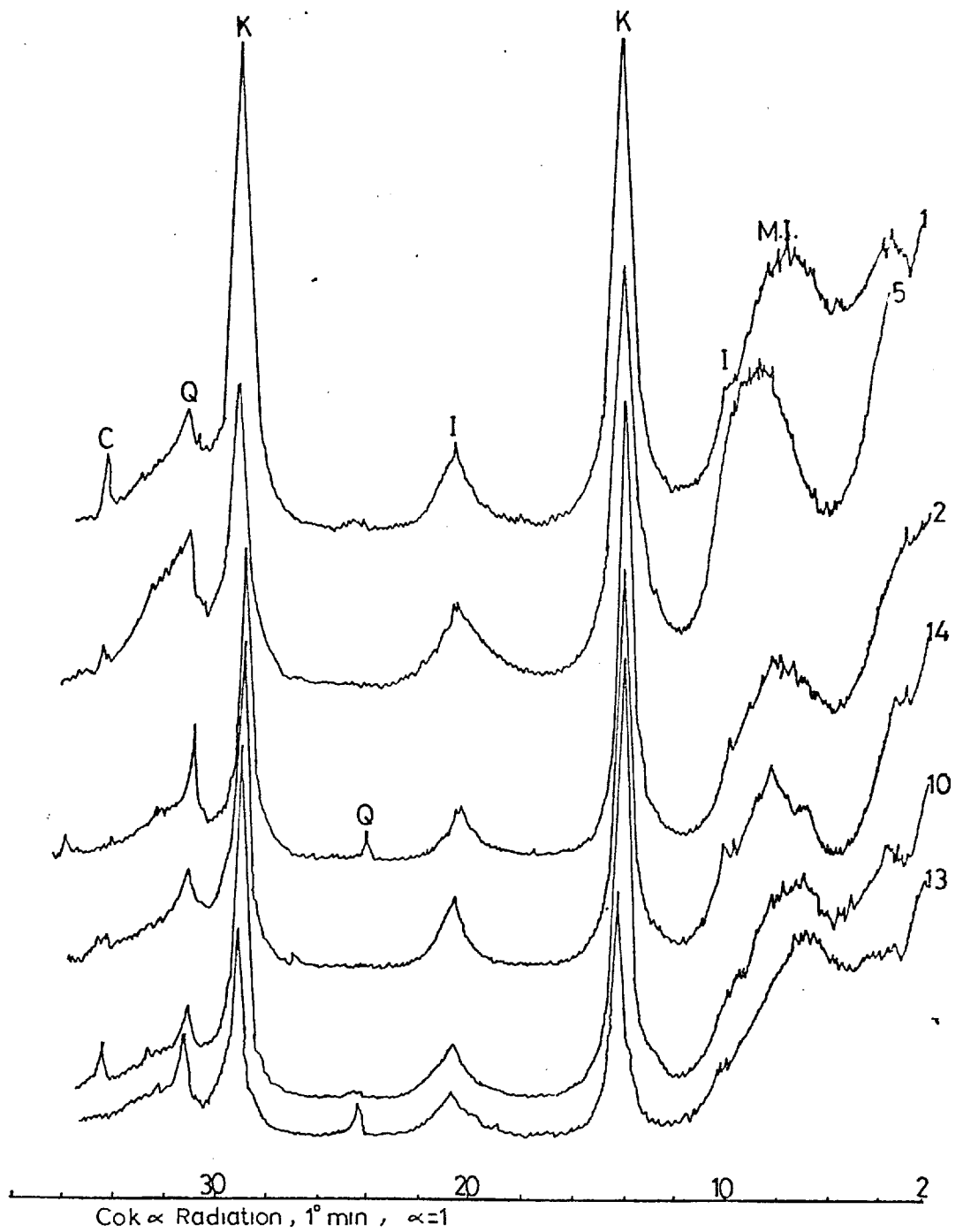
5. The small peak at 7.56\AA indicates the presence of gypsum.

In the light of the mineralogical studies it can be seen that the samples are composed mainly of montmorillonite, illite, kaolinite, quartz, calcite and dolomite, in that order of abundance.

Qualitative mineralogical analysis by X-ray diffraction on the oriented $<2\mu$ clay specimens, after the specimens were subjected to both glycerol and heat pre-treatment at 400°C and 550°C were carried out following the methods developed by Schultz (1964) and Shaw (1970).

The X-ray diffraction curves (Fig. 4.7) were interpreted as follows:

1. The broad peak 18\AA for the glycerated specimen indicates the presence of mixed layers of illite-montmorillonite. This peak shows a complete collapse to about 10\AA after heating.
2. The presence of illite is indicated by a series of peaks at 10\AA , 4.97\AA and 3.32\AA . None of these is affected by either glycerol or heat treatment.



NAUR - ADASIYE ROAD
CORRELATION OF THE X-RAY DIFFRACTION OF THE ORIENTED
MOUNT SPECIMENS

- M.I. — Mixed layer (Illite-Montmorillonit)
- I — Illite
- K — kaolinite
- Q — Quartz
- C — Calcite
- 1,2,5 — Landslide α
- 10,13,14 — Landslide β

Fig(4.7)

3. Kaolinite peaks were clearly observed at 7.16A° , 3.57A° and 2.38A° . Kaolinite gives a sharp peak at about 7A° . But this is mainly destroyed after heating at 550°C (Schultz, 1964).
4. Quartz, calcite, feldspar and dolomite were detected in minor amounts in all samples tested. Sharp peaks at 3.86A° and 3.03A° with basal reflections indicate the presence of calcite. The quartz peaks are at 4.26A° and 3.34A° ; dolomite has peaks at 4.02A° and 3.69A° , and feldspar has its strongest peak at 3.18A° .

The quantitative mineralogical results for the tested representative samples are shown in table 4.2.

Sample Number	Kaolinite %	Illite %	Mixed layer (I.M) %	Cation exchange capacity meg/100g
1	22	14	64	39
2	25	18	57	38
5	18	19	63	43
10	25	15	60	31
13	22	22	56	28
14	28	14	58	37

Table 4.2

The table of results shows that a I.M. mixed layer mineral is the predominant clay mineral in all the tested samples.

The cation exchange capacities of the tested clay minerals (using the Methylene Blue Adsorption method described fully elsewhere (Chapter.3)), show a high range, indicating that the clay could be a mixture of montmorillonite, illite, and kaolinite type. The cation exchange capacities' determinations tend to confirm the X-ray and D.T.A. analyses.

Chemical analyses of representative samples from the two landslide areas are presented in Table 4.3.

Chemical Analyses of the Representative Samples

Sample No.	MgO %	CaO %	Fe ₂ O ₃ %	K ₂ O %	N ₂ O %	MnO %	Al ₂ O ₃ %	SO ₃ %	SiO ₃ %	Loss on L.O.I. Ignition %
1	27.6	7.42	6.55	2.71	0.33	0.03	16.52	9.28	38.43	16.07
2	1.17	2.23	4.76	2.38	1.50	0.021	9.84		58.70	
3	3.00	26.82	6.00	1.40	0.11	0.02	11.35	0.78	23.97	26.72
4	0.11	2.23	4.90	2.40	0.12	0.03	10.98		59.40	
5	2.38	6.27	6.44	1.67	0.42	0.18	12.90		44.0	
6	2.66	7.80	5.90	1.33	0.24	0.05	20.27	0.29	44.46	16.97
7	0.99	20.99	3.58	1.00	0.11	0.05	8.08			
8	0.306	41.70	2.08	0.278	0.083	0.012	5.74		10.30	
9	1.918	29.80	3.27	1.40	0.12	0.019	8.20		21.90	
10	1.53	22.35	4.34	1.38	0.12	0.02	9.02		25.80	
11	1.35	36.51	2.26	0.65	0.08	0.04	4.26			
12	1.12	18.60	3.67	0.80	0.08	0.05	7.74			
13	1.96	4.66	3.96	1.87	0.14	0.08	8.40			

Table 4.3

4.3 DETAILED INVESTIGATIONS OF LANDSLIDE V

4.3.1 Geology and Hydrogeology

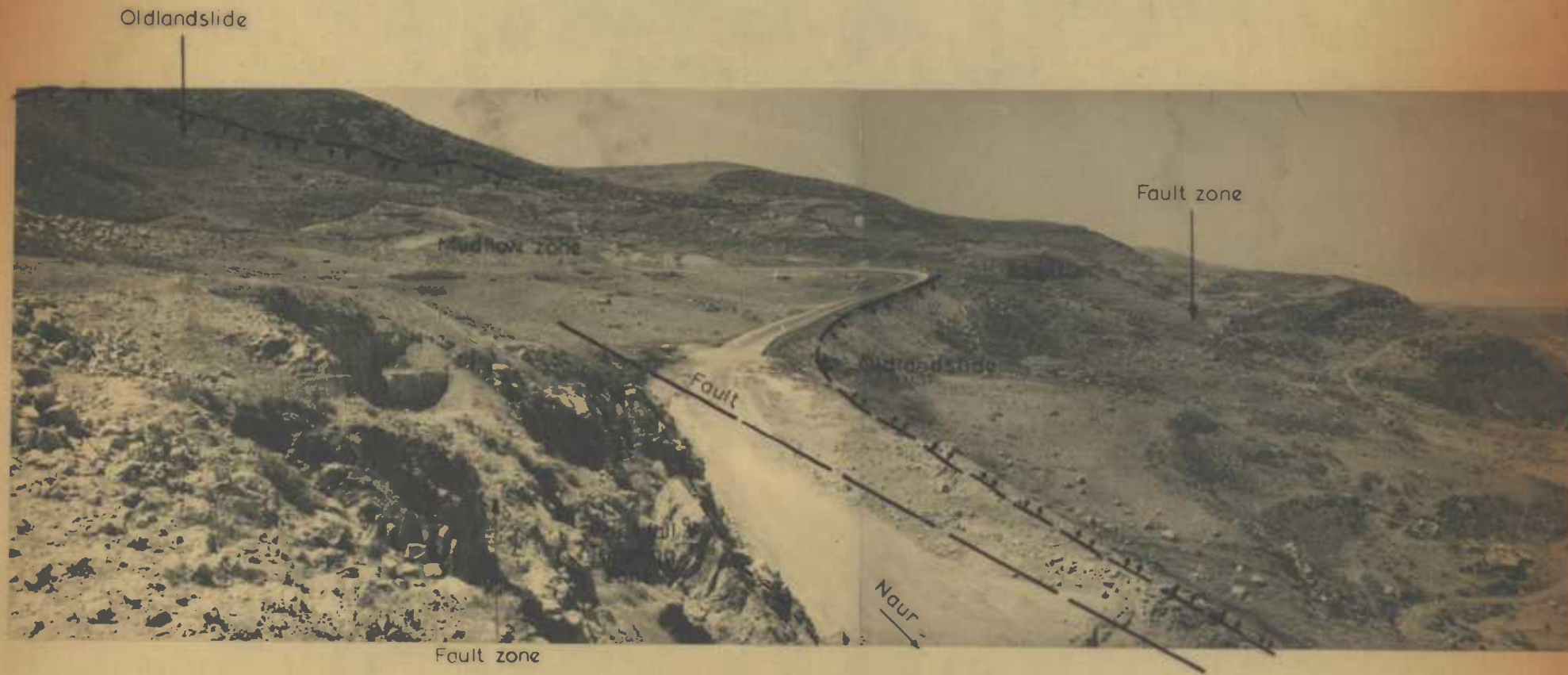
The slide area lies 25 Km south-west of Amman on the Amman-Jerusalem highway between Naur and Adasiye.

The area is mountainous with a highest elevation of 775 m, but the height decreases towards the northwest until it reaches 250 m at Wadi El-Bahhath.

The morphology of the area in the region of landslide V shows a hummocky terrain arising from the old landslide movements in the area (Plate 4.13).

Detailed geological investigations were carried out and maps were prepared on 1:1,000 and 1:5,000 scales. These were checked by the study of the aerial photographs on scales of 1:10,000 and 1:25,000.

The rock units exposed at the site of landslide V is the marl-clay unit of the Lower Ajlun Group (A1, 2, 3). This unit is composed of grey clay and dark green shale. These are overlain by rock of group A3, marly limestones alternating with thin bands of clay and marl. A3 rocks are exposed at the crest of the landslide and dip $3-5^{\circ}$ SE, thus the main scarp of the recent movement is located at the contact between the A2 and A3 groups.



LANDSLIDE V

Plate 4.13

General view of the study area in 1969.
Old landslides, faults and hummocky terrain.

The main structure at the site of landslide V is an anticline, whose axis trends northeast-southwest. The NW and SE limbs of this anticline are formed by the Lower Ajlun Group.

The region is severely affected by faulting and landslides, and many other small displacements which are apparent in the rock back slope (Plate 4.14). A major fault trending SE-NW passes through the left flank and the toe part of the landslide.

A particularly useful field indication of the activity and progressive nature of the slope failure is the development of the joints in the caprock which acts as a sensitive movement indicator. A detailed joint survey was made after the 1969 and 1971 movements, and the results are presented as stereographic plots in Fig. 4.8. The survey of 1969 shows that most of the joints are circumferential trending parallel to the hillside, and generally dipping out of the slope; some other types are radial and intersect the slope at an angle. Five joint sets were identified at this site. These are listed below:-

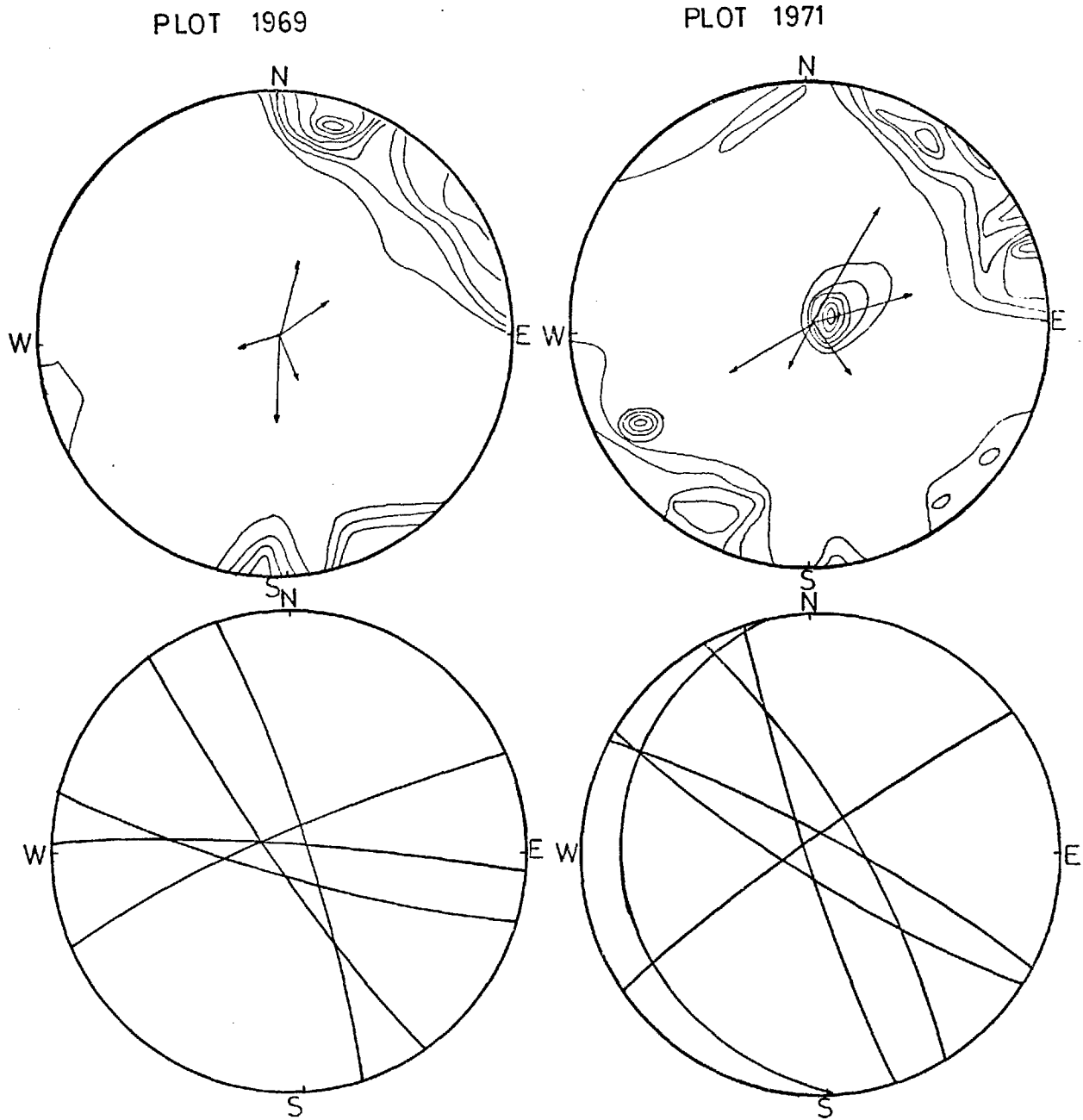
<u>Joint Set No.</u>	<u>Dip</u>	<u>Strike</u>
I	80 SW	N 72 W
II	82 NE	N 84 W
III	80 SW	N 33 W
IV	80 NW	N 68 E
V	76 NE	N 15 W



Plate 4.14 Jointing and faulting of the strata at the crown of landslide V. The bedrock is marly limestone underlain by marl and clay.



Plate 4.15 Toppling and rockfall at the crown of landslide V.



STEREOGRAPHIC PLOT OF JOINTS OF THE STRATA AT THE CREST OF LANDSLIDE V AFTER THE MOVEMENTS OF 1969 & 1971 .

Fig(4.8)

Set No. I is the one most strongly developed (circumferential) and might contribute to the most unstable slope conditions when these joints combined with the stratification and the other joint sets. In this situation, outwardly leaning blocks may become separated from the main mass by development of the backing joints. Se. No. I represents about 88% out of a total of 96 joints measured in this strata near the crest of the landslide (Fig. 4.8).

The survey of 1971 shows that the same joint sets were developed and were more strongly developed. In addition another shallow joint set No. III had developed. The dip and strike of these representative sets are listed below:-

<u>Joint Set No.</u>	<u>Dip</u>	<u>Strike</u>
I	80 SW	N 53 W
II	78 NE	N 60 W
III	10 SW	N 19 W
IV	82 NW	N 42 E
V	77 NE	N 31 W

It can be seen from the joint surveys that joint set no. I combined with the other sets divide the strata into many blocks which contribute to an overall potential instability and weakness of this hillside (Plate 4.16 and 4.17). Any undercutting of the underlying soft marls and clays would cause rockfalls and other rock instability (Plate 4.15).



Plate 4.16 Loose blocky appearance of the strata at the crown of landslide V. Rockfall and potential rockslips are the dominant mechanism at this site.



Plate 4.17 Shearing of the strata at the crown of landslide V.

Owing to the presence of impervious layers of marls and clays, alternating with layers of intensely jointed and highly disturbed limestones and marly limestones which can be considered reasonably permeable, the rainwater readily percolates through the limestones down to the clay. Many springs can be observed discharging from this formation of limited extent to the aquifers, these springs generally dry up very soon after the winter months. Thus it is highly probable that there is no permanent water table close to the ground surface in the area. The water table probably rises very fast during periods of heavy rainfall but falls equally rapidly when the rainfall ceases. A temporary spring probably discharging through the fault zone in the lower part of the hill was observed.

The rainfall is the only source of precipitation in this area. The rainfall station at Naur shows the following records for the months and years of the movements:-

Total Rainfall January 1967 (mm)	Total Rainfall 1966 / 1967 (mm)	Average Rainfall January/10 years (mm)	Total Rainfall March 1969 (mm)	Total Rainfall 1968 / 1969 (mm)	Average Rainfall March/ten years (mm)	Total Rainfall April 1971 (mm)	Total Rainfall 1970 / 1971 (mm)	Average Rainfall April / ten years (mm)
238	803.5	118	240	599	110	252	578	44

Table 4.4

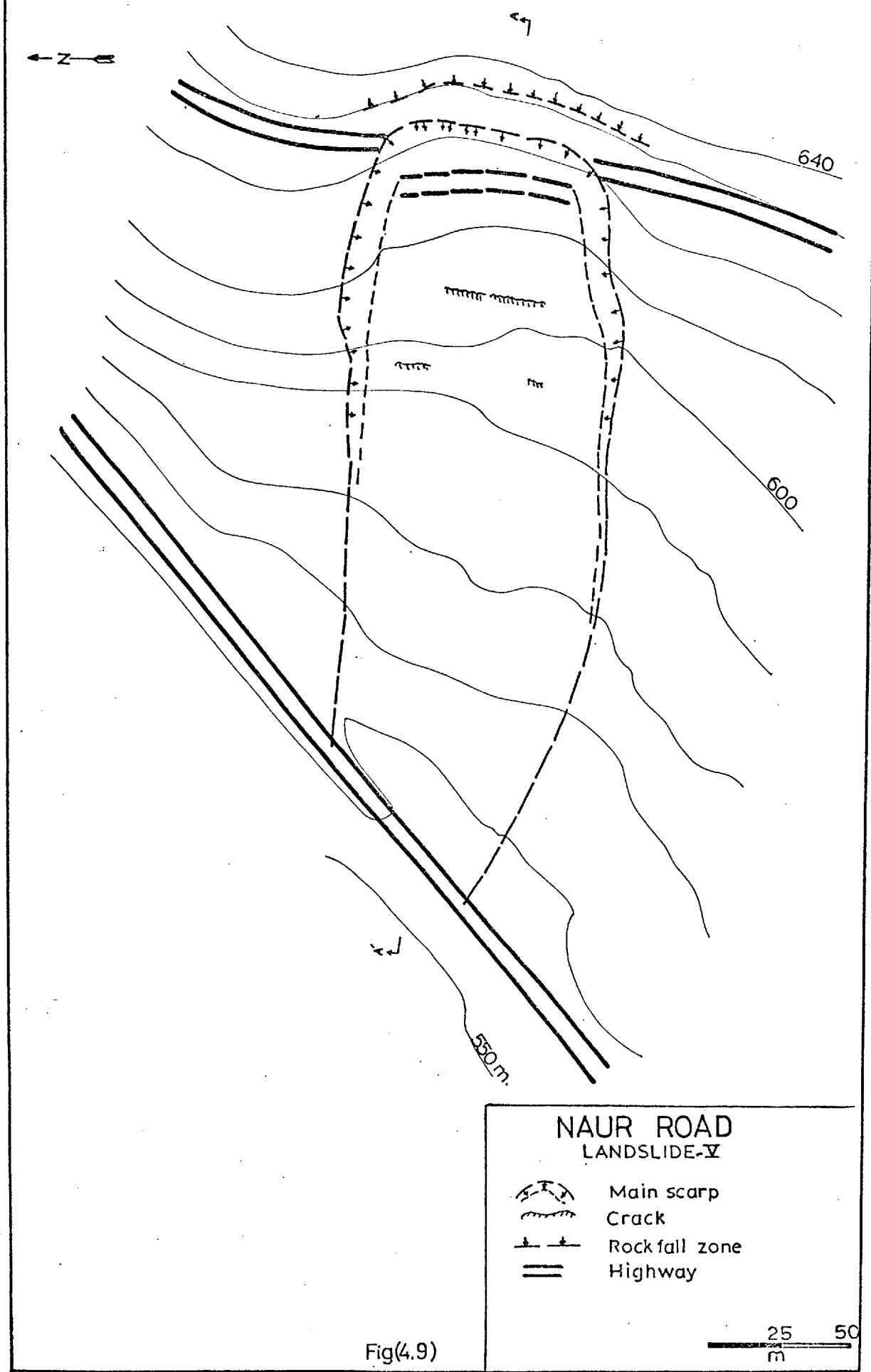
In 1967 rainfall was the highest recorded in ten years, and the January 1967 rainfall was twice the monthly average over the ten preceding years. The winter of 1968/69 was an exceptionally wet one. In March 1969, 240 mm of rainfall (compared with a March average of 110 mm) was over twice the monthly average for the previous year's record (Fig. 4.1). In the month during which the third movement took place, rainfall was approximately six times the monthly average. The annual rainfall for 1971 was also the highest over a ten year record.

4.3.2 Engineering Geology of the Landslide

4.3.2.1 General Description of Landslide V

In January 1967, there was 238 mm of rainfall after which a sudden landslide movement occurred. No investigations were made at the time of the movement. In March 1969, after periods of exceptionally heavy rainfall, a circular type of landslide occurred at 25 Km along the Naur-Adasiye highway. The landslide covers an area of about 25,000 m². The sliding mass moved as an almost monolithic body sinking about 10 m in the upper part (crown) of the slope where a steep clay wall marked as the main back scarp. At the main back scarp and on the flanks the slide had a clear-cut boundary, on which the rotation movement was clearly observed (Fig. 4.9 and Plates 4.2 and 4.20).

NAUR- ADASIYE ROAD MAP OF LANDSLIDE .V (1969)



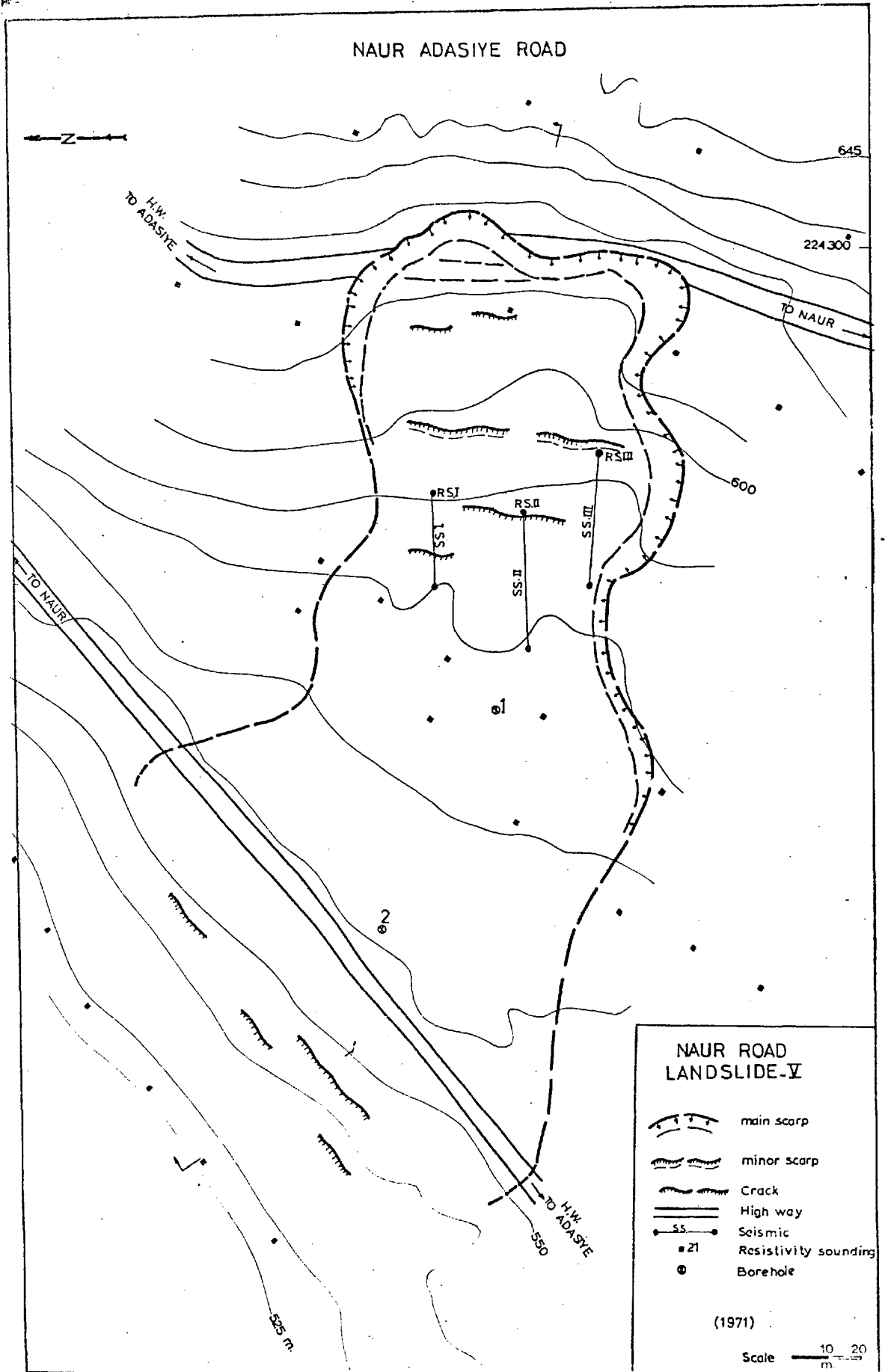
The breadth of the landslide was about 90 m, and its length approximately 250 m. The slide mass comprised an estimated total volume of approximately 500,000 m³. The slide mass sank at the rear, affecting the upper highway but causing little disturbance on the bedrock. The toe material overridden the lower highway (Fig. 4.9 and Plate 4.20). The movement was mainly towards the west. Immediately after the occurrence of this landslide, the Ministry of Public Works began excavating the toe part to open up the lower highway. In this way part of the resisting force was decreased. In April 1971, after a previous dry year and after 252 mm of heavy rainfall, a shallow debris slide occurred with a downward and outward movement. The near vertical main scarp 9.5 m high formed near the edge of the upper highway affecting approximately 3 m of its width, where also a steep clay wall was exposed. A spring discharging from the main scarp was observed (Plate 4.18). The total length of this second movement was about 225 m with a width ranging between 70 and 155m; the affected part of the upper highway was approximately 95 m and the moved material covered about 160 m of the lower highway (Fig. 4.10). The landslide mass was totally disturbed, and was probably in a saturated slurried state at the time movement was renewed. In an attempt to control the renewed movement, the Ministry of Public Works constructed a retaining wall at the edge of the lower highway and excavated the whole toe part of the present landslide. Fig. 4.11 shows three cross sections before and



Plate 4.19 Flow of the material near the main scarp.



Plate 4.18 A spring discharging from the bottom of the main scarp.



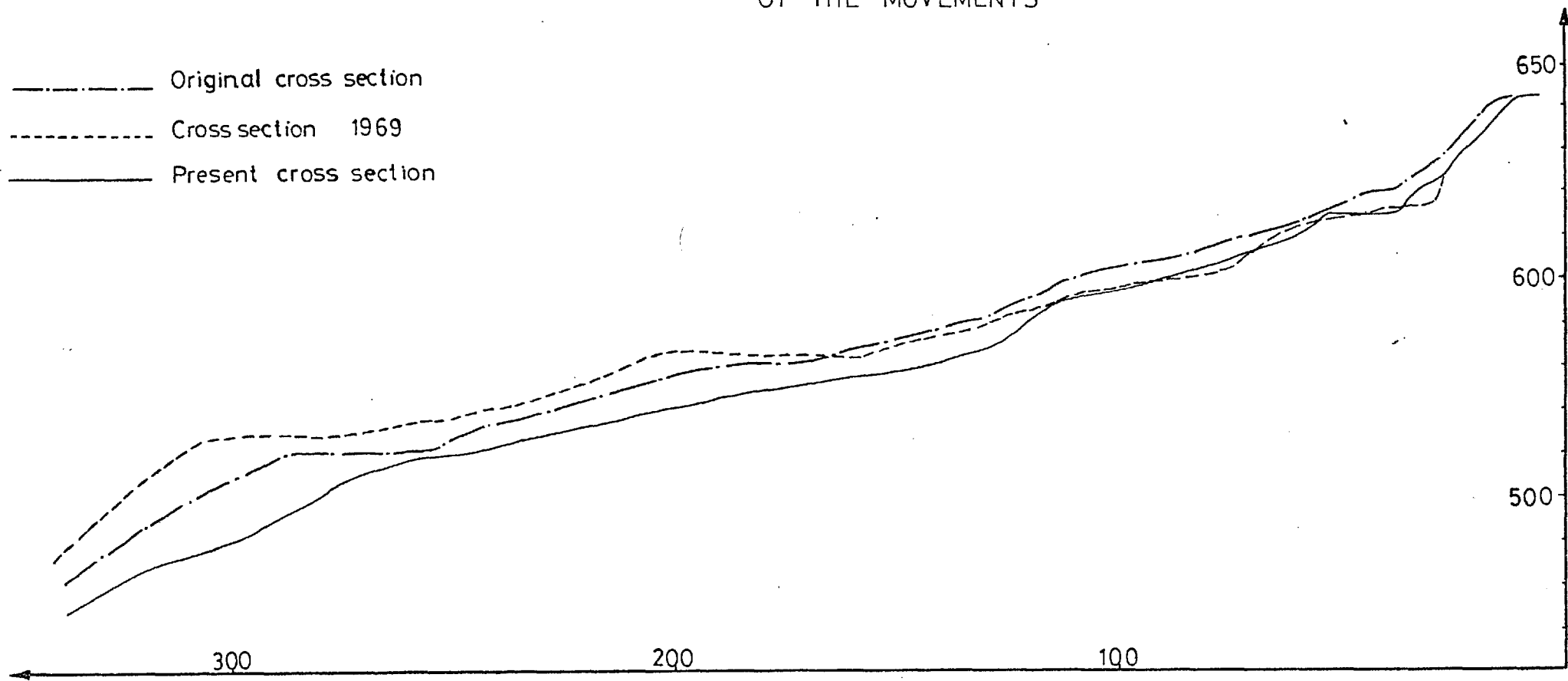
Fig(4.10)



Plate 4.20 General view of landslide V (looking up the slope). The main scarp, left and right flanks, the upper and lower road.

LANDSLIDE .V
CROSS SECTIONS SHOWING THE EVOLUTION
OF THE MOVEMENTS

— Original cross section
- - - Cross section 1969
— Present cross section



after the first movement of 1969 and the present cross section of 1971 after the final excavation.

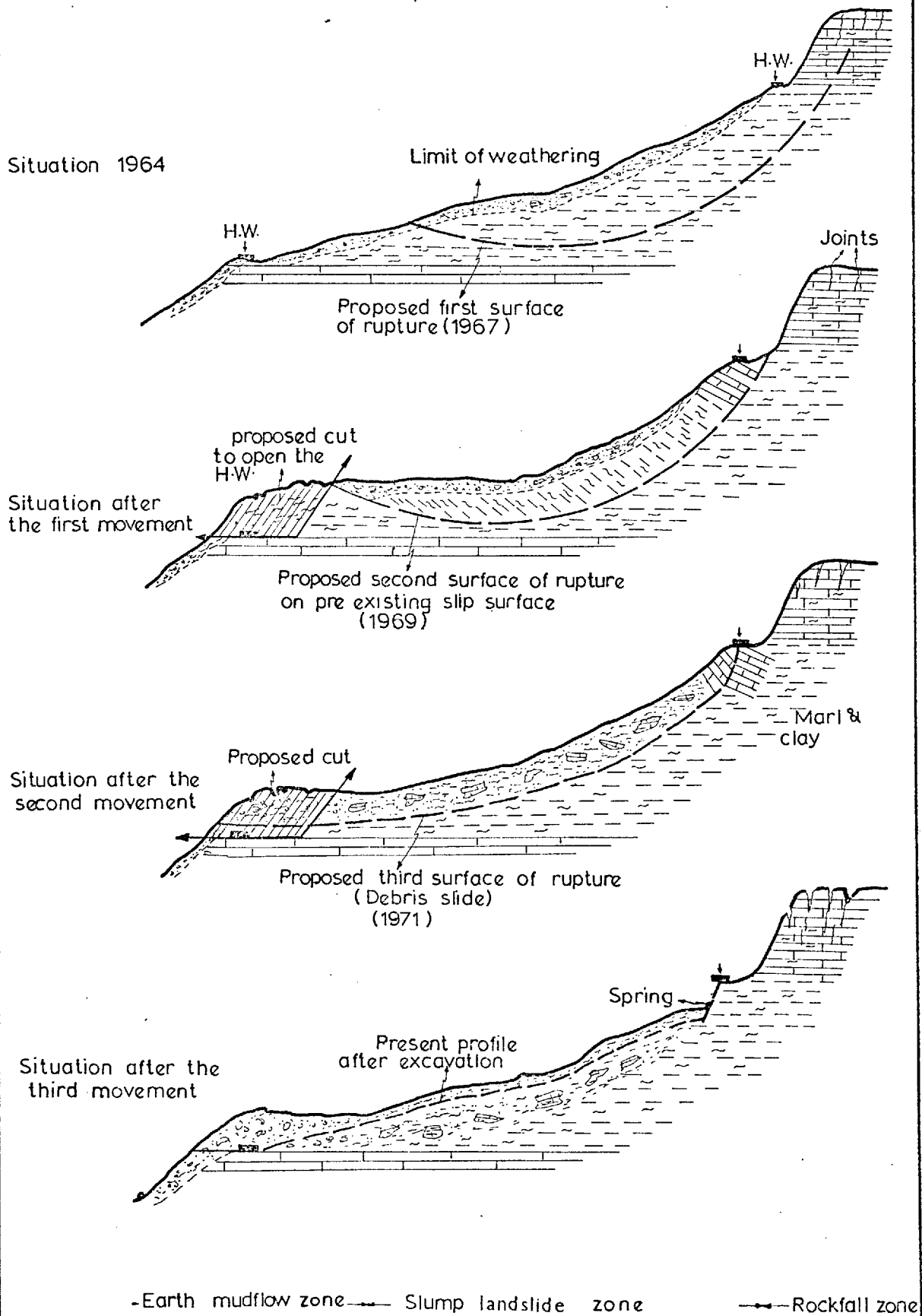
Following these main landslide movements, many types of rock instability were observed, such as rockfalls, rockslips, and probably toppling (Plates 4.2 and 4.15). The landslide area could be divided into three zones of instability.

- a) The main landslide mass (slump landslide zone).
- b) The lower part - earth and mudflow zone.
- c) Crown part - rockfall and potential rockslip zone.

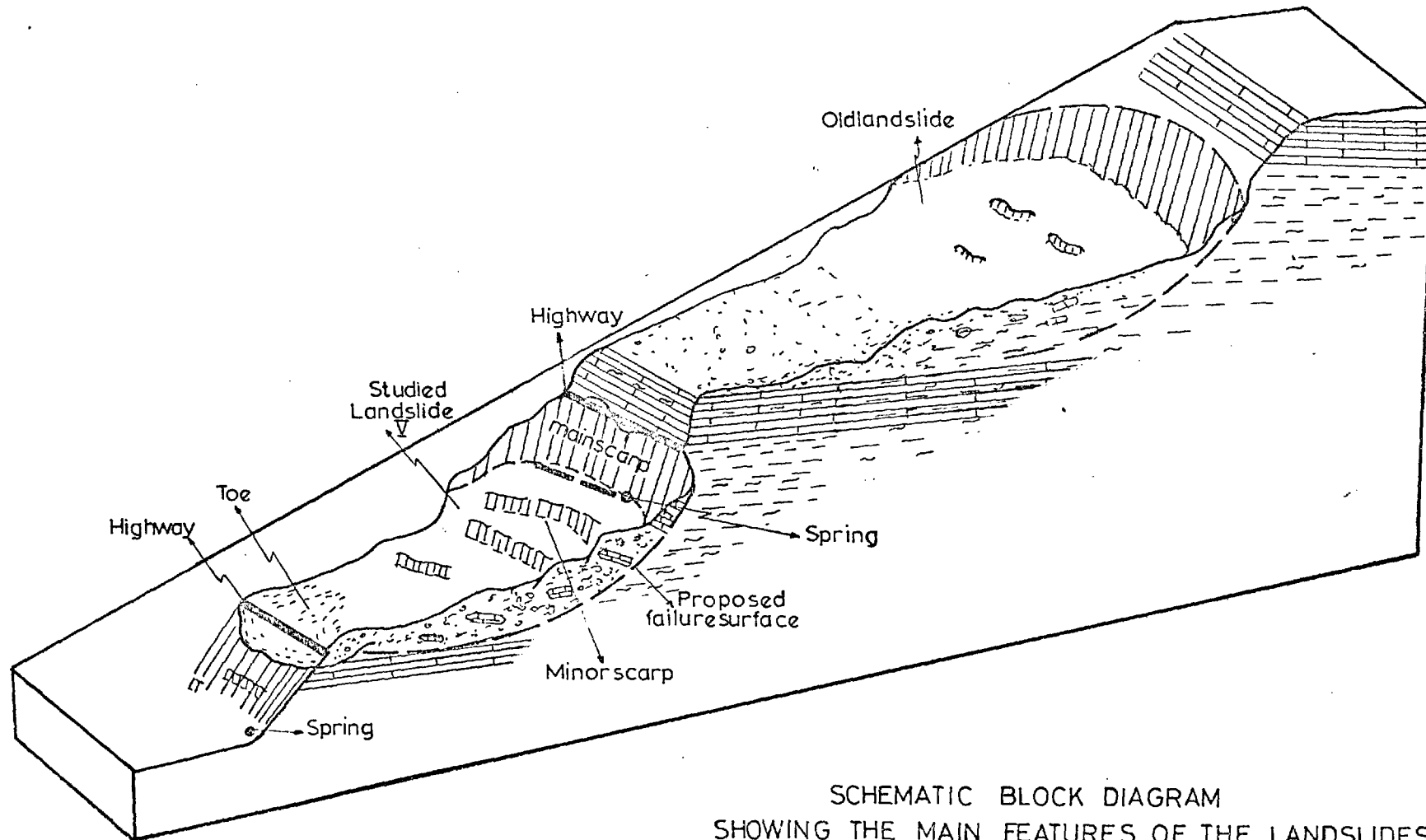
Fig. 4.12 shows the proposed instability zones and the movements in this area. Fig. 4.13 is a schematic block diagram showing the main features of the movements in the area.

It is worth mentioning that these recent movements were located within an old landslide area (Fig. 4.2). The section of the highway between observation points (5) and (9) is located within this old landslide area (Plate 4.13), and shows that the area is still active owing to the occurrence of continuous mudflows as shown on Plates 4.3, 4.4 and 4.5). The progressive opening up of the joints in the cap rock is a sensitive movement indicator.

NAUR- ADASIYE ROAD LANDSLIDE V PROPOSED EVOLUTION OF MOVEMENTS (PRINCIPAL SKETCHES)



Fig(4.12)



SCHMATIC BLOCK DIAGRAM
 SHOWING THE MAIN FEATURES OF THE LANDSLIDES

4.3.2.2 Field Investigations of Landslide V

Following the landslide movement of March 1969, field observations and surveying began and the relevant data were plotted on topographic maps on a scale of 1:1,000 (with a 2 metres contour interval). These maps were prepared by Aero Service Corporation. Many indications of the progressive nature of the slope instability were observed, such as tension cracks in the pavement at the crest of the movement and development of new sets of joints in the upper strata (Fig. 4.8). Very limited trial pits were excavated and some laboratory tests were carried out at the time of this failure (N.R.A.E. Geology Division Internal Report).

At the time of the April 1971 slope failure more detailed field investigations were carried out. Three boreholes were drilled in the vicinity of the landslide mass to locate the actual slip surface, determine the depth of the undisturbed strata, and to observe the groundwater level. It was found that the landslide mass consisted of highly jointed and weathered marls and clays alternating with thin layers of marly limestones underlain by the intensely jointed limestones probably of the Al formation. The slide mass was highly disturbed and remoulded, and many indications of minor failure surfaces were observed. It was therefore very difficult, indeed impossible, to decide

which surface was the actual one for the recent movement. For this reason it was necessary to try trial circles for the stability analysis on the original cross section using the peak strength parameters knowing the portion of the main scarp. Another definite point on the actual slip surface was located in B.H.3 at a depth of about 22.5 m. Typical profiles of the boreholes are shown in Fig. 4.14. The movement boundaries were clearly determined after the huge excavation at the lower part made by the Ministry of Public Works in an attempt to clear the lower highway and control the movement.

The surface geology and the exploratory drilling was supplemented by seismic refraction and resistivity soundings. Self potential profiles were also carried out to detect the occurrence of the ground water zones.

The seismic diffraction survey carried out in the vicinity of the landslide area shows that there are no major structural features, i.e. faults, and that the mass is composed of a weathered zone of low velocity ranging between 350-870 m/sec underlain by marls and clays with velocities in the range of 1200-1750 m/sec at a depth ranging between 2 to 3 metres (Fig. 4.1A).

The Schlumberger expanding method of the resistivity sounding, Fig. 4.2A, carried out suggested that the study area

BH3

BH2

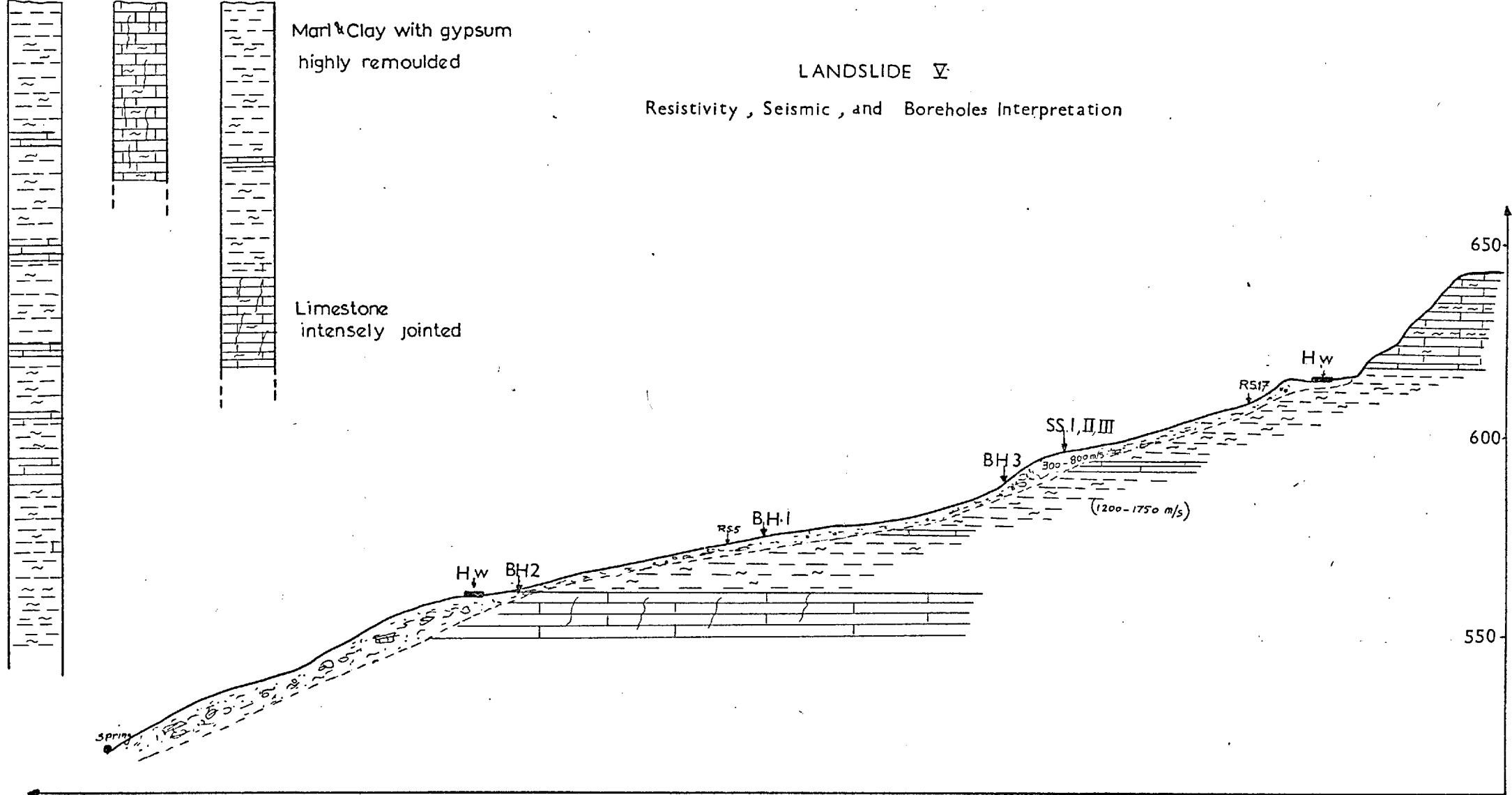
BH1

Marl & Clay with gypsum
highly remoulded

Limestone
intensely jointed

LANDSLIDE V

Resistivity, Seismic, and Boreholes Interpretation



Fig(4.14)

was influenced by one major fault, crossing the left flank and going through the toe part of the landslide. This was verified by the surface geological mapping and study of the aerial photographs.

The variation in seismic velocity and apparent resistivity correlate well with the surface geology and the information obtained from the exploratory drilling. The following table shows the average resistivity and velocity of the materials in the vicinity of the landslide:-

Zone	Apparent Resistivity Ω/m	Seismic Velocity m/sec
Mantle	7-42	300-870
Marl and Clay	42-100	1200-1750
Bedrock	>100	

Table 4.5

The self potential profiles carried out show that the water is flowing at most locations across the area. This observation is confirmed by the active seepages observed near the main scarp and at the lower point of the hill, probably discharging through the fault zone.

A lithological cross section of the site of the landslide was prepared based on all the information obtained, i.e. exploratory drilling, geophysical surveys and surface geological mapping. This cross section is shown in Fig. 4.14.

4.3.2.3 Laboratory Investigations

In the course of the 1967 movement, no field and laboratory investigations were made. Detailed field and laboratory investigations were carried out immediately after the 1971 movement took place. Representative disturbed and undisturbed samples were obtained, and laboratory testing programmes were devised and performed on these samples to establish the engineering properties of the materials in this area. A summary of the representative samples is compiled in Table 4.2B. The principal index test results are compiled in the following Table 4.6.

Index Properties		Range	Mean	No. of Samples
Liquid Limit	L.L.	54.7 - 89.3%	74.0%	7
Plastic Limit	P.L.	17.0 - 27.4%	21.9%	
Shrinkage Limit	S.L.	3.4 - 14%	8.8%	
Clay Fraction	<2 μ	65 - 84%	77.6%	
Activity		0.50-0.75	0.64	
Liquidity Index	L.I.	-0.18 - 0.15	0.02	
Max. Water Absorption		64.8-113.3%	89.7%	
Specific Gravity		2.56-2.72	2.63	
Wet Bulk Density	γ_B	1.83-2.04 g/cm ³	1.95 g/cm ³	
Natural Water Content	Wc	10.2 - 32.5%	21.6%	
Porosity	n	22.8 - 43.7%	38.3%	
Void Ratio	e	0.29-0.77	0.64	
Calculated Degree of Saturation		81.3 - 100%	91.0%	
Total Soluble Salts	%	0.07 - 3.0%	1.1%	

Table 4.6

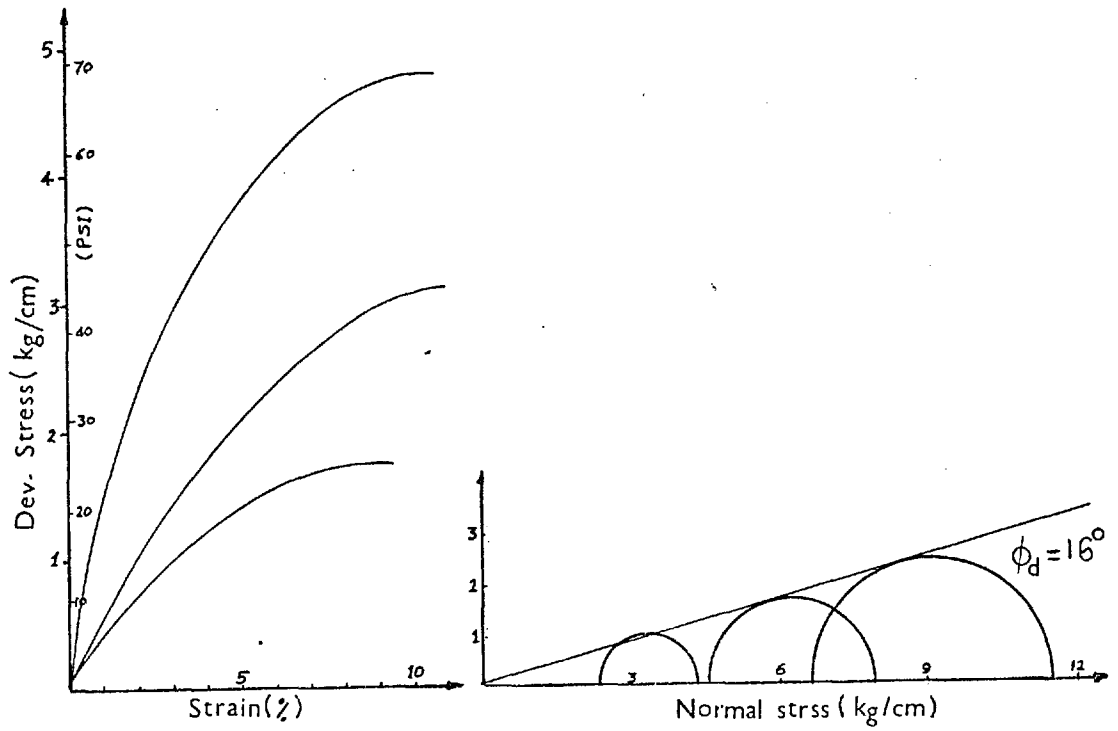
On the conventional plasticity chart (Fig. 4.3) points are plotted for the ten samples from which the average values in the above table have been obtained. All the points lie above the A-line and the clay is mainly CH (inorganic clays of medium to high plasticity). This type of clay is typically characterized by low shear strength and low workability as a construction material, and is usually impervious with a high compressibility when compacted and saturated. Such material should not be used as a foundation and surfacing for roadways owing to its low resistance against erosion.

The activity values show that this type of clay would be classified as inactive clay (Skempton, 1953) (Fig. 4.3). The liquidity index suggests that this clay could be classified as stiff clay (Terzaghi, 1936). The natural water content is slightly above the plastic limit, which indicates that the clay is slightly over-consolidated at the present time, but is partially saturated. The total soluble salts increase from 2245 ppm at a depth of 2.5 m to a maximum of 3017 ppm at a depth of 5.5 m and then decreases with depth to 1347 ppm at 10 m. The plastic limit decreases with depth from 21.1% at 5.5 m to 16.3% at 10 m, and also the liquid limit decreases with depth from 50.3% to 43% at a depth of 5.5 and 10 metres respectively. This decrease with depth is probably related

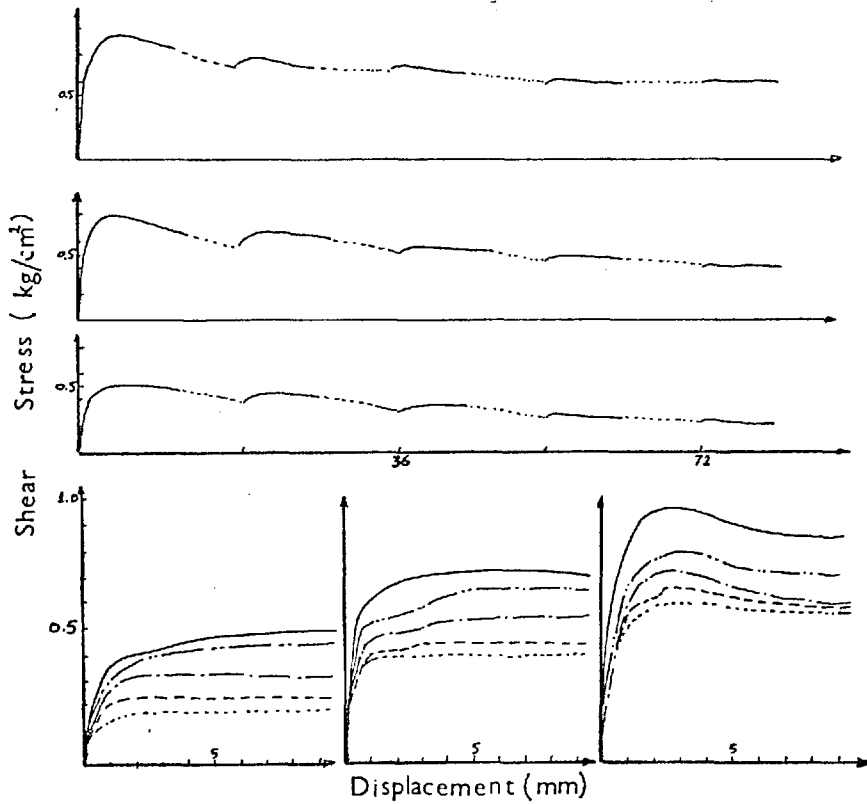
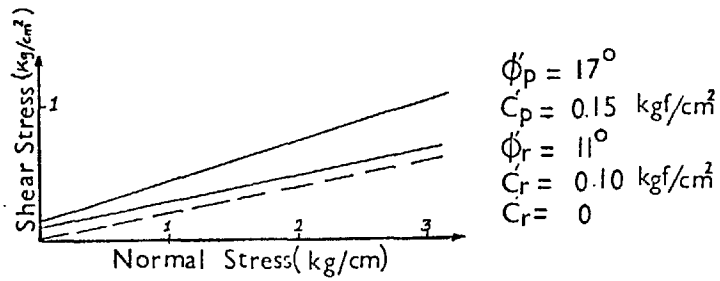
to the observed decrease in clay fraction (-2μ) with depth (Table 4.7). The chemical analyses of water issuing from the two springs from the main scarp and from the lower part of the landslide show that the lower spring water contains less salts than the upper one, indicating that the landslide mass probably has been subjected to leaching (Table 4.8).

Shear strength parameters in terms of effective stresses were determined by carrying out consolidated undrained triaxial compression tests with measurement of pore water pressure on three or four specimens 3 x 1.5" in diameter taken from the same sample. The tests show the following average shear strength parameters of three tests expressed by: $C'_p = 0.15 \text{ Kgf/cm}^2$, and $\phi'_p = 13^\circ$.

Representative peak and residual shear strength parameters were also determined by carrying out drained direct shear box tests on 6 x 6 x 2.5 cm with maximum relative displacement of about 9 mm, and subjected to reversals and reshearing until no further drop in shearing resistance was observed. The displacement rate was at a very slow speed (0.0000769 in/min) to avoid building up any excess of pore pressures. The test results could be represented by $C'_p = 0.15 \text{ Kgf/cm}^2$, $\phi'_p = 17^\circ$ and $C'_r = 0$, $\phi'_r = 11^\circ$ (Fig. 4.15).



Drained Triaxial Test



Multi reversal Shear Test

Fig(4.15)

Sample Depth (Borehole 1)	Atterberg Limits			Gradation Analysis			T.D.S.*
	L.L.	P.L.	S.L.	Clay %	Silt %	Sand %	
2.5 - 3.5 m	55.80	19.35	13.17	58	36	6	2245
4.0 - 4.5 m	50.28	21.15	4.69	74	26	0	2042
5.5 - 7.0 m	35.37	16.31	14.59	45	52	3	3107
8.6 -10.0 m	42.99	16.18	10.96	52	43	5	1347

Table 4.7

Sample Location	TDS ppm	Ca ⁺⁺ meg/L	Mg ⁺⁺ meg/L	Na ⁺ meg/L	K ⁺ meg/L	Cl ⁻ meg/L	SO ₄ ⁼ meg/L	CO ₃ ⁼ meg/L
Spring 1	896	4.7	5.6	3.8	0.07	5.19	4.7	0.0
Spring 2	409	3.5	2.1	1.05	0.06	1.38	0.64	0.0

Table 4.8

The materials in the area investigated suffered considerable shear displacement and probably leaching, therefore the observed drop from the peak to the residual is limited and the intercept cohesion is almost small. The greater the shear displacement suffered, the lower will be the drained peak strength and closer this will approach the residual value (Skempton, 1970), and also the greater the amount of leaching in the soils the lower will be the intercept cohesion. Reduction in salt content below 5 g/L in the material causes critically sensitive clay and may flow spontaneously and render the clay unstable (R.S. Liebling),

* T.D.S. Total dissolved salts.

and also when the leaching produced a salt content of less than 15 g/L, a noticeable increase in sensitivity resulted (Skempton and Northey, 1952).

The mineralogical analyses of these clays were carried out using the differential thermal analysis, and X-ray diffraction on cavity mount and oriented samples, which shows that this clay is mainly illite, montmorillonite, kaolinite, gypsum, calcite and traces or organic impurities (discussed in Section 4.2.2 and described in detail in Appendix C.1.

The chemical analyses of the representative samples from the slide area yielded the results summarized in Table 4.3 showing a high content of CaO, Al_2O_3 , K_2O and MgO, indicating that the montmorillonite is of the Ca-type compared with the low Na content.

4.3.2.4 Slope stability analyses

At the time of the original site investigations for the highway and after the first movement of 1967, no assessment of the stability of the existing slopes was made. After the movement of 1969 a stability analyses was made using the Fellenius method (N.R.A. Eng. Geol. internal report).

The stability analysis in terms of effective stresses in the form described by Bishop (1954) has now been made on the original cross section (before the movement occurred) and on the present cross section (after sliding).

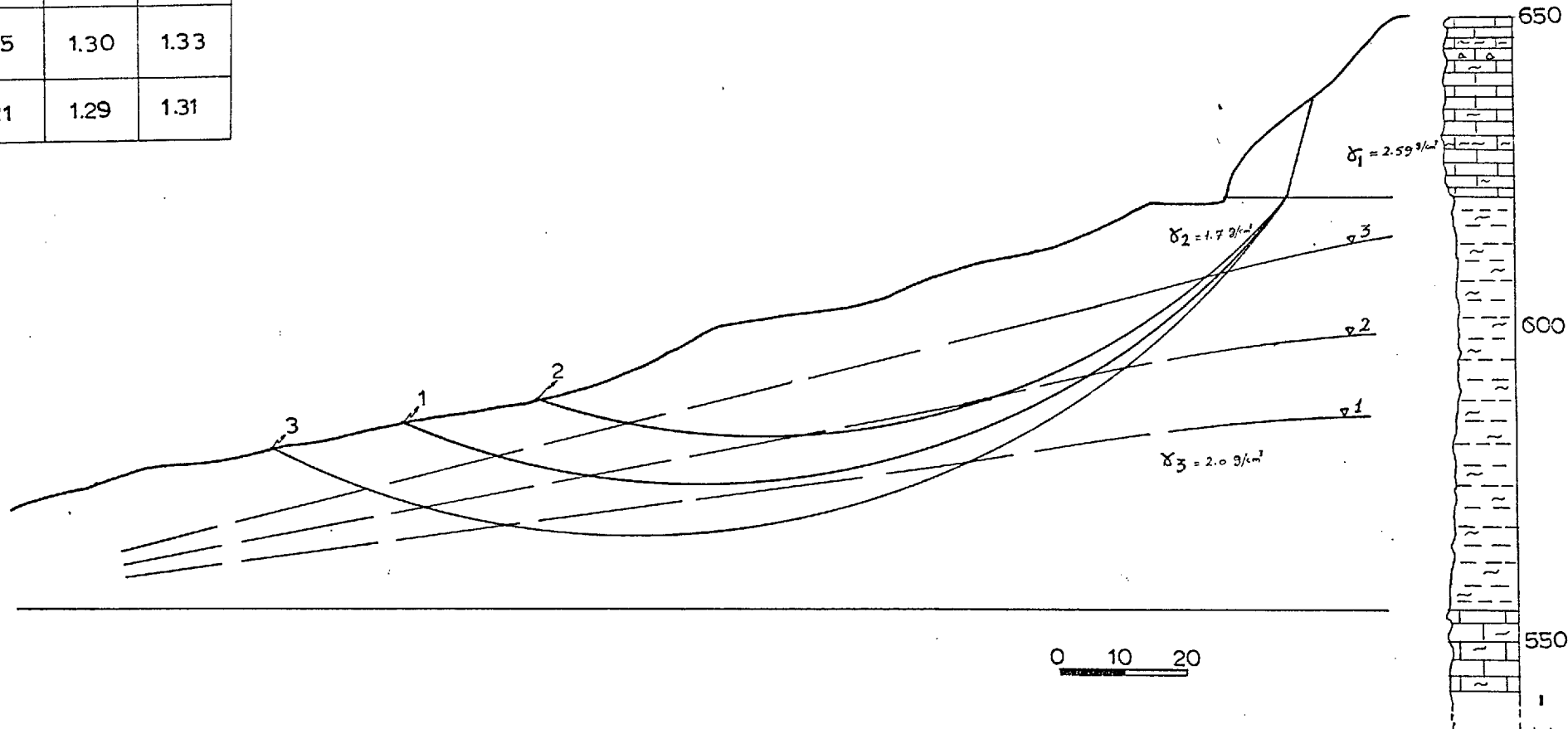
As can be seen from the cross sections, the slide mass is composed of three zones of different densities, the upper limestone strata, a weathered zone, and a clay zone. The average mass densities of the zones are 2.59 g/cm^3 , 1.7 g/cm^3 , and 2.0 g/cm^3 respectively.

Stability analyses for the original cross section (before sliding) were carried out using peak strength parameters in terms of effective stresses represented by $C'_p = 0.15 \text{ Kg/cm}^2$, $\phi'_p = 17^\circ$, knowing the location of the main scarp, one point along the slip surface and the approximate location of the toe part, and also assuming transient perched water tables in positions 1, 2, 3 respectively acting on the slip surface at the time of failure during a heavy rainfall (Fig. 4.16). It was found that the trial circle no. 3 with transient water table in position 3 is the most critical, where the movement would have occurred when the factor of safety is equal to unity.

To analyze the stability of the present slope (after the movements), trial circle no. 3R corresponding to the actual slip surface using the residual strength parameters represented

CIRCLE No.	FACTOR OF SAFETY			
	W.T. 3	W.T. 2	W.T. 1	NO W.T.
1	1.10	1.28	1.32	1.34
2	1.07	1.25	1.30	1.33
3	1.02	1.21	1.29	1.31

LANDSLIDE.V
ORIGINAL CROSS SECTION
(BEFORE SLIDING)



Fig(4.16)

by $C'_r = 0.10 \text{ Kgf/cm}^2$, $\phi'_r = 11^\circ$, it was found that these parameters under-estimate the factor of safety.

The analyses were also carried out on the present cross section using the fully softened strength parameters represented by $C'_d = 0$, $\phi'_d = 16^\circ$; it was found that the factor of safety is 1.06 assuming no excess water table and 1.05, 0.94, 0.73 assuming water table in positions 1, 2, 3 respectively (Fig. 4.17).

In the light of these analyses it was clearly shown that in its present condition the slope remains potentially unstable and it is sensitive to any perched water table present in the slipped material which will be sufficient to activate further movement. This situation is verified by field observation which indicates the progressive nature of the movement.

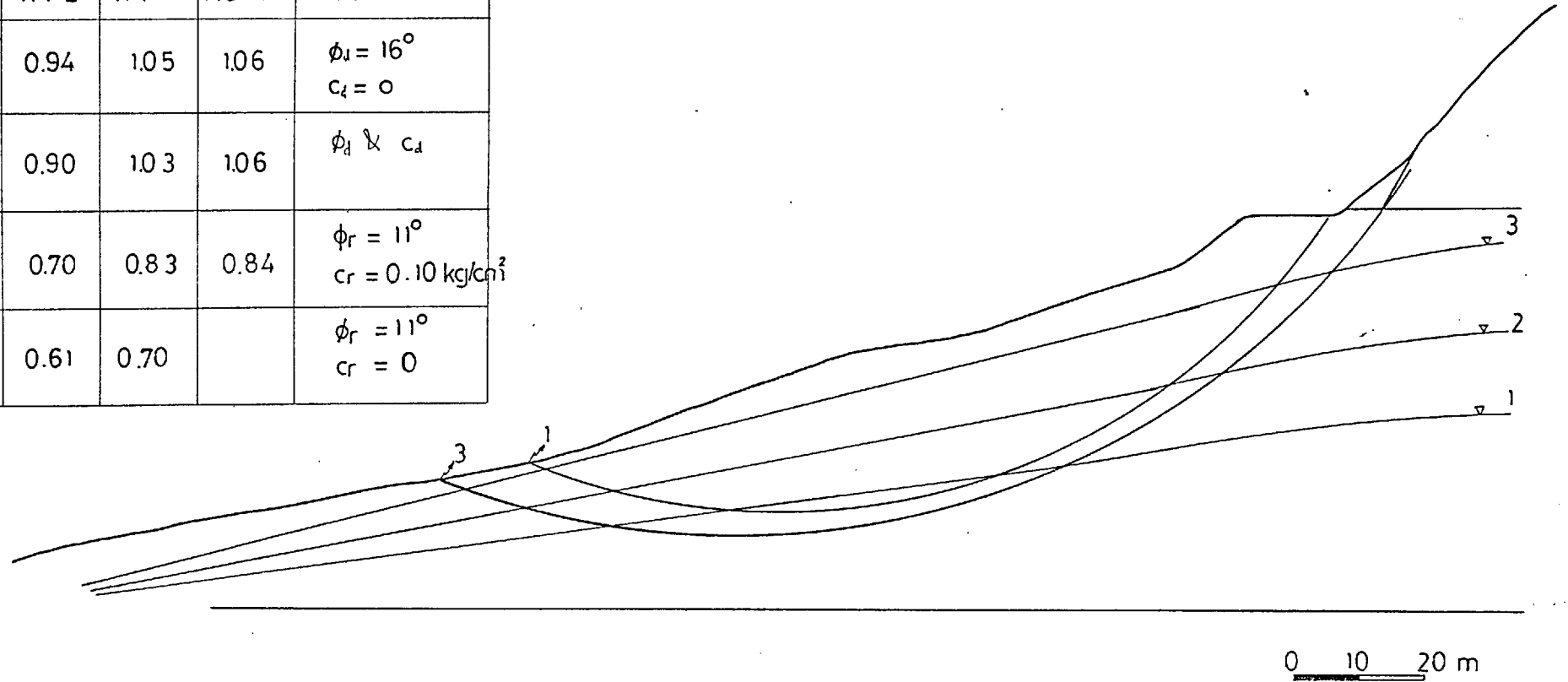
4.3.2.5 Remedial measures

The remedial measures for landslide V are shown in general outline in Fig. 4.18. These can be summarised as follows:-

- (i) Reducing the driving forces by excavating near the crown part of the landslide.
- (ii) Increasing the resisting forces by excavating the

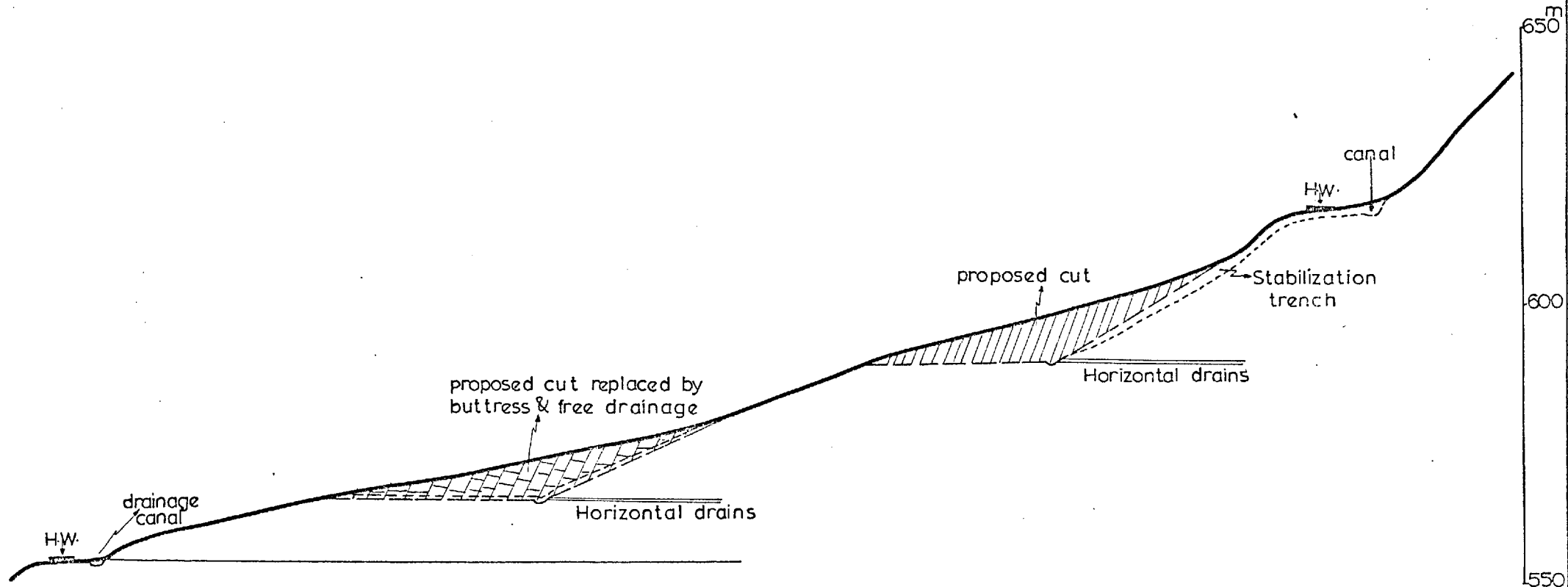
LANDSLIDE. V
PRESENT CROSS SECTION
(AFTER SLIDING)

CIRCLE No.	FACTOR OF SAFETY				REMARKS
	W.T. 3	W.T. 2	W.T. 1	NO W.T.	
1	0.73	0.94	1.05	1.06	$\phi_d = 16^\circ$ $c_d = 0$
3	0.71	0.90	1.03	1.06	$\phi_d \ \& \ c_d$
	0.57	0.70	0.83	0.84	$\phi_r = 11^\circ$ $c_r = 0.10 \text{ kg/cm}^2$
	0.48	0.61	0.70		$\phi_r = 11^\circ$ $c_r = 0$



Fig(4.17)

REMEDIAL MEASURES FOR LANDSLIDE ∇



Fig(4.18)

low strength material near the toe part and replacing it with a buttress. The bottom of the buttress should consist of a free draining blanket.

- (iii) Stabilizing and draining the embankment by constructing a stabilization trench within the embankment of the upper highway.
- (iv) Horizontal drains should be constructed at the proper places to carry away water from the slide.
- (v) Providing paved drainage canals to divert the water from the area.

4.3.2.6 Conclusions

In the light of the field and laboratory investigations and analyses, it is quite evident that the following factors probably contributed to the movements of landslide V:-

1. The presence of tectonic and old landslide movements in the area contributed to the weakening of the material in the region owing to disturbance of its structure.
2. Absence of surface and subsurface drainage.
3. Abnormally high precipitation.

4. The fill material of the embankment with steep gradients touched off the stability balance of this area.

All these factors combined to the disturbance of the natural equilibrium of this area and probably the occurrence of the movement.

The conclusions arising from these investigations may be summarized as follows:-

1. The movements of 1967 and 1969 were of rotational circular type followed by rockfall and potential rockslips at the crest of the slope. The movement of 1969 was re-activating movements along the pre-existing slip surfaces within the landslide of 1967 (Fig. 4.12). The movement of 1971 was a typical shallow debris slide.
2. The strength of the clay falls to its residual value when shear displacements are sufficiently large to develop a continuous slip surface (Skempton, 1972). The residual strength parameters obtained from multi-reversal shear test on undisturbed samples yields the following representative results; $C'_r = 0.10 \text{ Kgf/cm}^2$, and $\phi'_r = 11^\circ$. The residual values obtained from remoulded samples with pre-cut planes show that the cohesion disappears with $\phi'_r = 11^\circ$.

3. The results of drained triaxial compression tests performed on normally consolidated (remoulded) clay gave values of $C'_d = 0$, $\phi'_d = 16^\circ$. The absence of cohesion leaves it reasonable to conclude that this material reverted to its fully softened strength (after the idea by Skempton, 1970). These parameters are the most reliable for use in the stability analysis, owing to the amount of disturbance in the area, which suffered significant shear displacement.
4. The rainfall of 1967, 1969 and 1971 were very high compared with twenty years' record, and the hydrology of this area could be described as conduit hydrology. The landslide mass is considered to be in a fully saturated state during periods of high temporary water table, but no permanent water table near the surface was observed in the landslide area.
5. The clay in the slide area may be classified as a normal to inactive clay. The dominant minerals in the clay are illite, kaolinite, and montmorillonite. The main index properties of the clay are: $W_c = 22\%$, $LL = 74\%$, and $PL = 22\%$, $-2\mu = 77\%$.
6. Stability analysis of the original cross section using Bishop's method gave a minimum calculated factor of safety

of 1.02 on a critical circle corresponding closely to the actual slip surface. The slope is still potentially unstable and renewed movements can be expected in periods when the water table rises close to ground surface.

7. The proposed remedial measures of this area would improve the factor of safety by about 21%.

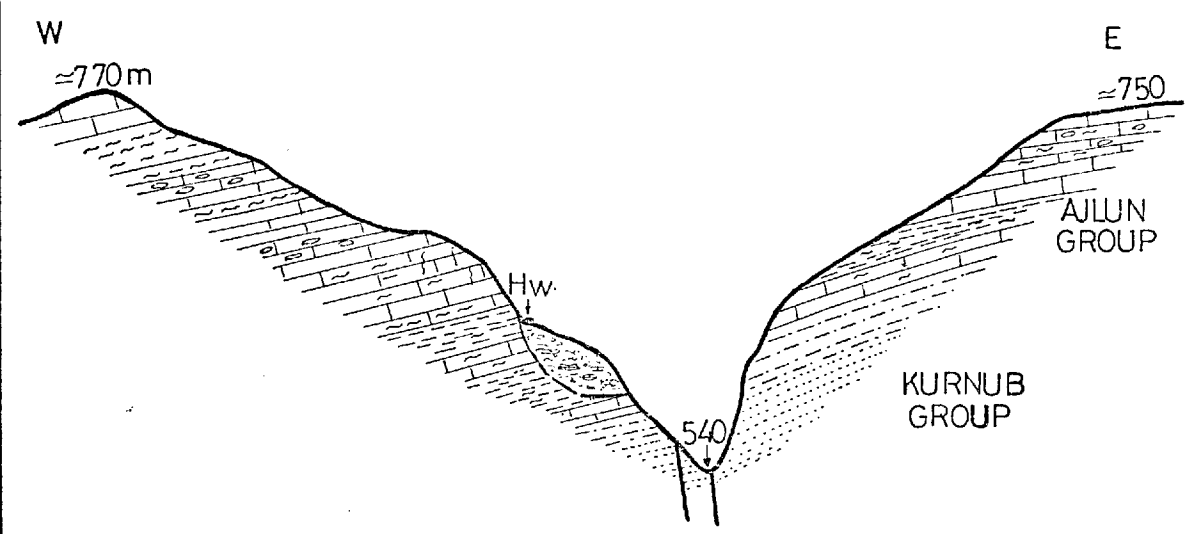
4.4 DETAILED INVESTIGATION OF LANDSLIDE VI

4.4.1 Geology and Hydrogeology

The slide area lies on the Amman-Jerusalem highway, approximately 20 Km southwest of Amman, between Naur and Adasiye. This area is mountainous with a highest elevation of 770 m towards the southwest, but the height decreases gradually to 540 m towards the northeast at the level of Wadi Umariye (Figs. 4.2, 4.19 and Plate 4.21).

Detailed geological maps were prepared on a 1:1,000 and 1:5,000 scale, checked by the study of the aerial photographs of 1:10,000 and 1:25,000 scales. The geology and main features of the movement were superimposed on the 1:1,000 scale map (Fig. 4.20).

Two distinctive rock units are exposed at the site of landslide VI; the Upper Kurnub Group and the marl-clay unit (A1, 2, 3) of the Lower Ajlun Group. The Kurnub Group is exposed as the oldest rock unit at about 2 Km west of Naur. Quennell (1951) and Burdon (1959) gave the age of this unit as Oxfordian to Albian. The uppermost part of this group consists mainly of grey marls, green clays and silty clays. The total thickness of the Kurnub Group in the area of landslide VI is probably around 250 m. The Kurnub Group is overlain by the



SCHEMATIC GEOLOGICAL CROSS SECTION

Fig(4.19)

Modified after (Ruef 1964)

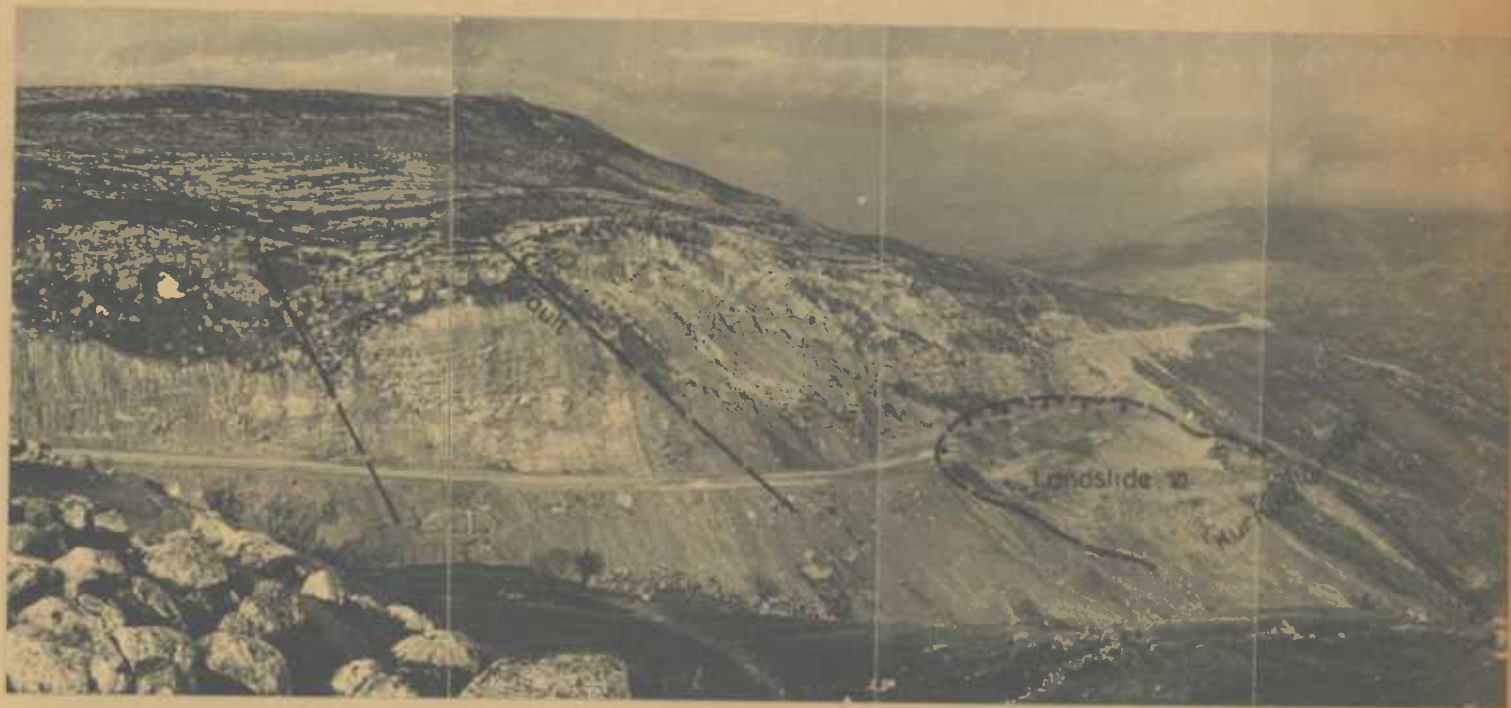


Plate 4.21 General view of the study area of landslide VI.

marl-clay unit of the Lower Ajlun Group. The latter is composed of yellow or grey marls, green clays and dark grey to black shales alternating with highly jointed limestones and marly limestones. The thickness of the marl beds within this unit reach 40 m thickness (Ruef, 1964). The total thickness of the marl-clay unit is between 300-370 m (Wiesemann, 1964).

At the site of landslide VI the strata is obscured by a mantle of weathered materials of an average of two metres in thickness. The bottom of the slopes in this area is covered by a thicker mantle consisting of soil, gravels, and huge boulders larger than 25 m^3 , indicating the amount of weathering and old landslide movements in the area. The bedrock is exposed at the crest of the landslide, and shows a distinctive loose blocky appearance owing to the weathering and jointing. The strata dip is 15° SW and the dip steepened to 70° , caused by flexure which is exposed in a wadi at Km 20.400. This wadi apparently follows a fault which forms an extension of the flexure. The main structural feature which dominates the area between the Wadi Bahhath to the NW and the upper course of Wadi Umtina to the SE is a broad anticline whose axis terminates towards the SW (Ruef, 1964). The NW and SE limbs are formed of the marl-clay unit. The study area is intersected by two major faults trending NW-SE and NE-SW which are approximately parallel to

the left and right flanks of the landslide (Fig. 4.20). However, the strike of the faults in the vicinity of the study area varies between 50° and 110° . At the western slope, at the level of the highway, the intensely jointed strata is trending at $N20^{\circ}E$ with a dip of approximately 8-16 NW. Three joint sets were mapped in this strata, one set trends $N25W$, the second trends $N22E$, and the third $N60W$. The dips of these sets are 46° NE, 82° SW and vertical respectively.

According to the hydrology observation station in Naur, the annual rainfall is 511 mm. The precipitation in the month during which the landslide took place (February 1964) was about 2.5 times the monthly average over the ten years and the total rainfall in 1964 was 610.5 mm.

Station	Total rainfall (mm)	Total rainfall (mm)	Average rainfall February/10 yrs. (mm)
Naur	141.5	610.5	66.5

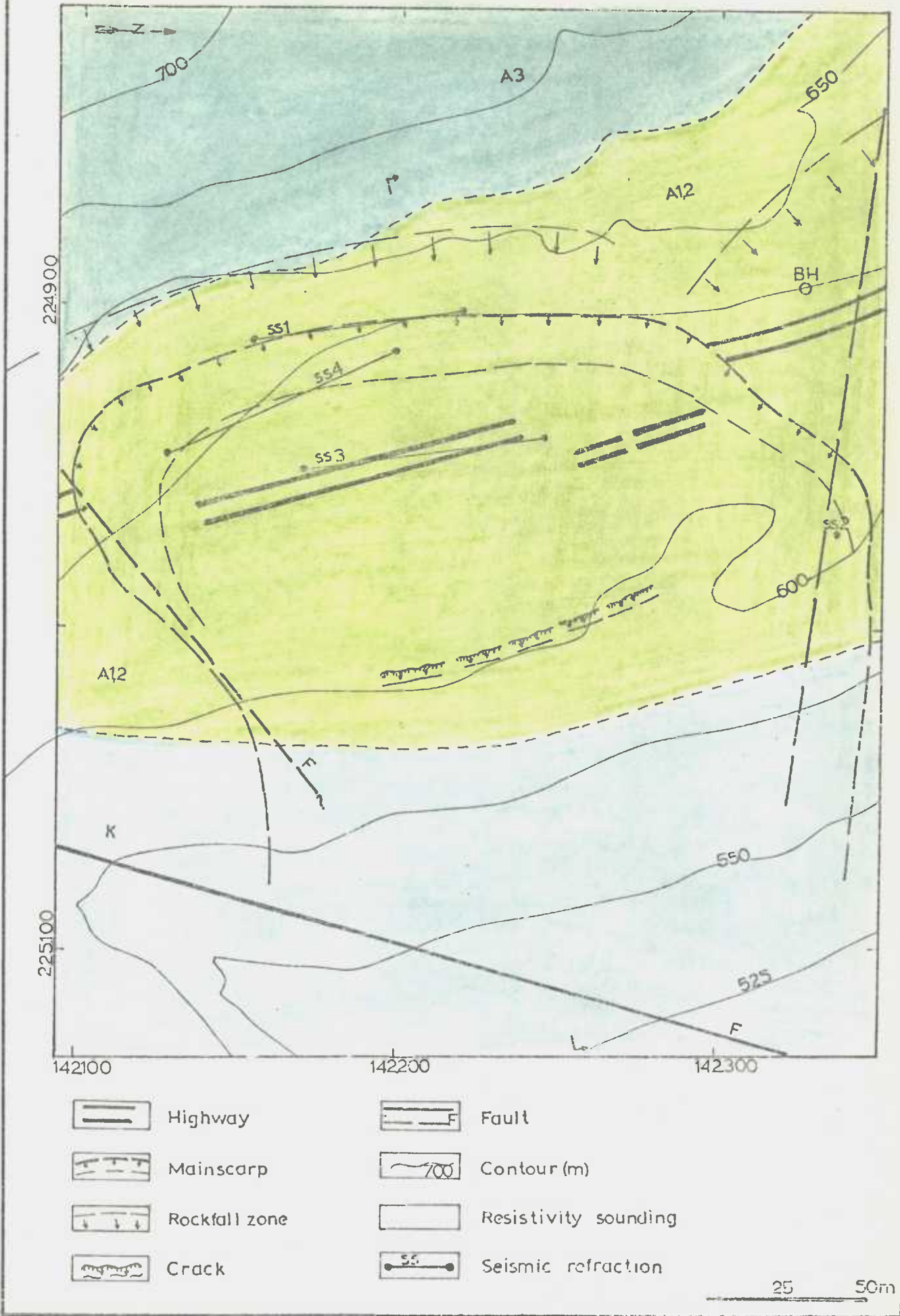
4.4.2 Engineering Geology of the Landslide

4.4.2.1 General description of landslide VI

The section of the Amman-Jerusalem highway at the site of landslide VI is situated at an elevation of approximately 620 m, on fill materials of nearly 20 m thick. During the

LANDSLIDE - VI

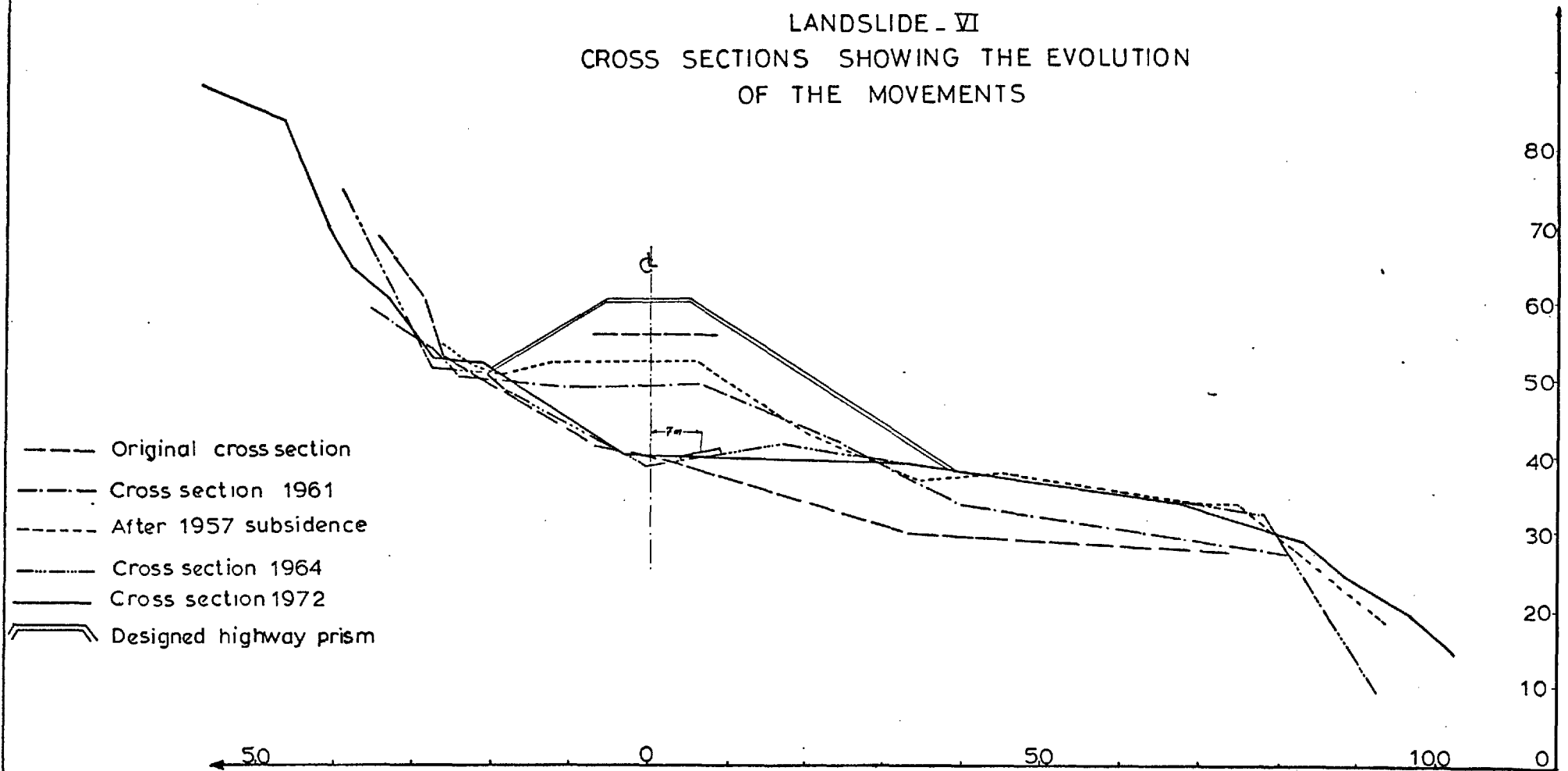
GEOLOGIC MAP



Fig(4.20)

construction of the highway in 1956 a subsidence of approximately 7.5 m vertical displacement occurred. Construction continued after repairs to the damaged section were completed. New fill was placed, but the required design height of the highway could not be reached, owing to the progressive nature of the movement. In 1957 a new movement of apparently 5.5 m vertical displacement commenced (Fig. 4.21). After the subsidence of 1957 numerous boreholes were made in the vicinity of the moved mass, but they were not deep enough to reach the undisturbed bedrock. In February 1964, following a month of 141 mm continuous heavy rainfall and 610 mm total rainfall in the winter season, the major landslide movement occurred. As a result of the translational movement the slide mass sank about 12 m at the main scarp with an outward horizontal displacement of 7 m northeast direction. The main scarp of the movement is at an elevation of 625 m, affecting all the width of the highway. The breadth of the landslide was about 245 m, and the length along the long axis is about 125 m, the axis approximately trending N74E on the west slope of Wadi Umariye. The slide mass covers an area of approximately 40,000 m². After the occurrence of the 1964 landslide, no direct indication of the progressive nature of this movement was apparent. As a result of the movement, internal disturbance in the strata and in the moved mass was

LANDSLIDE - VI
 CROSS SECTIONS SHOWING THE EVOLUTION
 OF THE MOVEMENTS



Fig(4.21)

observed, which can be a good indication of a non-circular movement. The first two-thirds of the failure surface of the landslide is in the plastic clay layers, while the last section was mainly tangential to the limestone bedrock (Fig. 4.22).

4.4.2.2 Field investigations of landslide VI

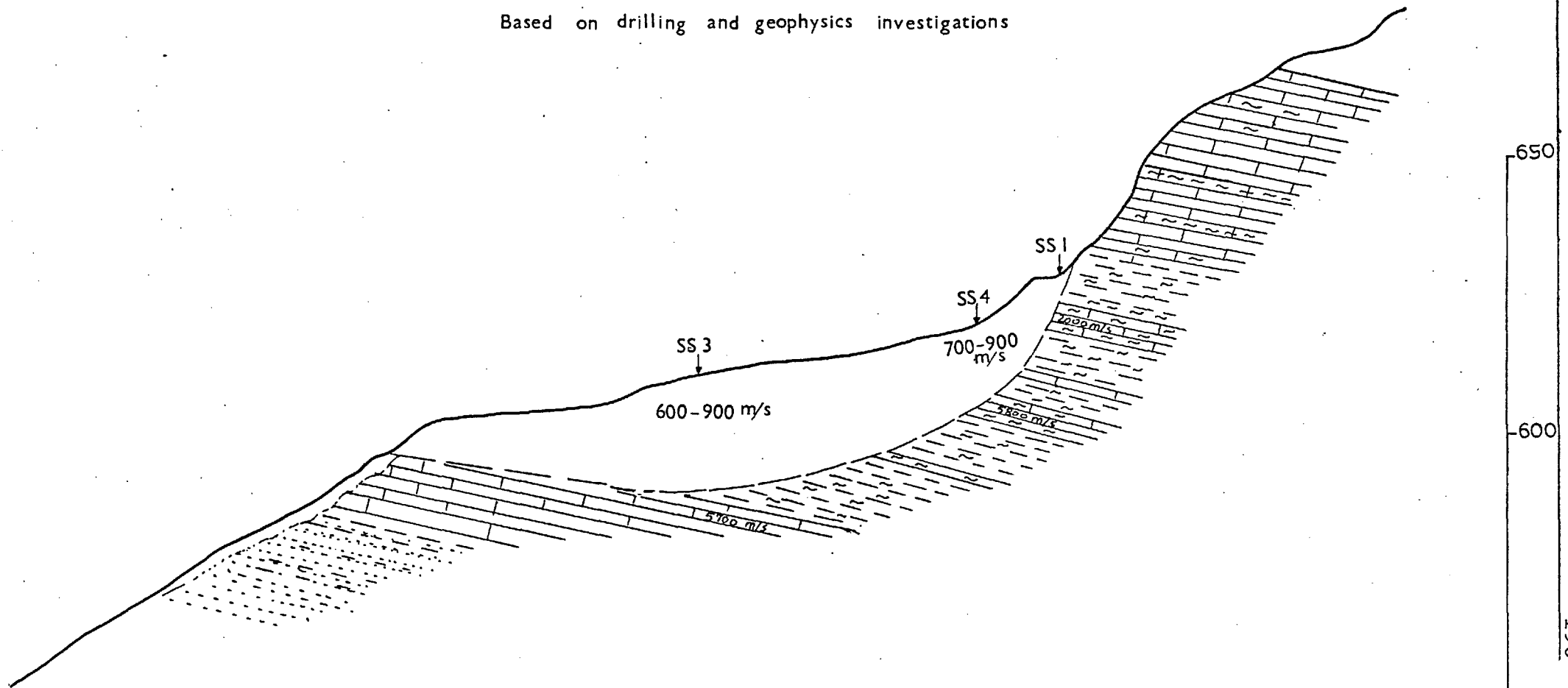
Following the landslide movement of February 1964, and after unsuccessful attempts to reconstruct this section of the highway, a temporary by-pass road 11 Km in length was proposed (Route 3, Fig. 4.2) by the Ministry of Public Works. The centre line of this route crosses the upper part of the A3 formation which is composed of limestones and marly limestones alternating with marls. No major landslides were observed along this line, during which a new route was proposed (Fig. 4.2). However, the proposed new route (3) was located on an old landslide area between observation points (4) and (9).

After the occurrence of landslide V along route (2), an intensive field investigation began. Three boreholes were drilled in the vicinity of landslide V, and one borehole was drilled in the area of landslide VI. In addition seismic refraction and resistivity surveying were carried out.

The cores from the exploratory boreholes in this area show that the strata is composed of limestones and marly

LANDSLIDE. VI
GEOLOGICAL CROSS SECTION

Based on drilling and geophysics investigations



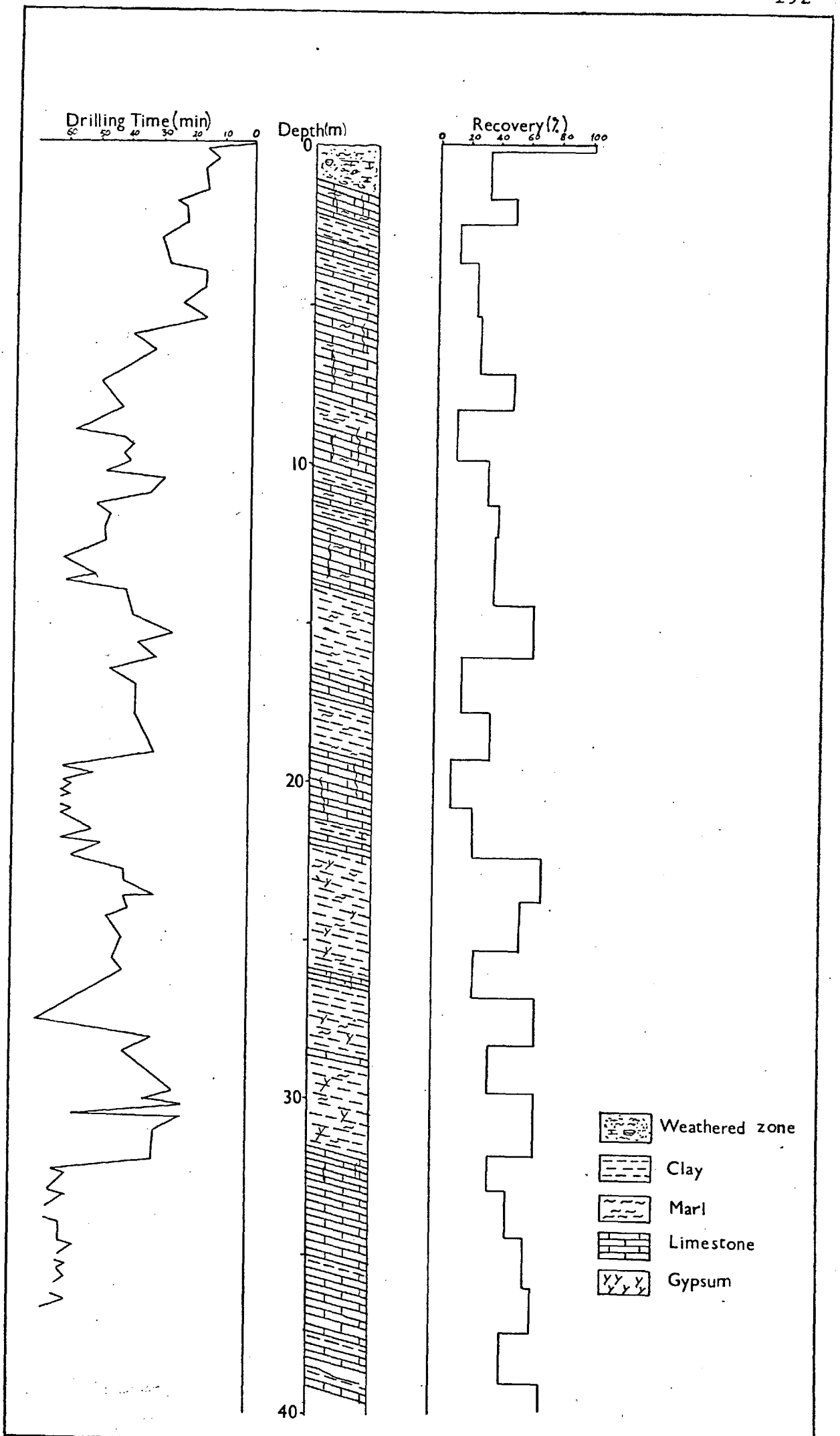
Fig(4.22)

650
600
550
- 190 -

limestones alternating with marl and clay (Fig. 4.23). However, the core samples were broken as small fragments and had many polished joint surfaces. The percentage recovery was low and the drilling rate was very fast (Fig. 4.23). Pressure tests performed in these boreholes show that the permeability of the strata was very high, and no water could be recovered at any stage. After the completion of drilling, the boreholes were used to observe groundwater levels but no permanent water table was observed.

The seismic refraction survey carried out at this site shows scattered readings, confirming the disturbed nature of the bedrock involved in the landslide mass. The interpretation of the best lines of these scattered readings on the time distance graphs shows that the bedrock is detected at different depths according to the shape of the moved mass. A lithological cross section of the site of the landslide was prepared based on information obtained from the surface geology, the exploratory drilling, and the seismic refraction survey and is shown in Fig. 4.22. The average velocity of the material involved in the moved mass ranged between 600-1000 m/s, while the bedrock velocity is in the range of 4500-5800 m/s (Fig. 4.3A).

The self potential profiles do not show any major water movement in the vicinity of the landslide area.



Fig(4.23)

4.4.2.3 Laboratory investigations

At the time of the 1964 landslide no laboratory investigations were carried out. For the purpose of the present study an intensive laboratory testing programme was devised and performed on representative disturbed and undisturbed samples obtained from the study area. A summary of the test results is presented in table 4.2B. The principal soil index test results are summarized in the table below.

Index Properties		Range	No. of Samples	Mean
Liquid Limit	L.L.	29.3 - 61.4%	9	50.1%
Plastic Limit	P.L.	13.3 - 19.2%	9	17.1%
Shrinkage Limit	S.L.	9.4 - 21.0%	6	13.3%
Clay Fraction	-2 μ	37.6 - 76.0%	9	56.7%
Activity		0.36 - 0.88	9	0.57
Liquidity Index	L.I.	0.017 - 0.64	9	0.25
Max. Water Absorption		69.2 - 84 %	9	70.5%
Specific Gravity	Sp.G.	2.58 - 2.70	9	2.63
Wet Bulk Density	γ_B	1.89-2.03 g/cm ³	7	1.91 g/cm ³
Natural Water Content	Wc	15.7 - 34.6%	9	* 23.4%
Porosity	n	37.1 - 43.6%	7	39.6%
Void Ratio	e	58.6 - 75.3	7	65.4
Calculated Degree of Saturation		66.6 - 100%	7	90.5%
Total Soluble Salts		0.07 - 0.2%	5	0.11%

Table 4.9

The Atterberg limits test results are plotted on the conventional Casagrande plasticity chart (Fig. 4.3) from which the average

values in the above table have been obtained. All the points lie above the A-line, and the clays are mainly CH (inorganic clays of medium to high plasticity). The activity values show that the clays could be classified as inactive to normal (Fig. 4.3). This suggests a predominantly illitic clay (Skempton, 1953). This was subsequently confirmed by an X-ray diffraction analysis. The dried and crushed samples finer than 0.15 mm show a medium to high water absorption (Fig. 4.5). The water absorption is related to the percentage and type of the clay. The liquidity index suggests that this clay could be classified as a stiff clay (Terzaghi, 1936). The natural water content is mainly slightly above the plastic limit, which suggests that this type of clay is over-consolidated at the present situation but is also partly saturated and few samples were fully saturated. The total soluble salts of these clays is mainly low.

Representative peak and residual shear strength parameters were obtained by carrying out drained direct shear box tests on specimens 6 x 6 x 2.5 cm with a maximum relative displacement of about 9 mm with reversals and reshearing until no further drop in shearing resistance was observed. The relative displacement rate was very slow (0.0000769 in/min) to avoid any build-up of excess pore pressures. The tests gave the following results:-

$$c'_p = 0.2 \text{ Kgf/cm}^2, \quad \phi'_p = 15^\circ, \text{ and}$$
$$c'_r = 0, \text{ with} \quad \phi'_r = 10^\circ \text{ (Fig. 4.24)}$$

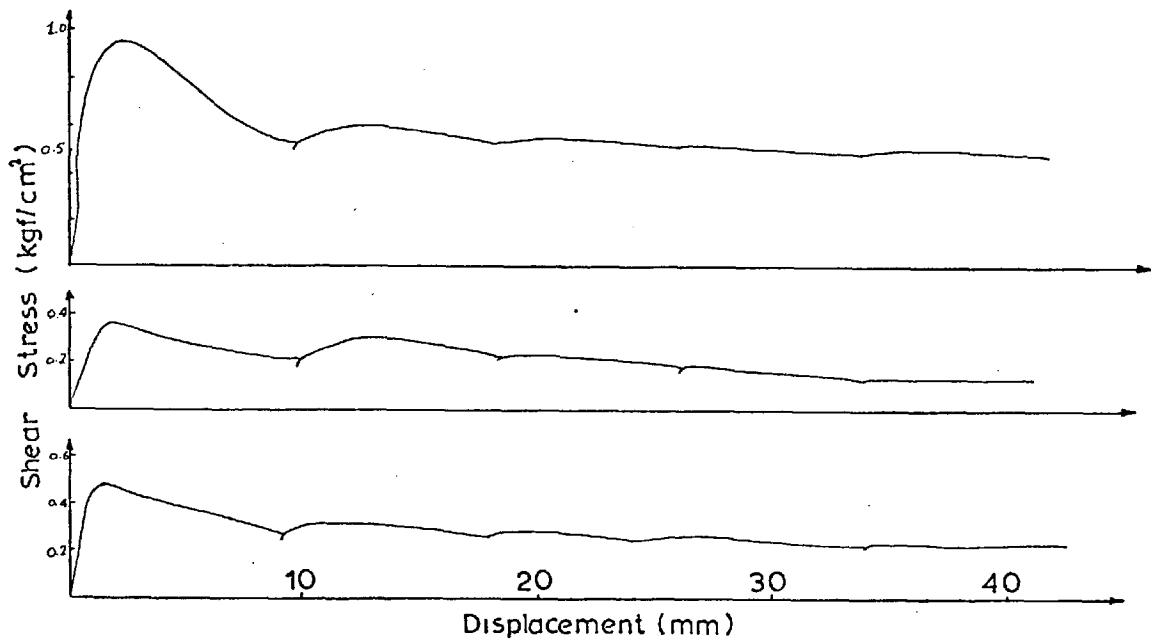
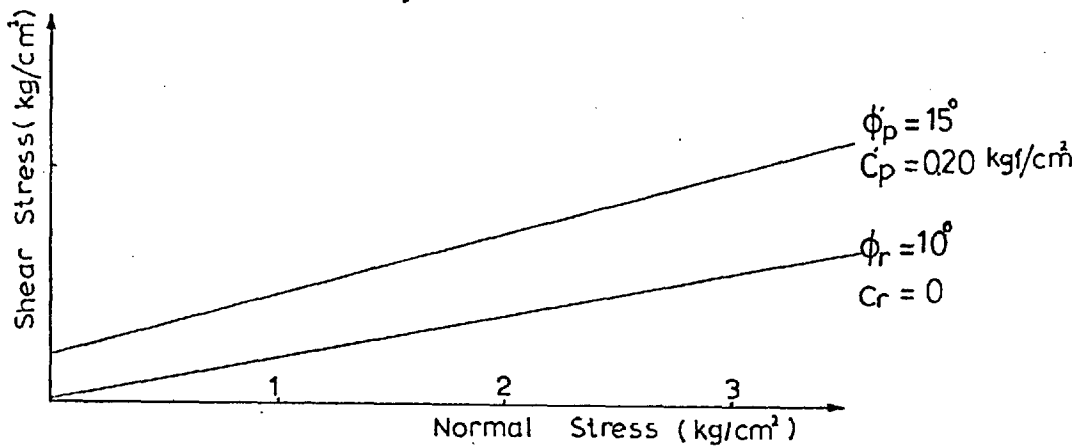
The mineralogy of the clay in the vicinity of the landslide area was studied by the differential thermal analysis method, X-ray diffraction on cavity mount and oriented samples, and showed the clay to consist mainly of illite, kaolinite, mixed layer with traces of gypsum, calcite and quartz (Figs. 4.6 and 4.7).

4.4.2.4 Slope stability analyses

Stability analyses in terms of effective stresses were performed on the cross section prior to the movement of 1964, and on the present cross section, using the methods of Janbu and Fellenius.

The simplifying assumptions, especially in respect to the geology of the site, that have been made for the purpose of stability analysis, are indicated in Fig. 4.25. The sole of the slip surface is assumed to be a curvature through the marly, clayey material and plane tangential to the limestone bedrock (Fig. 4.22).

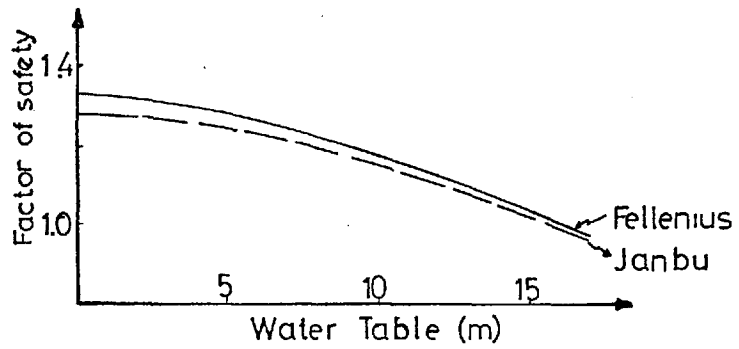
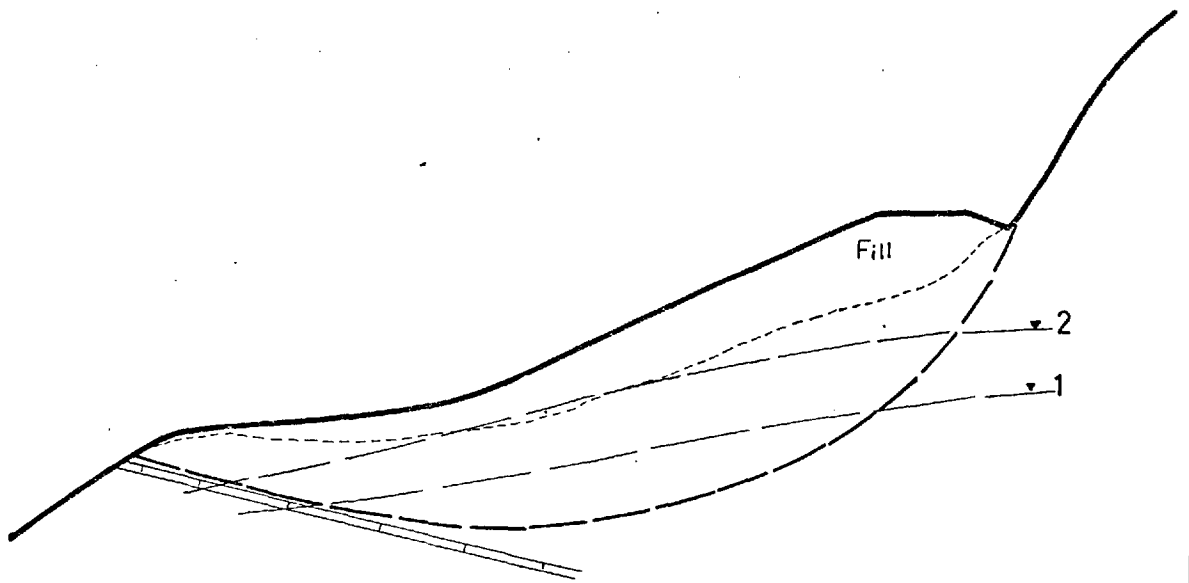
The main stability calculations were carried out for two different assumed positions of the water table in the slope corresponding to water tables 1 and 2 (Fig. 4.25).



TYPICAL CURVES OBTAINED FROM
MULTI-REVERSAL SHEAR TESTS
ON SAMPLE FROM LANDSLIDE. VI

Fig(4.24)

LANDSLIDE - VI
 CROSS SECTION PRIOR TO THE
 MOVEMENT OF 1964



Water table	Factor of safety		Remarks
	Fellenius	Janbu	
NO w.t.	1.33	1.28	Peak
1	1.23	1.21	Strength
2	1.04	1.04	Parameters

Fig(4.25)

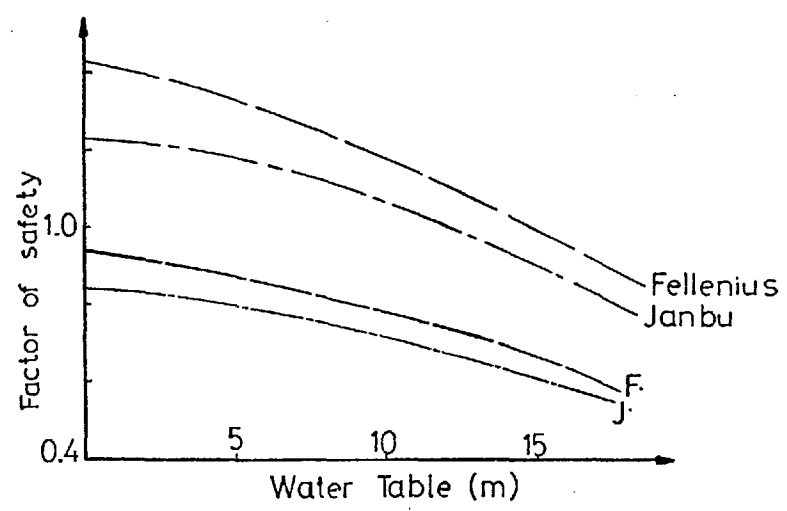
0 10 20 m.
 V & H

As can be seen from the cross section (Fig. 4.25), the slide mass is composed of two zones; the embankment fill material zone, and the marly limestone and marls zone. The average wet bulk densities of these zones are 1.99 g/cm^3 and 2.9 g/cm^3 respectively.

Stability analyses for the cross section prior to the movement of 1964 were carried out using peak strength parameters in terms of effective stresses represented by $C'_p = 0.2 \text{ Kgf/cm}^2$ and $\phi'_p = 15^\circ$, and assuming no water table in the slip mass and transient perched water tables in positions 1 and 2 respectively, at the time of failure during a heavy rainfall. It was found that the safety factors using Fellenius method were between 1.04 and 1.33, and by Janbu's method between 1.04 and 1.28. It can be seen clearly that for both methods movement could have occurred for a transient water table in position 2, and the agreement of the two methods used is good (Fig. 4.25).

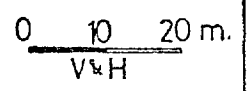
The stability analyses of the slope in its present state (Fig. 4.26) on pre-existing failure surface, and the residual strength parameters represented by $C'_r = 0$ and $\phi'_r = 10^\circ$ show that these parameters under-estimate the factor of safety. Therefore the fully softened strength parameters represented by $C'_d = 0$ and $\phi'_p = 15^\circ$ were used in the analyses of this

LANDSLIDE VI
PRESENT CROSS SECTION
(AFTER SLIDING)



W.T.	Factor of safety		Remarks
	Fellenius	Janbu	
NO w.t.	0.95	0.85	Residual Fully soft.
1	0.82	0.77	R.
	1.23	1.12	F. S.
2	0.64	0.60	R.
	0.96	0.85	F. S.

Fig(4.26)



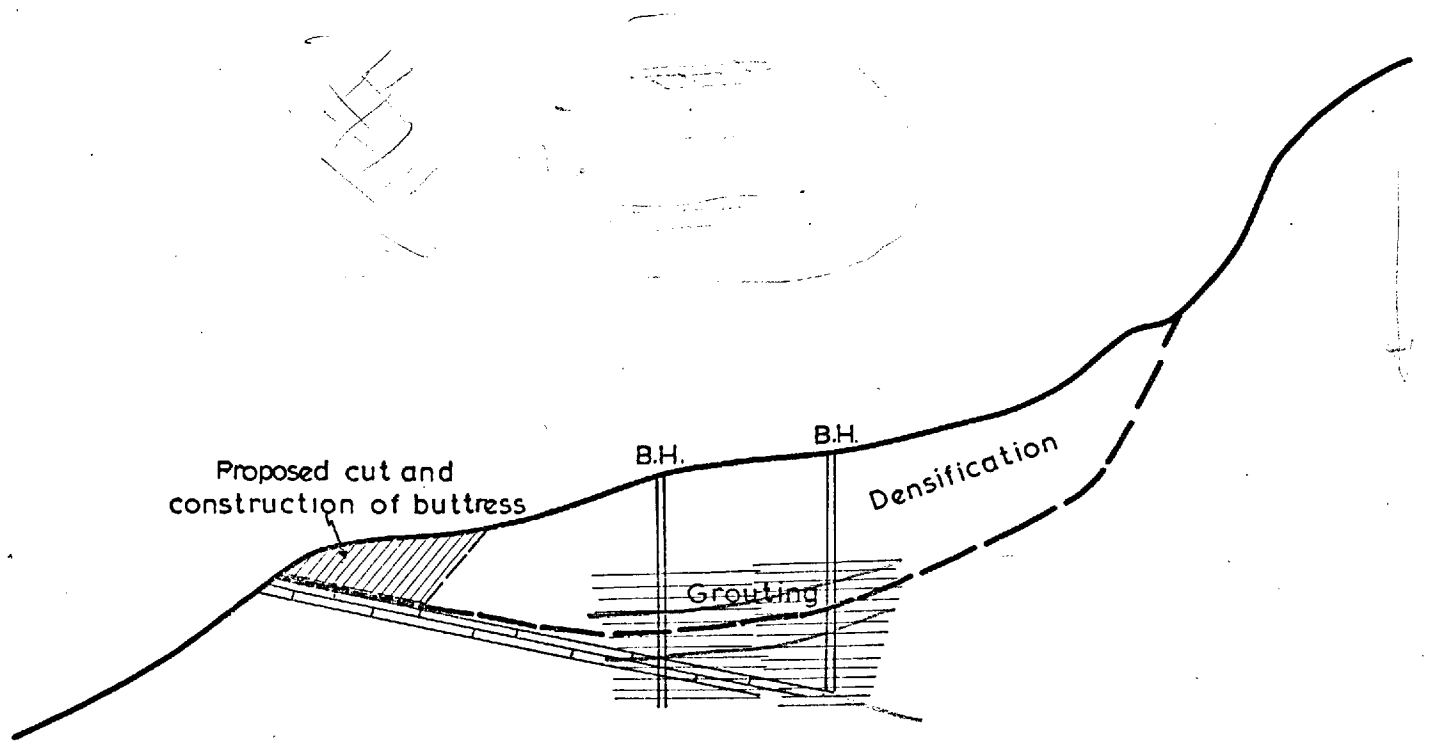
section, again assuming no water table in the slip mass and water tables in positions 1 and 2 respectively. It was found that the factor of safety was between 1.43 and 0.85 using Janbu's method.

The stability analyses clearly show that the area is almost stable with regard to water table in position 1 which might exist in the slipped mass. However, higher water table (position 2) will indeed be sufficient to re-activate the mass.

4.4.2.5 Remedial measures

The remedial measures for landslide VI are shown in outline in Fig. 4.27. They can be summarised as follows:-

- (i) Increasing the resisting forces by excavating the low strength materials at the toe part and replacing them by constructing a free drainage retaining buttress founded on the underlying bedrock. This construction will also probably increase the disturbing forces of the lower part, if there are many joints in the underlying bedrock, so it may be necessary to examine the bedrock in more detail and if the bedrock proves to be highly jointed, the retaining buttress should be replaced by sheet piling.



REMEDIAL MEASURES FOR LANDSLIDE VI

Fig(4.27)

0 10 20 m.
V&H

- (ii) Stabilizing the subgrade by densifying the materials beneath the embankment.
- (iii) Grouting the area above and below the failure zone to increase the cohesion and thus the resisting forces.
- (iv) Improving surface drainage by constructing culverts and canals to divert the rainwater from the landslide area.

4.4.2.6 Conclusions

In the light of the investigations and analysis reported here, it is quite clear that the following factors contributed to the movement:-

1. Presence of tectonic movements in the vicinity of the study area contributed to structural weakening of the strata.
2. Absence of surface and subsurface drainage facilities. The rainwater penetrates through the joints of the cap rock into the clay. A temporary water table probably exists, contributing to saturation and high pore water pressures.
3. Abnormally high precipitation in the month during which the landslide occurred (February, 1964).

4. The construction of a 20 m high embankment increased the driving forces and triggered movement in the slope.

The conclusions to be drawn from these investigations may be summarized as follows:-

1. The movements of 1956 and 1957, during the construction of the highway, were just vertical subsidence owing to the insufficient compaction of the fill material and the delicate balance of the area.
2. The fully softened strength parameters appear to be most reliable for use in the stability analysis of the slope in the present state owing to the amount of disturbance in the strata. The residual strength parameter consistently under-estimates the factor of safety of the slope.
3. The clay in the vicinity of the study area may be classified as normal to inactive. The main index properties of the clay are:- $W_c = 23\%$, $LL = 50\%$, $PL = 17\%$, $I_p = 57\%$.
5. The stability analyses of the slope in its present state clearly show that the area remains in a potentially unstable state with regard to any further high water tables which might develop following heavy rainfall. In addition, any additional fill material would disturb the delicate balance of the area.

4.5 THE AMMAN SLIDE VII (RAS-EL-AIN)

4.5.1 Introduction

This landslide is located at Ras-El-Ain in the central part of old Amman city, along the main road to Jerusalem. The site is an old quarry for building materials. A lack of experience in blasting techniques and the undesigned cutting slopes caused disturbance of the rock mass for some extent near the surface and contributed to instability in the slopes (Plates 4.22, 4.23, 4.24 and 4.25).

4.5.2 Geology

The bedrock in the vicinity of the landslide is limestone and marly limestones alternating with thin bands of clay and marl. The thickness of the clay bands is between 10-30 cm. The exposed face of the bedrock is highly jointed. Two joints were observed, one trending parallel to the slope dipping nearly vertical (circumferential); and other intersects the slope vertically (Plate 4.24).

The strata in this region are mainly horizontal but they dip at 29° out of the slope in the vicinity of the failure. The change in dip is caused by the presence of a fault (Plates 4.22 and 4.23). The fault trends $N85^{\circ}E$ and dips 44° in a south easterly direction.



Plate 4.22 Shows a general view of the study area of the landslide VII.



Plate 4.23 Shows the main features of landslide VII, (the moved mass, the faults and the clay bands).



Plates 4.24 and 4.25

Shows the old existing joint (A), the tension joint (B), then the failure surface (C) and the slipped mass (D).

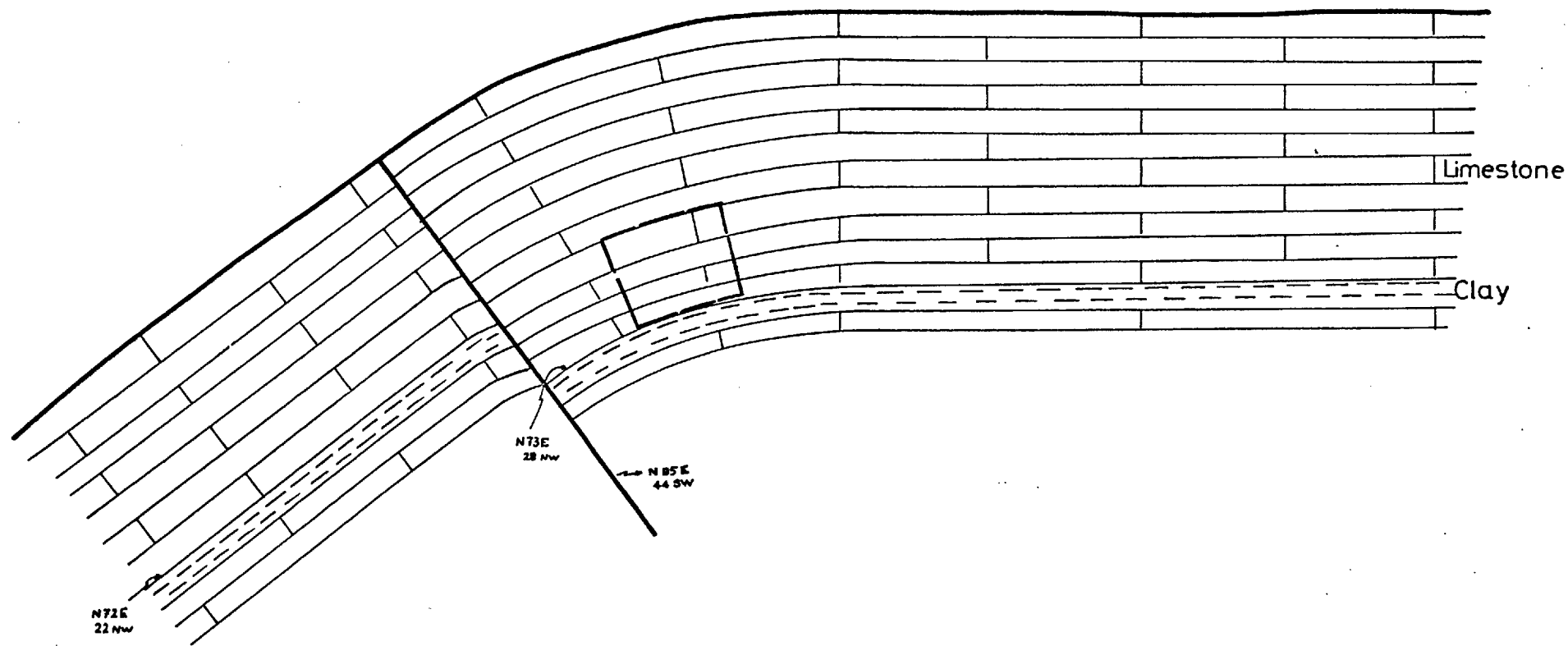
4.5.3 Topographic features

From the plan view of the area (Fig. 4.28) it can be seen that the failure is located on the west limb of an anticline intersected by a normal fault. The hillside cutting is approximately vertical, with an average height near the face of the cutting of about 18 m. The slope is made up of five large blocks which are bounded by master joints J1, J2, J3, J4 of circumferential type and another three discontinuous joints J5, J6, J7 intersecting the slope vertically (Fig. 4.29). The bedding surface on which the block rests dips at 29° out of the slope in the direction of the movement.

4.5.4 Failure mechanism

The stability of this particular slope is a function of the following factors:-

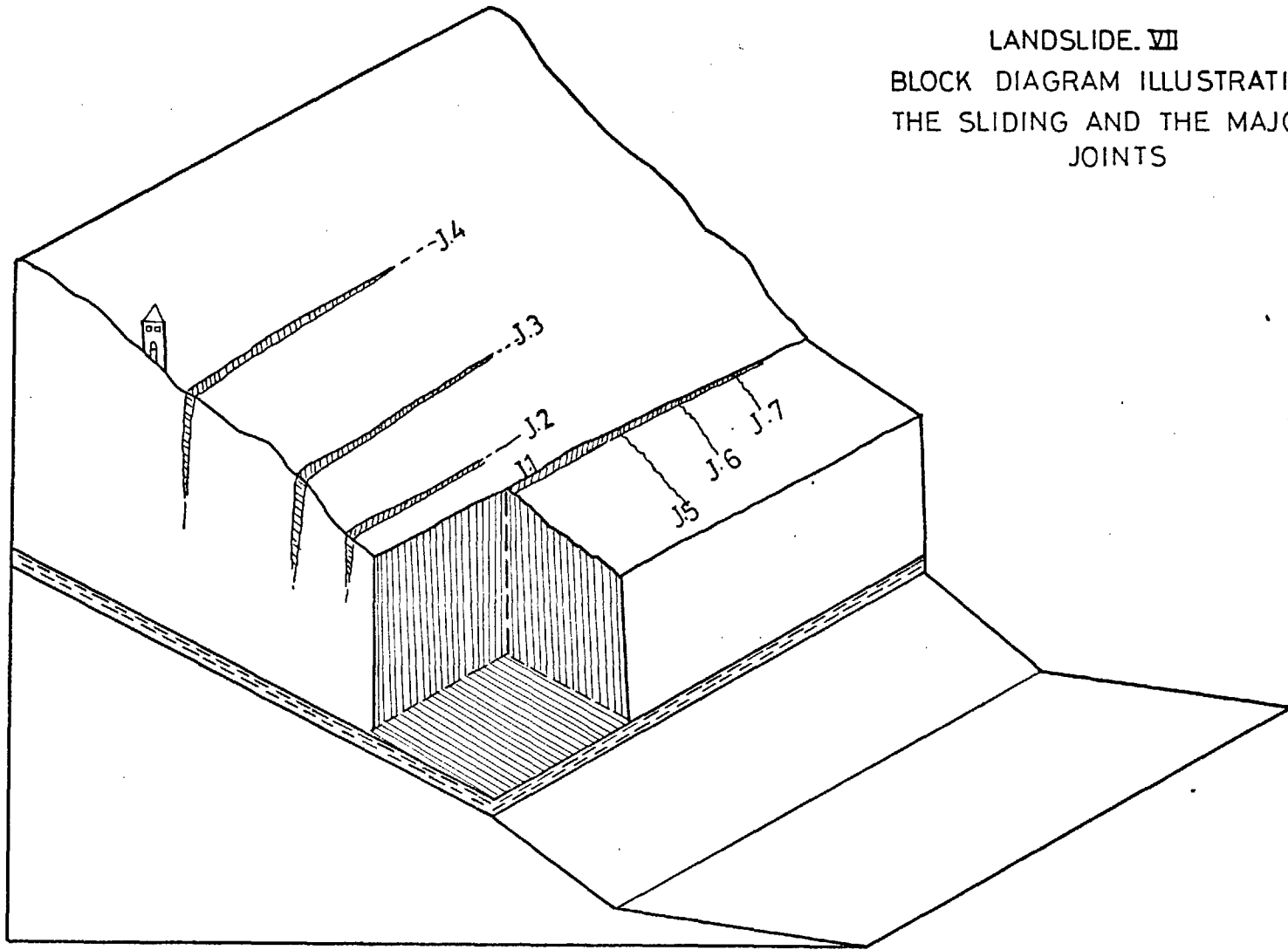
(i) The geometry of the slope, (ii) the orientation and strength of the major faults within the rock mass, and (iii) the tensile strength of the discontinuous joints (J5, 6, 7). The most critical situation would exist when the two joint sets combined. In such circumstances the seven blocks may become separated from the main mass by a progressive opening of the backing joint owing to the lateral stress release caused by the first failure. These blocks will move along the steep inclined bedding plane on the clay band. The angle of



SCHMATIC PLAN VIEW OF THE STUDY AREA OF
LANDSLIDE VII

Fig(4.28)

LANDSLIDE. VII
BLOCK DIAGRAM ILLUSTRATING
THE SLIDING AND THE MAJOR
JOINTS



Fig(4.29)

inclination of bedding planes had increased on account of tectonic movement, until the driving forces which acted on the slab become equal to the resistance against sliding. The resistance of the slab against possible sliding was also decreased due to the situation of the clay band between the slab and the base. Müller emphasized the fact that the rock mass is not always a continuum and that its behaviour is dominated by discontinuities such as faults, joints and bedding planes.

The simplified status of the slope stability analysis can be demonstrated by consideration of a block down an inclined plane under gravity (Fig.4.30). Consider a block of weight W resting on a plane surface which is inclined at an angle α to the horizontal. The driving force of this block is $W \sin \alpha$.

The resisting forces of the block is a function of the cohesion (c) and the friction angle between the block and the underlying clay, which is equivalent to $CA + W \cos \alpha \tan \phi$.

The block will be just on the point of sliding or in the

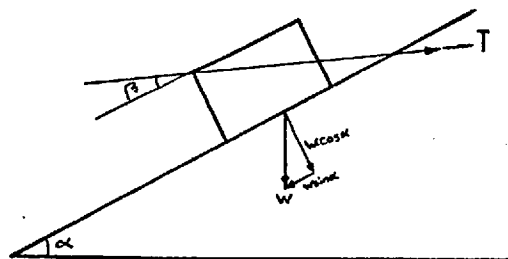


Figure 4.30

limiting equilibrium when the driving forces acting down the plane are equal to the resisting forces:

$$W \sin \alpha = CA + W \cos \alpha \tan \phi.$$

If the clay is in a fully softened strength condition ($C = 0$) then the limiting equilibrium would be when $\alpha = \phi$.

Considering the stability of the blocks ABCD and AEFB, $b/h < \tan \alpha$ and $\alpha > \phi$, thus the failure mechanism is by sliding and toppling, and also when considering the stability of the block AGHD, $b/h > \tan \alpha$ and $\tan \alpha > \phi$; sliding only can be expected (Figs. 4.31 and 4.32).

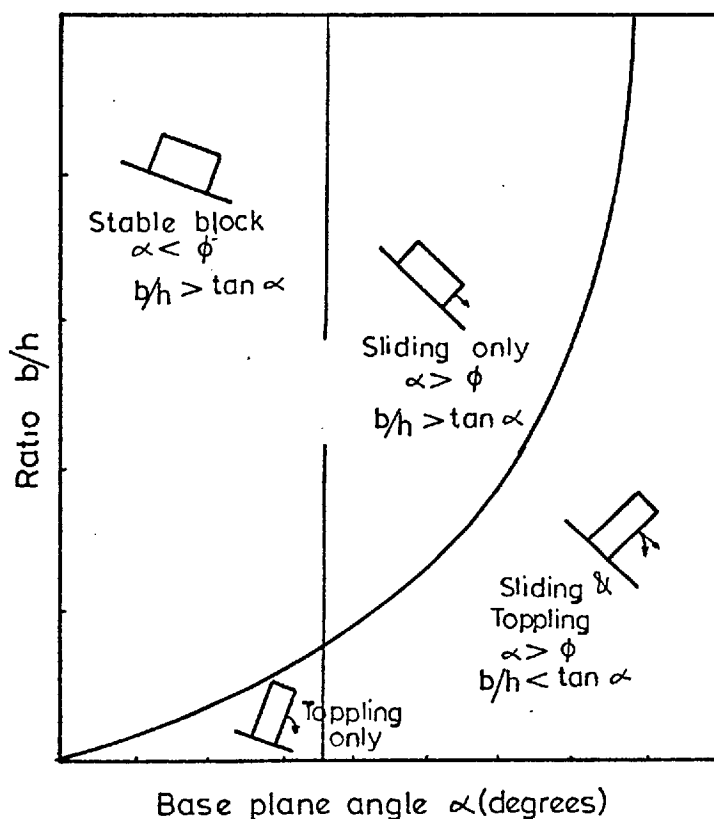


Figure 4.31

The peak strength parameters of the underlying clay give the following results: $C'_p = 0.31 \text{ Kg/cm}^2$, $\phi'_p = 19^\circ$.

The inclination of the failure surface is obviously critical to the stability of the proposed endangered blocks. Stability analysis for these blocks, ignoring any resisting forces acting along the open joint surfaces and using the peak

strength parameters of the underlying clay band show that the factor of safety is less than unity, i.e. the slope is still unstable with regard to the tensile strength of the discontinuous joints (J6, 7, and 8). Considering the case of the block AGHD (Fig. 4.32) being activated, assuming no excess water table and stabilized by a tensioned rockbolt, the factor of safety could be expressed as follows:-

$$F = \frac{CA + (W \cos \alpha + T \sin \beta) \tan \phi}{W \sin \alpha - T \cos \beta}$$

Londe has suggested that this equation is only valid for an active applied force, T, such as that generated by a tensional rockbolt or a pre-stressed cable. When the force T is given by passive anchor bars or cables which only come under load when relative movement of the block has taken place, the main effect is to increase the total resisting forces in the same way as this force is increased by cohesion and friction. Under these circumstances, the factor of safety is given by:-

$$F = \frac{CA + (W \cos \alpha + T \sin \beta) \tan \phi + T \cos \beta}{W \sin \alpha}$$

Both equations were solved for an assumed factor of safety of 1.5, with no excess water pressures on the slide mass. The minimum bolt tensions required to stabilize the blocks ABCD, AEFD and AGHD with respect to the angle ϕ for optimum bolt inclination are 24, 192 and 352 tons respectively.

LANDSLIDE VII
CROSS SECTION SHOWING THE MAJOR
JOINTS

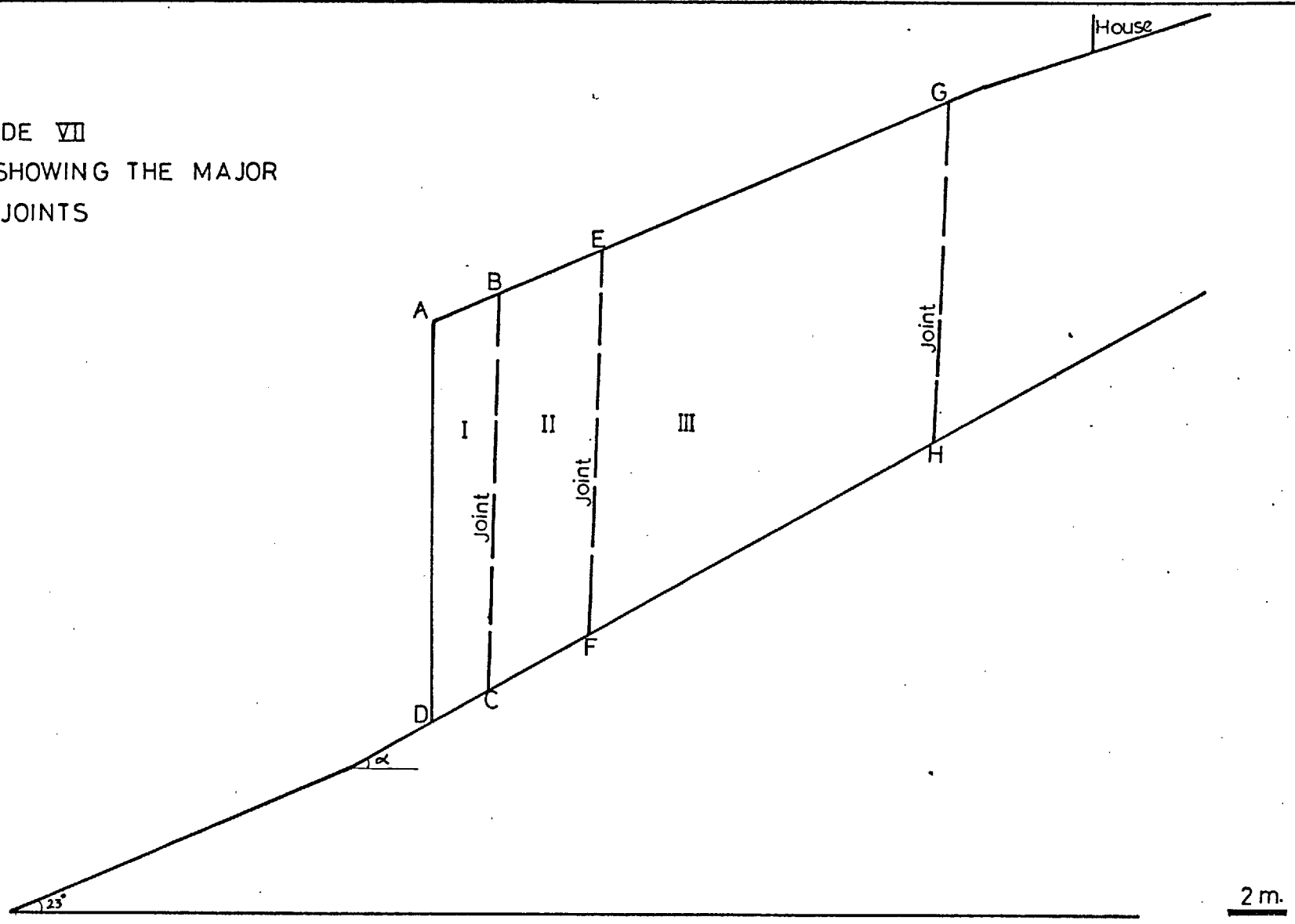


Fig (4.32)

4.5.5 Main causes of the slope failure

1. External causes: the change or increase in slope gradient such as excavation at the foot of the slope during the last twenty years in which quarrying at this site for building materials has taken place. The presence of tectonic process indeed contributed to the change of stress in the rock mass. The equilibrium is then distributed by the increase in shear stress.

2. Internal causes: are those which lead to slope failure owing to a decrease in the shearing resistance. The decrease in the shearing resistance of this slope is due to the progressive opening of the joints caused by blasting in the area, the cohesion of the material diminishes and the observed leakage from septic tanks penetrates through into the underlying clay band, causing reduction of the cohesion.

Both factors in combination contributed to a reduction of shearing resistance and increased the shearing stress, thereby disturbing the equilibrium of the rock mass.

4.5.6 Stabilization Measures

The stabilization of this rock slope can be effected by various measures, including:-

1. Sealing the joints in this area to protect any seepage of water through the underlying clay, and
2. Rock bolting (anchorage).

This measure is believed to be the most effective for this particular site and provides the most satisfactory means of successfully securing the endangered blocks near the surface rock. The required bolt inclination and tension are as calculated in Section 4.5.4.

CHAPTER FIVE

DETAILED INVESTIGATIONS OF LANDSLIDES

ALONG SWEILEH- JARASH ROAD

(LANDSLIDES I, II, III & IV)

5.1 INTRODUCTION

This chapter provides a brief description of the highway between Sweileh and Jarash, a summary of the field and laboratory testing for locations of the areas of instability and a detailed investigation of landslides I, II, III and IV. The landslide III is of the translational type, and stability analyses were carried out in terms of effective stress using the methods proposed by Fellenius (1926) and Janbu (1957). Landslides I, II and IV are of circular type, and the stability analyses were carried out using the method proposed by Bishop (1954).

5.2 GENERAL DESCRIPTION OF THE ROUTE

The area covered by the Sweileh-Jarash road lies at the northern edge of East Jordan, along Amman-Syria highway. The length of this road is about 35 Km, with a main south-north orientation.

The plan and design of this highway was based on air-photos on a scale of 1:25,000 carried out by Hunting Aerosurveys Ltd. in 1953. Construction was finished in 1961, and this was supervised by United States AID construction advisers and engineers of the Ministry of Public Works. The highway crosses

a distinctive topographical region varying from 1000 metres altitude at Sweileh in the north to 600 metres at Jarash towards the south, and crossing the Baqa'a depression at an altitude of 600 metres and Zerqa river at 250 metres.

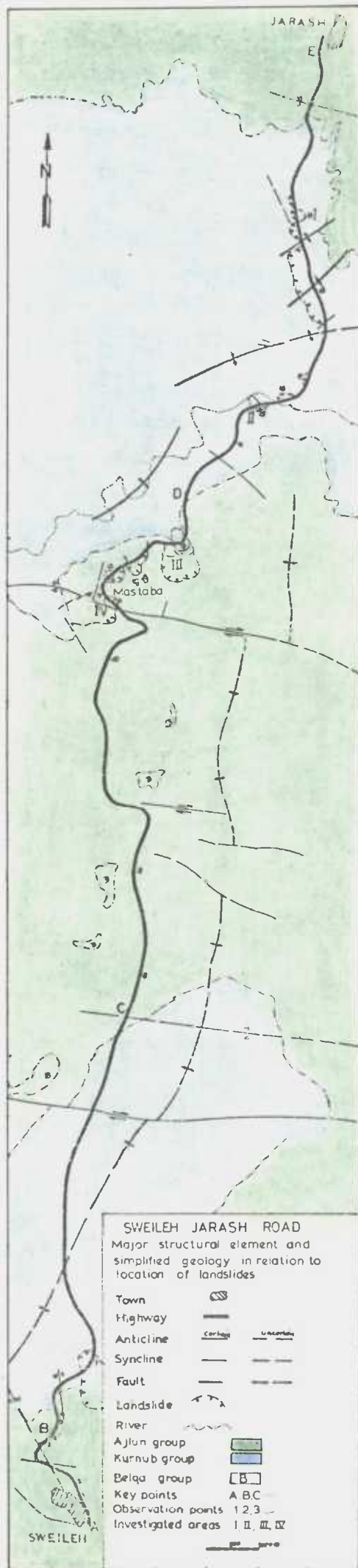
From the topographical and geological point of view, the highway may be divided into four sections starting from Sweileh city, referred to as AB, BC, CD and DE in Figure 5.1 & 5.1A.

Two types of geological formation are crossed by the highway:

- Group A: Upper Kurnub group (K_2).
- Group B: Marl-clay unit (Lower Ajlun group, $A_{1,2,3}$ and 4).

The main sedimentary formations which appear along this highway are listed and briefly described in Table 2.2, Chapter II, and a measured columnar section showing these different formations is shown in Figure 5.2. The sections AB and CD cut the Lower Ajlun formation, and sections BC and CD cross the Upper Kurnub group.

The Lower Ajlun formation in this area is mainly represented by limestone, marly limestone interbedded with marls and clays. The following sub-units are recognised:

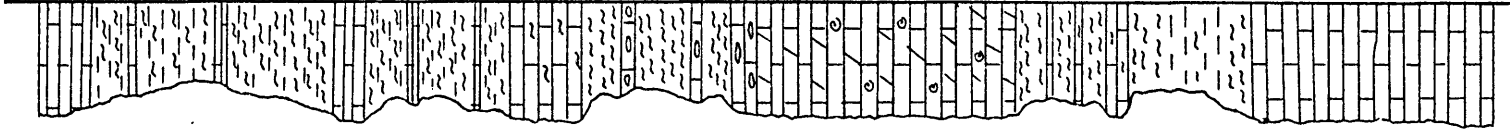


Fig(5.1)

NORTH JARASH

LOWER AJLUN FORMATION (A1,2,3)
≈ 198 m

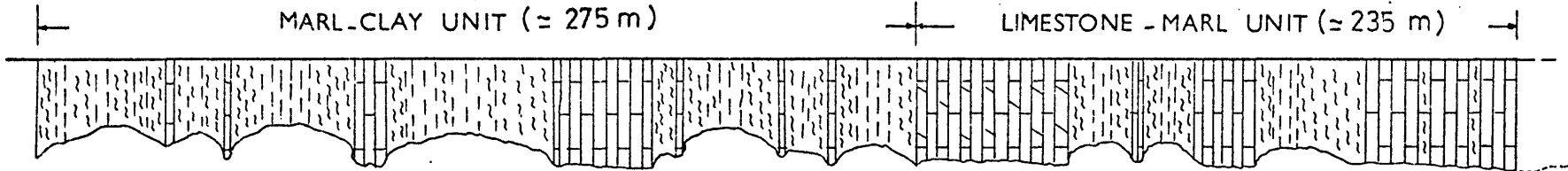
UPPER AJLUN FORMATION (A4,5,6)
≈ 220 m



BETWEEN SWEILEH & JARASH

MARL-CLAY UNIT (≈ 275 m)

LIMESTONE - MARL UNIT (≈ 235 m)



COLUMNAR SECTIONS

Fig(5.2)

20m

A₁: clayey, marly formation.

A₂: limestone, marly, nodular and cherty.

A₃: marl and clay.

These three sub-units are combined and classified as the marl-clay unit in the engineering geology classification.

The Upper Kurnub group in the study area consists of sandstones, siltstones, silty clays, clays and shales.

Due to the occurrence of shale and clay layers interbedded with weakly cemented sands, many slope problems have arisen. Ultimately several of the slopes have become unstable due to the following reasons:

1. Unfavourable orientation of the bedding planes and stratification. Figure 5.5.
2. Unfavourable orientation of the joints. Figure 5.3.
3. Weathering of the lower soft clays and undermining the lower siltstones used as construction materials.
4. Artificial factors (excessive height of the cut slopes, undercutting, etc.). (Plate 5.1).

AB Section of the highway:

This section of the highway drops gently down to



Plate 5.1 Landslide activated by the undercutting of the river near the Zerqa River bridge.

the wide Baqaa depression, from 1000 metres altitude at Sweileh to 600 metres at Baqaa, within a distance of 5 kms, and crosses the marl-clay unit of the Lower Ajlun group. This group is characterized by erosion of the underlying soft clay and marls, and by intense jointing of the marly limestones.

The areas indicated by the field observation points 1, 2, 3 and 5 along this section of the highway have been affected by mudflows, now contained by retaining walls. The materials involved in these movements comprise yellow, green silty clays and marls mixed with limestone fragments. These areas were recently planted with deep rooted trees in an attempt to control the movements by absorbing some of the precipitation.

Observation point no. 4 shows a small mudflow area planted by trees. The material involved is mainly a brown soil with yellow silty clays. The average liquid and plastic limits of this soil are 50% and 25% respectively. The grain size distribution indicates that the clay percentage is as high as 60% with 20% silt, 10% sand and 10% gravel. The hillside cuttings along this section, at about 3 km from Sweileh city, show 10 metres of limestone and marly limestone underlain by an average of 5 metres of marl and clay. The dip of the strata is about 25-35 degrees out of the slope towards the highway on the right side and into the hill on the left side of the highway (Figure 5.3).

The representative joint sets dip between $60-80^{\circ}$ with a strike of N20E, N85W and N55W (Figure 5.4). The inclination of the slope is between $70-80^{\circ}$ E. The unfavourable condition regarding the dip of the strata as well as the dip of the jointing together with the steep inclination of the slope renders block sliding and toppling probable, thus endangering the traffic. These probable types of failures might occur due to the stress release after the removal of lateral support by cutting the roadway, causing successive opening of the joints.

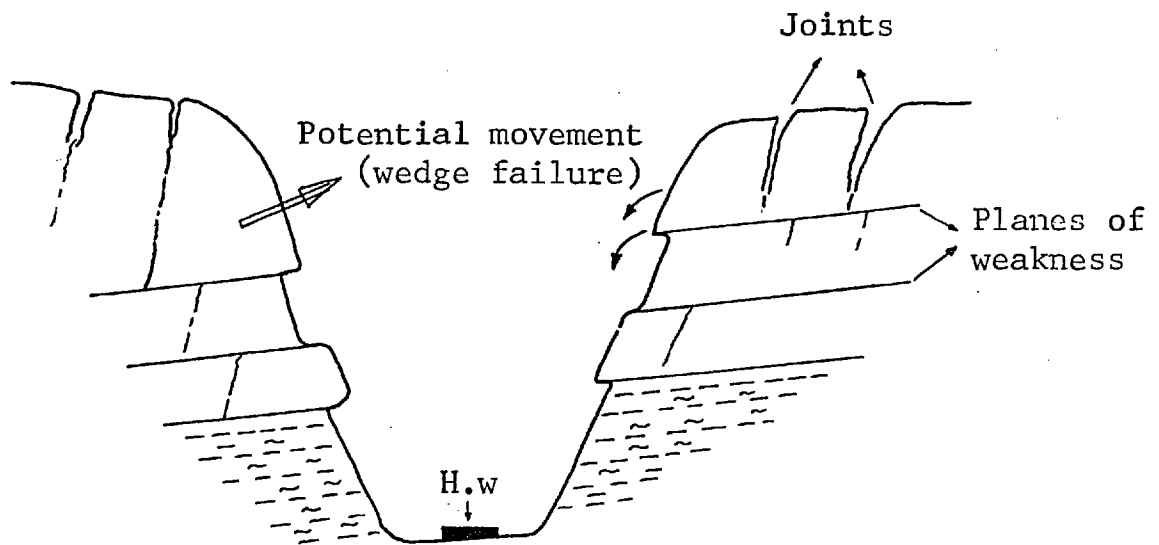


Figure 5.3

If the slope is to fail, it might fail along the least resistant plane, which is a function of the geologic planes of weakness inherent in the earth materials comprising the slope. Geological planes of weakness are those structural or lithologic elements or surfaces in a rock or soil-rock which result in a mechanical discontinuum (D. Evans, 1966). The probable types of failure in the right side of the road could be summarized as toppling

or sliding along a plane of weakness; or deep seated sliding through the underlying clay, which is related to the driving forces tending to produce a failure arc, resisted by the peak strength of the clay through the increased load onto the arc. In the left side, wedge shape potential movement is expected.

Only one major NW-SE fault intersects this portion of the highway at two locations.

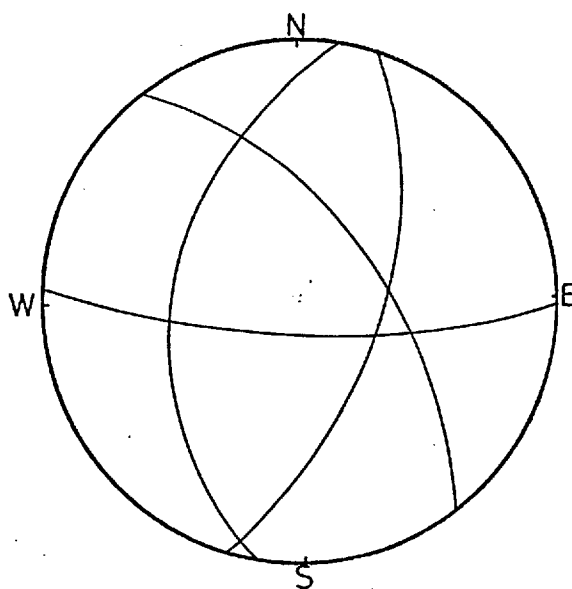


Figure 5.4

BC Section of the highway:

The highway between key points B and C crosses the Upper Kurnub group which comprises mainly of silty clay, shale and weakly cemented sands. This formation is also called the Baqaa formation since it outcrops in Baqaa depression which is 6 Km long, being mainly covered by superficial deposits comprising silty clays mixed with varying percentages of gravels.

A representative sample from this depression showed the following grainsize distribution: 70% clay, 18% silt, 8% sand, and 4% gravel. The liquid and plastic limits are 55% and 35% respectively, which could be classified as an organic silty clay of low plasticity.

Two major faults intersect this portion of the highway trending NE-SW and E-W and there is only old landslide at observation point no. 6. The outcrop of the Kurnub group ends at key point C. (Figure 5.1.)

CD Section of the highway:

The rock units along this section are mainly marly clays (lower Ajlun group A_{4,3,2,1}). The measured section, between observation points 8 and 9, being as follows, from top to bottom:

400 cm highly weathered jointed limestone.

72 cm yellow-green soft clay.

68 cm cream, highly jointed, marly limestone.

76 cm cream, white, intensely jointed limestone.

275 cm yellow-green clay.

North of the Baqaa depression, between key points C and D, the terrain initially becomes higher with steep natural

slopes until the road reaches 700 metres in elevation before dropping to about 250 metres at the Zerqa river crossing.

Many different types of instability have been observed along this section of the highway, indicating both active and ancient major landslides which are concentrated between Mastaba village and Zerqa river bridge (Figure 5.1A).

The gradient of this slope is about 75° to 80° , with a length of about 200 metres oriented north south and with a maximum height of 12 metres. The strata trends about 80° and dip 12° SE. The major joints show a dip ranging between 85° and 90° SW with a strike of 55-80 NW.

Two types of failures have been observed: (a) block sliding, and (b) toppling. The stability of this type of slope is mainly controlled by orientation and inclination of the planes of weakness relative to the slope face and the shear resistance along the discontinuities. These planes of weakness are represented by stratifications and joints within the rock mass. When the inclination of the stratification is greater than the friction angle between the block and the plane, sliding occurs, and when the vertical line passing through the centre of gravity of the block falls outside the base of the block, toppling occurs (following the idea of Hoek and Boyd), Figure 5.5.

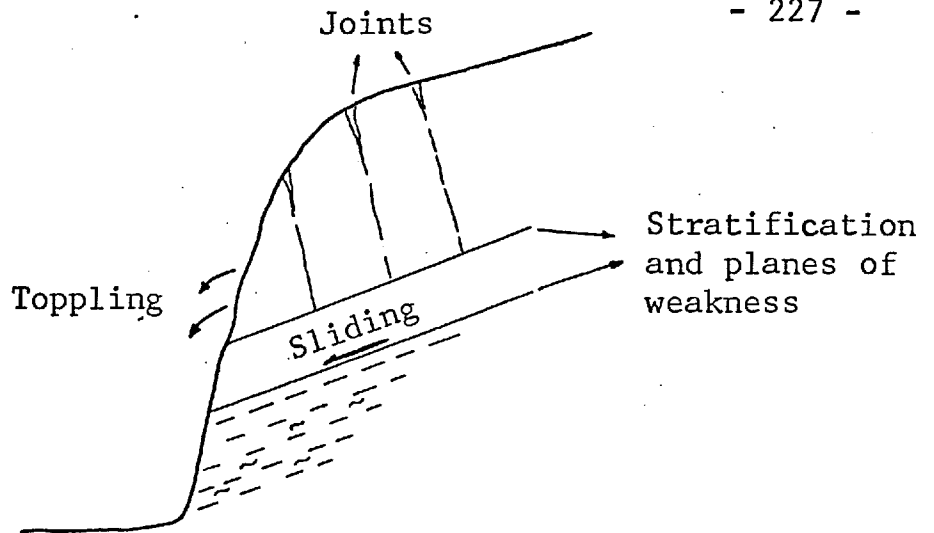


Figure 5.5

Observation No. 10:- an old landslide (stable).

Observation No. 11:- landslide IV.

Observation No. 12:- old landslide, and recent small landslide activated in 1962; 50 metres breadth along the highway, within $A_{1,2}$ formation. In addition the development of many tension cracks was observed.

Observation No. 13:- landslide III.

Observation point (D):- Measured section on the cutting slope is as follows from top to bottom:

185 cm, red clay weathered zone mixed with rock fragments.

410 cm, marl, weathered.

18 cm, dark grey shale.

227 cm, hard jointed marly limestone to limestone.

56 cm, cream, yellow, medium hard clay.

60 cm, white, yellow, hard intensely jointed limestone.

250 cm, yellow soft marl and clay.

The joints in this slope mainly dip at 84° NE into the slope with a strike of N30W and some trending N56E with an 80° SE. The joints are parallel to the road and the incombination with each other allows blocks to fall out of the slope. The massive beds are being undercut by undermining of the marl and clay which allows blocks to fall into the highway. At this observation point a small old landslide was observed within the silty clayey material together with some subsidence in the pavement due to the embankment failure.

DE Section of the highway:

The last portion of the highway, extending from two kilometres north of Mastaba village to Jarash city, between key points D and E, is mainly in a steep hillside cutting within the Upper Kurnub group. Many different types of instability including cracking and subsidence in the pavement, earth and mudflows, in addition to major progressive landslide movements. Observation point 14:- Earth and mudflow within the silty clayey material. Plate 5.2.

Observation point 15:- Landslide II.

Observation point 16:- Old landslides are present and a recent landslide occurred in 1964. The bedrock is mainly sandstone underlain by clayey, silty, shaley material of the pper Kurnub group. Springs discharge from this area.



Plate 5.2 Earth and mudflow within the silty clayey materials along the Sweileh-Jarash road (observation point 14).



Plate 5.3 Earth fall along the Sweileh-Jarash road.

Observation point 17:- This is an old landslide within the same formation as above. Few trees are planted in this area. A measured section from top to bottom:

180 cm, cream white sandstone.

350 cm, varicoloured clayey silts.

120 cm, grey siltstone with thin bands of shale.

220 cm, brown clay and clayey silts.

The average slope of the hillside cut is 55° .

Observation point 18:- A large old landslide area mainly within the same sequence of material which seems to have been activated due to the recent hillside cuts. Measured sections from top to bottom:

12 cm, brown siltstone.

22 cm, yellow, weakly cemented silty clay.

100 cm, massive siltstone.

65 cm, grey, green, silty, sandy clay and clay.

28 cm, brown, rusty sandstone.

30 cm, grey, yellow clay and silty clay.

58 cm, grey, brown, medium hard siltstone.

62 cm, grey, rusty, clayey, silty, sandy clay.

42 cm, medium hard siltstone.

21 cm, grey, green, clay and silty clay.

61 cm, weakly cemented siltstone.

Observation point 19:- Landslide I.

From the above mentioned cases of instability four particular landslide areas were selected for detailed study.

This study started with the field work jointly with the laboratory analysis.

The field work comprises the following:-

1. Detailed description of the existing problems along the highway.
2. Field observations of the existing problems by constructing observation points.
3. Geology, morphology, identification and classification of the slope instability in relation to the origin, causes and types.
4. Joint survey in the overlying bedrock and its relation to the existing problems.
5. Geophysical study of the selected landslide areas.
6. Study of the air photos jointly with the field geology.
7. Exploration drilling (core boring, trenches, pits).
8. Collecting disturbed and undisturbed samples for laboratory testing.
9. Field density and natural water content.

The laboratory work comprised:

1. Consolidated undrained and drained triaxial compression tests and unconfined compression tests.
2. Specific gravity.
3. Direct shear tests.
4. Grain size analysis.
5. Atterberg limits.
6. Maximum water absorption.
7. Complete chemical analysis of soils and cation exchange capacity.
8. D.T.A. and X-ray diffraction studies.
9. Total soluble salts of the soil in water.
10. Thin section studies.

A summary of the testing results of the representative samples taken from the selected four landslide areas along this highway is shown in Tables 5.1B and 5.2B.

5.3 DETAILED INVESTIGATION OF LANDSLIDE III

5.3.1 Geography and Geomorphology

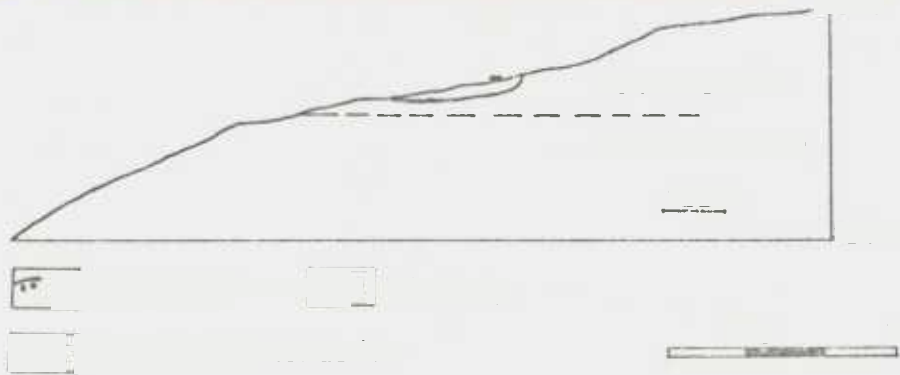
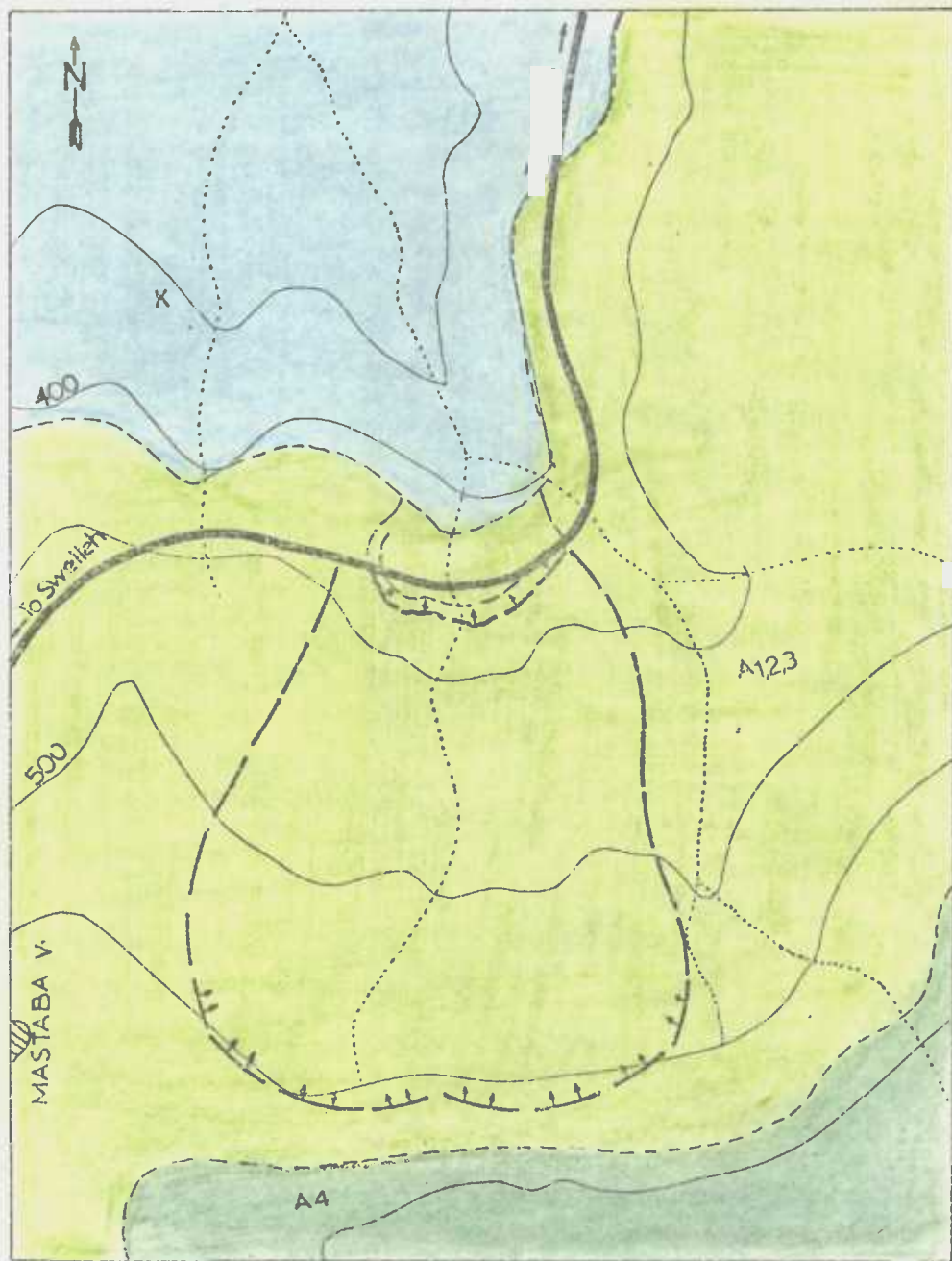
The slide area lies at Km 24 on the Sweileh Jarash road north east of Mastaba village at a distance of 3.75 Km from the Zerqa river bridge (location map, Figure 5.1). The landslide is on the southern slope of the tributary Wadi of the Zerqa river. This area is mountainous with a highest elevation of 650 m towards the south west, but the height decreases gradually to 200 m towards the north west at the level of Zerqa river (Figure 5.1A).

The high rainfall and presence of faulting have combined to form a hill region of diversified scenery with many outcrops of limestone, sandstone and marl (Burdon 1953, page 13).

The morphology of the area in the region of the recent landslide shows a hummocky terrain with rock outcrops in the relatively steep valley sides.

5.3.2 Geology of the study area

Detailed geological maps were prepared on 1:10,000 and 1:25,000 scales, and checked by the study of aerial photographs of 1:10,000 and 1:25,000, Fig.5.6. In 1970 a new contour map on



a scale of 1:1,000 was prepared by the Ministry of Public Works Surveyors for the recent landslide area on which the mapping of the slide area was superimposed.

Stratigraphy:

The rock units exposed at the site of landslide III:-

- a. Marl-clay unit (lower Ajlun group $A_{1,2,3,4}$).
- b. Upper Kurnub group (K_2).

The thickness of the marl-clay is about 130-150 m. This formation is highly weathered and disturbed as a result of tectonic and old landslide movements. This lowermost part of the Ajlun group is overlain by the bedded, highly jointed, crystalline cherty limestones of the A_4 formation with a total thickness of about 40 m. The limestone in the upper part can be readily differentiated from the lower parts of the sequence in the field by its characteristic topographical features and lithological properties arising from its strong resistance to weathering (Figure 5.2).

Marly limestone with chert nodules is exposed near the crest of the slide and as a result of its weathered and intensely jointed condition the rock mass has a rather distinctive loose blocky appearance. These beds are underlain

by thin bands of greyish clay, and dark greenish grey shale with a dip of 12° out of the slope and in the direction of the movement. Two major joint sets were observed in the limestone, one trending N 20 W and the other N 72 E, with dips of 80 NE and 80 NW respectively (Figure 5.2A). These joint sets have a critical orientation, dividing the strata into cuboidal, loose blocks which contribute to rockfalls and often rock instability. A measured vertical section along the highway was as follows:-

100 cm, red clay mixed with rock fragments.

166 cm, weathered zone made up of cream, white

limestone and marly limestone.

12 cm, grey shale.

61 cm, intensely jointed limestone.

72 cm, cream, yellow clay and marl.

7 cm, dark grey shale.

61 cm, cream, yellow clay.

Structure:

The main structural feature which dominates the study area is an anticline trending with a NE-SW axial trace which is disturbed by E-W striking normal and shear faults, the highway passing mainly through the western flank of this anticline. The anticline terminates north east of Mastaba

village, and is intersected by an E-W trending associated shear fault, which passes through the site of landslide IV; this fault zone is highly disturbed and many springs discharge from the vicinity of the fault.

The area to the north of this fault, around Mastaba village, is located on the western flank of an anticline trending in a N-S direction, dipping towards the Zerqa river. Many landslides can be seen on this flank, in addition to the recent landslides III and IV, together with other zones of instability (Figure 5.1).

The section of the highway between the Zerqa river and Jarash city is characterised by steep hillside cuttings within the Upper Kurnub group. The structural pattern, 5 Km north of the Zerqa river, is formed by a NE-SW trending anticline, followed by a syncline and a further anticline on its northern flank. Landslides are concentrated on the flanks of these anticlines.

5.3.3 Climate and Hydrology

The study area is characterised by semi-arid climate, warm and dry in summer with a mild rainy winter. The rainfall is of medium to high intensity for short periods. The rainfall

west of the highway is somewhat greater than the east.

Monthly rainfall relationships at various recording stations along this highway are shown in Figure 5.7 . The average mean rainfall is about 400 mm and this is limited to the winter months between November and April.

According to the Hydrology Observations Stations along the Sweileh-Jarash road, the mean annual rainfall is 382 mm at Jarash, 12 Km from the site, and 549 mm at Sweileh station, 24 Km from the site, and at Rumman station, 8 Km from the site it is 328 mm. The precipitation in the month of failure to be described was about twice the monthly average over the ten years record (Table 5.1).

Station	Total rainfall in March, 1969 (mm)	Total rainfall in 1968 (mm)	Average rainfall in March/in 10 years (mm)
Jarash	131.0	437.6	87.0
Sweileh	297.4	740.0	127.0
Rumman	195.0	368.7	91.8

Table 5.1

It is worth mentioning that the rainfall is the only significant source of precipitation in the study area, which is mainly uncultivated, except for a few trees recently planted near the slide area. The natural vegetation consists of shrubs and bushes.

SWEILEH - JARASH ROAD
 ANNUAL PRECIPITATION
 (1962 - 1972)

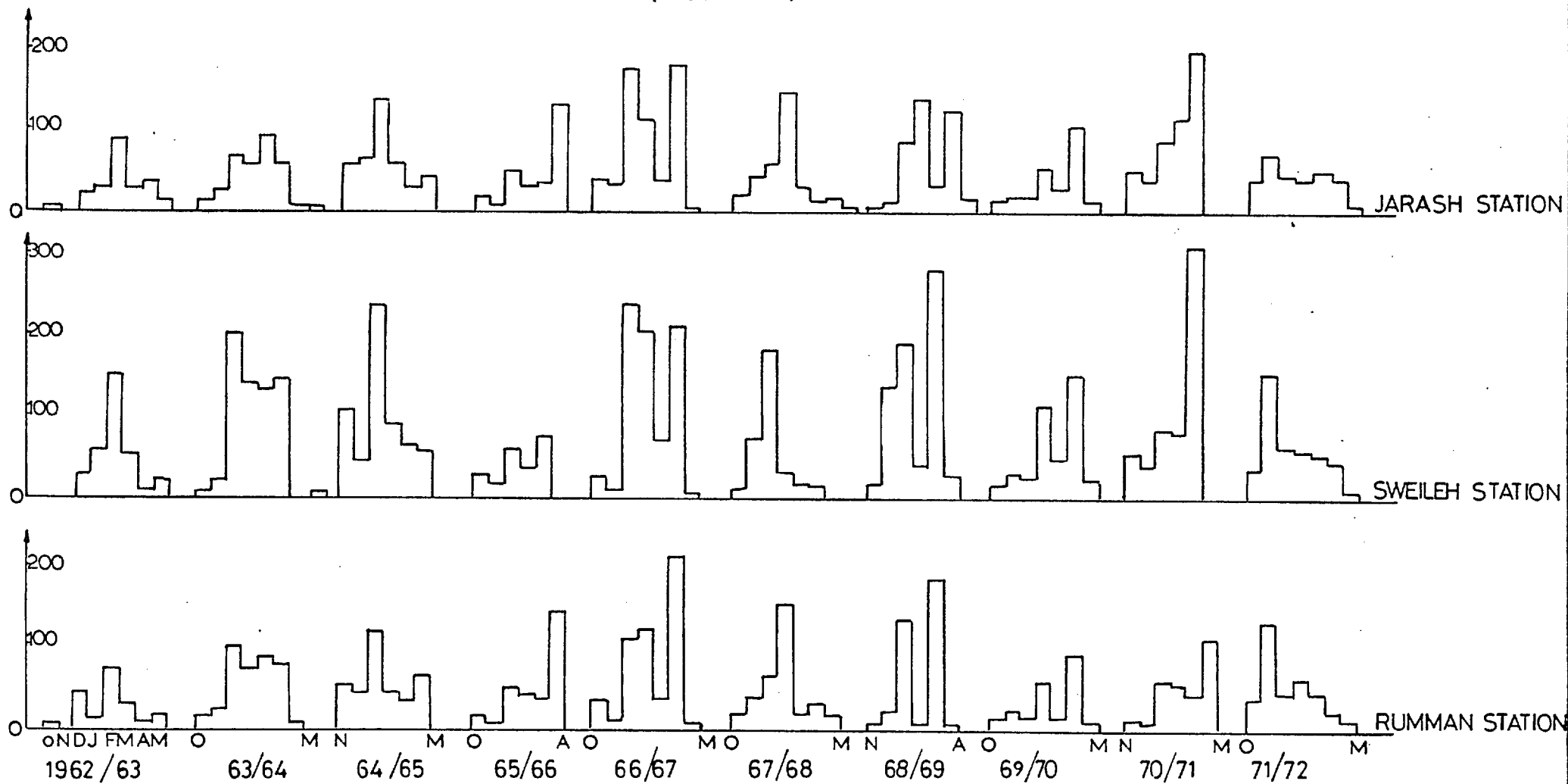


Fig. 5.7

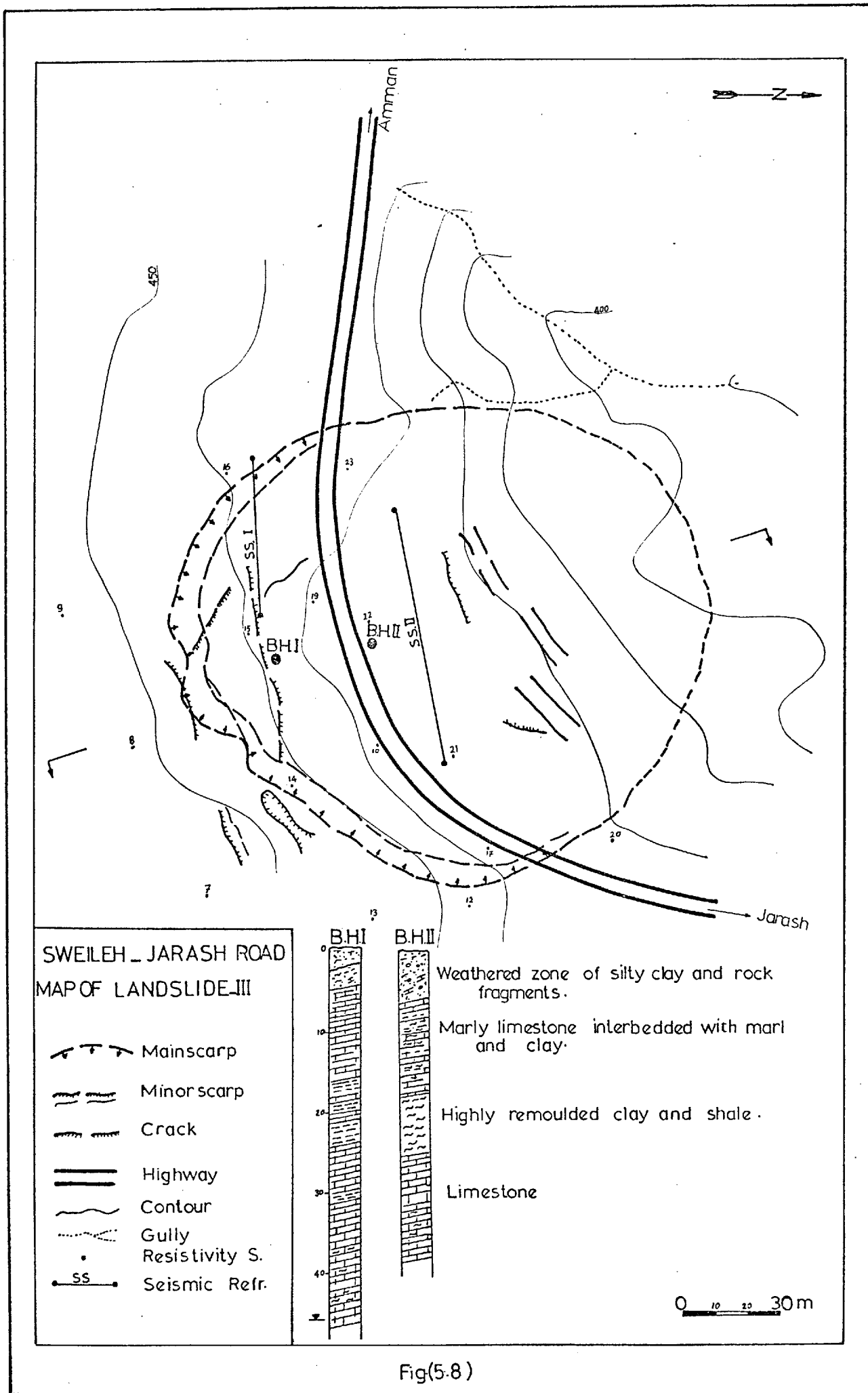
The deep incision of the Zerqa valley drains off much of the ground water in the form of base flow. The observed springs in the area issue from fault zones and generally cease to flow within a few months after the rainfall period, confirming the limited extent of the aquifers.

From borehole I (Figure 5.8) it was observed that there is a perched water table at the depth of 46 m probably within the A.1 formation. A spring discharging from this formation in the lower part of the hill had also been depleted after a few months following winter. The self potential profiles which were carried out in this area show two zones of water movement, one of which is along the left flank of the landslide whereas the second one is along a fault zone.

5.3.4 Engineering Geology of the Landslide

5.3.4.1 Recognition and General Description of the Landslide III

The recent landslide III occurred in an area of an old landslide which covers a total area of about 370,000 m². The main scarp of the new landslide is at an elevation of 445 m, about 25 to 45 m from the existing highway which is here at an elevation of 428 m (Plate 5.4 & Figure 5.8).



Fig(5-8)

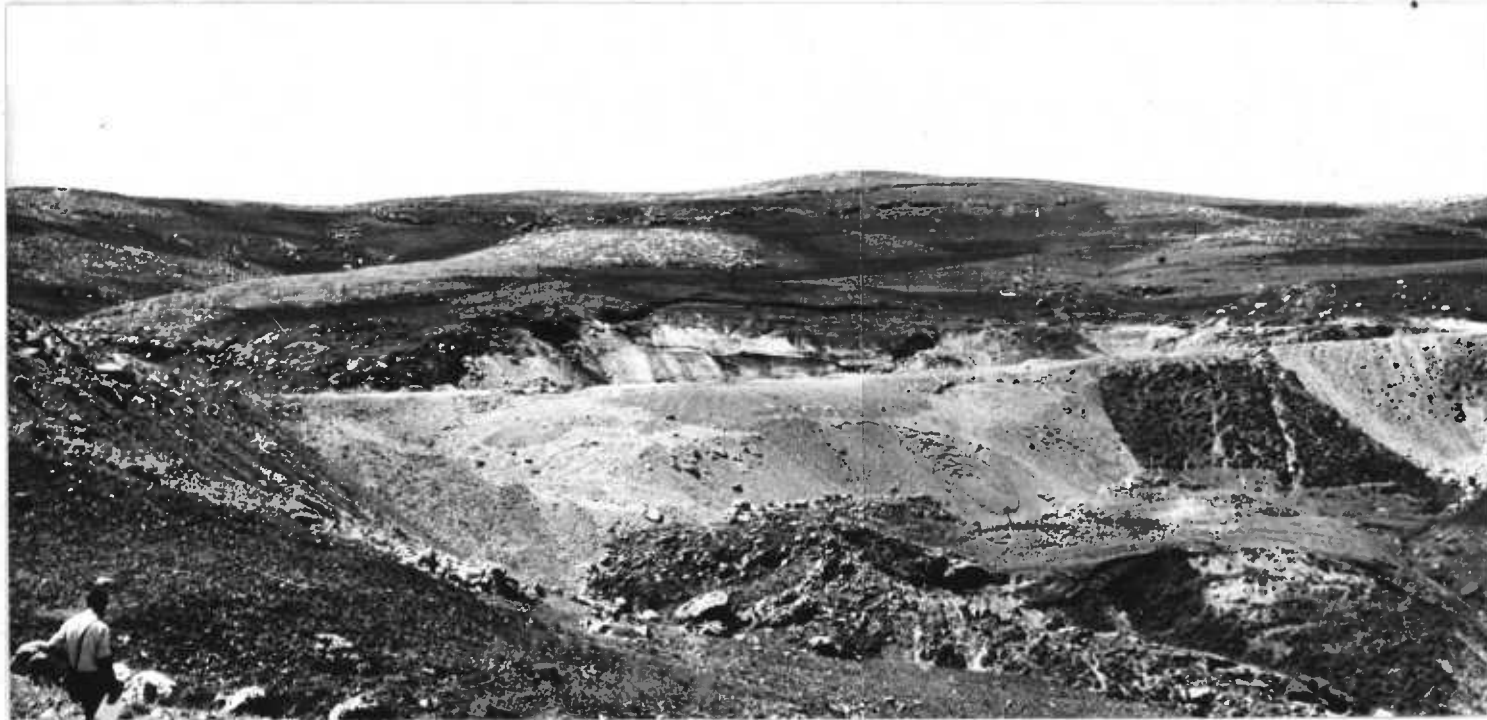


Plate 5.4 General view of the landslide III in 1969.

The breadth of the slide was about 160 m measured along the highway, and the length along the long axis about 170 m, the axis trends about N 20° W. The slide mass comprised a total volume of about 400,000 m³, and covers an area of about 15,000 m², which is 1/20th of the ancient landslide area. The surface of slide mass was relatively wet during the movement, the mass consisting of clay and weathered rock fragments ranging in size from clay to boulders. The soil is yellowish-brown, with large included marlstone and marly limestone boulders.

This section of the highway was constructed partially on the natural hillside and partially on the fill. The ground slope originally had an average inclination of approximately 14°. Landslide III occurred in 1969 after periods of heavy rainfall and caused damage to the highway and consequential traffic delays.

As a result of this transitional movement, the slide mass sank about 3 m in the crown where a grey, yellow clay (Wc = 28%) was exposed along the scarp. The highway was displaced about 30-50 m north west in the direction of the slope. At the main scarp, and on its left and right flanks, the slide has clear cut lateral boundaries on which the slide surface could be clearly traced.

The slide mass consists of soft clays and marls alternating with marly limestone, dipping gently in a north-

west direction out of the slope. It is confined wholly within the weathered zone extending to a depth of about 6 m below the surface. The slip surface runs parallel to the slope, inclined at 12° , as proved by drill holes and other exploration methods.

The slide mass remains active. After the highway was reconstructed, many tension cracks were observed above the highway, which suggests that the area is still moving. Also, continued cracking and settlement in the highway pavement demonstrate that the movement is of a progressive nature.

After the 1969 landslide, many minor scarps were observed in the area, as well as the many tension cracks which were observed at the north edge of the fill, which contributes significantly to the stability of the area. Any reduction in the resisting forces of the lower part by erosion would cause a consequential failure in the embankment.

The highway was reconstructed immediately after the landslide occurred, and also trees were planted in the fill area, north and south of the highway, and these trees have shown a remarkable growth, Plate 5.5. The total length of the reconstruction is about 175 m.

This section of the highway was constructed in the toe of the old landslide area (Figure 5.6) which would be observed clearly from the aerial photographs taken in 1953 and 1965.



Plate 5.5 Landslide III in 1971.



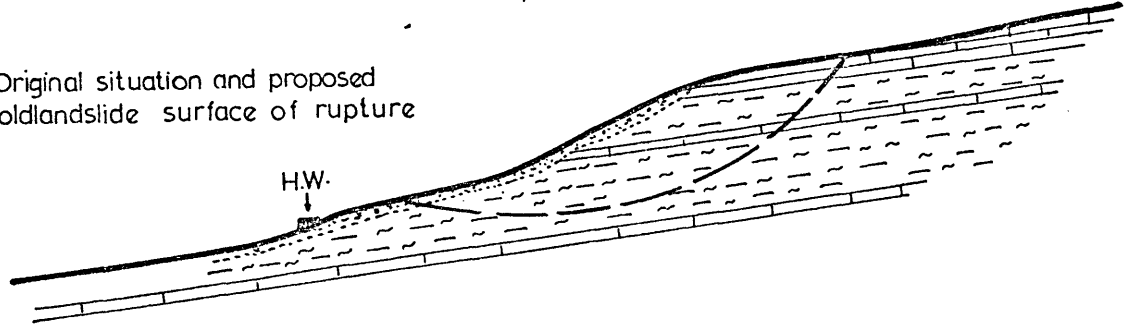
Plate 5.6 Landslide III in 1971.
Establishment of tension
cracks at the crown part
of the landslide.

The ancient movements of this area seem to be deep seated, circular-type movements without significant intense disruption in the bedrock but with a change in the dip of the strata as the result of tilting (Figure 5.9). In contrast to this situation, the present landslide shows intense disturbance in the bedrock, and in the moved mass, which can be a good indication of a non-circular movement. The main movement occurred along the plastic clay layer and tangential to the limestone beds at an average depth of about 22 m, where a remoulded clay zone was found in the boreholes. The upper stratum is intensely jointed and this is believed to have failed progressively.

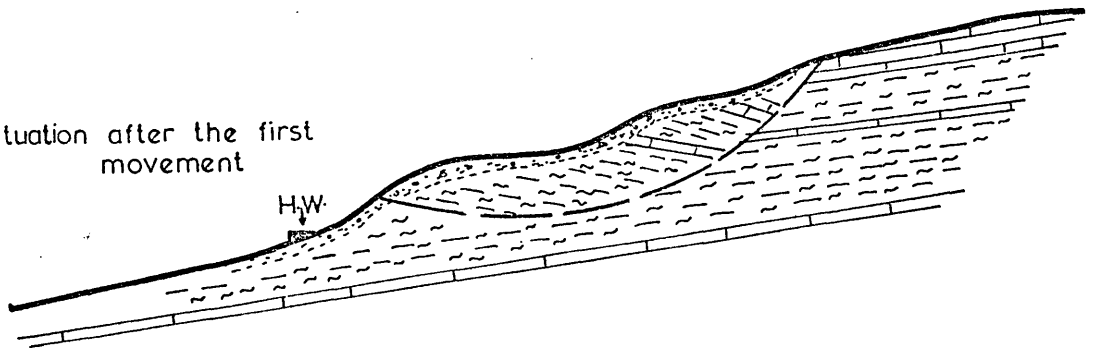
This movement of landslide III occurred immediately after exceptionally heavy rainfall, and led to bulging and cracking of the soil above and below the level of the road. The joints in the rigid strata show progressive opening up of tension cracks in the clay leading to loss of interlock between the rock joints. Most of these joints are open and parallel to the ground contours dipping in the direction of the ground slope (circumferential to the slide outline). The joints divide the bank into many blocks which causes consequential loss of coherence in the layered strata and leads to a progressive reduction in strength (Terzaghi, 1936).

SWEILEH - JARASH ROAD LANDSLIDE III PROPOSED EVOLUTION OF MOVEMENTS (PRINCIPAL SKETCHES)

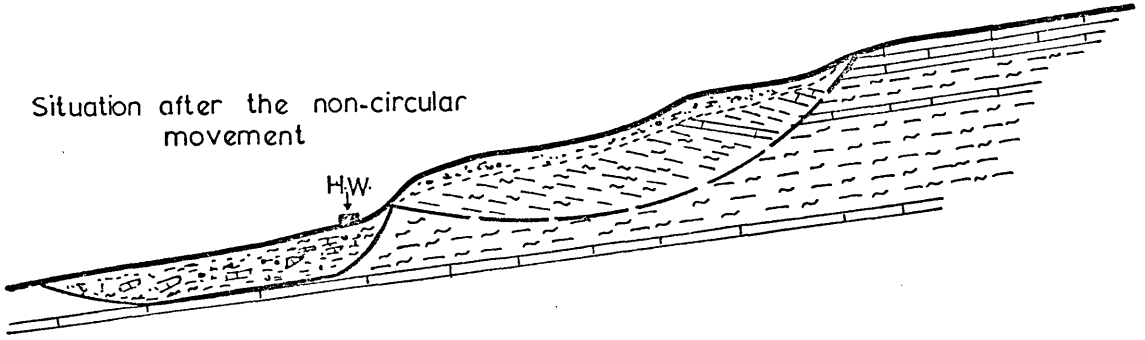
Original situation and proposed
oldlandslide surface of rupture



Situation after the first
movement



Situation after the non-circular
movement



- | | | | |
|---|-----------------|---|-----------|
|  | Weathering zone |  | Clay |
|  | Marl |  | Limestone |
|  | Highway | | |

Fig(5.9)

After the first movement in the area, stress relief would have occurred causing opening of the joints in the clay and marls, thus increasing the permeability of the rock mass. These joints act also as discontinuous planes of weakness and stress concentrators which the sliding shear surface will tend to follow (Skempton, 1970).

5.3.4.2 Field investigations

Movement of the landslide commenced in March, 1969 after 200 mm exceptionally heavy rainfall over a period of one month. Field observations and surveying were started and the relevant data plotted on contour maps of 1:10,000 scale (with a 25 contour interval) carried out by Hunting Aerosurveys Ltd. In 1970, a 1:1,000 scale contour map was prepared, and further detailed geological mapping was carried out.

Between 1969 and 1971 many indications of the progressive nature of the slope failure were observed, such as tension cracks just above the crown of the slide (Plate 5.6), opening of joints in the bedrock, bulging and cracking in the pavement, and tilting of the recently planted trees.

Two boreholes were drilled in the vicinity of the landslide to locate the slip surface, determine the depth of the undisturbed bedrock and to observe the ground water level.

The core samples obtained from the first 20 m of these boreholes were intensely jointed marly limestone with slickensides and polished surfaces, together with remoulded marl and clay. The water content of materials in this zone increases with depth from 22% to 30%. The strata between 20-21.7 m are highly disturbed, being composed of marly limestone and marls with a 25% water content. 3 m below this level the strata are remoulded to very soft marl and clay with cavities observed during the drilling. Hard limestone was located at a depth of about 24 m interbedded with thin bands of marl and clay; the natural water content of these bands is as low as 12%. A typical profile of the boreholes in the slide area is shown in Figure 5.8.

The surface mapping and the exploratory drilling was supplemented by seismic refraction and resistivity soundings. Self potential profiles were also carried out to detect the occurrence of the ground water zones.

The seismic refraction survey carried out at the first location, SS.1, shows that the strata above 21 m has been disturbed and that bedrock is located at a depth of 27.7 m with an apparent dip of 12° out of the slope in the direction of the movement. The second location, SS.II, showed thickening of the marl and clay zone towards the northwest, with bedrock located at a depth of 21.6 m (Figure 5.3A).

The Schlumberger expanding method of the resistivity sounding carried out suggested that the area is influenced by two major faults besides smaller displacements, and also indicates that the thickness of the soil mantle ranges between 5-10 m.

The faults located by the seismic investigation were detected by the difference between resistivity soundings no. 21 and 22; and also the thickening of the marl and clay zone was demonstrated by resistivity soundings nos. 13, 14, 15 and 16 (Figure 5.4A).

The variation in seismic velocity and apparent resistivity correlate well with the surface geology and the information obtained from the exploratory drilling. The following table shows the average resistivity and velocity of the materials in the vicinity of the landslide:

Zone	Apparent resistivity (Ω /m.)	Seismic velocity (m./sec.)
Mantle zone	4-30	550-800
Marl & Clay zone	30-80	1000-2500
Bedrock	>100	3700-7000

Table 5.2

The intense jointing and disturbance of the upper zone, the soft remoulded clay, the shear zone, and the slip surfaces at 21 m depth indicated by geophysical methods, together

with the position of the main scarp and toe of the landslide, allow the geometry of the slipped mass to be determined with reasonable accuracy.

A lithological cross-section of the site of the landslide was prepared based on information obtained from the interpretation of the exploratory drilling, geophysical surveys and surface geology, and is shown in Figure 5.10.

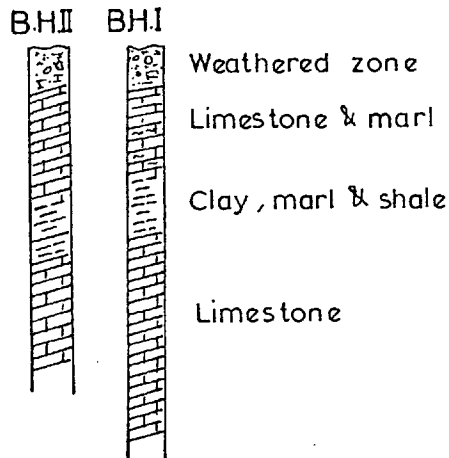
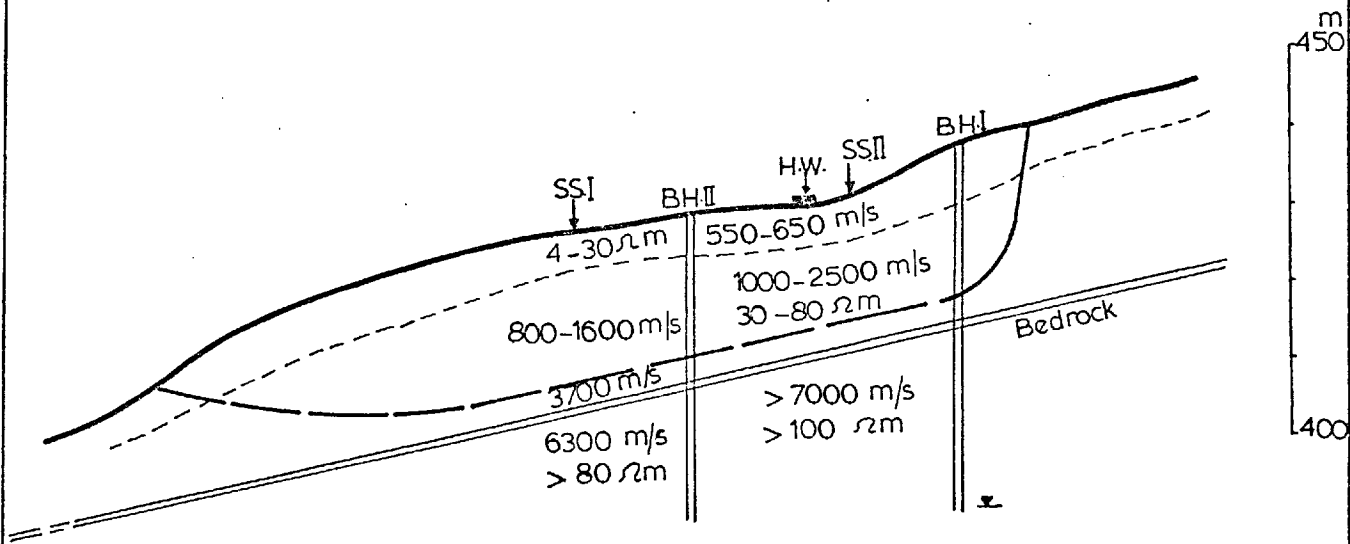
5.3.4.3 Laboratory investigations

Representative disturbed and undisturbed samples were obtained from this site in order to establish the engineering properties of the clay material in this area.

A summary of the representative results of the analyses is compiled in Tables 5.1B & 5.2B. The principal classification results are summarised in the table on the page following. (Table 5.3).

The Atterberg limits test results are plotted on the conventional Casagrande plasticity chart (Figure 5.11) from which the average values in the following table have been obtained. All the points lie above A line, and the clay is mainly CH (inorganic clays of high plasticity). This type of clay has the following properties (according to U.S.B.R.):-

LANDSLIDE-III RESISTIVITY , SEISMIC AND BOREHOLES INTERPRETATION



SS. Seismic refraction
 BH. Borehole
 H.W. Highway

Fig(5.10)

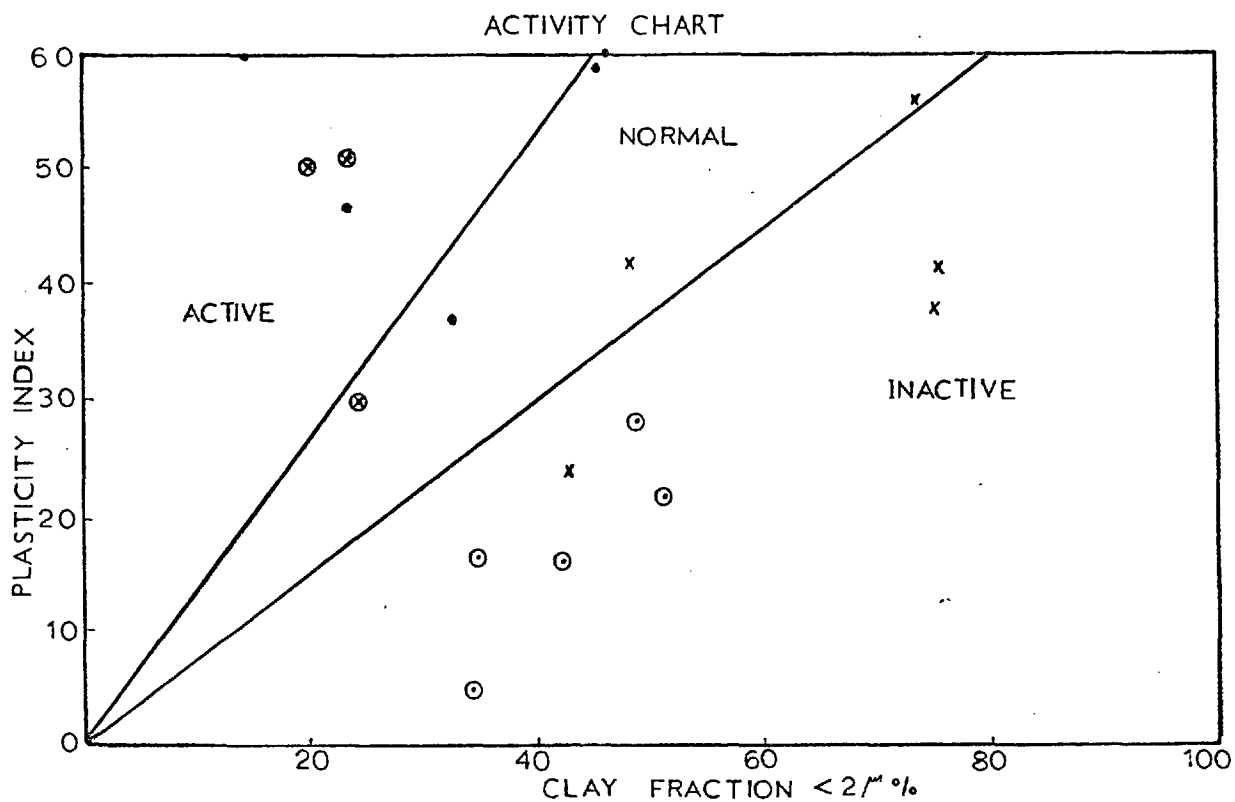
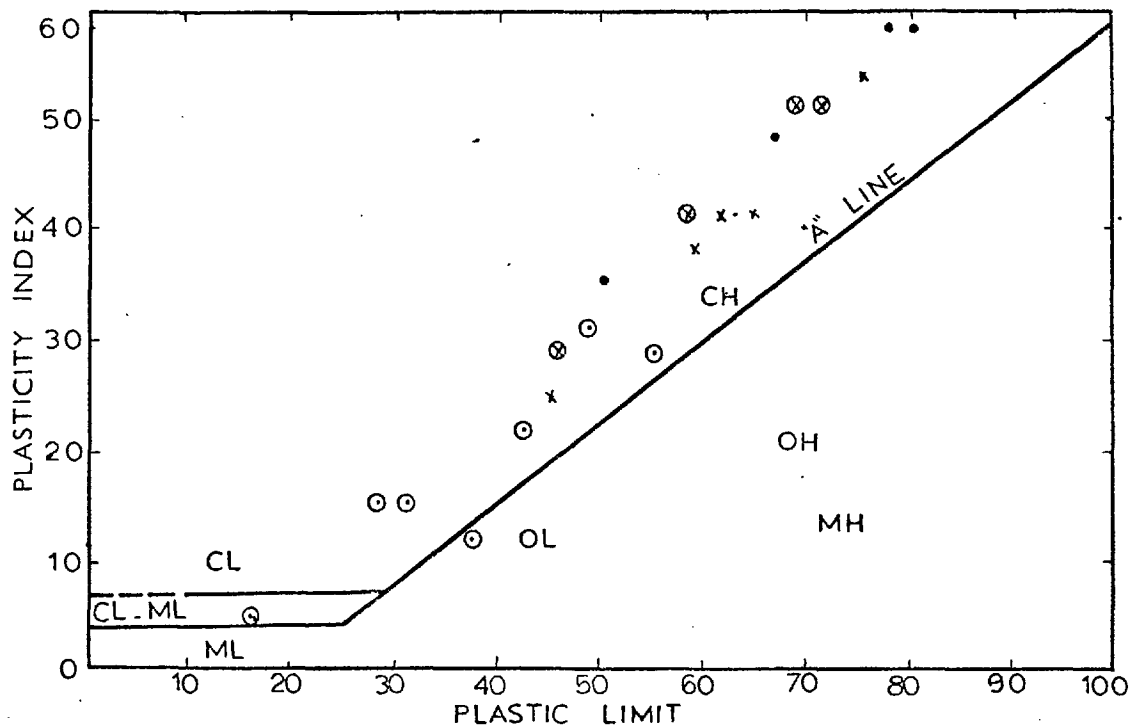
Index Properties	Range	Number of Samples	Mean
Liquid Limit (L.L.)	50-88%	5	71.8%
Plastic Limit (P.L.)	14-20%	5	17.6%
Shrinkage Limit (S.L.)	10-12%	5	10.8%
Clay Fraction (<2 μ)	13-45%	5	31.4%
Activity	1.1-4.7	5	1.96
Liquidity Index (L.I.)	0.08-0.37	5	0.20
Max. Water Absorption	52-99%	5	75.6%
Specific Gravity	2.60-2.66	5	2.64
Wet Bulk Density γ_s	1.83-2.08 g/cm ³	5	1.93 ₃ g/cm ³
Natural Water Content (W _c)	17-40%	5	29.0%
Porosity (n)	33-49%	5	43.0%
Void Ratio (e)	0.74-0.98	5	0.77
Calculated Degree of Saturation	92-100%	5	95.4%

Table 5.3

1. Impervious when compacted.
2. Poor shearing strength and high compressibility when compacted and saturated.
3. Poor workability as a construction material.
4. Suspect to erosion resistance, and should not be used as surfacing in the roadways.
5. Poor as a fill and foundation material.

The activity (as the ratio of plasticity index to the content of the clay fractions) shows that this type of clay would be classified as a normal to active clay (Figure 5.12). This suggests a predominantly Illitic, Montmorillonitic clay

SWEILEH - JARASH ROAD
 PLASTICITY AND ACTIVITY CHARTS
 OF REPRESENTATIVE SAMPLES



- x LANDSLIDE I
- ⊗ LANDSLIDE II
- ⊙ LANDSLIDE III
- LANDSLIDE IV

Plasticity chart (above) and Activity chart (below)
 Fig(5.11) & Fig(5.12)

(Skempton, 1953) and was subsequently confirmed by X-ray analysis. The dried and crushed samples finer than 0.15 mm show a medium to high water absorption related to the percentage and type of the clay; the greater the content of a Montmorillonite or mixed layer mineral, the higher the water absorption (Figure 5.5A). The liquidity index suggests that this clay could be classified as stiff clay (Terzaghi, 1936). The natural water content is mainly above the plastic limit; this type of clay is over-consolidated in the present situation, but is also partially saturated. The grainsize distribution of the representative samples shows 13-45% clay fraction, Figure 5.6A.

Shear strength parameters in terms of effective stresses were determined by consolidated-undrained triaxial compression with pore water pressure tests performed on three or four specimens 3 x 1.5 in. in diameter taken from the same sample. The results of tests are summarised in Table 5.2B. The average shear strength parameters of five tests for the clay involved in landslide III, as an approximation represented by a straight line can be expressed with sufficient accuracy by $\phi'_p = 13^\circ$, $C'_p = 0.2$ Kgf/cm²; and for the same clay horizon taken from ambient clay outside the landslide area is $\phi'_p = 14^\circ$, $C'_p = 0.51$ Kgf/cm² (Figure 5.13).

Representative peak and residual shear strength parameters were also obtained by carrying out drained direct

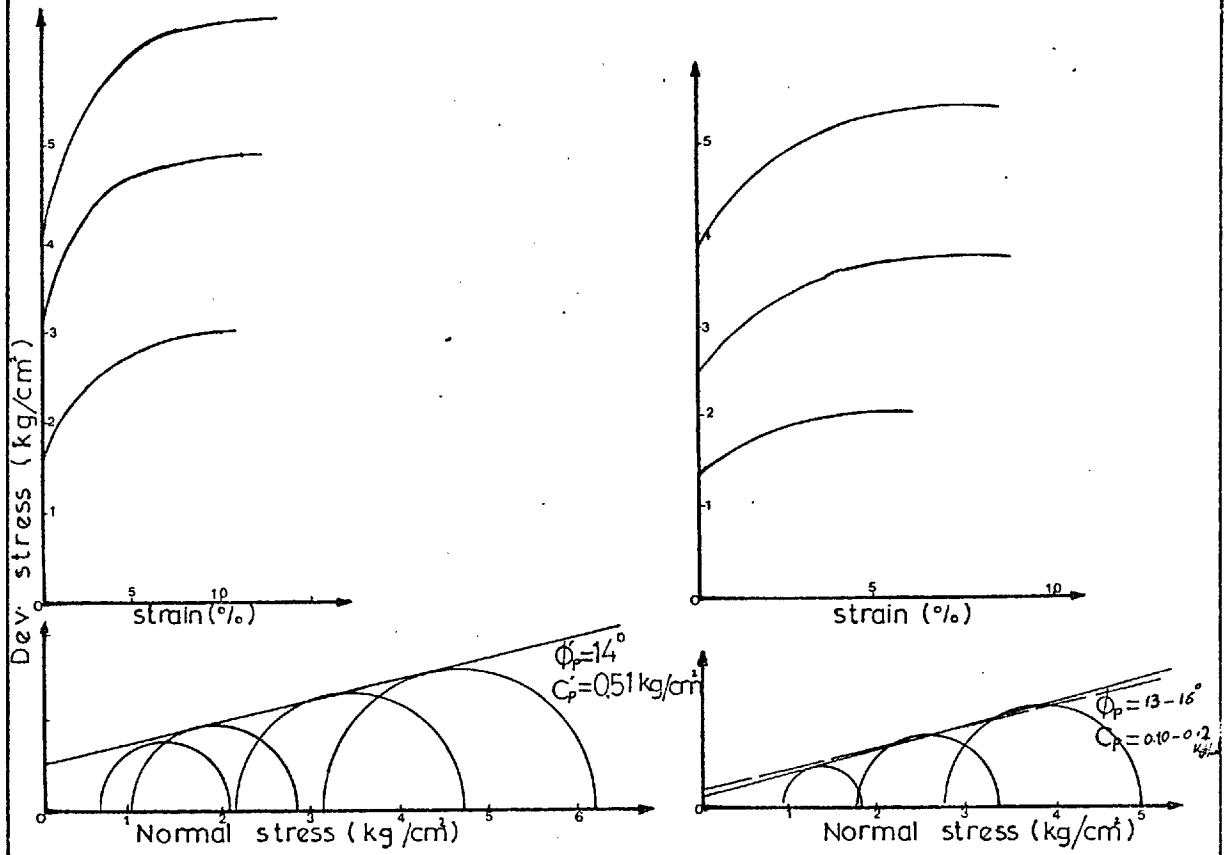


Fig: (5.13) - CONSOLIDATED-UNDRAINED TRIAXIAL TEST

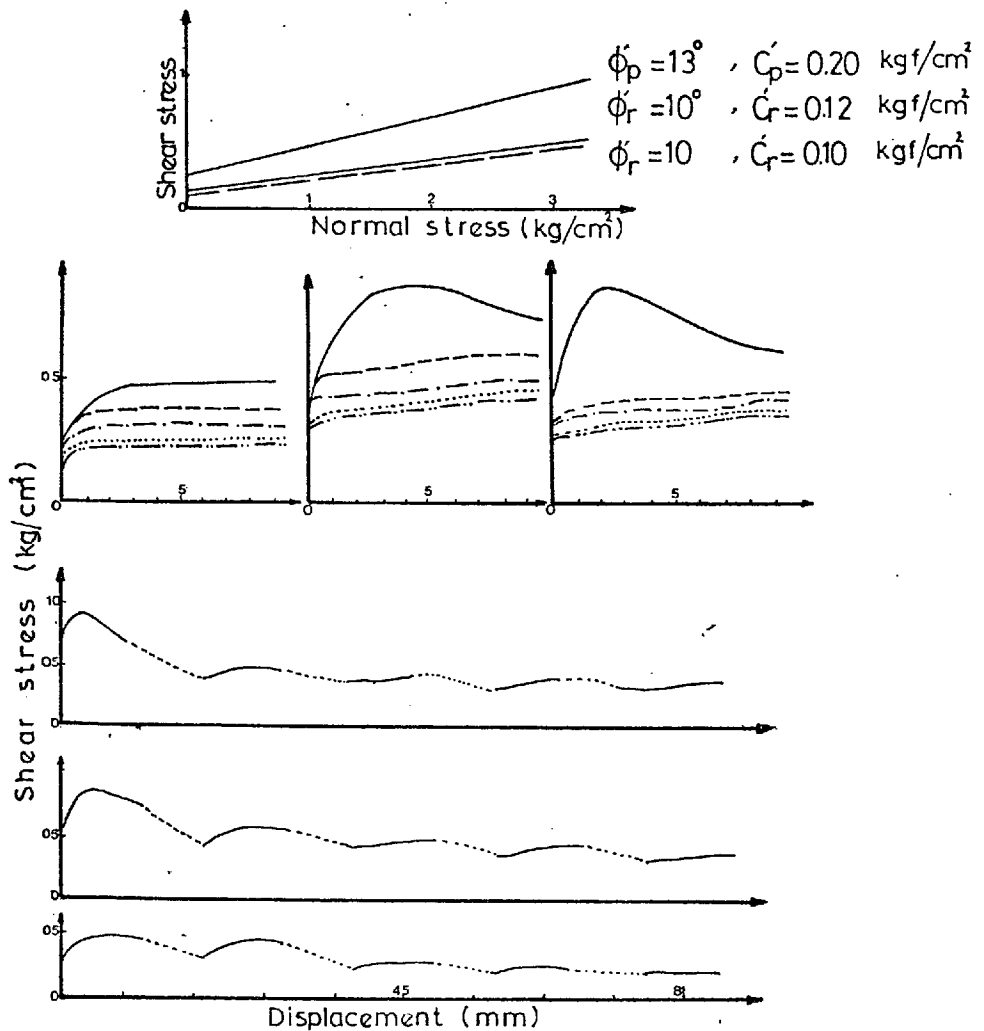


Fig (5.14) - MULTI-REVERSAL SHEAR TEST

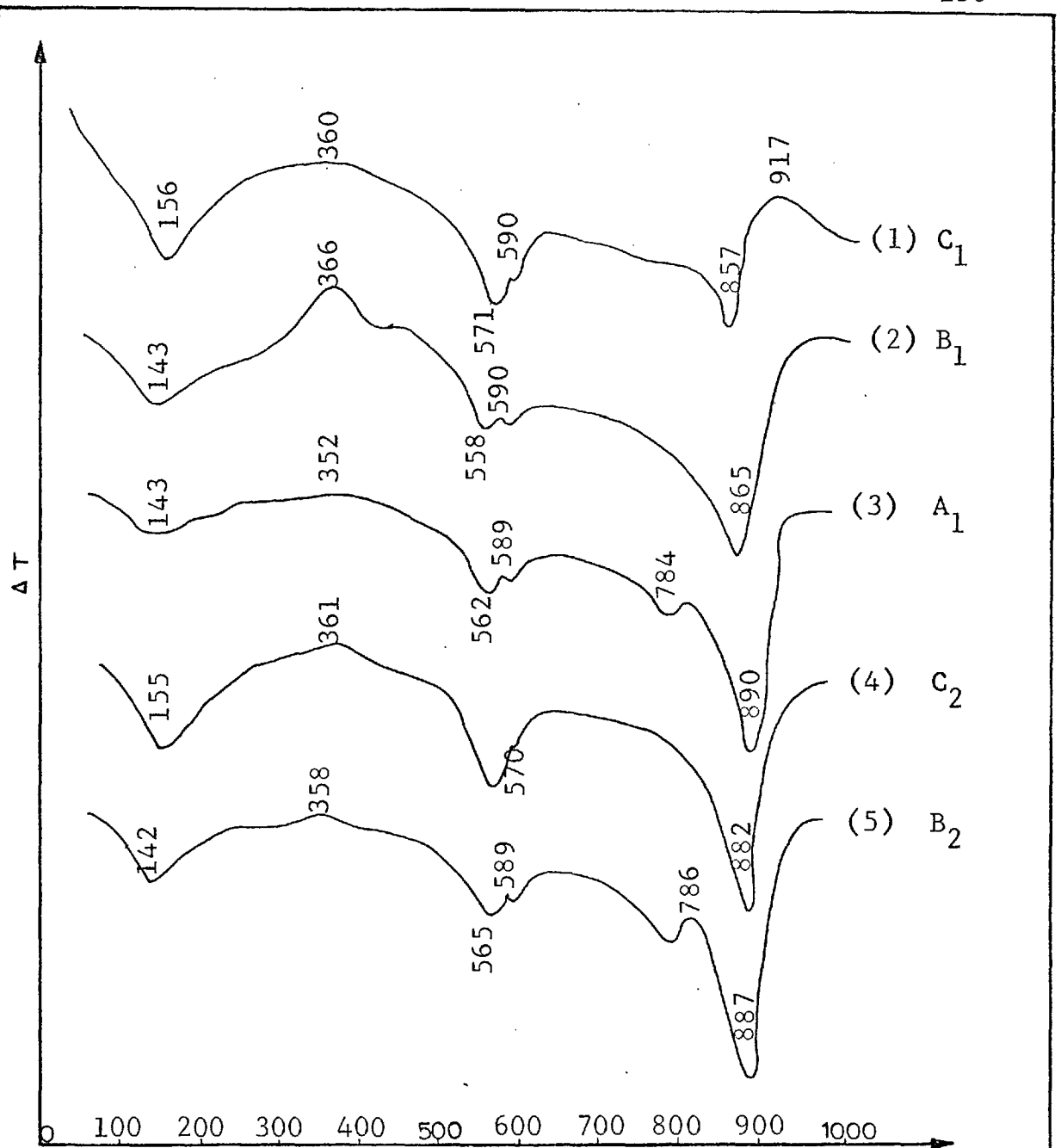
shear box tests on specimens 6 x 6 x 2.5 cm with a maximum relative displacement of about 9 mm, and subjected to reversals and reshearing until no further drop in shearing resistance was observed (Skempton and Petley, 1968). Movement in both directions was at a very slow speed (0.0000769 in/min) to avoid building up excess pore pressures. The tests show the following results:-

$$\phi'p = 13^{\circ}, C_p' = 0.26 \text{ Kgf/cm}^2, \text{ and } \phi'r = 10^{\circ}, C_r' = .12 \text{ Kgf/cm}^2$$

(Figure 5.14). These results agreed very well with the results obtained from the triaxial test.

The material in the area investigated suffered considerable shear displacement, therefore the drop from the peak to the residual strength is limited. The greater the shear displacement suffered, the lower will be the drained peak shear strength and closer this will approach the residual value (Skempton, 1970).

The mineralogical composition of these clays was studied by the Differential Thermal Analysis, which shows that this clay is mainly Illite, montmorillonite, poorly crystallised kaolinite, quartz, calcite and traces of organic impurities (Figure 5.15, and Table 5.4). The curves obtained show the following types of peaks at the appropriate temperatures.



Correlation of the D.T.A. of the representative samples along Sweileh - Jarash road

- Sample C₁:- Illite + Montmorillonite, poorly crystalline kaolinite, with quartz, carbonates and traces of organic materials.
- Sample B₁:- Illite + Montmorillonite + Calcite, poorly crystalline kaolinite, with quartz and carbonates.
- Sample A₁:- Illite + Montmorillonite + Calcite, Kaolinite, quartz and carbonates.
- Sample C₂:- Illite + Montmorillonite + poorly crystalline Kaolinite, calcite, quartz, carbonates and organic material.
- Sample B₂:- Illite + Montmorillonite, Calcite, poorly crystalline Kaolinite, quartz, carbonates and traces of organic material.

Expected Minerals

Fig(5.15) and Table(5.4)

Sample No.	Type of Peak + temp. in °C	Probable Explanation
C1	Endotherm 142-156	The evolution of absorbed water from atmosphere
B1	Exotherm 352-365	Decomposition of carbonates
A1	Endotherm 558-571	Evolution of Hydroxyl water
C2	Endotherm 589-590	α - β quartz inversion
B2	Endotherm 857-890	Evolution of CO ₂

Table 5.5

The X-ray diffractometer traces for cavity mount specimens show that all the whole samples proved to give nearly the same reflections but of different intensities according to the percentages of the minerals present. The following interpretations can be applied to the analysed samples:-

1. The first peak appearing at about 10 \AA° indicates the presence of non-expanding mica type layers such as illite, The presence of a 10 \AA° basal reflection, a relatively broad peak, could be attributed to one or more of the following reasons:-
 - a. poorly crystalline and/or very fine grained illite.
 - b. the presence of illite in the form of exceedingly thin flakes.
 - c. imperfections of illite crystals due to random displacement of the lattice layers in two directions.
2. The second peak which appears at about 7.13 \AA° is characteristic of the first order basal reflection (001)

of the mineral kaolinite; the second order basal reflection of kaolinite (002) occurs at 3.57 \AA° . It is possibly of a poorly crystalline type because of the absence of many other reflections and the broadening of the peaks. Chlorite has the same spacing characteristic of kaolinite but in view of the absence of the 19 \AA° basal reflections in most of the samples studied, it is almost certainly absent from all the samples examined.

3. The following minerals show the following basal reflections:-

Calcite	3.82 \AA°
Quartz	$4.25 \text{ \AA}^\circ, 3.33 \text{ \AA}^\circ$
Dolomite	$2.91 \text{ \AA}^\circ, 2.88 \text{ \AA}^\circ$
Feldspar	$3.43 \text{ \AA}^\circ, 3.22 \text{ \AA}^\circ$
Gypsum	7.56 \AA°

It can be seen that the tested samples are mainly composed of quartz, calcite, illite-montmorillonite, illite, kaolinite, dolomite, and accessory feldspar.

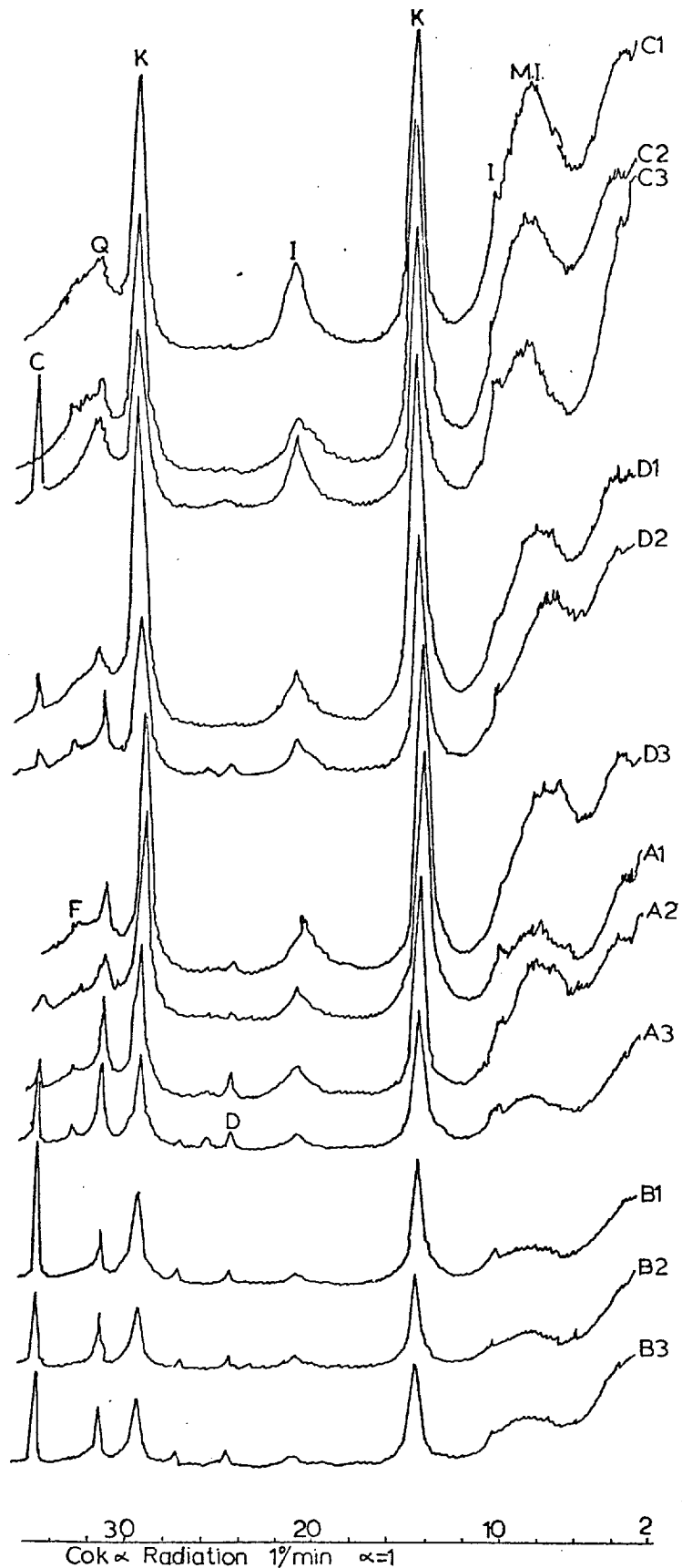
The quantitative mineralogical analysis X-ray diffraction on the orientated $<-2\mu$ clay specimens was also carried out after the samples were subjected to both glycerol and heat treatment at 400 and 550° to distinguish between certain types of clay minerals, following the method developed by Schultz (1964) and Shaw (1970).

The interpretations of the curves obtained (Figure 5.16 and Table 5.7) are as follows:-

1. The Illite basal reflection peaks were found at 10 \AA , 4.97 \AA , and 3.32 \AA , that are not appreciably affected by either glycerol or heat treatment, except very slight shift after glycerol.
2. The kaolinite reflection peaks were found at 7.16 \AA , 3.57 \AA and 2.38 \AA . This peak is mainly destroyed after heating at 550° C .
3. The mixed layer is characterised by a broad peak near $15\text{-}18 \text{ \AA}$ after glyceration, and complete collapse to about 10 \AA after heating. The broad band of reflections between 15 \AA and 18 \AA was interpreted as series of montmorillonite and mixed-layer illite-montmorillonite (Shaw, 1972).
4. The following minerals were found as minor amounts in the tested samples; they show the following basal reflections:-

Calcite	3.86 \AA and 3.03 \AA
Quartz	4.26 \AA and 3.34 \AA
Dolomite	4.02 \AA and 3.69 \AA
Feldspar	3.18 \AA

The most important conclusions that could be drawn from this analysis are:-



SWEILEH-JARASH ROAD
 CORRELATION OF THE X-RAY DIFFRACTION OF THE ORIENTED
 MOUNT SPECIMENS

M.I. - Montmorillonite illite
 I - Illite
 K - Kaolinite
 Q - Quartz
 C - Calcit
 D & F - Dolomite & Feldspar

A - LANDSLIDE I
 B - LANDSLIDE II
 C - LANDSLIDE III
 D - LANDSLIDE IV

Fig(5.16)

1. The mixed-layer illite-montmorillonite is the principal clay mineral in the tested samples.
2. There are no significant mineralogical differences between the tested samples. All the samples show the same reflections, but with different intensities according to the percentage of the minerals.

The chemical analyses of the representative samples from the slide area, along the Sweileh-Jarash road, yielded the results summarised in the following table:-

Sample No.	MgO %	CaO %	Fe ₂ O ₃ %	K ₂ O %	Na ₂ O %	MnO %	Al ₂ O ₃ %	SO ₃ %	SiO ₂ %	L.O.I. %
C1	0.75	12.01	5.72	0.73	0.14	0.06	10.63	0.40	56.35	13.36
B1	0.98	11.50	3.80	0.67	0.13	0.05	6.90	0.26	52.32	
A1	0.97	17.24	3.10	0.80	0.09	0.06	9.97	0.37	51.63	
C2	1.82	17.24	4.05	0.80	0.06	0.05	8.90	0.31	47.58	18.89
B2	1.90	17.24	4.29	0.67	0.08	0.04	6.19	0.21	50.17	

Table 5.6

The cation exchange capacities of various clay minerals using Methylene Blue Absorption Method, are summarised in Table 5.7. They show a high range, which indicates that this clay is probably of a mixed Kaolinitic, illitic, montmorillonitic type.

Summary of the X-ray diffraction analysis

(Semi-quantitative)

Oriented specimens

Sample No.	Kaolinite	Illite %	Mixed Layer	Cation Exchange Capacity meq/100 g
A1	29	15	56	30
A2	19	17	64	38
A3	27	13	60	30
B1	39	17	44	26
B2	22	39	39	32
B3	27	17	56	30
C1	17	19	64	42
C2	20	17	63	43
C3	20	16	64	
D1	20	14	60	39
D2	23	21	56	37
D3	20	17	63	43

Table 5.7

Whole Rock Specimens

Sample No.	
1 (C ₁)	Illite-Montmorillonite, quartz, calcite, kaolinite, illite, dolomite, feldspar.
2 (B ₁)	Illite-Montmorillonite, quartz, calcite, kaolinite, illite, dolomite, feldspar.
3 (A ₁)	Illite-Montmorillonite, quartz, calcite, dolomite, kaolinite, illite, feldspar.
4 (C ₂)	Illite-Montmorillonite, calcite, kaolinite, quartz, illite, dolomite (access.), feldspar (trace).
5 (B ₂)	Illite-Montmorillonite, quartz, calcite, dolomite, kaolinite, illite, feldspar (accessory).

Table 5.8

5.3.4.4 Slope stability analysis

At the time of the original site investigations for

the highway, no assessment of the stability of the existing slopes was made. After the first landslide, a stability analysis was made in terms of total stresses using the Fellenius method (N.R.A. Engineering Geology, internal report, 1968).

An analysis in terms of effective stresses has now been made on the original cross section (before the landslide occurred) and so on the present cross sections (after sliding) using the methods of Janbu and Fellenius.

As can be seen from the cross sections, the slide mass is composed of three zones; a weathered zone, a marly limestone interbedded with marl zone, and a clay zone. The average densities of these zones are 2 g/cm^3 , 2.2 g/cm^3 , and 1.8 g/cm^3 respectively.

The exploratory drilling showed that the material involved in the slide, particularly close to the slip surface, had been sheared and is remoulded.

Stability analyses for the original cross sections (prior to the movement) were carried out using peak strength parameters in terms of effective stresses, and assuming transient perched water tables in positions 1, 2, 3, 4 respectively at the time of failure during a heavy rainfall

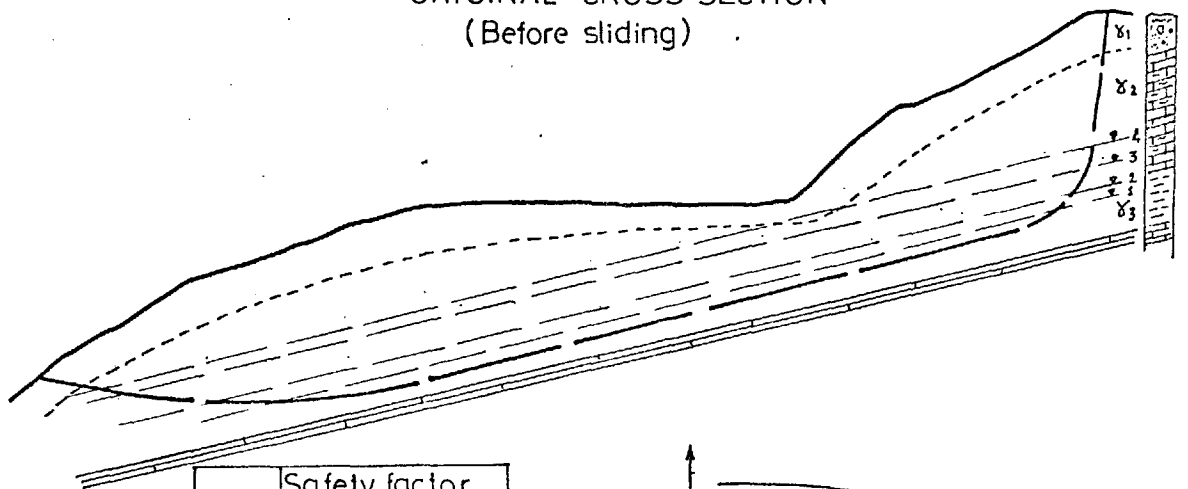
(Fig. 5.17). It was found that the safety factor using Janbu's method ranged between 0.89 and 1.155 and by Fellenius's method between 0.89 - 1.15. It can be seen clearly that the movement would have occurred for a transient water table in position 3, when the factor of safety is equal to unity for both methods. The perched water table was found by the drilling at a depth of 46 m.

The shear strength of the material in the slide was greatly diminished after the initial movement by the presence of joints and slickensides. Therefore the material in the slide mass was not able to mobilise its peak strength during any subsequent movement on the existing slip surface. For subsequent movement residual strength would have to be used in a stability analysis (Skempton, 1964).

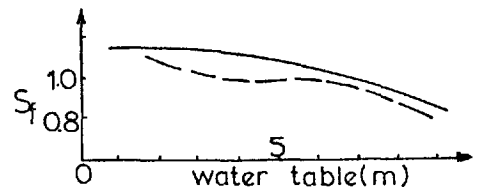
To analyze the stability of the slopes in their present state, cross sections 1, 2, 3 were chosen and the residual strength parameters represented by $C'r = 0.12 \text{ Kgf/cm}^2$, $\phi'r = 10^\circ$, and $C'r = 0$ with $\phi'r = 10^\circ$ being used in Janbu's and Fellenius's methods.

For cross section 1 with a pre-existing slip surface and assuming no excess water pressures on the slip surface and water tables in positions 1, 2, 3 it was found that the factor

LANDSLIDE. III
ORIGINAL CROSS SECTION
(Before sliding)

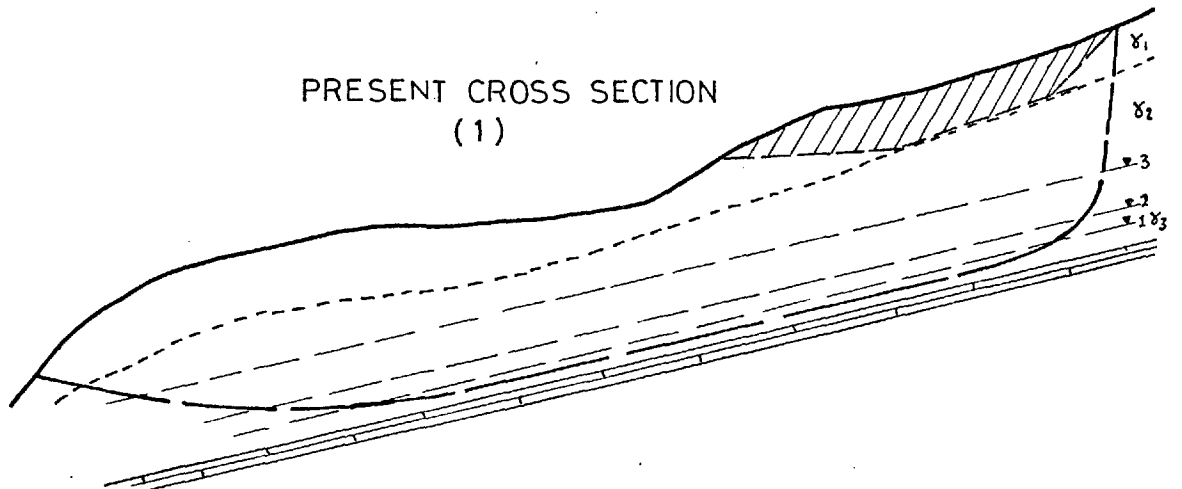


W.T.	Safety factor	
	Fellenius	Janbu
1	1.15	1.155
2	1.11	1.007
3	1.036	0.996
4	0.89	0.827

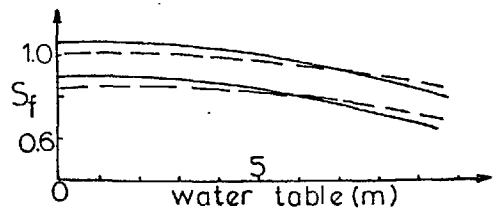


Fig(5.17)

PRESENT CROSS SECTION
(1)



W.T.	Safety factor		Remarks
	Fellenius	Janbu	
No	1.08	1.002	c_r & ϕ_r
W.T.	0.92	0.86	$c_r=0, \phi_r$
		1.062	$c=0, \phi_r=13^\circ$
1	1.08	1.001	c_r & ϕ_r
	0.914	0.845	$c_r=0, \phi_r$
2	1.048	0.985	c_r & ϕ_r
	0.878	0.813	$c_r=0, \phi_r$
3	0.85	0.862	c_r & ϕ_r
	0.68	0.695	$c_r=0, \phi_r$



Fig(5.18)

- Janbu
- Fellenius
- S_f Safety factor
- proposed cut

10 m

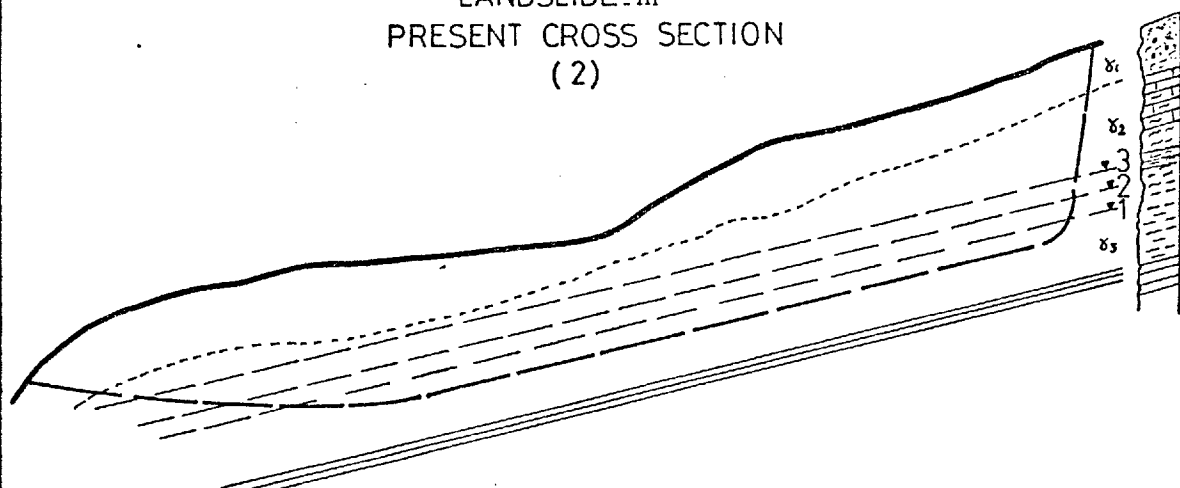
of safety, by Janbu's method, ranges between 0.862 and 0.995 for $C'r = 0.12 \text{ Kgf/cm}^2$ and $\phi'r = 10^\circ$, for $C'r = 0$ and $\phi'r = 10^\circ$ the factor of safety ranged between 0.695 and 0.824. The comparison between the results obtained from both methods is presented in Fig. 5.18.

For cross section 2, Fig. 5.19, the failure surface is assumed to be shallower than the original slip surface, and assuming no excess water pressures on the slip surface, and water tables in positions 1, 2, 3 and using the same shear strength parameters, it was found that the factor of safety by Janbu's method ranged between 0.994 - 1.26 for $C'r = 0.12 \text{ Kgf/cm}^2$, and $\phi'r = 10^\circ$, and 0.79 - 1.046 for $C'r = 0$, and $\phi'r = 10^\circ$. These values are 3-4% higher than the factors of safety obtained by the Fellenius method.

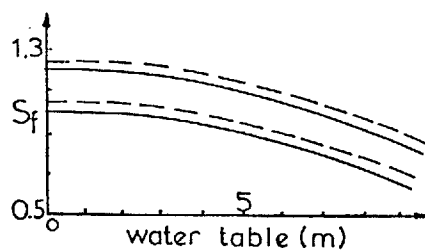
Using cross section 3, Fig. 5.20, assuming an even shallower failure surface with no excess water pressure and water tables in positions 1, 2 it was found that the factor of safety by Janbu's method was in the range of 1.040 to 1.15 using $C'r = 0$ and $\phi'r = 10^\circ$, and 1.334 - 1.45 using $C'r = 0.12 \text{ Kgf/cm}^2$, and $\phi'r = 10^\circ$. These values are about 8-12% higher than the factors of safety obtained by Fellenius method.

The stability analyses clearly show that the slopes remain in a critical state with regard to further movement and

LANDSLIDE .III
PRESENT CROSS SECTION
(2)

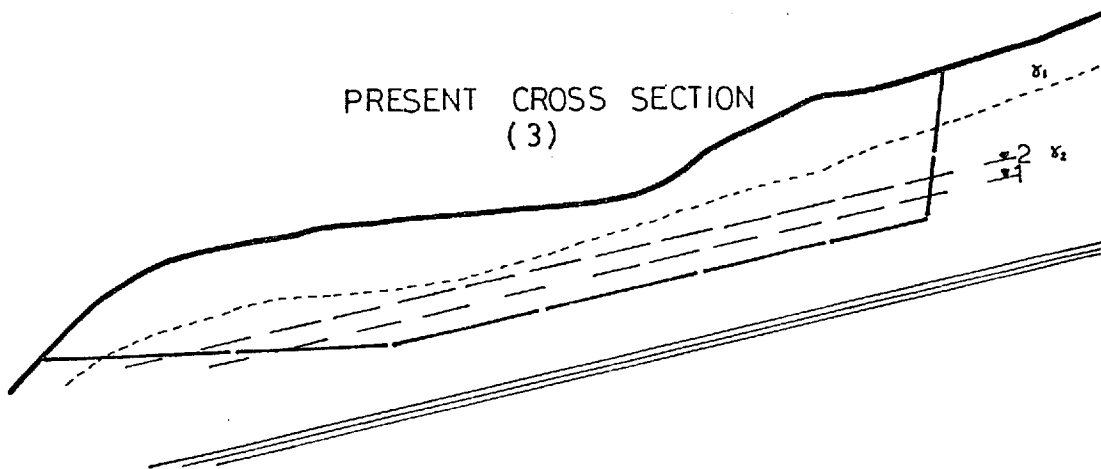


W.T.	Fellenius	Janbu	c_r & ϕ_r
no w.t.	1.22	1.26	$c_r=0$
1	1.176	1.223	c_r & ϕ_r
	0.97	1.12	$c_r=0$
2	1.13	1.17	c_r & ϕ_r
	0.93	0.96	$c_r=0$
3	0.93	0.994	c_r & ϕ_r
	0.73	0.79	$c_r=0$

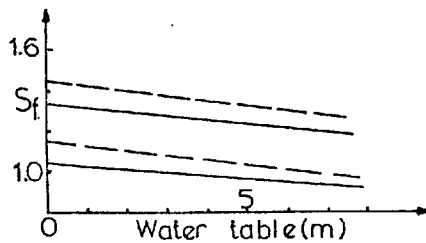


Fig(5.19)

PRESENT CROSS SECTION
(3)



W.T.	Fellenius	Janbu	c_r & ϕ_r
No W.T.	1.35	1.45	c_r & ϕ_r
	1.06	1.15	$c_r=0$
1	1.27	1.39	c_r & ϕ_r
	1.0	1.10	$c_r=0$
2	1.246	1.334	c_r & ϕ_r
	0.976	1.04	$c_r=0$



Fig(5.20)

- - - Janbu
 — Fellenius
 S_f Factor of safety
 W.T. Water table

that temporary perched water tables in the slip material will be sufficient to activate further movement.

5.3.4.5 Remedial measures

The remedial measures for landslide III are as follows:-

- (i) Reducing the driving forces by excavating material at the crown of the landslide, Figure 5.18.
- (ii) Densification of the surface material and sealing off the joints to reduce the amount of rainwater percolating into the ground.
- (iii) Improving surface drainage by diverting rainwater from the landslide area.
- (iv) Constructing a buttress at or near the toe part of the landslide to increase the resisting forces and eliminate toe erosion.

5.3.4.6 Conclusions

In the light of the field and laboratory investigation and analysis, it is quite clear that many factors contributed to the movement, including:-

1. Successive old landslide movements in the area contributed to structural distortion of the strata.

$$C'_r = 0.12 \text{ Kfg/cm}^2 \quad \phi'_r = 10,$$

while the residual parameters obtained from remoulded samples with pre-cut planes shows the following results:

$$C'_r = 0 \quad \phi'_r = 10^{\circ}.$$

4. The stability analysis for the original cross section using the peak strength parameters and assuming four transient water tables during a heavy rainfall shows that the movement probably has occurred for a transient water table in position 3, when the factor of safety is equal to unity for both methods of Fellenius and Janbu.

5. The stability analysis of the slope in its present state shows that the residual parameters underestimate the factor of safety; and the fully softened strength parameters appear to be most reliable for use for the stability analyses of the slope, owing to the amount of disturbance in the strata involved in the slide mass.

6. The method of stability analysis proposed by Fellenius (1926) and Bishop (1954) seems to be the most reliable for use for the non-circular failures; and the safety factor by both methods is very close to each other.

7. The results of these analyses clearly show that the area remains potentially unstable with regard to any further high water tables which might develop in the slip mass.

5.4 DETAILED INVESTIGATIONS OF LANDSLIDE IV

5.4.1 Geology and Hydrology

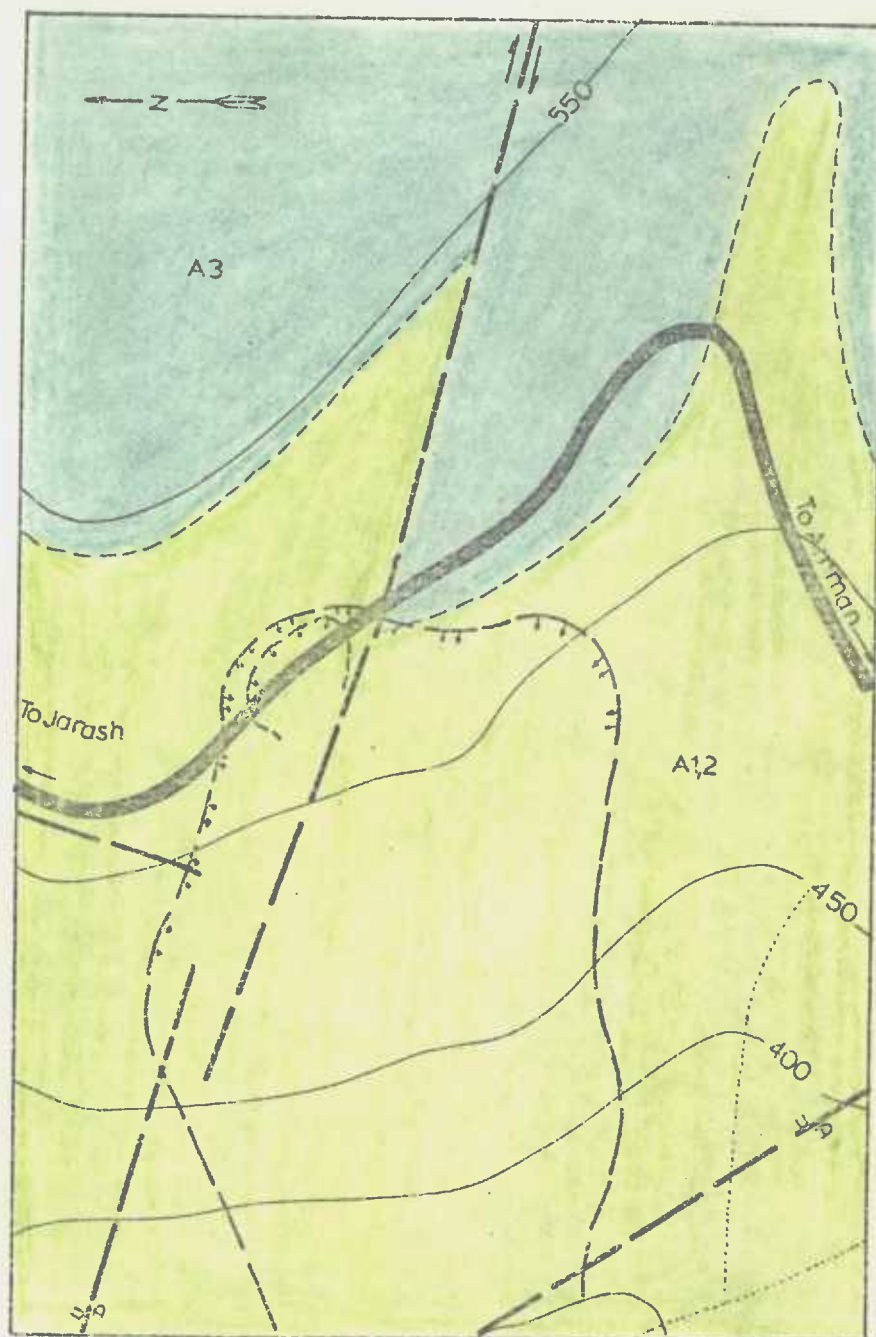
In early March 1967, a sudden landslide occurred at 37 Km on the Sweileh-Jarash road to the south west of Mastaba village, at a distance of 6 Km from Zerqa river bridge. The highway is at an elevation of about 500 metres in this area. A detailed geological investigation was carried out on the available contour maps of a 1:25,000, 1:12,500 and 1:1,000 scale (Figs. 5.21 and 5.22). The geology and the main features of the movement were checked by a study of the aerial photographs produced by Hunting Aerosurveys.

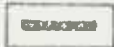
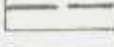
The landslide is on the left flank of a North-South trending anticline, intersected by a NW-SE striking major shear fault, which passes through the landslide zone (Figs. 5.21, 5.1, and Plate 5.7).

Faulting phenomena are a dominant element in the structural geology of the area. The change of dip and lithology at the south-eastern side of the landslide area (at or near the left flank of the landslide), is the result of the shear fault; in addition the strata in the vicinity of the backslope of the landslide show evidence of structural deformation (Plate 5.7 and 5.8).

LANDSLIDE - IV

GEOLOGIC MAP



- | | |
|---|------------------------|
|  | Highway |
|  | Old landslide |
|  | investigated landslide |
|  | Fault |
|  | Contour (m) |

250 m

Fig(5.21)

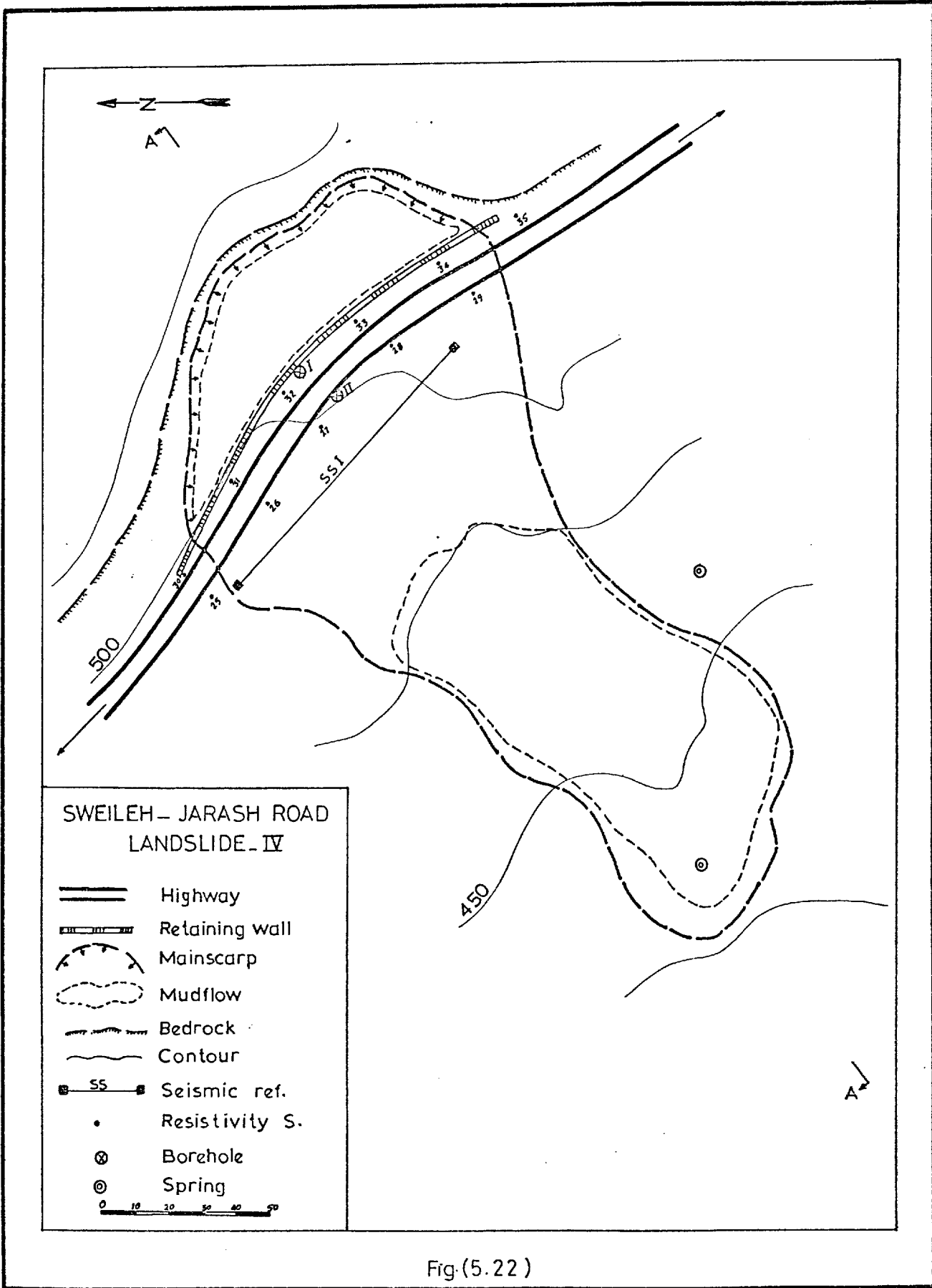


Fig.(5.22)



Plate 5.8 The main features of the upper part of landslide IV.



Plate 5.7 The main features of the lower part of landslide IV including simplified geology.

Two joint sets were observed in the stable bedrock to the south east of the landslide; the first set trends N 21° W dipping 52° NE while the second set trends N 66° E with nearly vertical dips.

The bedrock in the region of the landslide area consists of the marl-clay unit of the lower Ajlun group (A1, 2, 3). The present movement occurred within the A1, 2 formation, near to its contact with A3. The main scarp of the landslide is located in the A2 area. The strata strike almost parallel to the highway. The A3 bedrock is exposed at the southern flank of the present landslide, whilst the north flank is mainly composed of clay and marl (Plate 5.7).

The mean annual rainfall in this area is similar to that at landslides II and III (Section 5.3.3 and Figure 5.7). Rainfall stations along the Sweileh-Jarash road show the following records of the precipitation in the month and year of the recent movement.

Station	Total rainfall March 1967 (mm)	Total rainfall 1967 (mm)	Average rainfall in March in ten years
Jarash	192.2	612.3	87.0
Sweileh	226.7	807.4	127.0
Rumman	221.7	551.5	91.8

Table 5.9

During the month in which the landslide took place, rainfall was approximately twice the monthly average for the ten preceding years (Table 5.9).

As a conclusion, the hydrogeology of this area could be described as being based on fracture permeability. Because of the highly faulted and disturbed nature of the beds, it is probable that the water table rises very rapidly during periods of heavy rainfall, and falls perhaps equally rapidly immediately after the rainfall ceases.

Two springs were observed at the lower part of the landslide area (i.e. to the south-west of the highway). These were probably discharging from the fault zone. The chemical analyses of the water samples from these two springs are shown in Table 5.10.

Spring	Ca	Mg	Na	K	Cl	SO ₄	CO ₃	Total Soluble Salts	Na %	Total Cations
(1)	2.49	3.64	7.40	0.15	6.92	3.26	0.0	896	54.09	13.68
(2)	5.68	4.61	6.50	0.03	6.98	2.25	0.0	1056	38.64	16.82

Table 5.10

The above analyses show that the material from which spring (2) discharges contains a high percentage of soluble salts and is also being subjected to leaching.

5.4.2 General Description of Landslide IV

It has already been noted that landslide IV occurred in March, 1967 following a period of heavy rainfall. As a result of this movement the slide mass sank about 15 metres at the crown of the slope with a horizontal outward movement estimated to be approximately 80 metres downward of the slope in the direction of the movement. The width of the landslide was 80 metres and the crown of the landslide was approximately 20 metres above the road level, at an elevation of 520 metres. Prior to the movement the slope at this part had an inclination of 32° .

Immediately after the movements began, the Ministry of Public Works started reconstruction of the highway; a concrete retaining wall about 155 metres long and 2.0 metres high was constructed. However, due to a complete lack of provision of surface and subsurface drainage and the incorrect location of the retaining wall, water was impounded behind the wall, and this probably led to a softening of the clay material causing the mud flow (Plate 5.9). The shear fault zone also probably concentrated some of the precipitation from a large catchment area into the unstable zone in the lower part of the slide mass, thus contributing to the saturation of the



Plate 5.10 Shifted and curved backward trees at the crown of landslide IV indicating the progressive nature of the movement.

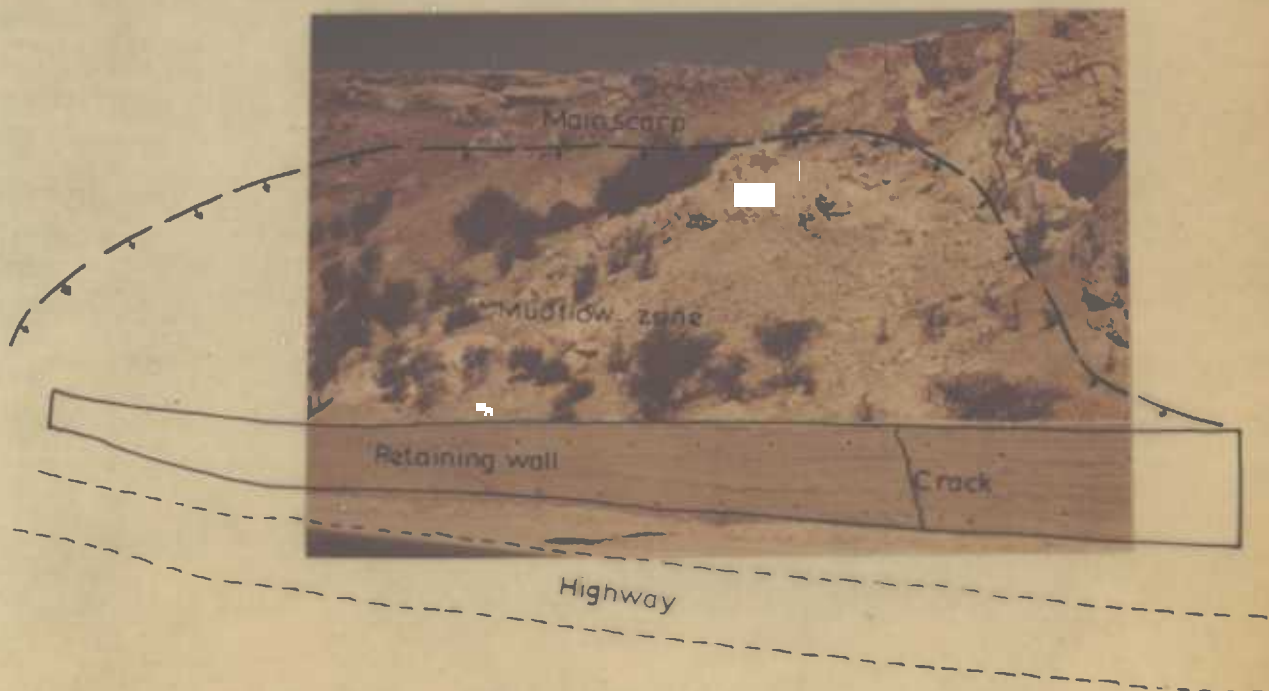


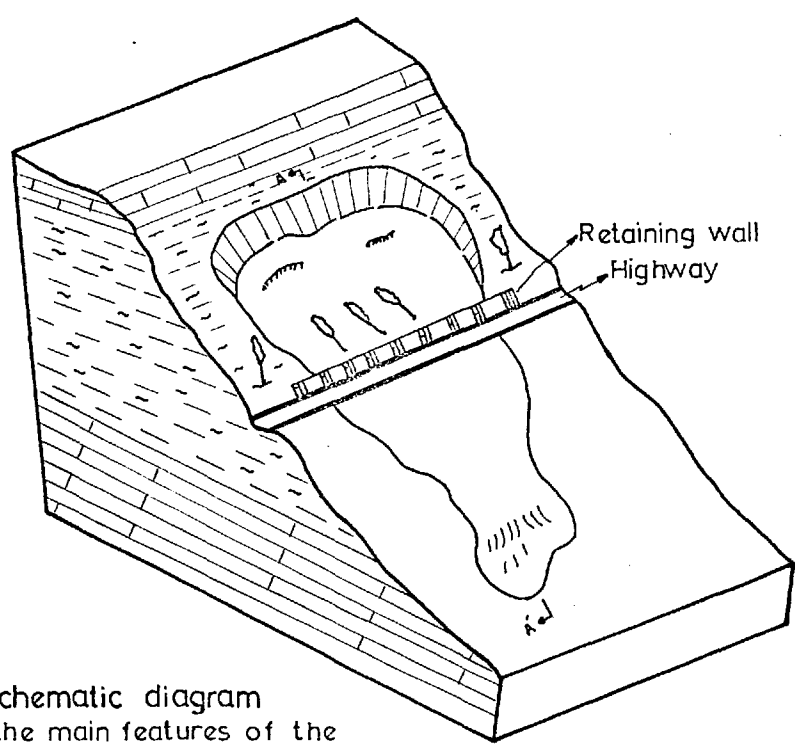
Plate 5.9 Earth and mudflow at the crown part of landslide IV. Notice cracking in the retaining wall.

material and leading to other mudflows (Fig. 5.22). It is believed that these secondary mudflow movements contributed to the reduction of the restraining forces on the whole hillside and could well have initiated the major movement at a higher elevation.

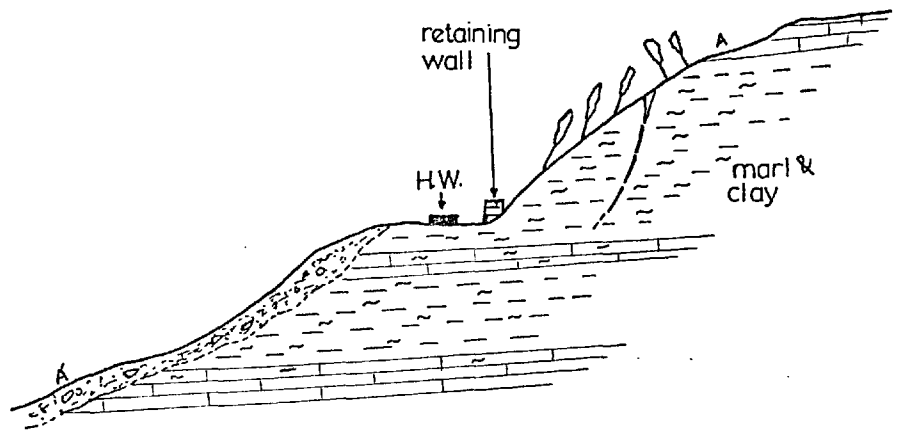
Recently many tension cracks have been observed near the crown of the landslide and in the concrete retaining wall (Plate 5.9). In addition the trees planted behind the retaining wall shifted and curved backward near the crown, indicating that continuation of the movements is occurring (Fig. 5.23, schematic cross section and Plate 5.10).

5.4.3 Field Investigations

Following the landslide movement in 1967, the site investigation started with two boreholes to determine the actual failure surface. These holes were drilled in the vicinity of the displaced mass to depths of 12 and 27 metres. The core samples obtained show a direct indication of shear surfaces at a depth of 11 metres and 12.5 metres in boreholes I and II respectively. The strata above the slip surface consisted of marls, clays and marly limestone. The core recovery was 0% in the weathered zone, between 20 and 40% in the marl-clay zone, and about 80% in the marly limestone



Schematic diagram showing the main features of the landslide area IV.



Schematic cross section showing the trees shifted and curved backward near the crown indicating the movement is in progress.

Fig(5.23)

strata. The moisture content of the clay shows an increase with depth down to the failure surface but then decreases below this level. The clay close to the slip surface is remoulded and it has a noticeably higher moisture content. A third borehole was drilled 8 metres from borehole II, but was abandoned because of technical difficulties.

The Schlumberger expanding method of the resistivity sounding which was carried out at this site showed the weathered zone had a low resistivity and a thickness of about 5 metres; bedrock is probably at a depth of 25 metres. Relative displacements between resistivity zones were also detected from these profiles (Figure 5.7A).

A seismic refraction profile carried out in the middle of the moved mass to the south-west of the highway revealed that the material above a depth of 9 metres had a low velocity, and bedrock was also detected at a depth of about 30 metres (Fig. 5.8A).

The range of apparent resistivities and seismic velocities of the materials in the vicinity of the study area are presented in the table on the following page.

A lithological cross section at the site of the landslide, based on information obtained from the interpretation

Zone	Apparent Resistivity Ω/m	Seismic Velocity m/sec
Weathered Zone	10-30	450-750
Marl and Clay	≈ 30	1000-1100
Limestone and marly limestone	> 90	5600-9000

Table 5.11

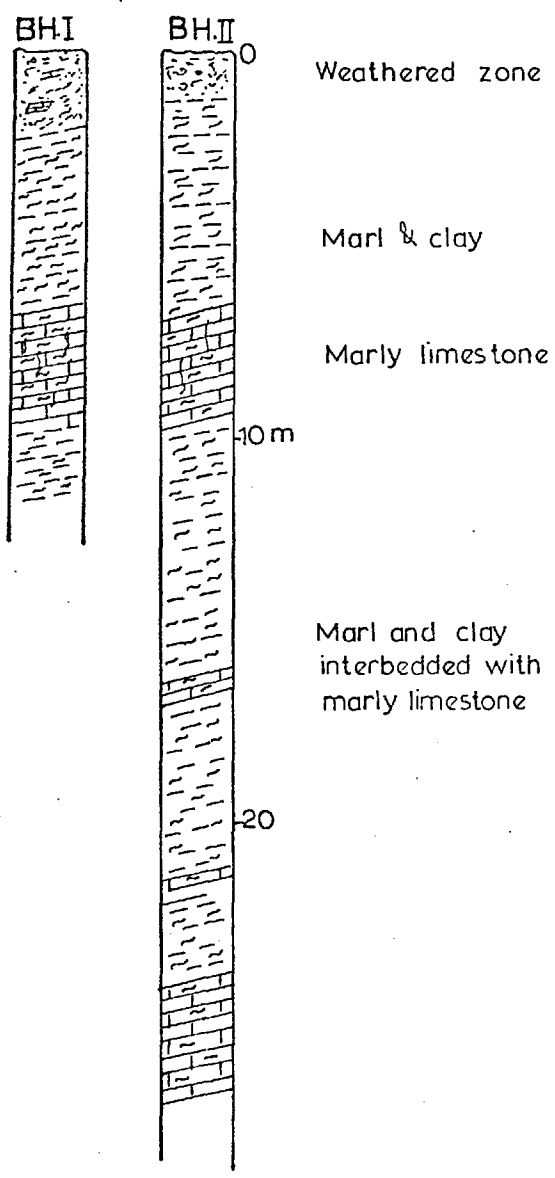
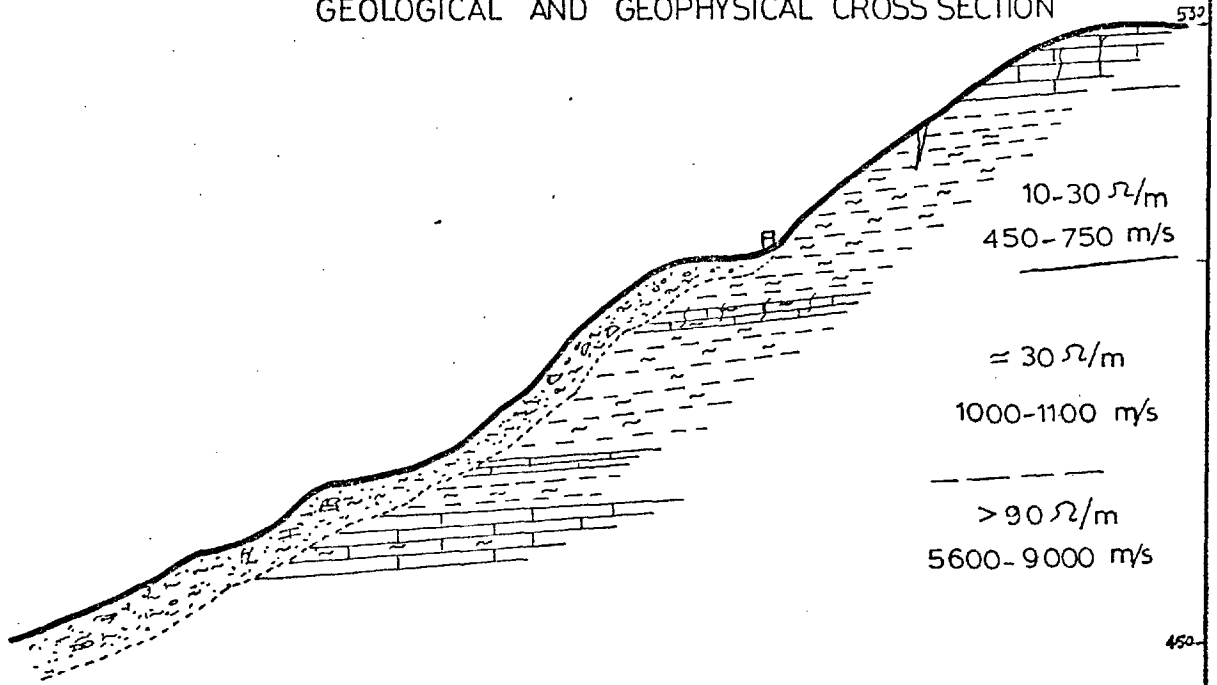
of the exploratory drilling, geophysical surveys and surface geology is shown in Fig. 5.24.

5.4.4 Laboratory Investigations

A laboratory testing programme was devised and performed on representative samples taken from the landslide area, for the purpose of classifying the materials and to establish the shear strength parameters of the clay for use in the stability analysis. The summary of the test results is presented elsewhere in Table 5.2B.

The typical range of values for the various parameters is given in Table 5.12. Atterberg limit test results are plotted on the Casagrande plasticity chart (Figure 5.11) which shows that all the points lie above A line, indicating that the clay materials are mainly CH type (inorganic clays of medium to high plasticity).

LANDSLIDE .IV GEOLOGICAL AND GEOPHYSICAL CROSS SECTION



50 m.

Fig(5.24)

Index Properties	Range	Mean	Sample Number
L.L.	45-71%	62.3%	
P.L.	16-20%	18.2%	
S.L.	9.7-10.4%	10.3%	
>2 μ	20-25%	22.7%	
Activity	1.1-2.45	1.9	
L.I.	0.02-0.4	0.14	
Max. Water Abs.	74-94%	84.8%	
Specific Gravity	2.65-2.66	2.655	
Wet Bulk Density	1.76-2.01	1.91 g/cm ³	
γ_B	g/cm ³		
Natural Water Content (Wc)	21-27%	23.8%	
Porosity (n)	40-48%	42.2%	
Void Ratio (e)	0.66-0.91	0.720	
Calculated Degree of saturation	77-98%	87.8%	

Table 5.12

The activity values show that the clay could be classified as normal to active clay (Fig.5.12, Section 5.3.4.3) suggesting a predominantly montmorillonitic clay (Skempton, 1953); this was subsequently confirmed by the D.T.A. and X-ray diffraction tests (Tables 5.4 & 5.8, Section 5.3.4.3). The maximum water absorption test of the clay shows high percentages, probably due to the presence of montmorillonitic mixed layer clay minerals (Fig. 5.5A & Section 5.3.4.3). The water content of the clay is above the plastic limit, which indicates that this clay is over-consolidated at the present time.

The soil strength tests included direct shear box, consolidated undrained and consolidated drained triaxial

compression tests to obtain C' and ϕ' , the shear strength parameters in terms of effective stresses (sampling preparation and procedure are described in detail in Chapter 3); the results of these soil strength tests are presented in Table 5.2B.

Consolidated-undrained triaxial compression tests provided variable results; the intercept C' of the clay ranges from 0.18 to 0.32 Kgf/cm^2 , and ϕ' is in the range of 14.5° to 18.5° . There was no marked difference between the samples taken within and samples taken from outside of the slide mass.

Peak and residual strength parameters were determined by means of direct shear box tests, subjected to five reversals and reshearing until no further drop in shearing resistance was observed. The following test results were obtained:-

$$\begin{array}{ll} C'_P = 0.26 \text{ Kgf/cm}^2 & \phi'_P = 16^\circ \\ C'_r = 0.12 \text{ Kgf/cm}^2 & \phi'_r = 9.5^\circ \end{array}$$

Residual strength parameters were also determined by carrying out direct shear tests on a remoulded sample with pre-cut planes, and these gave the following results:-

$$C'_r = 0.05 \text{ Kgf/cm}^2, \text{ and } \phi'_r = 9.5^\circ$$

(Fig. 5.25). The fully softened strength parameters of this clay were determined by carrying out consolidated (remoulded) samples. The following test results were obtained:-

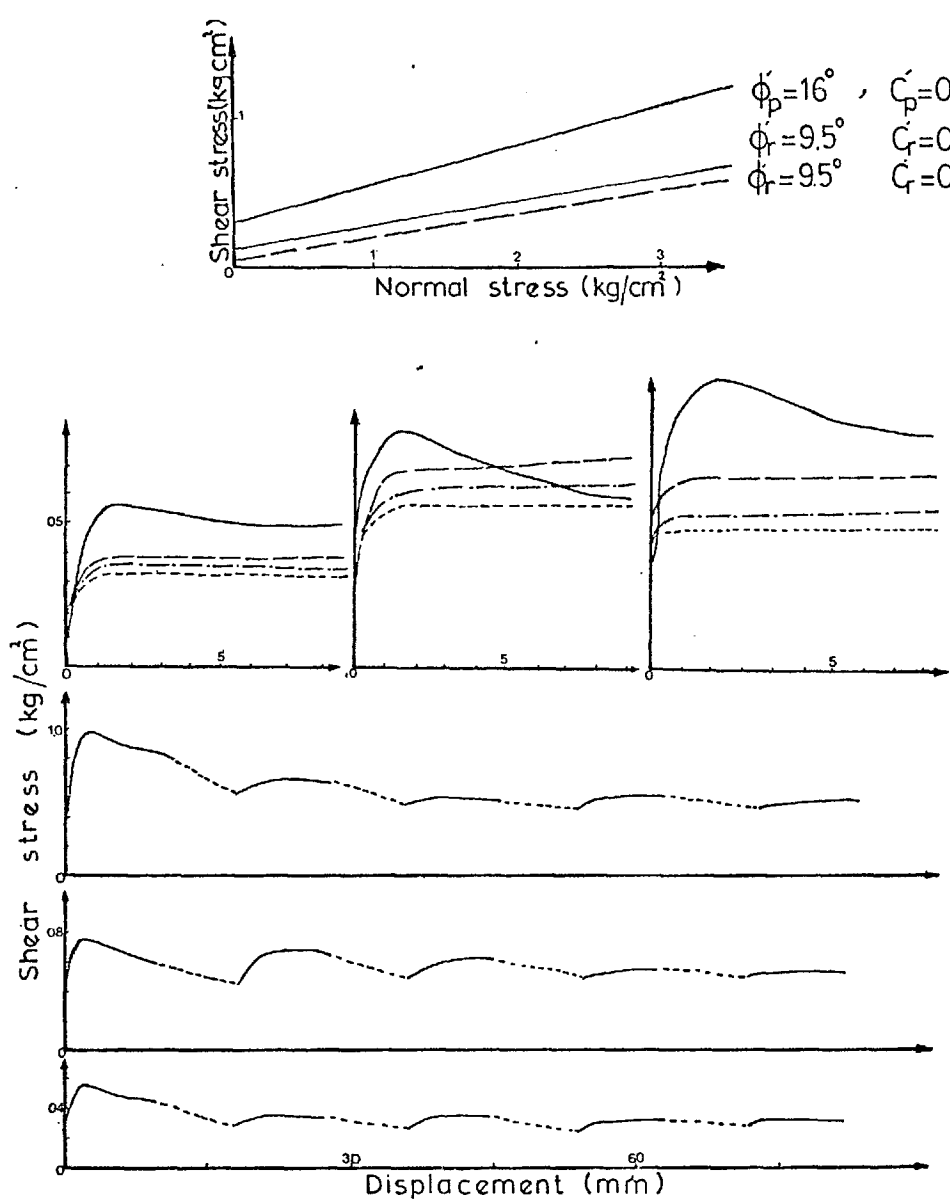
$$C'_d = 0.18 \text{ Kgf/cm}^2, \text{ and } \phi'_d = 11.5^\circ.$$

The test curves and Mohr's envelopes are shown in Fig. 5.25.

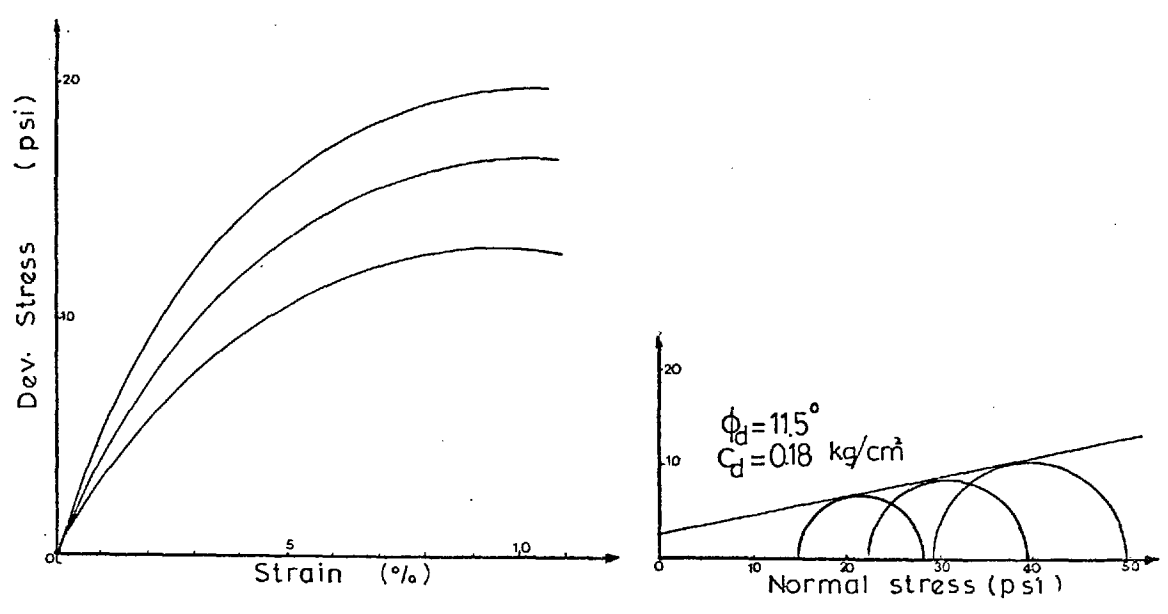
A mineralogical analysis of the sample obtained from the landslide area is given in Table 5.8, Section 5.3.4.3. The mineralogical tests indicate that the clay is mainly composed of kaolinite and illite, with mixed layer of illite-montmorillonite, and traces of quartz, calcite and feldspar. The cation exchange capacity shows a high range, confirms the above results.

5.4.5 Slope Stability Analysis

Stability analysis in terms of effective stresses in the form derived by Bishop (1954) were carried out on the present cross section shown in Fig. 5.26. The calculations were made assuming three positions of transient water tables at the time of failure, during periods of heavy rainfall. Residual strength parameters represented by $C'_r = 0.12 \text{ Kgf/cm}^2$ and $\phi'_r = 9.5^\circ$ were used for the actual slip surface (IR). The factors of safety were found to be 0.94 and 0.88 for



MULTI-REVERSAL SHEAR TEST



DRAINED TRIAXIAL TEST

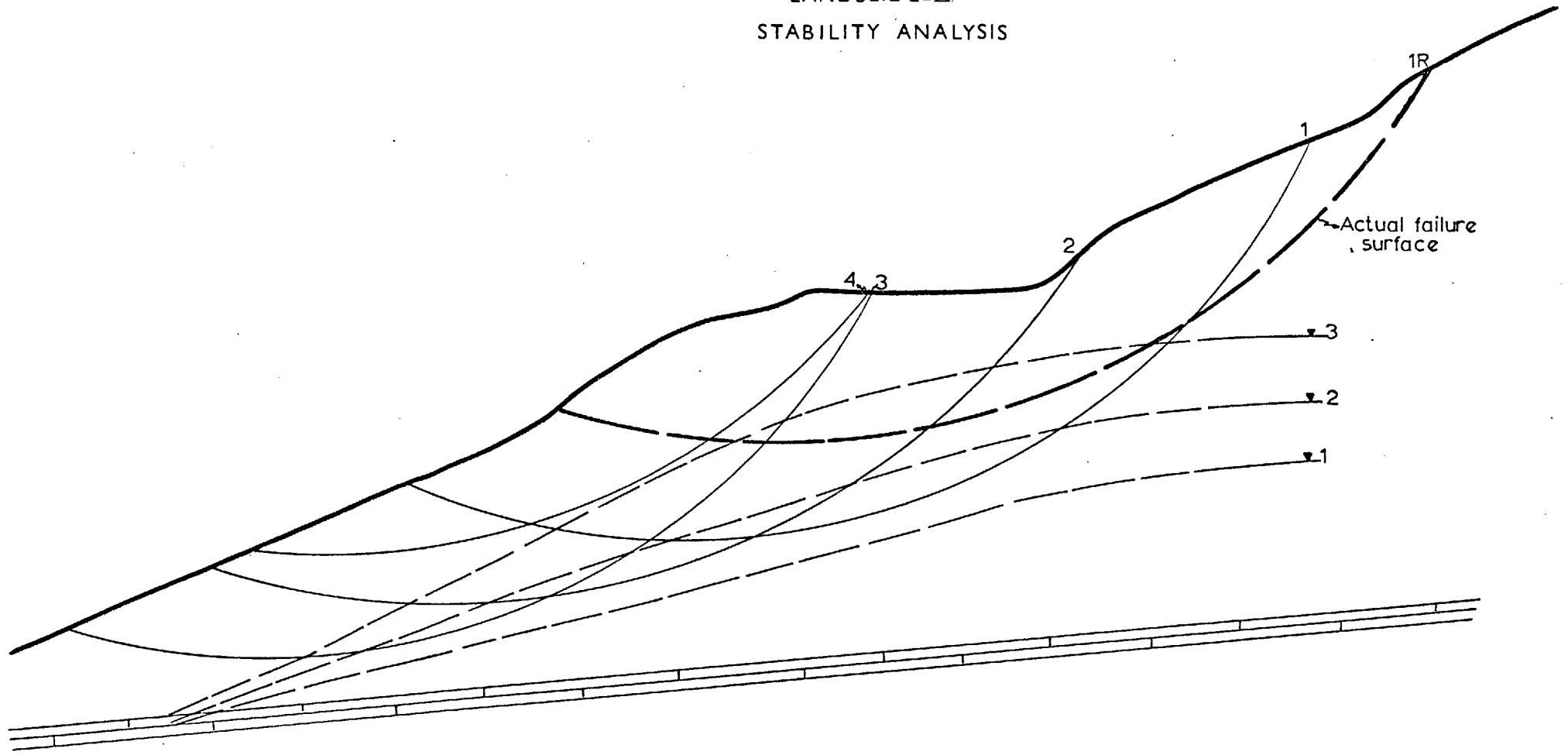
Fig(5.25)

water tables in positions 2 and 3 respectively.

To analyse the stability of the present slope, trial circles 1, 2, 3 and 4 were chosen (Fig. 5.26) and the peak, fully softened, and combination parameters were used. It was found that the peak strength parameters represented by $C'_p = 0.26 \text{ Kgf/cm}^2$ and $\phi'_p = 16^\circ$ overestimate the safety factor (Fig. 5.27). The stability analysis was also carried out using fully softened strength parameters represented by $C'_d = 0.18 \text{ Kgf/cm}^2$ and $\phi'_d = 11.5^\circ$, with the same three positions of the water tables acting on the slip surface. For this case it was found that the factors of safety ranged between 0.83 and 0.93 for the highest positions of water table 2, and was in the range of 0.90 and 1.10 assuming no water pressures on the slip surface.

The same analyses were also made using a combination of strength parameters; the fully softened parameters were used along the portion of the trial circle which goes through the landslide mass while peak strength parameters were used along the rest of the trial circles which go through the intact part of the material. It was also found that this type of analysis over-estimated the factor of safety for this particular area. The result of the analysis is shown in Fig. 5.27.

LANDSLIDE-IV
STABILITY ANALYSIS

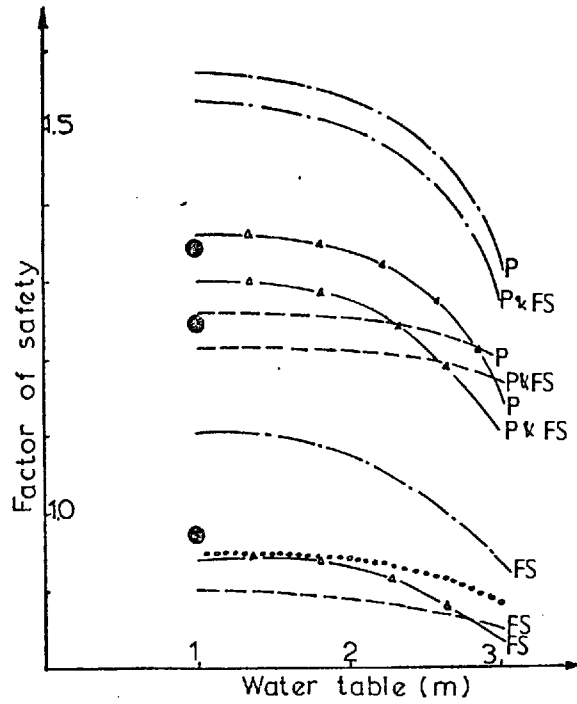


Actual failure surface

0 5 10m

Fig.(5.26)

LANDSLIDE-IV RESULTS OF THE STABILITY ANALYSIS



CIRCLE NO.	PARAMETER	NO WATER TABLE	WATER TABLE (2)	WATER TABLE (3)
1R	Residual	0.94	0.94	0.88
1	P	1.57	1.54	1.31
	FS	1.10	1.08	0.93
	P & FS	1.53	1.50	1.27
2	P	1.36	1.34	1.15
	FS	0.94	0.94	0.83
	P & FS	1.30	1.28	1.10
3	P	1.26	1.25	1.20
	FS	0.90	0.89	0.85
	P & FS	1.23	1.21	1.20
4	P	1.35		
	FS	0.97		
	P & FS	1.25		

P Peak
 FS Fully softened
 ——— Circle 1
 —△—△— Circle 2
 - - - - - Circle 3
 Pre-existing surface
 ● Circle 4

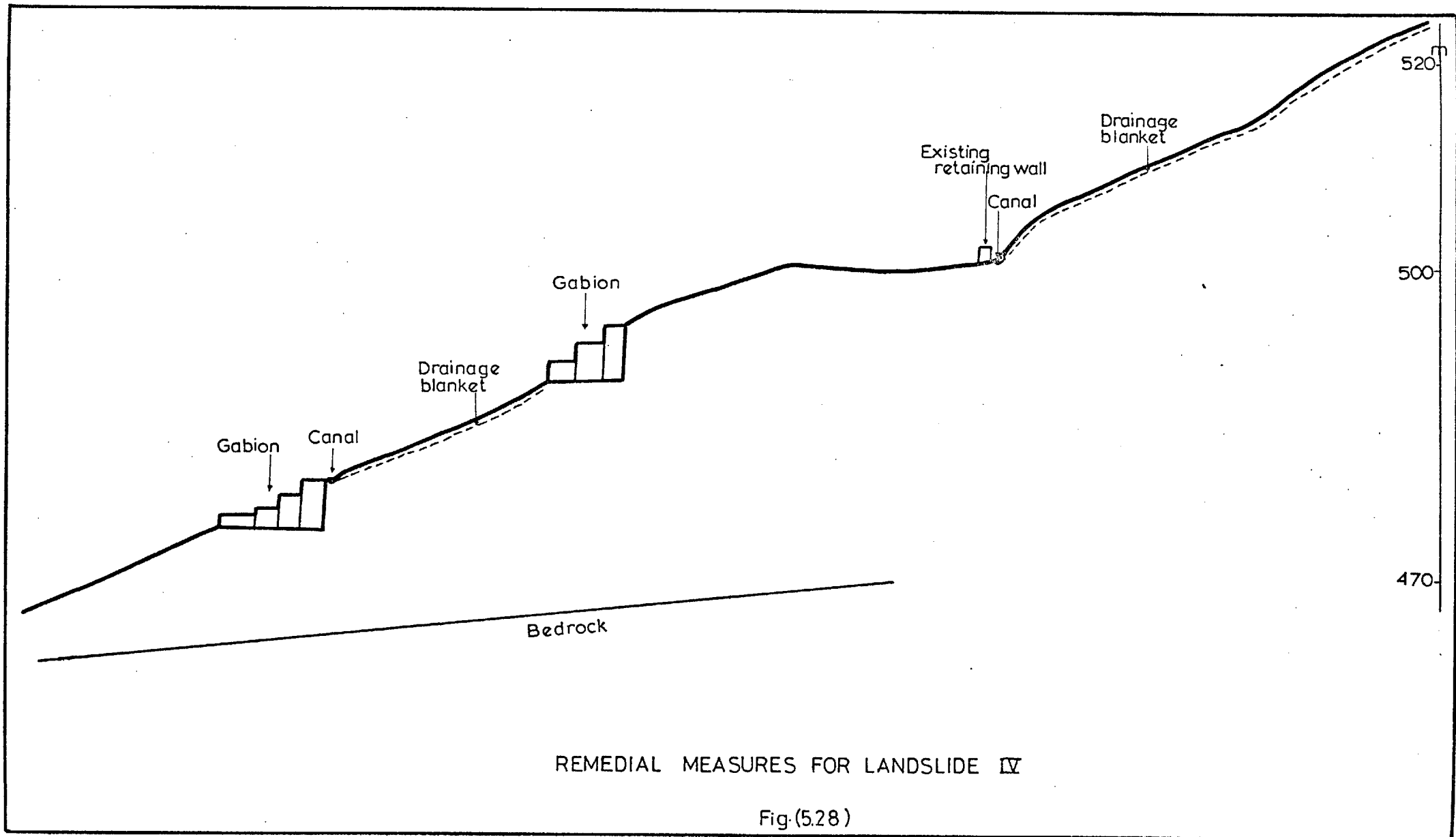
Fig(5.27)

The analysis clearly showed that trial circle no. 3 was the most critical in the fully softened case, and that subsequent movements might occur; this is confirmed by the field observations.

5.4.6 Remedial Measures

The proposed remedial measures for landslide IV are presented in general outline in Figure 5.28. They consist of the following main works:-

- (i) Increasing the resisting forces and protecting the toe from erosion by constructing two gabions at or near part of the landslide indicated by the trial circles 1R, 2, 3, and 4.
- (ii) Improving surface drainage by means of constructing a drainage blanket of coarse sand and gravel between the two gabions with a paved canal to channel surface water and carry it away from the landslide area. In addition a drainage blanket on the crown area behind the existing concrete retaining wall should be provided after first scarifying and compacting the softened and loose materials here. This would provide the crown area with an improved surface drainage after densification and effectively reduce percolation of rainwater into the slide mass causing softening.



5.4.7 Conclusions

From the above investigations and analysis, it is quite evident that several factors contributed to the landslide in 1967 and these are summarised as follows:-

1. The presence of major shear faults contributed to the weakening of the strata in this region.
2. Poor surface and subsurface drainage.
3. An improperly constructed retaining wall.
4. Abnormally high precipitation.

All the factors combined to result in the disturbance of the natural equilibrium of this area and the probable occurrence of the landslide.

The conclusions to be drawn from this investigation may be summarised as follows:-

1. The movement was initially a rotational type and was followed by mudflow at the crest and near the toe of the movement.
2. The residual strength parameters obtained from remoulded samples with pre-cut planes shows the following results: $C'_r = 0.05 \text{ Kgf/cm}^2$ and $\phi'_r = 9.5^\circ$, while the

residual parameters obtained from multi-reversal shear test on undisturbed samples yields the following results:
 $C'_r = 0.12 \text{ Kgf/cm}^2$ and $\phi'_r = 9.5^\circ$.

3. The fully softened strength parameters represented by $C'd = 0.18 \text{ Kgf/cm}^2$ and $\phi'd = 11.5^\circ$ are the most applicable for use in the stability analysis due to the amount of disturbance in the area, which suffered significantly from shear displacement.
4. The annual rainfall in 1967 was the highest in the year's record.
5. The hydrogeology of this area could be described as fracture-induced and the water table probably rises only during a heavy rainstorm and falls very rapidly. The landslide material probably only approaches saturation during periods of high temporary water table.
6. The clay in the landslide area may be classified as normally active to active and it is predominantly composed of montmorillonite-illite, illite and kaolinite.
7. The proposed remedial measures would increase the factor of safety by 12%.

5.5 DETAILED INVESTIGATION OF LANDSLIDE I

5.5.1 Geology and Hydrology

The landslide area is located on the Sweileh-Jarash road 5.5 Km south of Jarash city.

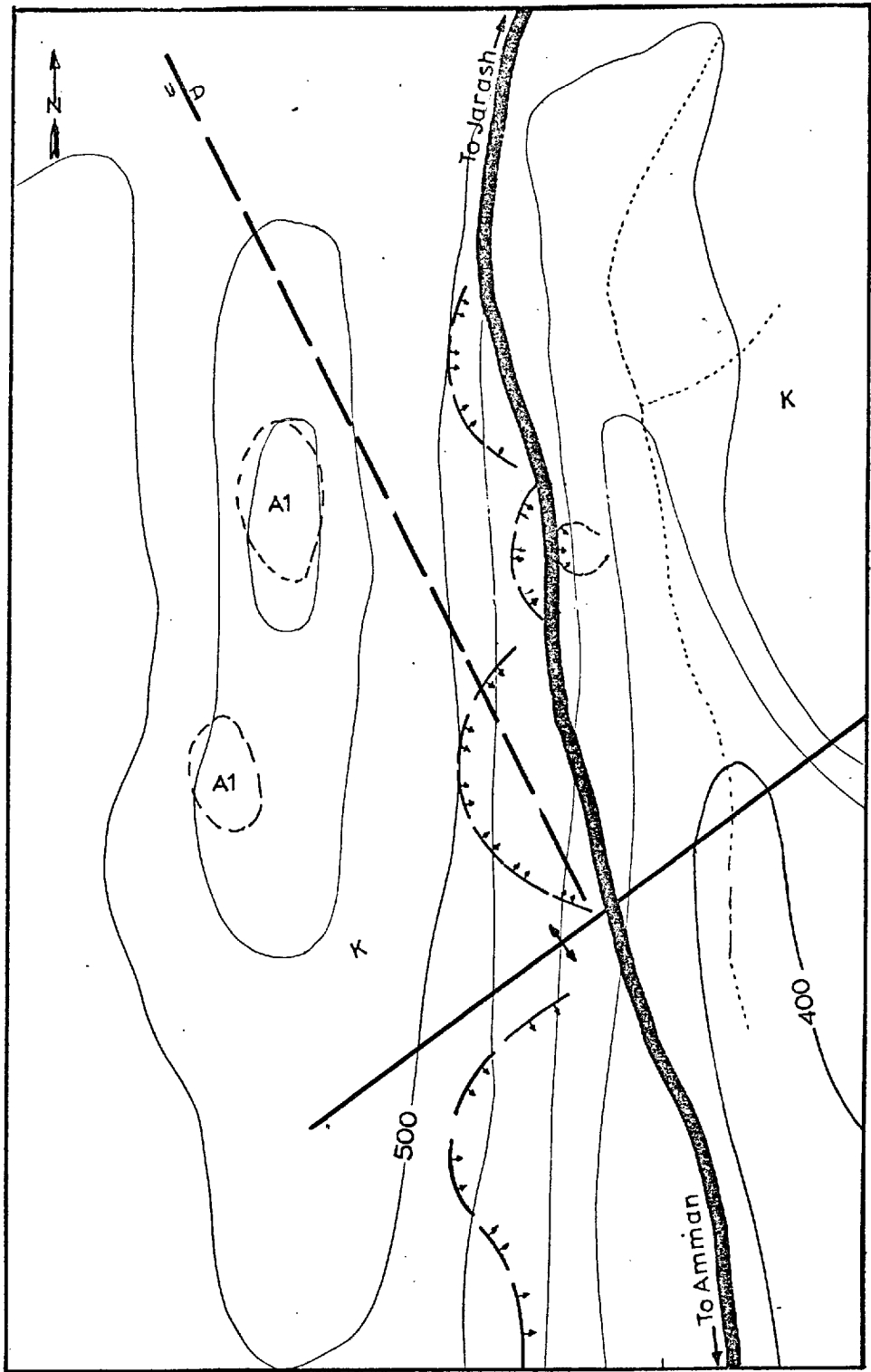
The geology of this area is superimposed on a contour map of 1:10,000 scale (Fig. 5.29). A geological cross section through the landslide area, showing the geology and main features of the movement is presented in Fig.5.30. The main geological formation exposed at the site of landslide I is part of the Upper Kurnub group, which here consists predominantly of silty clays alternating with grey shale.

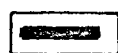
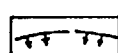
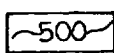
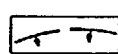
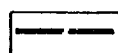
Landslide I lies to the north-east of an anticline whose axis trends NE-SW, east of the existing highway, on the downthrown side of a NW-SE trending major normal fault. The strata strike almost parallel to the highway and dip at about 5° towards the east.

The first movement commenced in December, 1966 (Plate 5.11) after a period of continuous heavy precipitation of 612 mm and 191 mm during December. The total December precipitation was approximately 2.5 times the monthly average for the ten preceding years' record. The month during which the second

LANDSLIDE I

GEOLOGIC MAP

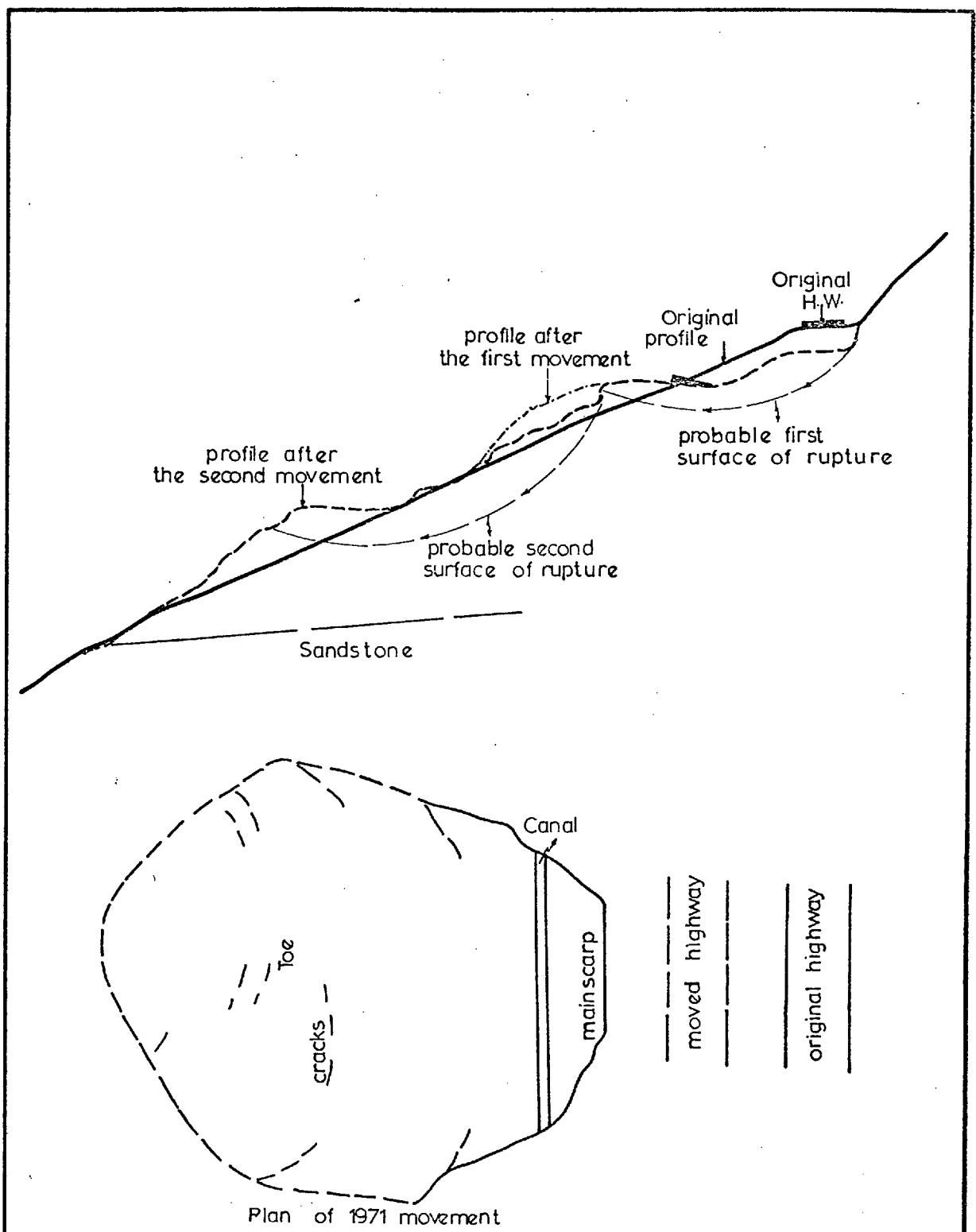


- | | |
|--|--|
|  Highway |  Anticline |
|  Old landslide |  Contour(m) |
|  Investigated landslide | |
|  Fault | |

224000

Fig(5.29)

250 m



LANDSLIDE-I
CROSS SECTIONS AND PLAN SHOWING
THE MAIN FEATURES OF THE MOVEMENTS

Fig(5.30)



Plate 5.11 Showing the moved highway after the movement of 1966 - landslide I.

movement occurred, the rainfall was exceptionally high and was approximately 6 times the monthly average over ten years' record (Table 5.13).

Station	Total Rainfall Dec.1966 (mm)	Total Rainfall 1966/67 (mm)	Average Rainfall in Dec. 10 years (mm)	Total Rainfall April.71 (mm)	Total Rainfall 1970/71 (mm)	Average Rainfall in April 10 years (mm)
Jarash	190.9	612.3	77.4	210.6	513.8	36.9
Sweileh	250.8	807.4	87.4	332.9	611.7	51.9
Rumman	114.5	551.5	53.2	115.1	280.6	25.9

Table 5.13

5.5.2 General Description of Landslide I

Immediately after the first movement commenced in December 1966, the Ministry of Public Works started reconstruction of the affected section of the highway, but did not undertake an investigation into the main causes and the probable future activation of the movement. Approximately four years later, in April 1971, following a month of 211 mm heavy precipitation a new circular landslide took place, which affected the main irrigation canal which supplies the farms south of the area (Plates 5.12 & 5.13). In the upper part of the landslide there is little disturbance but the toe part shows earth and mudflow. The length of the movement along the long axis was approximately 100 m, with a breadth of 110 m and 3 metres near vertical



Plate 5.13 The main scarp of 1971 movement, showing the moved gabion at the crown of landslide I.



Plate 5.12 Main features of the 1971 landslide, showing the moved irrigation canal at the main scarp of landslide I.

displacement. The horizontal outward movement was approximately 7 m. The ground slope prior to the 1971 movement was 27°.

A borehole was drilled in the vicinity of landslide I and was unsuccessful in locating the slip surface owing to the amount of disturbance in the strata and technical difficulties.

Three trial pits were also dug for exploration and sampling purposes. The materials obtained were friable and highly disturbed.

5.5.3 Laboratory Investigations

During the 1966 movement no investigations took place. After the movement of April 1971, a soil testing programme was devised and carried out on disturbed samples obtained from the landslide area to establish the engineering properties and strength parameters of the clay.

The principal index properties of the soil properties are given in the following table:

Index Properties	Range	Mean	Sample Number
Liquidity Limit L.L.	43.8 - 76%	60.6%	5
Plasticity Limit P.L.	19.0-21.5%	20.5%	5
Shrinkage Limit S.L.	5.3-12.3%	9.3%	5
Clay Fraction <2μ	42 - 74%	61.6%	5
Activity	0.52-0.89	0.66	5

Index Properties	Range	Mean	Sample Number
Liquidity Index L.I.	-0.12 - 0.15	-0.15	5
Max. Water. Absorption	72.7 - 83.2%	77.3%	5
Specific Gravity Sp.G.	2.53-2.65	2.58	5
Wet Bulk Density γ_B	1.78-2.01 g/cm ²	1.90 g/cm ²	5
Natural Water Cont. Wc	15.1 - 28.9%	17.5%	5
Porosity n	32-40%	37.4%	5
Void Ratio e	0.47-0.66	0.59	5
Calculated Degree of Saturation	60-100%	72.4%	5

Table 5.14

Atterburg limits are plotted on the Casagrande plasticity chart in Fig. 5.11; all points lie above the A-line, the clays are mainly CH (inorganic clays of medium plasticity). The activity values show that the clays would be classified as inactive to normal clays (Skempton, 1953), Fig. 5.12, and would suggest that clays are composed of mainly kaolinite and illite.

The range of liquidity index shows that this clay is stiff (Terzaghi, 1934). The natural water content of the tested samples is mainly above the plastic limit, indicating that the clay is over-consolidated at the present moment.

Owing to the degree of weathering, disturbance and general structural deformation of the material in the vicinity of the area, no undisturbed samples could be obtained.

Shear strength parameters of the clays were obtained from the consolidated-drained triaxial compression tests

performed on normally consolidated (remoulded) samples, to obtain the fully softened strength parameters. The following values were obtained (Fig. 5.31):

$$c'_d = 0, \quad \phi'_d = 20^\circ.$$

The absence of cohesion leaves it reasonable to conclude that this clay had reverted to its fully softened strength (after Skempton, 1970).

Mineralogical analyses of the clays were carried out using Differential Thermal Analysis, X-ray diffraction and chemical analysis. The mineralogical composition is given in Table 5.8 and curves Fig. 5.16. These analyses show that the clay is mainly montmorillonitic, kaolinitic clay, with minor quantities of calcite, feldspar and dolomite.

5.5.4 Slope Stability Analysis

At the time of the original investigation of the highway and after the first movement, no stability analyses were carried out.

Owing to the amount of structural deformation, the fully softened strength parameters are the most realistic parameters to be used for the stability analyses of the present

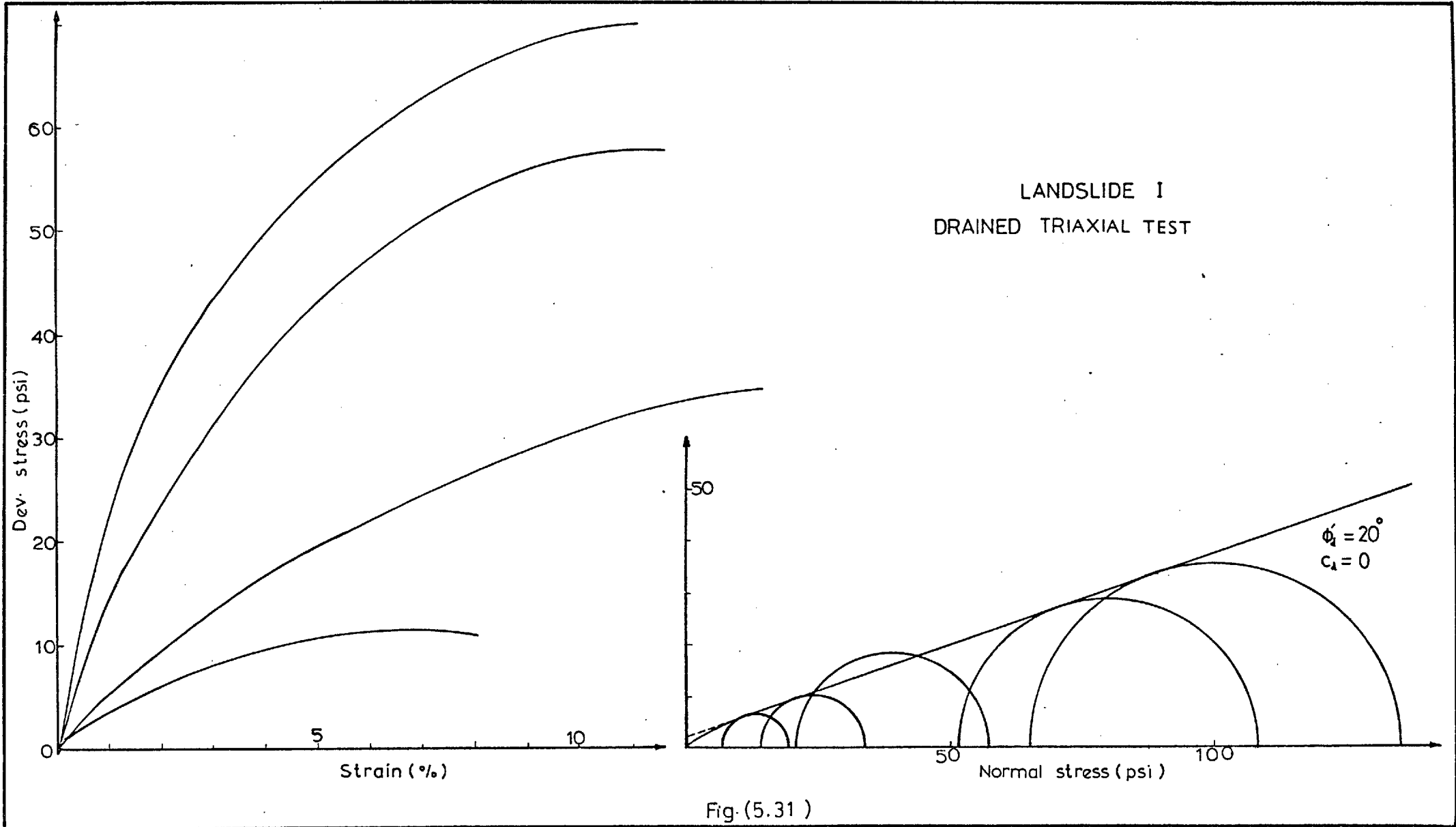


Fig. (5.31)

slope. To analyse the stability of the slope in its present state, cross section (Figure 5.32) was chosen; the fully softened strength parameters represented by $C'_d = 0$ and $\phi'_d = 20^\circ$ were used in the form derived by Bishop (1954). The average wet bulk density of the material, 1.89 g/cm^3 , was used in the analysis. Three trial circles were chosen to be analysed. It was found that the factors of safety 1.07, 0.72 and 1.12 for circles 2, 3 and 4 apply respectively.

It is worth mentioning that in the lower part of circle 3 the soil was still creeping as a mudflow, the resisting forces of the mass confined by circles 2 and 4 will be reduced, a progressive nature of the movement will be produced.

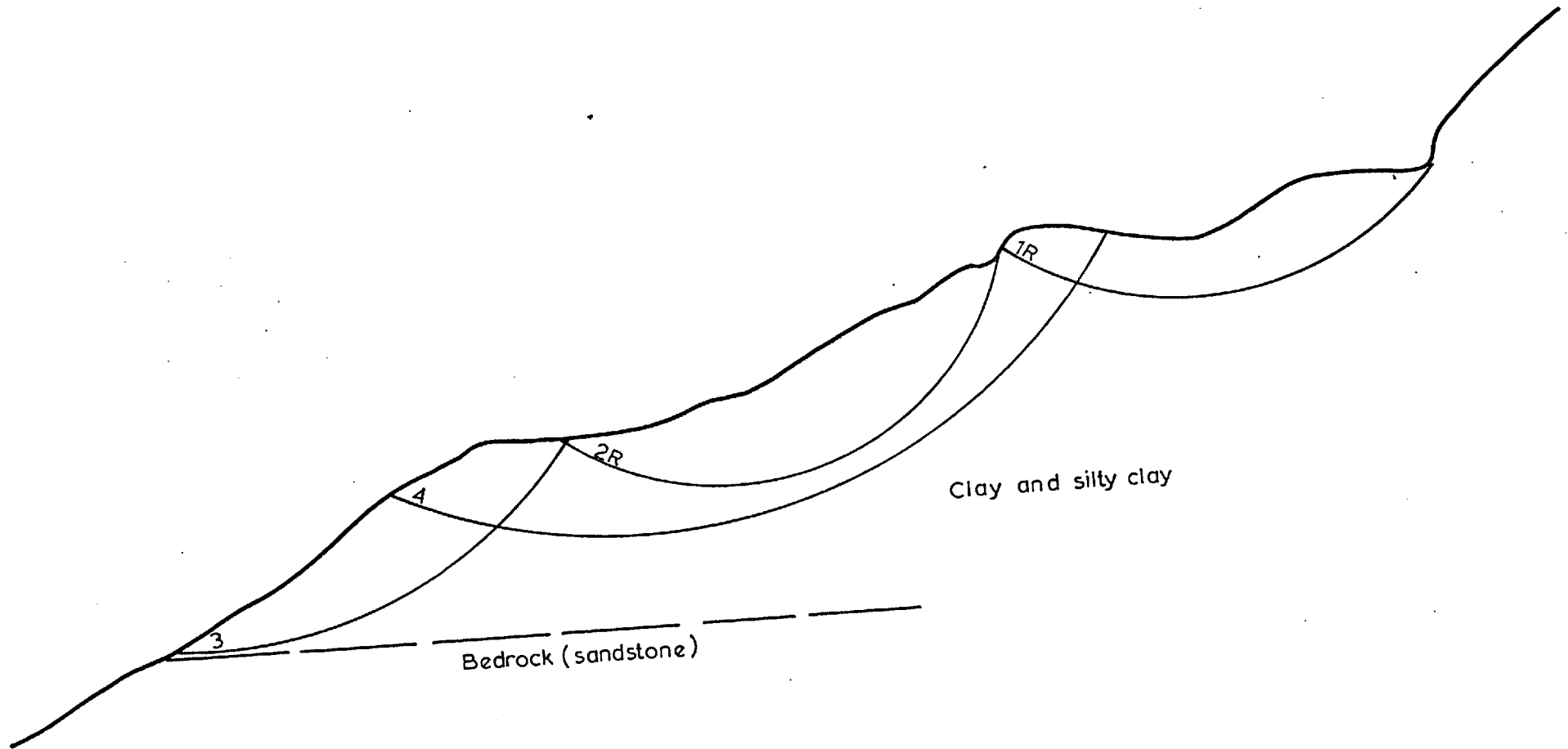
In the light of the above analysis, it was found that the slope remains unstable with regard to any further softening which may occur arising from the percolation of the precipitation or irrigation water.

5.5.5 Remedial Measures

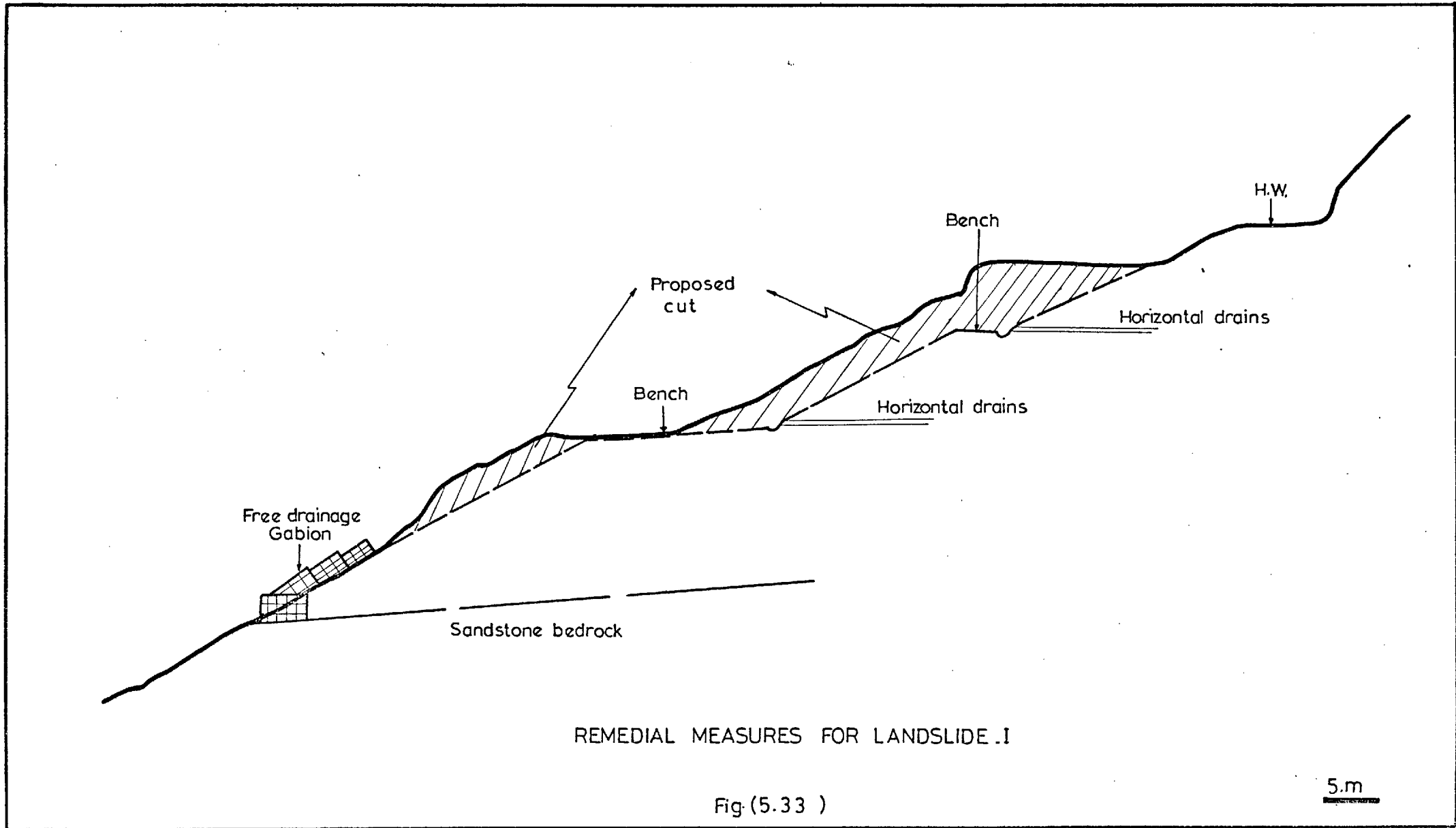
The proposed remedial measures for landslide I are indicated in general outline in Figure 5.33. They consist principally of the following:-

- (i) Reducing the driving forces by means of excavation at the top of the landslide and flattening the slope and

LANDSLIDE I
STABILITY ANALYSIS



Fig(5.32)



REMEDIAL MEASURES FOR LANDSLIDE .I

Fig (5.33)

5.m

benching; the benches should be wide enough to allow a larger area to be cultivated.

- (ii) Increasing the resisting forces by constructing a gabion at or near the toe part of the landslide. This gabion is to be founded on the sandstone bedrock and provided with free drainage material.
- (iii) Providing subsurface drainage by installing horizontal drain pipes discharging to a paved drainage canal to carry the water out of the area.

5.5.6 Conclusions

In the light of the site investigation and slope stability analyses of the landslide area, it was found that the probable main causes of the present movement may be summarised as follows:-

1. Increase of the driving forces at the crown of the recent movement (1971) arising from the accumulation of the toe material of the first movement of 1966 (as shown in cross section, Figure 5.30).
2. Inadequate surface and subsurface drainage.
3. Critical slope angle with regard to the strength of the involved material.

4. The amount of structural deformation in the area permits the rain water to percolate, causing softening of the material.
5. Saturation of the materials by seepage from the newly created irrigation canal, which might have reduced the stability in the following ways:
 - a) It may have reduced the shearing resistance of the material by increasing the p.w.p. along the failure surface.
 - b) It may have reduced or eliminated a small cohesion intercept by removing soluble salts or the chemical binder.
6. Abnormal precipitation in the month and year of the movement.

One or more of the above mentioned factors might have caused the disturbance of the natural equilibrium of the area and probably the occurrence of the landslide.

The main conclusions to be drawn from the investigations may be summarised as follows:

1. Major slope movements were initially of the rotational type and these were followed by mudflows near the toe.
2. The fully softened strength parameters represented by $C_d = 0$ and $\phi'_d = 20^\circ$ are the most appropriate for use

in the stability analysis due to the amount of disturbance in the strata, which suffered very high shear displacement.

3. In December 1966 rainfall was the highest record over ten years. No permanent water table was observed in the landslide area. The water table probably rises only during a heavy rainfall and falls very rapidly. It is reasonable to assume the landslide mass to be fully saturated during periods of high temporary water table.
4. The stability of the lower part of the slope was triggered by the accumulation of the material of the first movement.
5. The stability analyses of the present slope indicate that the area remains unstable and that it will be sensitive to any further fluctuations in the water tables.
6. The proposed remedial measures would increase the factor of safety by about 23%.

5.6 A DETAILED INVESTIGATION OF LANDSLIDE II
 SWEILEH-JARASH ROAD

5.6.1 Geology and Hydrogeology

Landslide II occurred in the slopes of the Zerqa river valley at Km 42 on the Sweileh-Jarash road, at a point 600 metres west of Zerqa river bridge (Fig. 5.1A).

The area is in mountainous terrain with 60-70° slopes inclined towards the north and west. In the vicinity of landslide II, the hill slope has a highest elevation of about 600 metres, but the height decreases gradually to 210 metres at the Zerqa river level. The highway at the crown of landslide II is 50 metres above the river level. Fig. 5.34 and Plate 5.14.

Shortly after a major landslide commenced in April 1971, a detailed geological map on a scale of 1:1,000 was prepared, and the main features of the movement were plotted (Fig. 5.34). The studies were supplemented by aerial photographs on scales of 1:10,000 and 1:25,000.

The rock unit exposed in the landslide area is part of the Upper Kurnub group of the lower Cretaceous. The part of this formation involved in the landslide consists mainly of brown or green silty clays, grey-greenish clays and black shale;

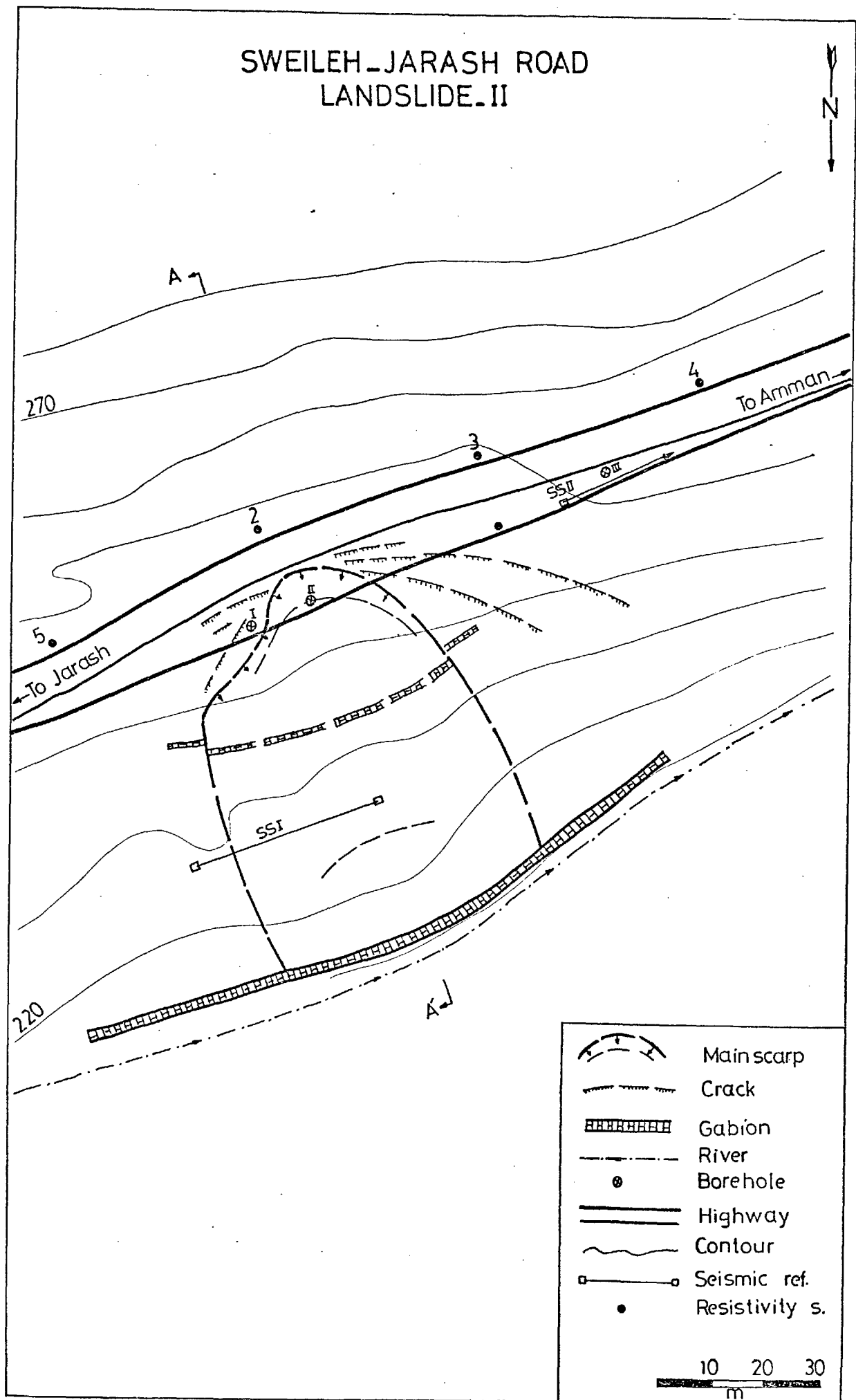


Fig.(5.34)

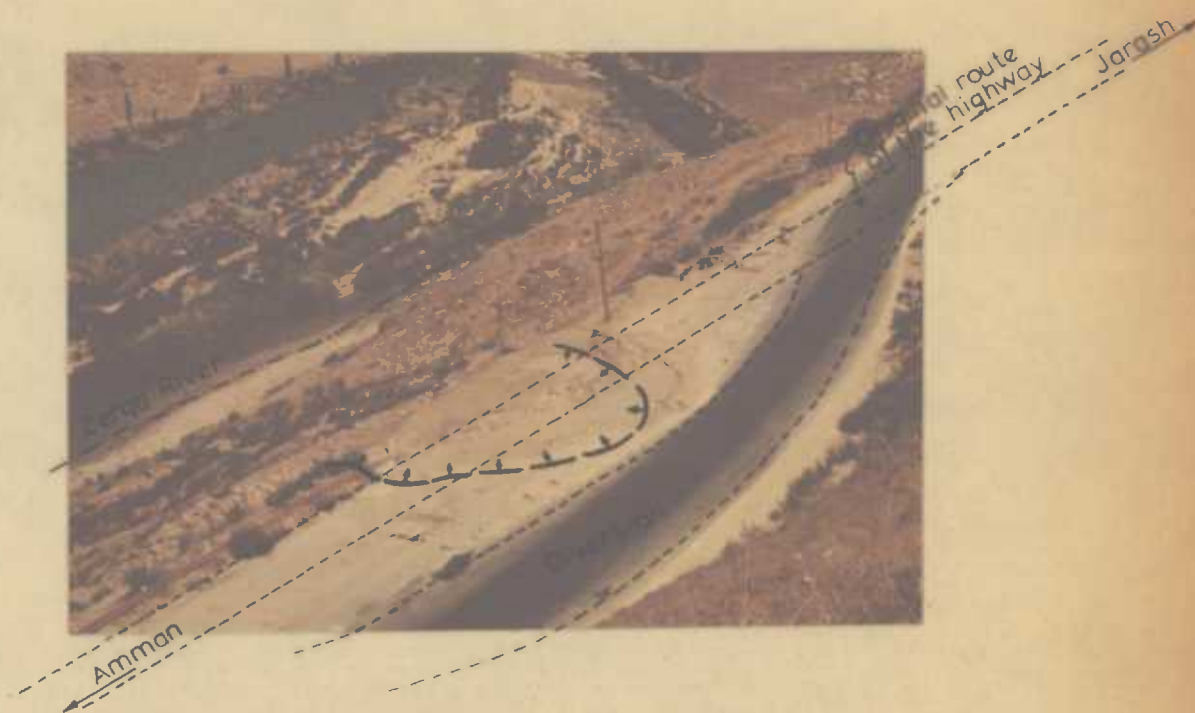
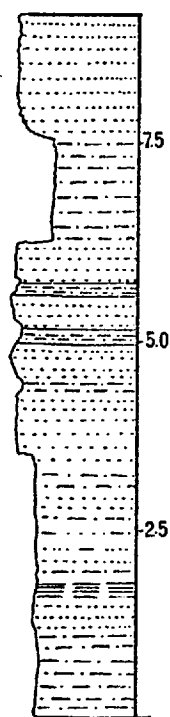


Plate 5.14 General view of landslide II showing the original route of the highway and the diversion.

the lower part of this formation consists of vari-coloured sandstone.

Silty clay is exposed at the road level and is in a highly weathered and intensely jointed condition with small relative displacements on fissures (Plate 5.15).

A measured vertical section above the road level was as follows:-



Grey-brown sandstone, medium to fine grained.

Grey-green, highly fissured plastic silty clay with a soapy texture.

White-creamish sandstone and siltstone, alternating with thin bands of greyish silty clay, weakly cemented and intensely jointed.

Green-brown siltstone, alternating with thin bands of black shale.
0.52 m highly fissured silty clay; the fissures were filled with iron oxide.

Highway level.

The strata in the vicinity of the landslide dip at $3-5^{\circ}$ in a direction of 210° . This part of the Kurnub group is regarded as an aquiclude, but the lower sandstone part can be viewed as an aquifer.



Plate 5.15 Jointing and weathering of the silty clay at the highway level in the backslope of landslide II.

The mean annual precipitation in the area is similar to that in landslide III (see Section 5.3.3 and Fig. 5.7).

Rainfall stations along Sweileh-Jarash road show the following records in the month and year of the movement:

Station	Total Rainfall April 1971 (mm)	Total rainfall in 1970/1971 (mm)	Average rainfall in April / in ten years (mm)
Jarash	210.6	523.8	36.9
Sweileh	332.9	611.7	51.9
Rumman	115.1	280.6	25.9

Table 5.15

The above table shows that most of the rainfall was concentrated into short periods of heavy rainfall in April. The precipitation, in April 1971, was almost the highest on record in the last ten years, and was about five times the monthly average over the last ten years of records. The landslide occurred very soon after this period of high precipitation.

5.6.2 General Description of the Landslide

Shortly after a shallow debris slide occurred in March 1969, the authorities started reconstruction of the highway but did not undertake any investigations into the causes of the movements. Two gabions were constructed, one near the crest of

the landslide and the other at the Zerqa river level. In April 1971, following periods of heavy precipitation, a circular type landslide took place. The crown of the slide is partially on a roadbed and affects the complete width of the highway. The upper part of the landslide shows slumping while the middle and lower parts of the landslide show tilting and bulging respectively. The upper gabion was sheared along the left and right flanks of the slide (Plates 5.16 & 5.17). Lower down the slope, materials accumulated at the top of the lower gabion, pushing it north-westwards, i.e. in the direction of the movement. Plate 5.18.

The breadth of the slide is approximately 55.0 metres and the slide exceeded 70 metres in length along its long axis. The vertical scarp was 4 metres high at the crest of the landslide. The original ground slope was 33° and approximately $60,000 \text{ m}^3$ of the material was involved in the landslide. It is reasonable to assume that the soil mass was approaching a fully saturated state when movement occurred and that a temporary high water table must have existed. After the main movement had ceased, many tension cracks developed on the road near the main scarp (Fig. 5.34), indicating that the movement was still taking place.

5.6.3 Field Investigations

Field observations started immediately after the occurrence of the first movement in 1971.

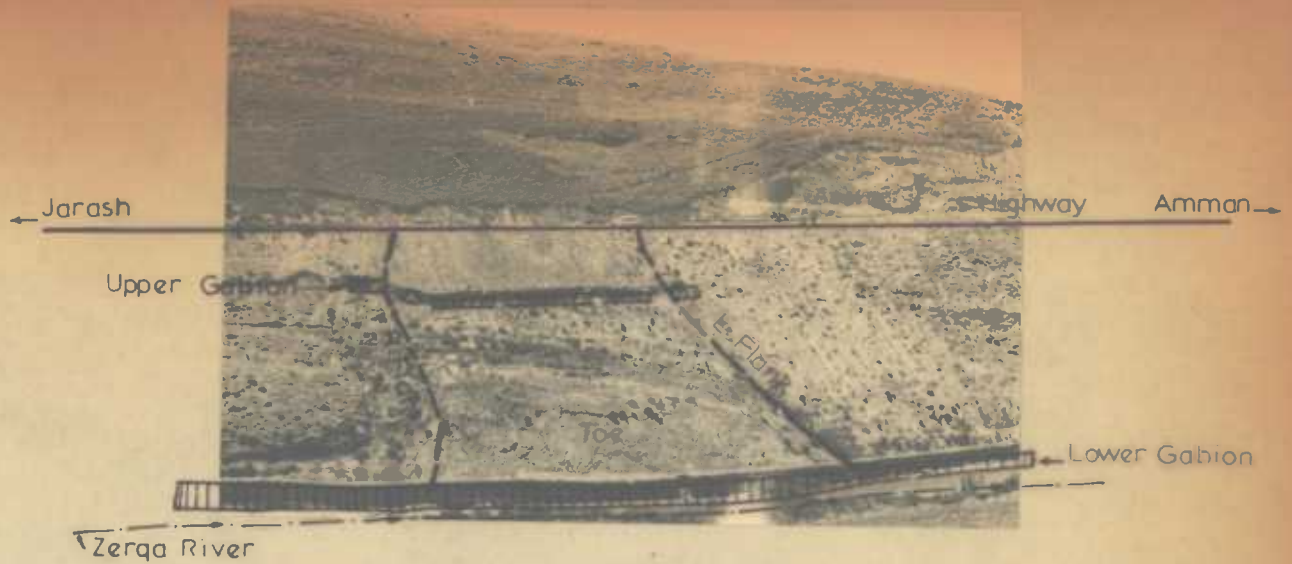


Plate 5.16 General view of landslide II showing the main features of the movement.



Plate 5.17 Shearing of the upper gabion at the crown of landslide II.



Plate 5.18 Tilting of the lower gabion at the level of Zerqa River - landslide II.

The exploration stage started with deep core drilling to investigate the subsurface geology and observe ground water levels. The core samples obtained consisted of silty clays interbedded with bands of shale; solid sandstone bedrock was located at a depth of about 26 metres (Fig. 5.35). Two boreholes were drilled specifically to locate the actual slip surface; however, this drilling was only partly successful due to technical difficulties arising from cavities in the area. However, at a depth of 7 and 5 metres in boreholes I and II respectively the clay was found to be highly remoulded and shear surfaces were observed in the core samples. In addition to the exploratory drilling, two seismic refraction profiles were made, the first profile, S.S.I, in the middle of the slipped mass, shows that the first 5-8 metres had a low velocity being composed of loose material, with solid bedrock at an average depth of 25 metres. The second profile S.S.II, was located away from the slide mass and showed that the weathered zone has a thickness of about 2 metres; weakly cemented material is approximately 10 metres thick. Bedrock was located at a depth of about 13 metres (Fig. 5.9A).

The Schlumberger expanding method of the resistivity sounding profiles revealed no major faults and showed that the weathered zone covering the study area is about 2-5 metres in thickness. Intact silty clays and siltstones were detected

LANDSLIDE II EXPLORATION BOREHOLES

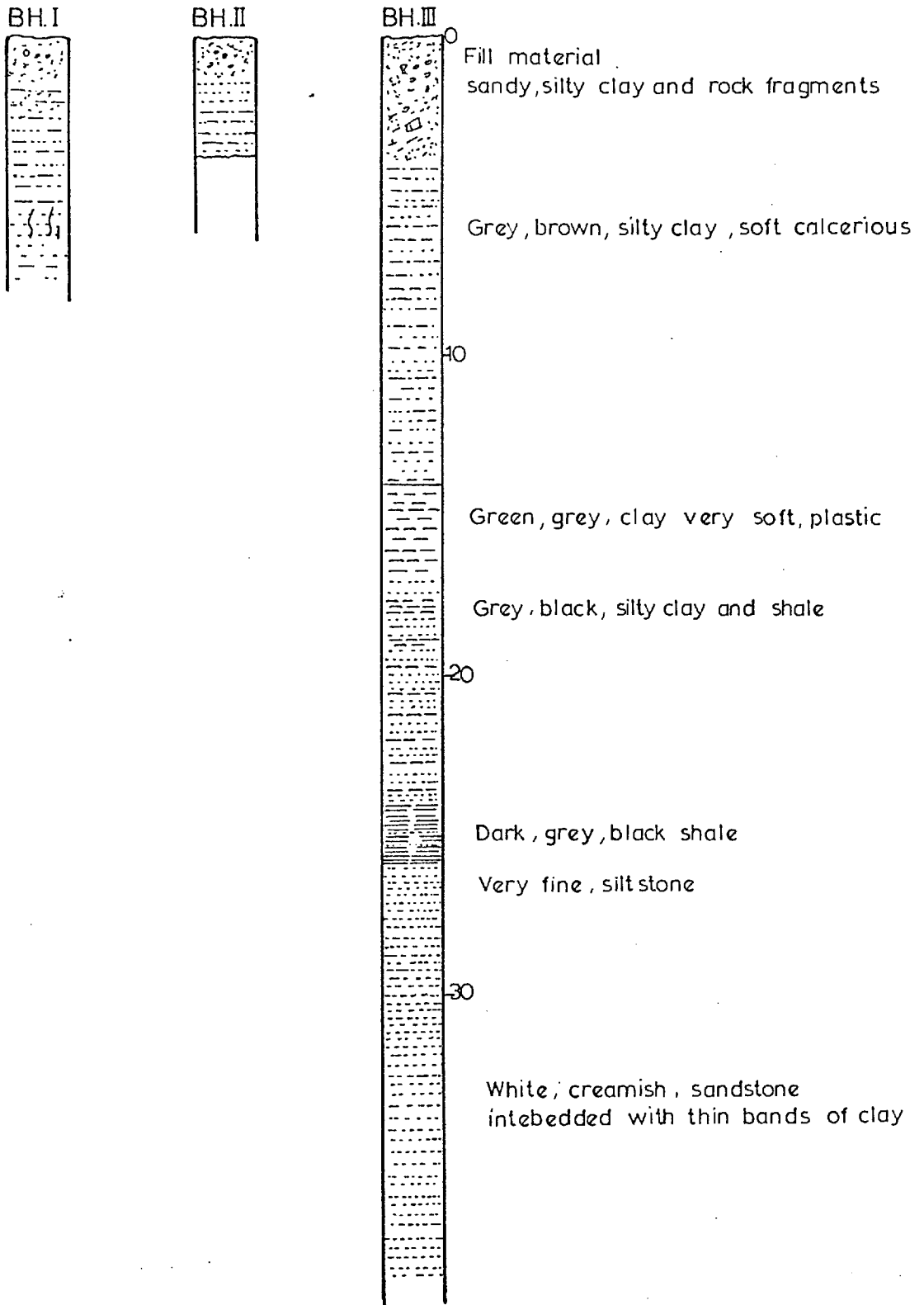


Fig.(5.35)

below this depth (Fig.5.10A). The range of seismic velocity and apparent resistivities of the materials in the study area are summarised in the following table:

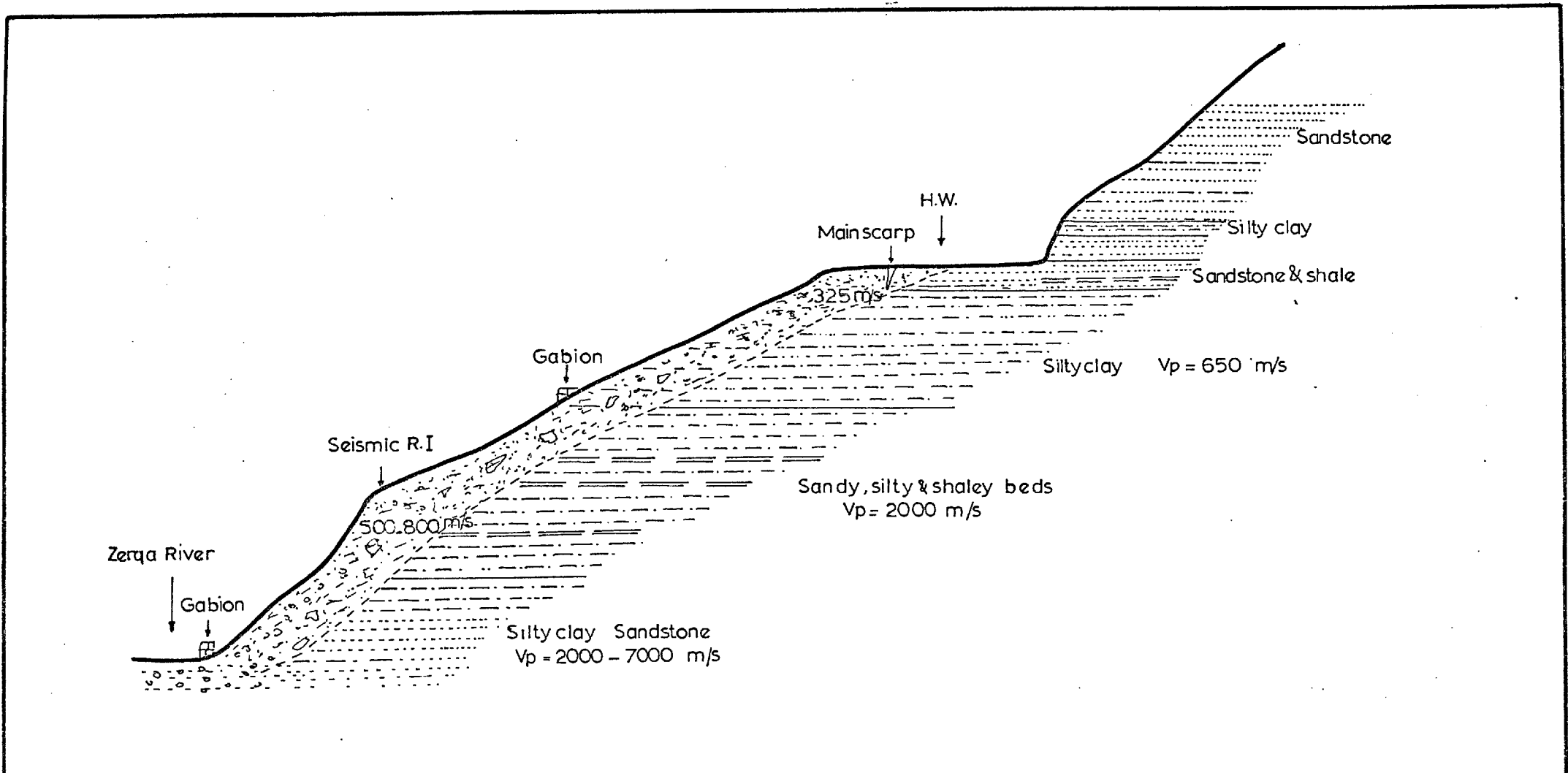
Zone	Apparent resistivity (Ω/m)	Seismic velocity (m/sec)
Mantle (Weathered zone)	15 - 34	325 - 800
Silty clay zone	48 - 60	800 - 1200
Sandy, silty shaley beds.	60 - 94	2000
Cemented sandstone bedrock.	≈ 95	2000 - 7000

Table 5.16

A lithological cross section at the site of the landslide was prepared based on information obtained from the interpretation of the exploratory drilling, the geophysical surveys and surface geology (Fig. 5.36).

5.6.4 Laboratory Investigations

A soil testing programme was devised and carried out on disturbed and undisturbed samples taken from the landslide area, to establish the index properties and strength parameters of the clay for use in the slope stability analysis.



LANDSLIDE . II
 Geological cross section based on drilling and geophysics investigations

0 5 10m

Fig(5.36)

A summary of the results is presented elsewhere in Table 5.1B and Section 5.3.4.3. The typical range of values for the various soil parameters is given in the table below.

Index Properties		Range	Sample Number	Mean
Liquid Limit	L.L.	18 - 49%	5	33.4%
Plastic Limit	P.L.	13 - 18%	5	16.2%
Shrinkage Limit	S.L.	10 - 12%	5	11.2%
Clay Fraction	2μ	33 - 51%	5	41.4%
Activity		0.15-0.64	5	0.41
Liquidity Index	L.I.	-0.2-0.31	5	0.11
Max. Water. Abs.		58 - 72%	5	64.7%
Specific Gravity	Gs	2.60-2.65	5	2.61
Wet Bulk Density	γ_B	1.79-2.0g/cm ³	5	2.93 g/cm ³
Natural Water Content	Wc	11 - 28%	5	18.9%
Porosity	μ	33 - 40%	5	38.2%
Void Ratio	e	0.43-0.67	5	61.6
Calculated Degree of Saturation	S	67 - 95%	5	79.8%

Atterberg limit values are plotted on the conventional plasticity chart, Fig. 5.11 (Section 5.3.4.3) which shows that all the points lie above A-line, and the materials are mainly CL (inorganic sandy silty clays of low to medium plasticity).

The activity values of the material show that the clay could be classified as inactive (Fig. 5.12) and of a mainly kaolinite, illitic composition (Skempton, 1953).

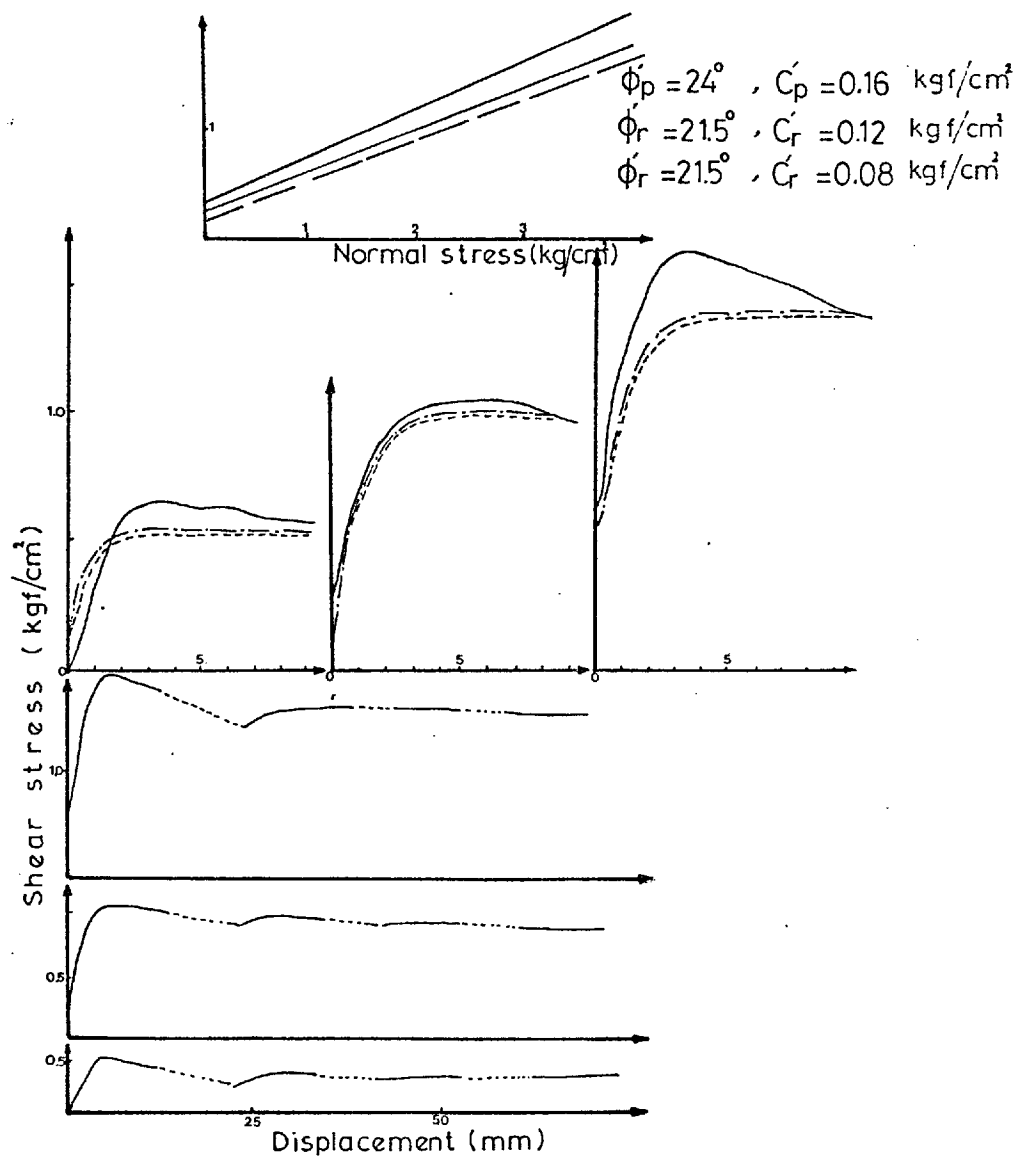
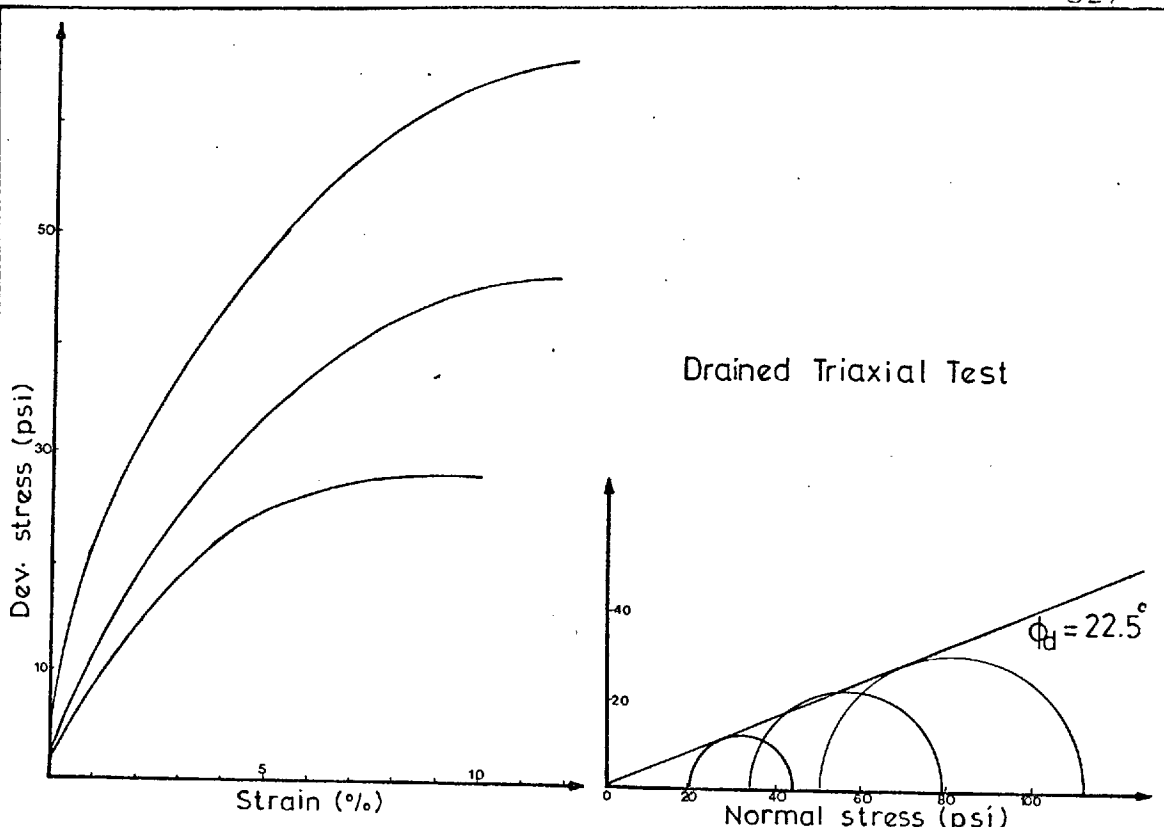
The range of liquidity index indicates that the clays are stiff (Terzaghi, 1936). The natural water content of the samples is mainly above the plastic limit, confirming that the clay is over-consolidated at the present time.

Shear strength tests were performed on both disturbed and undisturbed representative samples (in the manner described in detail in Chapter 3) to find out peak and residual strength parameters in terms of effective stresses.

Peak strength parameters obtained from the direct shear tests on undisturbed samples were: $C'_p = 0.16 \text{ Kgf/cm}^2$, $\phi'_p = 24^\circ$, and the residual parameters were: $C'_r = 0.12 \text{ Kgf/cm}^2$ and $\phi'_r = 21.5^\circ$. Residual parameters obtained from the same samples in a remoulded state with pre-cut planes were $C'_r = 0.08 \text{ Kgf/cm}^2$ and $\phi'_r = 21.5^\circ$.

Consolidated-drained triaxial compression tests were carried out (as described in Chapter 3) to obtain the "fully softened" strength parameters, and the following values were obtained: $C'_d = 0$; $\phi'_d = 22.5^\circ$ (Fig. 5.37).

A mineralogical analysis of the clays was carried out using Differential Thermal Analysis, X-ray diffraction analysis and chemical analysis. The tests are described in detail



Multi-Reversal Shear Test

Fig.(5.37)

elsewhere (Chapter 3). The mineralogical compositions are given in Tables 5.7 & 5.8 which show that the clay is mainly composed of illite, kaolinite, mixed layer of illite-montmorillonite and traces of gypsum, calcite and quartz.

5.6.5 Slope Stability Analysis

As previously stated, the main movement of 1971 was rotational in nature. The surface of soil involved in the movement was not significantly disturbed and clear-cut boundaries were to be seen at the main scarp and at the left and right flanks. The slip surface is assumed to be circular. The point of the breakout at the toe is not known exactly and five alternative positions of the lower part of the slip circles were considered. The original cross-section upon which the stability analysis was made is shown in Fig. 5.38.

An effective stress analysis in the form derived by Bishop (1954) has been used on the original cross section (before sliding), using peak strength parameters of the clay. The outlines of the stability method used is presented and described in detail in Chapter 3. By this method the shear strength is expressed as a function of the apparent C' , ϕ' in terms of effective stresses, which makes it possible with certain accuracy to solve the long term stability problems.

Two simplifying assumptions concerning the geology of the area are: (i) the slipped mass is homogeneous, and (ii) the slipped mass was fully saturated immediately prior to this movement. No observations were made of the pore water pressures acting on the slip surface.

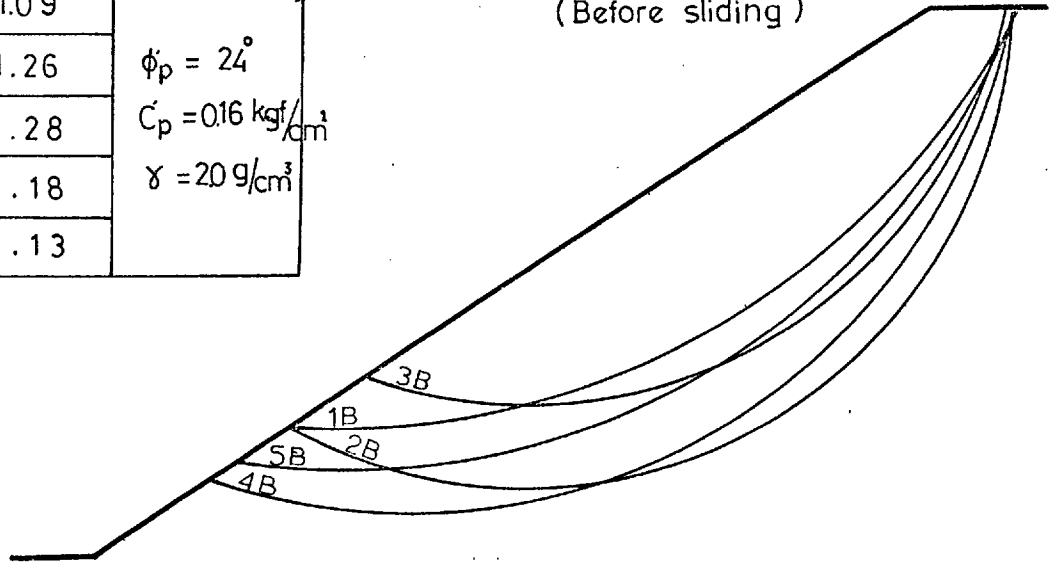
The stability analysis for the original cores section, using peak strength parameters represented by $C'_p = 0.16 \text{ Kg/cm}^2$, $\phi'_p = 24^\circ$, with $\gamma_B = 2.0 \text{ g/cm}^2$, showed that the factors of safety ranged between 1.09 and 1.28 for the five proposed slip circles, which go through the main scarp of the landslide. Slip circle no. 1B is considered to be most likely approximation to the surface, on which slide movement occurred (Fig. 5.38).

The clay is highly fissured and jointed; and the joints act as planes of weakness (Skempton, 1966) and softening of the whole mass takes place commencing along the joints and fissures (Terzaghi, 1936). Due to the stress relief following the excavation of the highway, these joints would have opened, thus allowing precipitation to percolate through the soil mass, causing softening along the joint surfaces. Non-uniform softening will take place from the face of an open joint under zero effective stress, and this leads to further softening (Skempton, 1973). The fully softened strength parameters which could be represented by the normally consolidated (remoulded)

LANDSLIDE - II

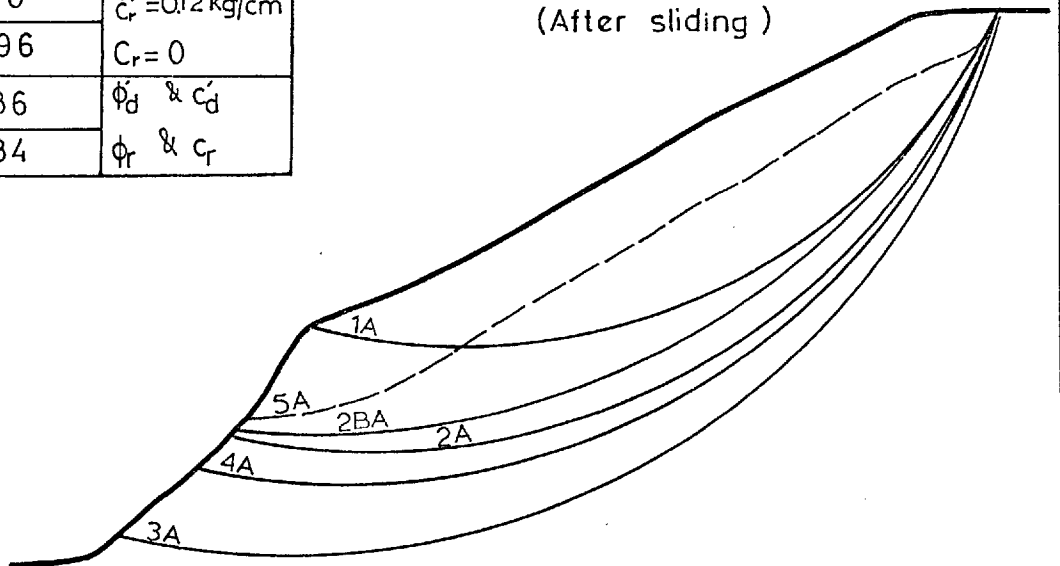
Circle	Factor of safety	Remarks
1 B	1.09	$\phi_p = 24^\circ$ $C_p = 0.16 \text{ kg/cm}^2$ $\gamma = 20 \text{ g/cm}^3$
2 B	1.26	
3 B	1.28	
4 B	1.18	
5 B	1.13	

ORIGINAL CROSS SECTION
(Before sliding)



Circle	Factor of safety	Remarks
1 A	1.082	Fully softened
2 A	1.041	$\phi'_d = 22.5^\circ$
3 A	1.005	
4 A	1.040	$\phi_r = 21.5^\circ$ $C_r = 0.12 \text{ kg/cm}^2$
1 BA	0.96	
5 A	0.86	ϕ'_d & C'_d
	0.84	ϕ_r & C_r

PRESENT CROSS SECTION
(After sliding)



ORIGINAL AND PRESENT PROFILES OF
LANDSLIDE.II WITH THE RESULTS OF STABILITY ANALYSIS

Fig(5.38)

5.m

parameters are the more realistic parameters to use rather than the residual values for the drop in strength preceding the first-time slides (Skempton, 1970). The use of these parameters as the limiting value for design was implied by Henkel (1956) and proposed by Skempton (1961). However, stability analysis of the slope in its present state was carried out using the residual strength parameters for the actual slip surface represented by: $C'_r = 0.12 \text{ Kgf/cm}^2$, $\phi'_r = 21.5^\circ$ and $C'_r = 0$ (assumed with $\phi'_r = 21.5^\circ$). It was found that the factors of safety 1.10 and 0.96 were valid for both sets of parameters.

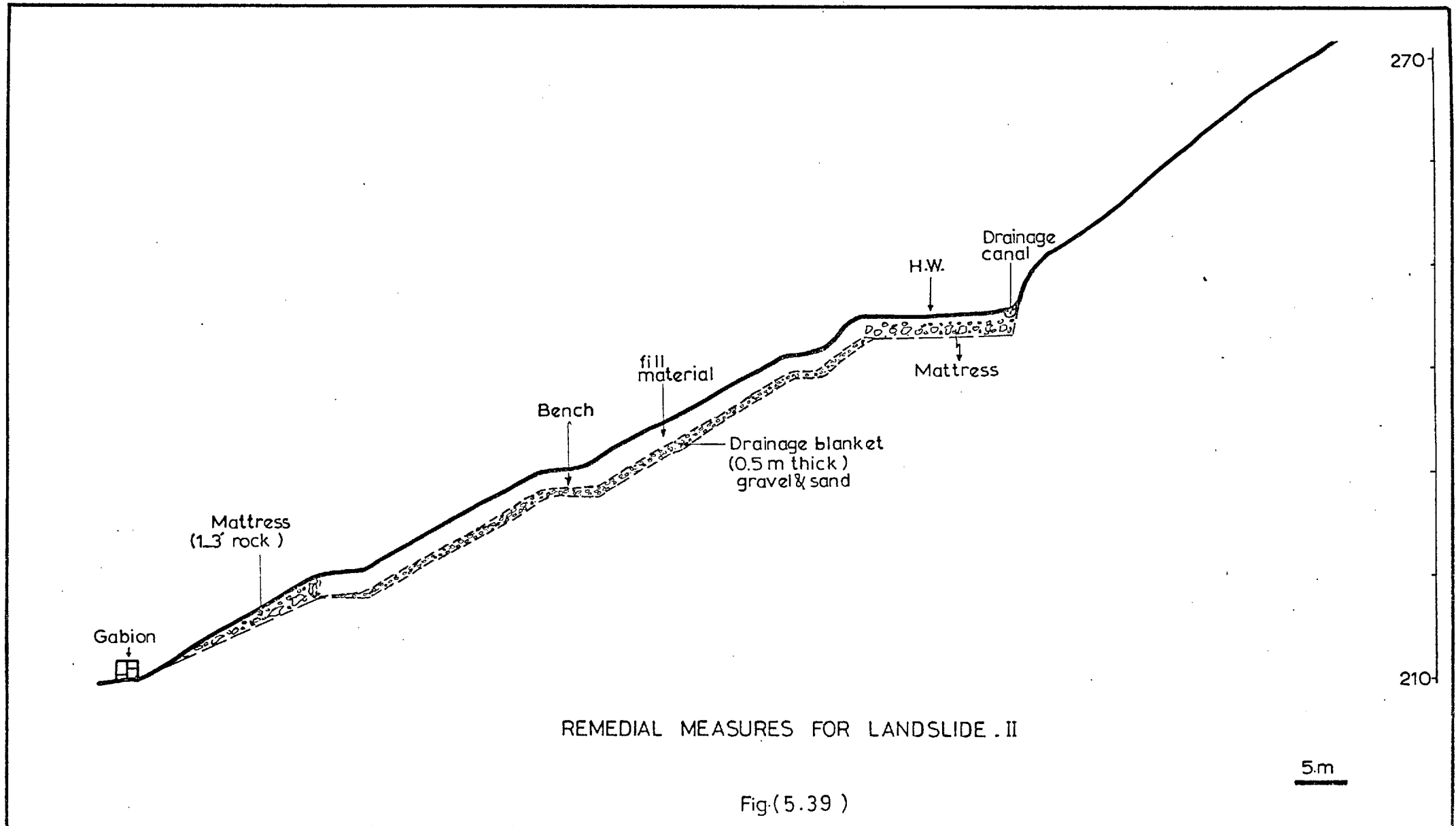
The stability analyses carried out on trial circles 1A, 2A, 3A and 4A using the fully softened strength parameters represented by $\phi_d = 22.5^\circ$, $C_d = 0$, show that the factors of safety range between 1.04 and 1.08. The stability analyses were also carried out assuming a shallow non-circular failure surface 5A, and using the fully softened and residual strength parameters. It was found that the factors of safety are 0.89 and 0.84 respectively. Cross sections and tabulation of the results are shown in Fig. 5.38.

The stability analysis carried out on the present cross section shows that the slope remains in a potentially unstable condition with regard to any further softening which may occur due to the percolation of the surface water.

5.6.6 Remedial Measures

The proposed remedial measures for landslide II, Fig. 5.39, would consist principally of the following:-

- (i) Removing the low strength sliding materials particularly the weathering zone and replacing it with a proper material. The fill should be compacted in layers of 6 inches thickness to a maximum dry density.
- (ii) Removing the low strength materials of the embankment to a depth of at least 2 metres along the affected section of the highway and replacing them with free drainage granular fill designed as a drainage mattress or layers of permeable material. This would provide two benefits; it would replace the poor quality material and at the same time provide material with the necessary drainage characteristics to remove surface water from the area. The inner edge of the highway should be provided with a paved drainage canal to divert the rainwater from the landslide area.
- (iii) Removing the existing upper gabion near the crown of the landslide which has increased the driving forces and has allowed rainwater to percolate into the landslide zone.
- (iv) Flattening the slope and providing benches; benches widths to be 5 m and to dip at 1 in 15, to assist in rapid



REMEDIAL MEASURES FOR LANDSLIDE . II

Fig.(5.39)

runoff of rainwater.

- (v) Diverting the river to its original channel and constructing a gabion 2 metres high and 1 metre wide. This will protect the lower toe from erosion along the unstable area of the hillside between the Zerqa river bridge and the end of the slide area II.
- (vi) The slide area should be provided with a drainage blanket of coarse sand and gravel prior to the placement of the fill material. The toe should be protected by construction of a pervious mattress filled with rock fragments (1 to 3 feet approximate size) to protect the landslide from erosion and provide extra resisting forces. This mattress should be in direct connection with the drainage blanket to provide a continuous drainage layer.

5.6.7 Conclusions

In the light of the field, laboratory and stability analyses, it was found that the probable main causes of the movement may be summarised as follows:-

1. Stress release following the excavation of the highway allowed joints to open and act as planes of weakness.
2. Abnormally high precipitation in the month of the movement contributed to a temporarily high water table.

3. Critical slope angle with regard to the height.
4. Lack of the surface and subsurface drainage.
5. Increase of driving forces caused by the construction of gabions at or near the crown of the landslide.
6. Undercutting of the slope by the Zerqa river reducing the resisting forces.

In addition, the absence of engineering geological investigations prior to route selection, design and construction of the highway led to routing of the highway through an unstable area.

The main conclusions arising from this study may be summarised as follows:

1. The first minor movement in March 1969 was a shallow debris slide. This was caused by a heavy rainstorm which saturated the weathered material and turned into the mudflow or debris slide.
2. The second, and major, movement was a typical rotational landslide where the strength of the clay falls to its residual, due to the large shear displacement. The residual strength parameters were represented by $C'_r = 0.12$ Kgf/cm² and $\phi'_r = 21.5^\circ$.

3. Tests on remoulded samples with precut planes show the following residual parameters: $C'_r = 0.08 \text{ Kg/cm}^2$ and $\phi'_r = 21.5^\circ$.
4. The fully softened strength parameters are the most reliable to be used for the stability analysis, owing to the present condition of the material, which suffered considerable shear displacement causing disturbance of the clay structure. These parameters could be represented by: $C'_d = 0$, and $\phi'_d = 22.5^\circ$.
5. The use of the peak strength parameters would overestimate the factor of safety of the existing slope, owing to the progressive nature of the movement.
6. The stability analysis of the slope after the proposed remedial measures shows that the factor of safety increased by 24%.

CHAPTER SIX

SLOPE STABILITY ON MA'AN-AQABA ROAD
(RAS-EN-NAQAB ESCARPMENT)

SLOPE INSTABILITY ON MA'AN-AQABA ROAD

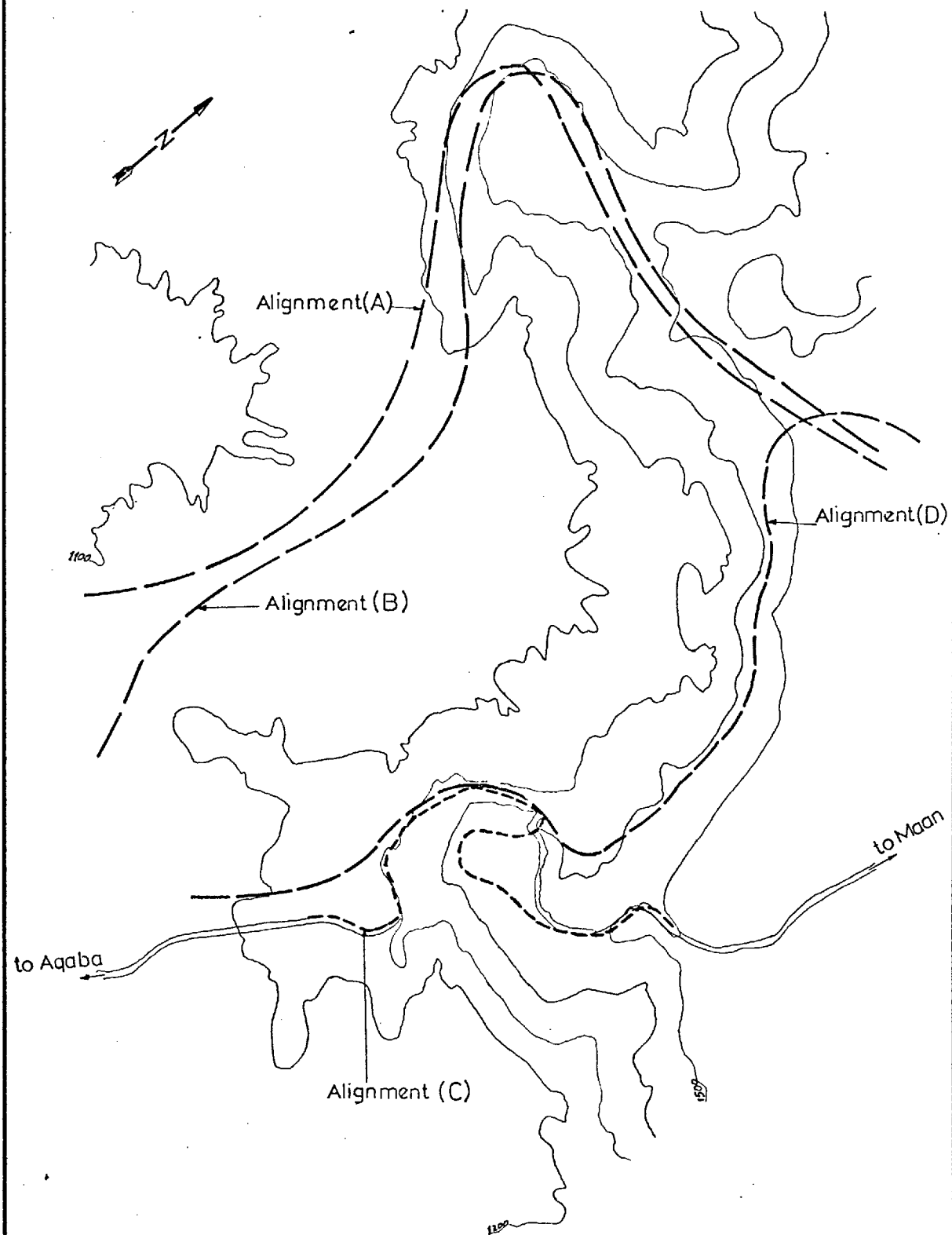
(Ras-En-Naqab Escarpment)

6.1 INTRODUCTION

The Ministry of Public Works in Jordan is planning to improve or to relocate the existing section between Ma'an and Queweira along the Amman-Aqaba highway. This section of the highway is considered to be the most difficult in the county as the design of the curves and highway grade is not of primary standard.

In 1968, British Consulting Engineers, Scott, Wilson, Kirkpatrick and Partners carried out a reconnaissance survey of this section of the highway using available air photographs together with topographic and geological and hydrological information in the Natural Resources Authorities in Amman. The proposed realignment sections are shown in Fig. 6.1 . It was apparent in the course of their investigations that geological and topographical conditions would govern the direction of the proposed realignments. Therefore the realignment "B" in Fig. 6.1 is considered to be the most stable in an active geological area (Scott Wilson Report, 1968). The engineering geological problems are concentrated on Ras-en-Naqab escarpment section. The length of this section is about 7 Km, with an average highway grade along the three proposed alignments of 7%. In 1970, the writer

MAAN-AQABA ROAD RAS ENNAQAB ESCARPMENT PROPOSED ALIGNMENTS



Modified after
Scott Wilson &
Kirk Patrick
1968

0 500 1000 m.

Fig (6.1)

received the opportunity to examine the previous studies made on the subject and decide the most suitable alignment for the proposed road following a request from the Ministry of Public Works.

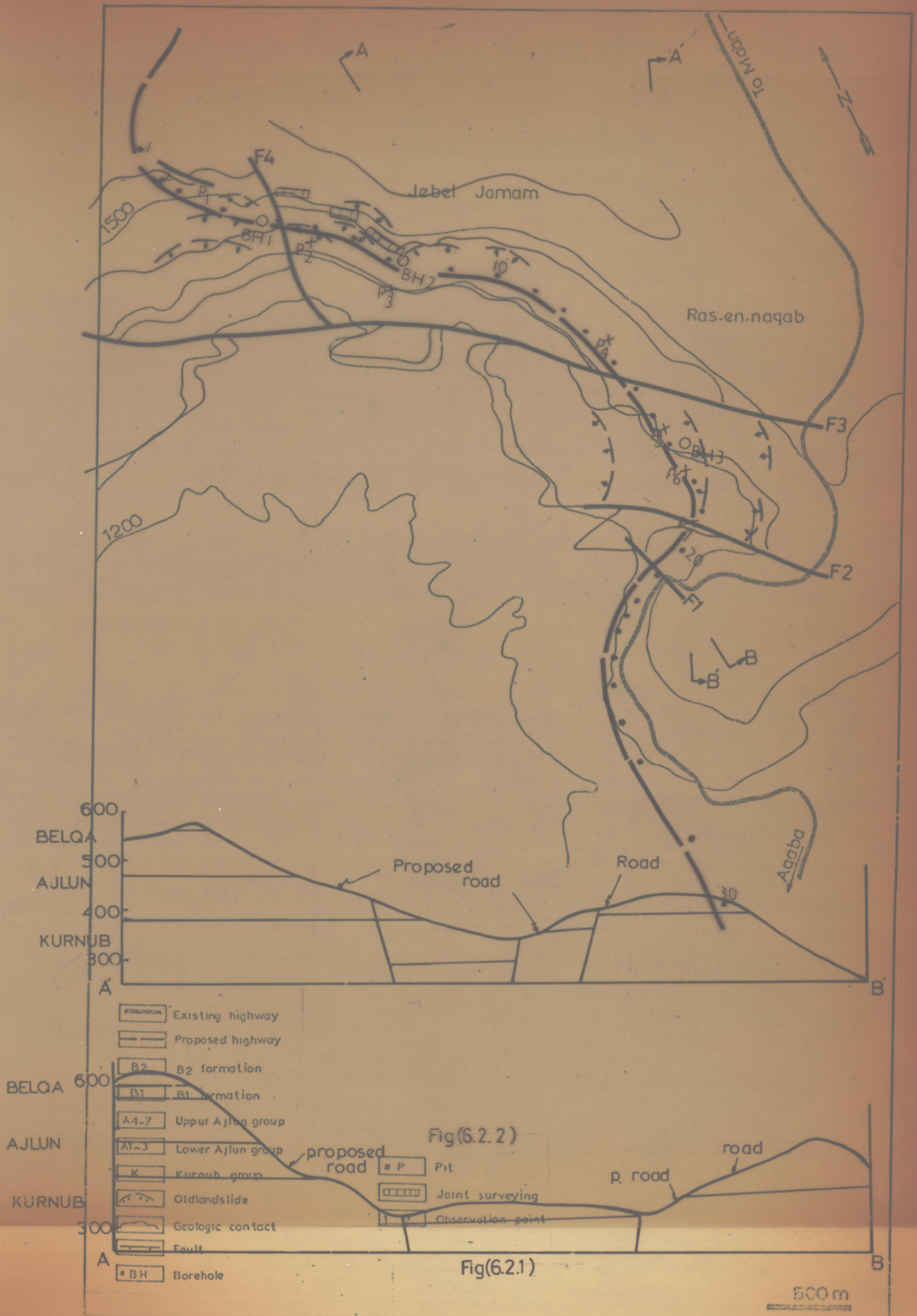
In this Chapter, a brief description of the latest proposed highway* between Km 35 and Km 41, Fig. 6.2.2, is given together with detailed field and laboratory testing of the soils along the highway. The problems of stability of the highway and recommendations for prevention of instability are presented.

6.2 GEOGRAPHY AND GEOMORPHOLOGY

The area covered by this study lies at the south western edge of east Jordan, along the existing highway between Amman and Aqaba, within the steep wall of the escarpment, between coordinates 933-938N, and 193-197E. The Ras-en-Naqab area is in rugged mountainous terrain with steep slopes bearing towards the south. The proposed highway crosses a distinctive topographical region varying from 1600 m in the north at the top of the escarpment, to 1200 m at the bottom of the escarpment, with an average ground slope of 25%. The escarpment is traversed by a well-marked pattern of steep gullies which drain the area towards the southwest and at the bottom of the escarpment the

* This highway was proposed by the Ministry of Public Works Engineers and Dar-El-Handash Eng. Office in Amman.

MĀAN AQABA ROAD
RAS-EN-NAQAB ESCARPMENT



- Existing highway
- Proposed highway
- B2 formation
- B1 formation
- A1-7 Uppur Ajlun group
- A1-3 Lower Ajlun group
- K Kuroub group
- Old landslide
- Geologic contact
- Fault
- Borehole
- Pit
- Joint surveying
- Observation point

Fig(6.2.2)

Fig(6.2.1)

500 m

area is characterized by wide steep and deep valleys. The gradients of the proposed highway on the hillside are in the range of 2.5 - 5.5% over a 7 km distance. The morphology of the area shows a hummocky terrain owing to the combined action of weathering, tectonic and old landslide movements in the area (Plate 6.1).

6.3 GEOLOGY OF THE STUDY AREA

A detailed geological map was prepared on an available topographic map of 1:25,000 scale, Fig. 6.2 and a detailed geological description of the route is given in Appendix G2. The approximate geological mapping of the area is also shown in Plate 6.2.

6.3.1 Stratigraphy

The rock units exposed in the study area are:

- a. Recent deposits.
- b. B₂ formation - "Silicified limestone unit".
- c. B₁ formation - "Sand-Marl unit".
- d. Upper Ajlun formation - "limestone-marl unit".
- e. Lower Ajlun formation - "marl-clay unit".
- f. Kurnub sandstone unit.

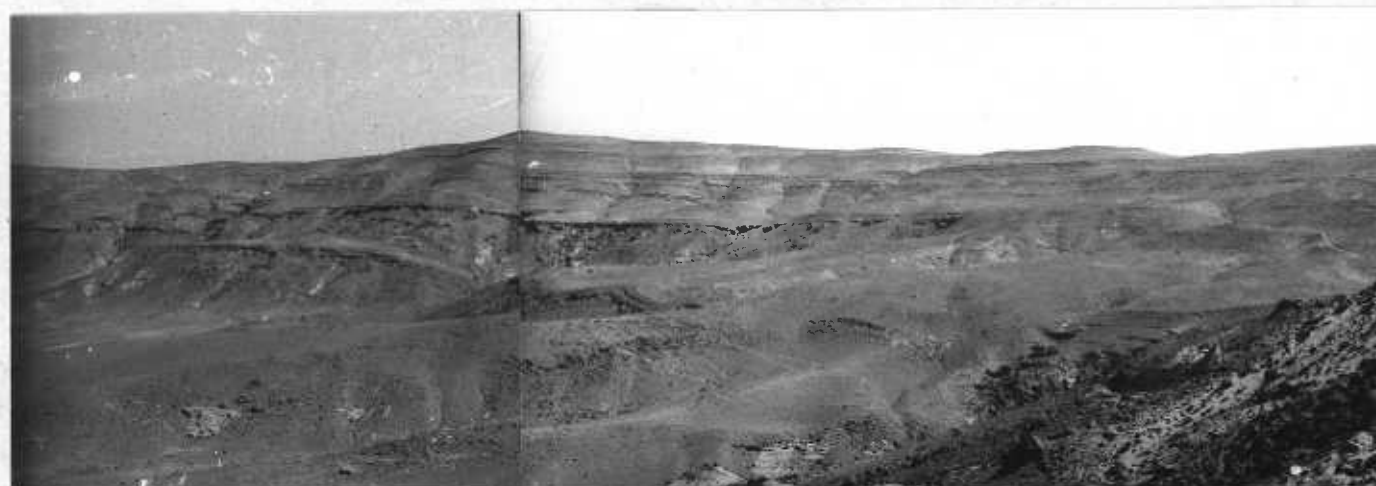
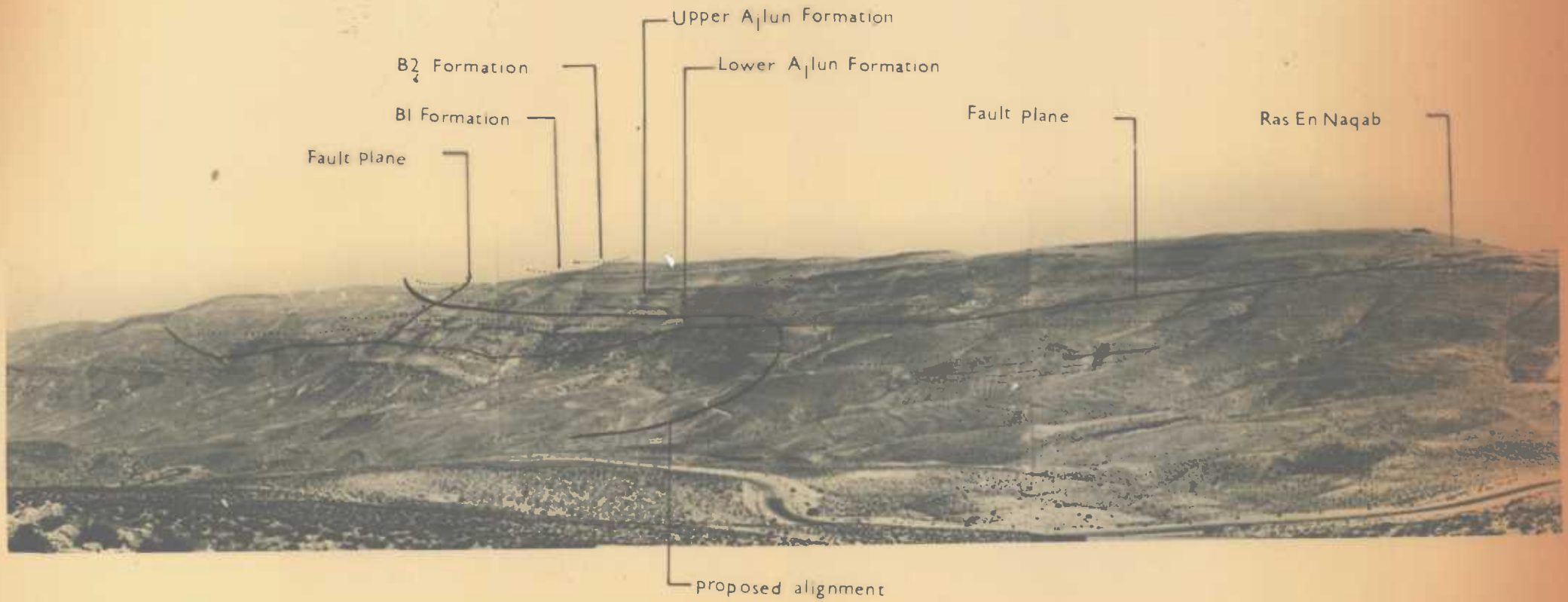


Plate 6.1 General view of the study area of the Ras-en-Naqab escarpment showing a hummocky terrain owing to the combined action of the tectonic, old landsliding and weathering.



PLATE(6.2)-GENERAL VIEW OF THE STUDY AREA, SHOWING THE APPROXIMATE GEOLOGY ALONG THE PROPOSED ALIGNMENT.

A measured columnar section showing these units is given in Figure 6.3 , and described in detail in Appendix C3.

a. Recent deposits:

The bedrock in the study area is often covered by these deposits, which range in thickness from 0 to 20 m and may be any of the following types:

i) Residual soils formed by the decomposition of the bedrock in situ. Deposits of this type occur on the upper plateau of Ras-En-Naqab.

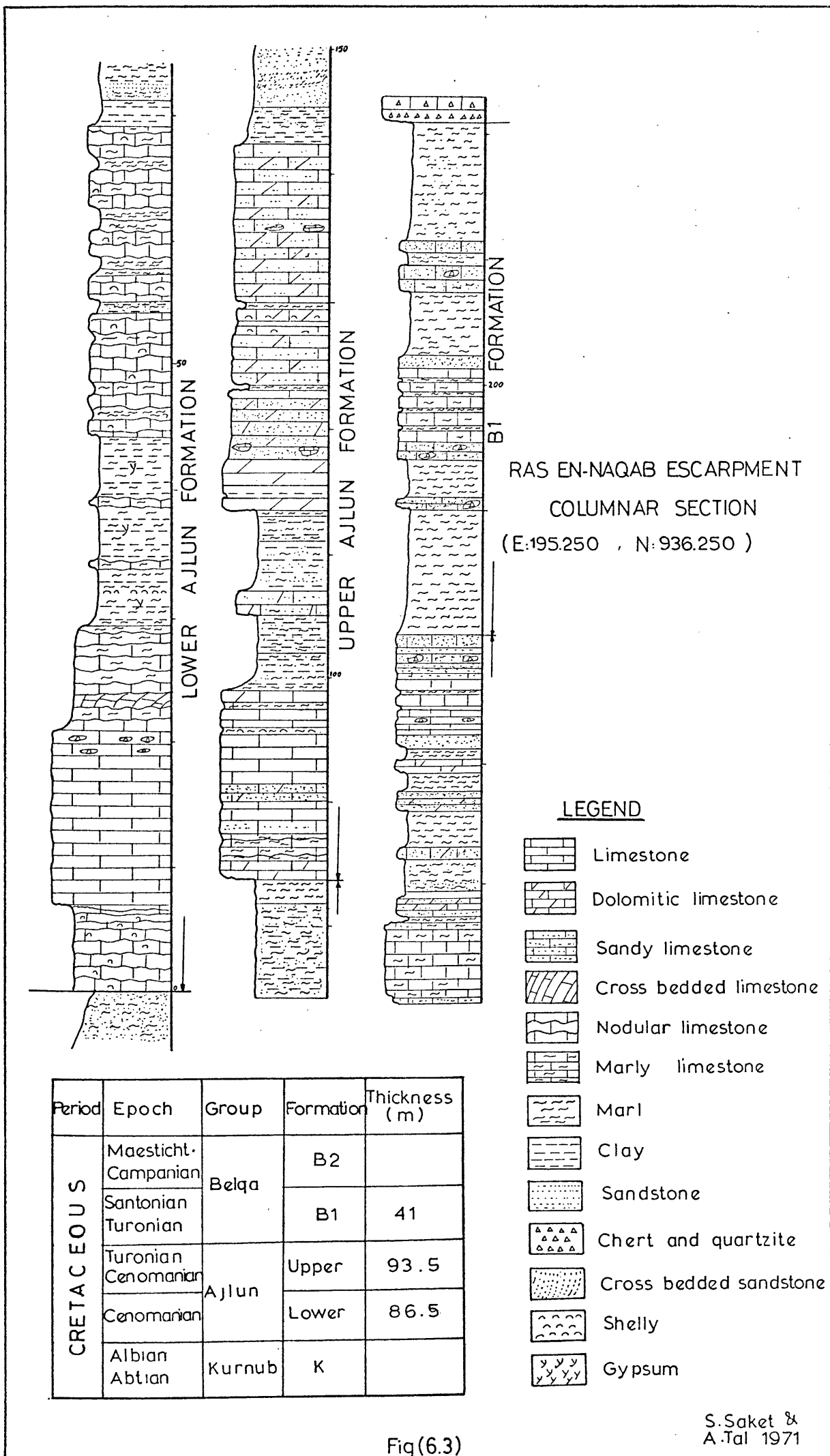
ii) Detrital soils in the form of boulders, cobbles, gravels and sands in a matrix of silty clay generally found mantling the hillsides. These are predominantly observed within the escarpment.

iii) Poorly sorted alluvium formed by the transportation of the residual soils. These are observed in the gullies and wadis.

iv) Fans of marl and clay cover the underlying Kurnub sandstone.

b. B₂ formation - "Silicified limestone unit":

The unit is exposed at the top of the escarpment and is mainly composed of a highly weathered chert and silicified limestone.



Fig(6.3)

S.Saket &
A.Tal 1971

c. B₁ formation - "sand-marl unit":

This unit is composed of sandy, silty marls alternating with sandy limestones and brown white cross-bedded calcareous sandstones. The lower boundary has been placed at the top of brown to yellow thin cross-bedded, calcareous sandstones with lenses of dark brown hard crystalline limestone and quartzite.

The thickness of B₁ is about 41 m.

The Belqa group is assigned to Santonian-Maestrichtian (Lloyd 1969), younger Belqa sediments ranging in age up to the Eocene.

d. The Upper Ajlun Formation - "limestone-marl unit":

This unit is mainly composed of sandy limestones, sandy dolomites and calcareous sandstone alternating with thin bands of marl. The lower boundary of this unit has been placed where the marl-clay sequence of the lower Ajlun formation becomes limy and sandy, and the topographical relief becomes steeper. The thickness of this unit is about 94 m. It is assigned to Turonian-Cenomanian.

e. Lower Ajlun Formation - "Marl-clay unit":

The formation is composed of marls and clays alternating with dolomitic limestones and nodular limestones. The

lower boundary of the unit is marked by the first thick limestone bed overlying green yellow sandy marls of the Kurnub sandstone. The upper contact has been placed below the sandy-dolomitic limestone beds where the morphology changes from steep in the Upper Ajlun Formation to gentle in the Lower Ajlun Formation. The thickness of this unit is about 79 m. It is Cenomanian age.

f. Kurnub sandstone group:

Only the uppermost part of this unit is exposed in the study area. It begins at the base of 15 m thick limestone bed of the Lower Ajlun group and is composed of sandy and silty shales and marly sandstones with gypsum laminae on bedding planes, with intercalations of discontinuous bands of hard ferruginous quartzitic fine sandstones.

At Ras-En-Naqab the Kurnub group is 120 m thick and it is considered to be of Albian age (Lloyd 1969).

6.3.2 Structure

The Ras-En-Naqab escarpment lies on the southern borders of the block faulted area of the central and north-eastern province of Jordan. Faults occur in two main directions: NW-SE and NNE-SSW; their intersection is seen in the Ras-En-Naqab

escarpment, Figure 6.2B. Faults No. F_1 and F_2 (NW-SE) have a 30 m downthrown; F_3 has an almost NNE-SSW direction and also has a 30 m downthrown.

F_1 and F_2 form a step-shaped structure, while F_2 and F_3 form a graben-shaped structure which downfaults down the Ajlun formation. F_3 and F_4 intersect approximately at right angles.

6.4 HYDROLOGY AND HYDROGEOLOGY

According to Long (1957), the investigated area lies within the Mediterranean arid-warm variety of the bioclimatic region sub-divisions. The average annual rainfall is 150 mm, average minimum temperature in the coldest month (January) of -5°C to 7°C and an average maximum temperature of hottest month (August) of 34°C to 40°C . The mean annual relative humidity is 40%. According to the hydrology observatory station at Ras-En-Naqab, the distribution of monthly precipitation is as shown in the following table .

Station	Month	Observation	Mean monthly rainfall mm	Max.monthly rainfall mm	Min.monthly rainfall mm
Ras-En-Naqab	October	14	3.0	18.8	00
	November	13	9.5	46.2	00
	December	13	34.7	93.8	00
	January	13	33.5	160.5	00

Station	Month	Observation	Mean monthly rainfall mm.	Max. monthly rainfall mm.	Min. monthly rainfall mm.
Ras-En-Naqab	February	13	32.2	87.2	00
	March	13	17.6	48.0	00
	April	13	11.0	43.0	00
	May	13	4.3	39.5	00

TABLE 6.1 (Continued)

The mean monthly rainfall figures show that the wettest period is from December to February.

The characteristic statistics of annual precipitation are summarized as following (Lloyd 1969).

Station	Ras-En-Naqab
Years of Record	14
Mean annual rainfall (mm)	139.0
Max. annual rainfall (mm)	254.0
Min. annual rainfall (mm)	64.0

TABLE 6.2

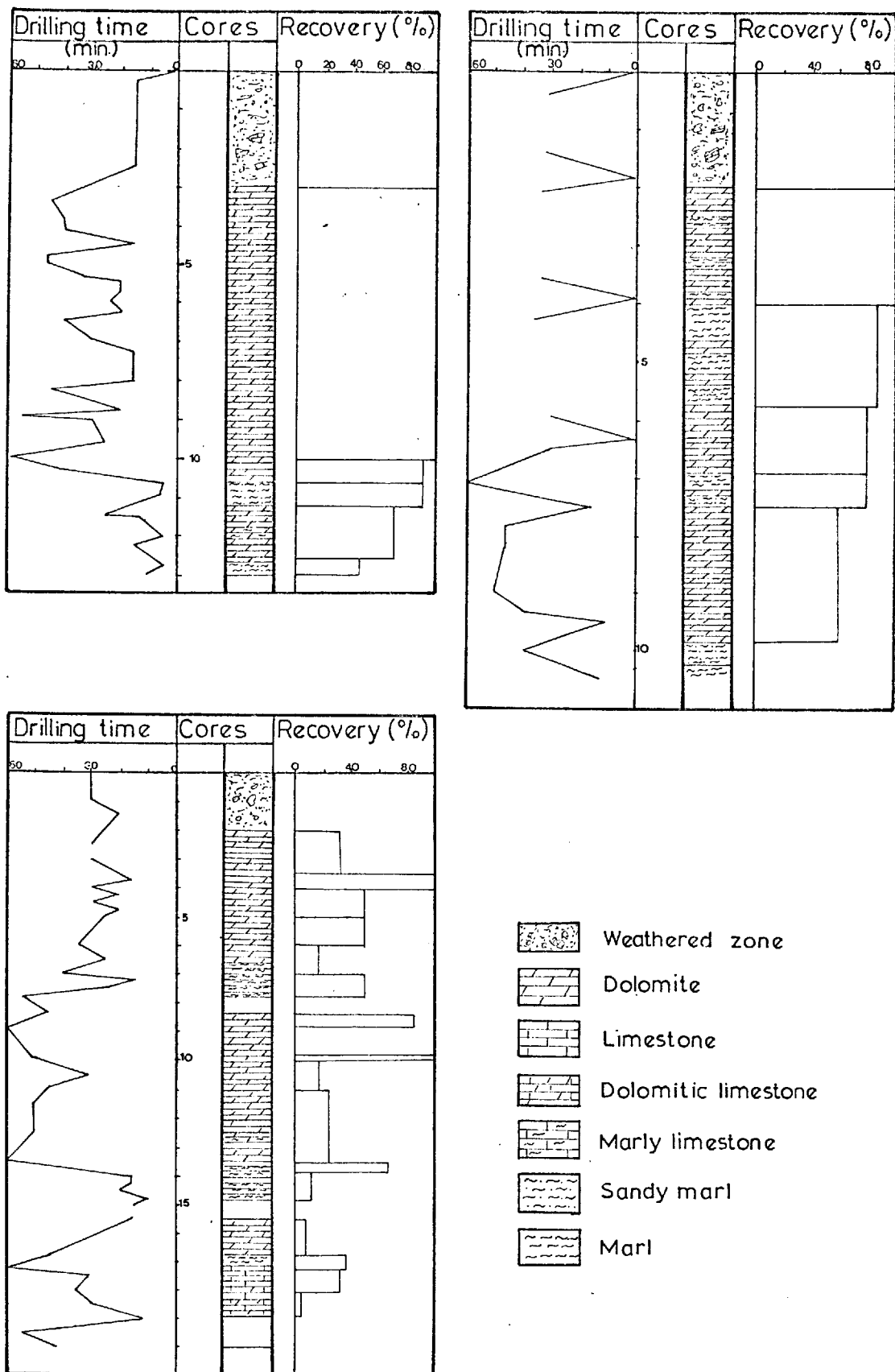
The evaporation in the study area is moderate (1-3 mm/day), and the infiltration is low due to the steepness of the ground surface and the impervious nature of the ground although a certain rate of infiltration occurs through the jointed rock formations particularly when the escarpment is capped with snow in winter. Many springs can be seen discharging probably from the fault zones within these sediments in the

study area. The Lower Ajlun group (marl-clay unit) is regarded as an aquiclude because of the thick clayey portions in this unit; while the Upper Ajlun group, "limestone-marl unit", is regarded as an aquifer when the jointing is well developed. The B₁ formation, "sand-marl unit", is considered as a poor aquifer owing to the presence of calcareous cement. The inadequate recharge, small catchment area, the steep slope and faulting in the vicinity of the study area appear to be unfavourable for the development of large ground water body close to the ground surface.

6.5 FIELD INVESTIGATION AND SURVEY

Field investigations began with the preparation of a geological map of 1:25,000 scale. A detailed columnar section was recorded and is described in detail elsewhere in Appendix C3. Three boreholes were drilled along the centreline of the road to explore the subsurface materials, the depth to bedrock and to obtain information on old landslide movements. Generally the cores recovered were intensely broken with small fragments of rock intercalated with marls and clays; joints and cavities were observed.

In borehole no. 1 (Figure 6.4), the bedrock was found to consist of alternations of intensely jointed limestones,



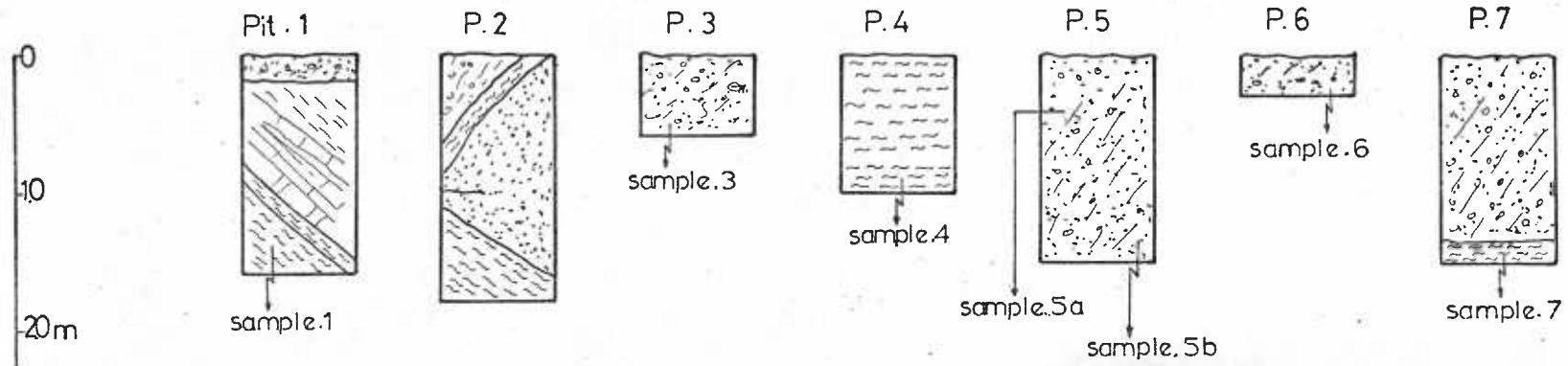
EXPLORATION BOREHOLES LITHOLOGY INCORRELATION WITH THE DRILLING TIME AND CORE RECOVERY PERCENT

Fig(6.4)

dolomitic and marly limestones, and marls. In borehole no. 2, soft clay was encountered at a depth of about 20 m. All the overlying material was composed of sandy to silty clay with rock fragments and brownish weathering soil. In borehole no. 3, softened marl was encountered at a depth of 13 m. This marl was overlain by intensely weathered silty clayey materials. The disturbed nature of the bedrock and presence of polished joint surfaces indicated the action of an old landslide movement (these three boreholes are described in detail elsewhere (Appendix C4)). In addition to the boreholes, seven trial pits, Figure 6.5, were excavated along the proposed re-alignment, to permit sampling and detailed visual examination of the soil profile. (These pits are described in detail in Appendix C5.) They also show direct indication of the old movements in the area (Plate 6.3). Eight samples, three disturbed and five undisturbed, were obtained from these pits for complete analysis and these were regarded as representative of the materials along this road (location of the boreholes and pits is shown in Figure 6.2.2).

The harder members of the Upper Ajlun group were affected by different sets of joints which are mostly open and continuous. Detailed joint surveys were carried out in this material at three locations along the proposed road, Figure 6.2.2.

MA'AN - AQABA ROAD
 RAS EN-NAQAB ESCARPMENT
 PITS LITHOLOGY



-  Marly Limestone
-  Marl
-  Sand
-  Weathered zone



PLATE(6.3) - Exploratory pit shows the disturbed nature of the bedrock indicating the old movements in the area.

In the upper and middle part of this rock unit area 1 (Figure 6.6), three joint sets were defined as follows:-

Joint Set	Dip	Strike
I	73 SW	123
II	72 SW	163
III	78 SE	227
Strata (bedding)	4 NW	70

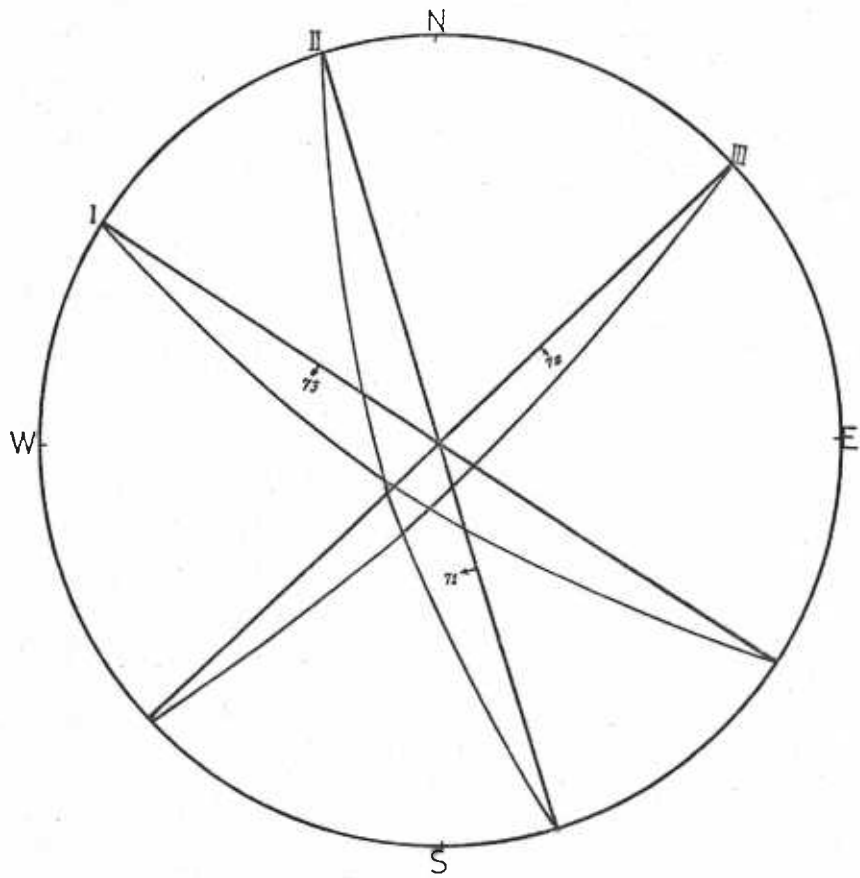
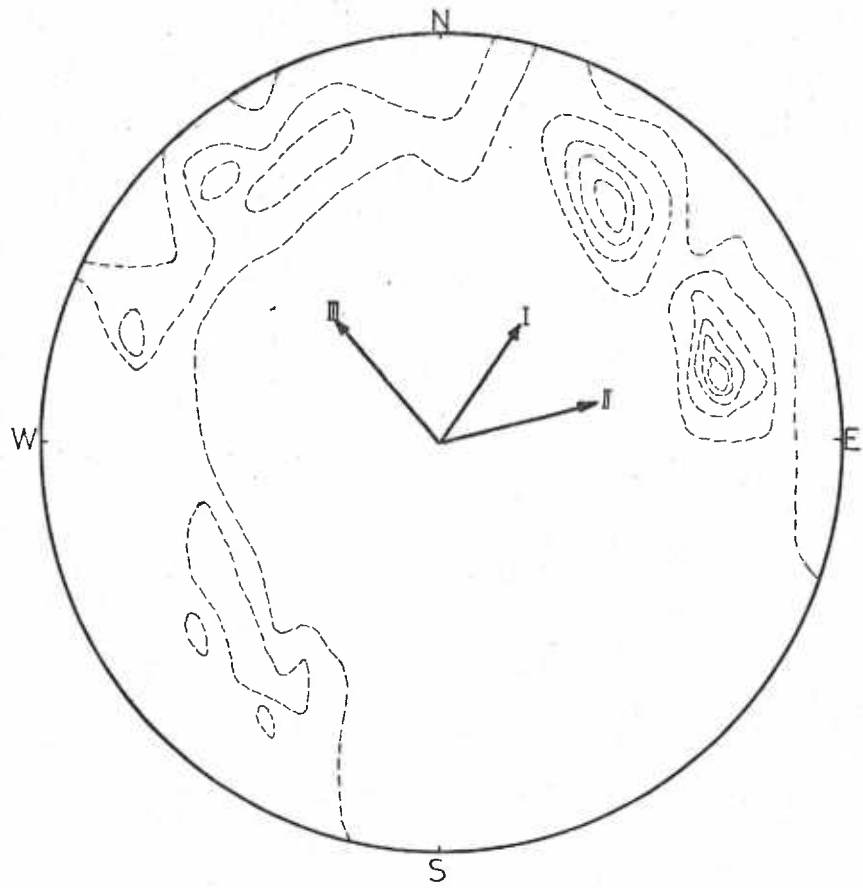
The joint surveys indicate that 76% of all joints are very steep and nearly vertical and parallel to the hillside dipping out of the slope (circumferential). The three sets divide the rock into many cuboidal blocks ranging in size from 0.5 m³ to 2 m³ (Plate 6.4).

In the lower part of the Ajlun rock unit two sites were selected for joint surveys. At the first site (area 2, Figure 6.7) the following joint sets were measured:-

Joint Set	Dip	Strike
I	78 SW	354
II	80 SE	21
III	80 SE	62
Strata (bedding)	4 NW	70

about 60% of these joints are of critical types (circumferential), most of them are open and continuous, Plate 6.5.

At the second site (area 3, Plate 6.8), the following joint sets were recorded:-



AREA(1)_ CONTOUR DIAGRAM AND REPRESENTATIVE JOINT SETS
(LOWER HEMISPHERIC PROJECTION)

Fig(6.6)



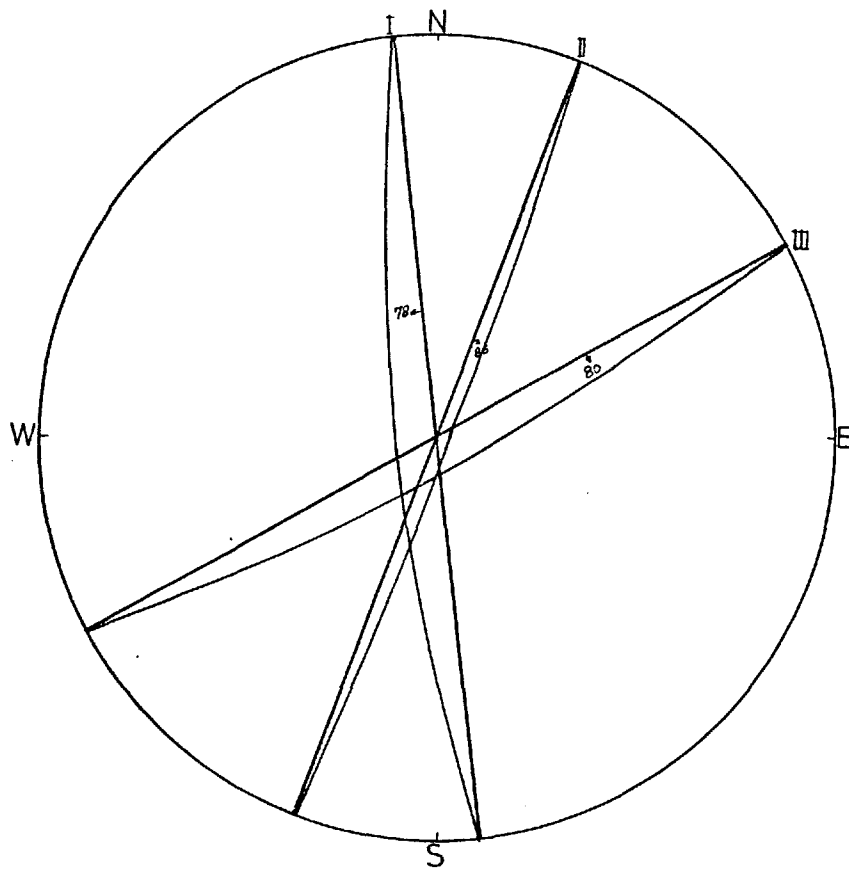
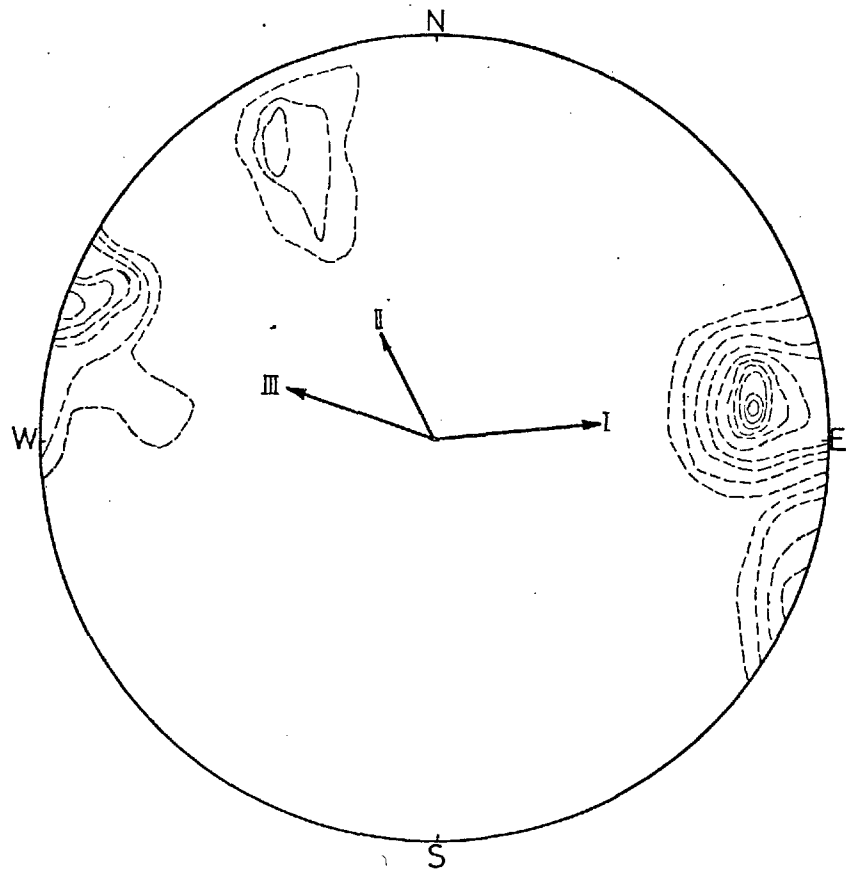
Plate 6.4 The intensely jointed bedrock of the Upper Ajlun Formation (joint surveying area 1).



Plate 6.5 The upper part of the Lower Ajlun rock unit showing intense jointing and expected toppling (joint surveying area 2).

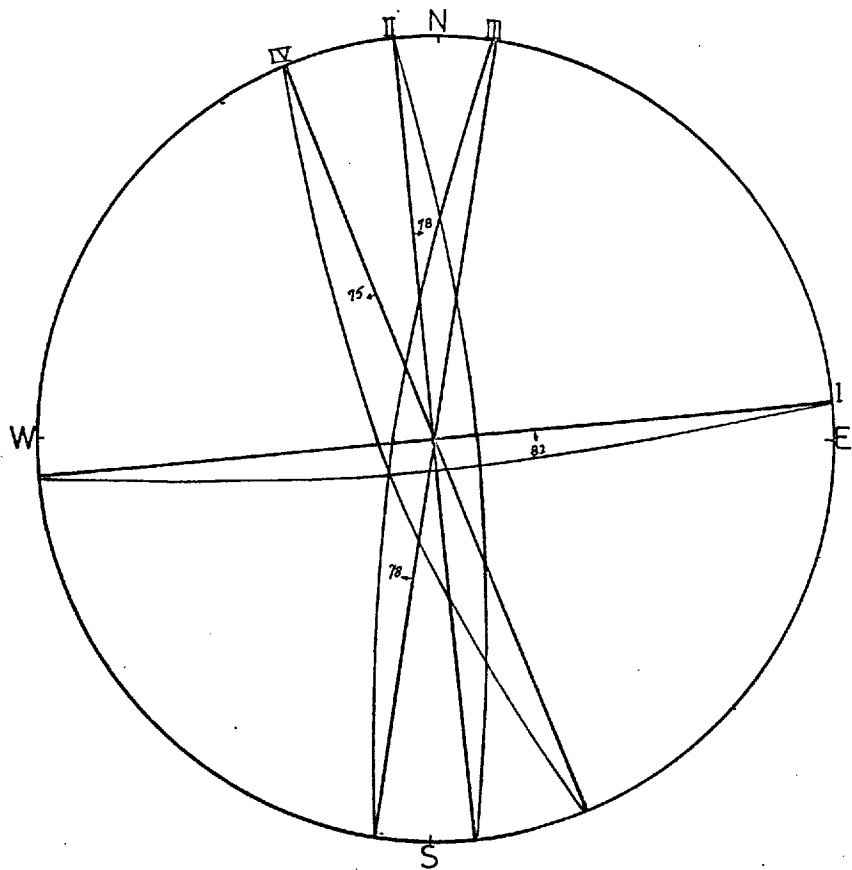
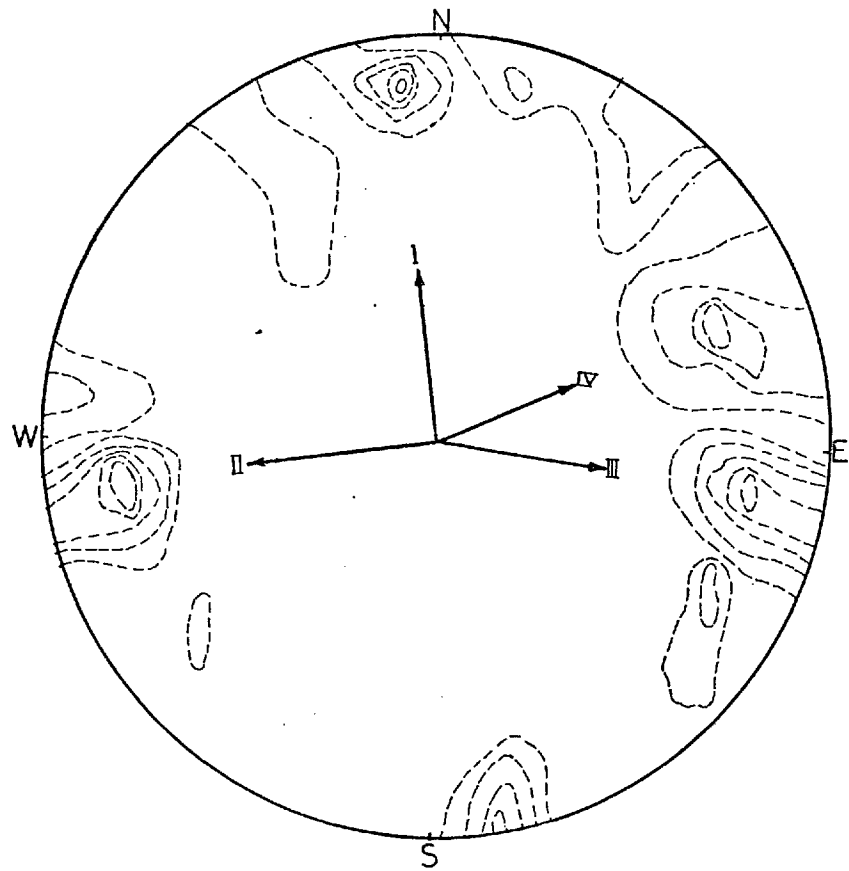


Plate 6.6 The intensely jointed Lower Ajlun rock unit (joint surveying area 3).



AREA(2)_ CONTOUR DIAGRAM AND REPRESENTATIVE JOINT SETS
LOWER HEMISPHERIC PROJECTION

Fig(6.7)



AREA(3). CONTOUR DIAGRAM AND REPRESENTATIVE JOINT SETS
(LOWER HEMISPHERIC PROJECTION)

Fig(6.8)

Joint Set	Dip	Strike
I	82 SE	84
II	78 SE	173
III	78 NW	8
Strata	4 NW	70

Few of these joints intersect the hillside at an angle; some are of circumferential type, some others in combination divide the strata into cuboidal blocks ranging in size between 1 m^3 to 4 m^3 . The most critical joints are those nearly vertical and parallel to the hillside and dipping out of the slope. All these joints are related to either past tectonic activity or old landslide movements in the area. Many types of slope instability were observed within the Ajlun rock unit; e.g. rockfalls, rockslips and toppling. (Detailed descriptions of the existing problems along the route are in Appendix C2).

6.6 LABORATORY INVESTIGATIONS

For the purpose of the present study an intensive laboratory testing programme was devised and performed on eight representative samples obtained from the pits to establish the engineering properties of the materials along the proposed alignment.

A summary of these results is compiled in Table 6.1.B. The principal classification results are summarized in Table 6.3.

Index Properties		Range
Liquidity Limit	L.L.	32.3 - 80.5%
Plastic Limit	P.L.	13.7 - 27.4%
Shrinkage Limit	S.L.	10.1 - 24.1%
Clay Fraction	<2 μ	16 - 80 %
Activity		0.5 - 2.2
Liquidity Index	L.I.	0.02 - 0.07
Max. Water Absorption		54 - 117%
Specific Gravity	Gs.	2.59 - 2.75
Wet Bulk Density	γ_B	1.47-1.85 g/km ³
Natural Water Content	Wc.	13 - 57.3%
Porosity	n	27 - 55%
Void Ratio	e	12 - 66
Total Soluble Salts		0.43 - 7.0%
Max. Dry Density		1.20-1.78 g/km ³
Optimum Moisture		15 - 27%
C.B.R.		2.5 mm 2-14%
		5.0 mm 3-10%

TABLE 6.3

The Atterberg limits test results are plotted on the Conventional Casagrande plasticity chart (Figure 6.9); all the points lie above A line, and the tested samples fall generally into two types; the first type is CH highly plastic clay and has the following properties (according to U.S.B.R.):-

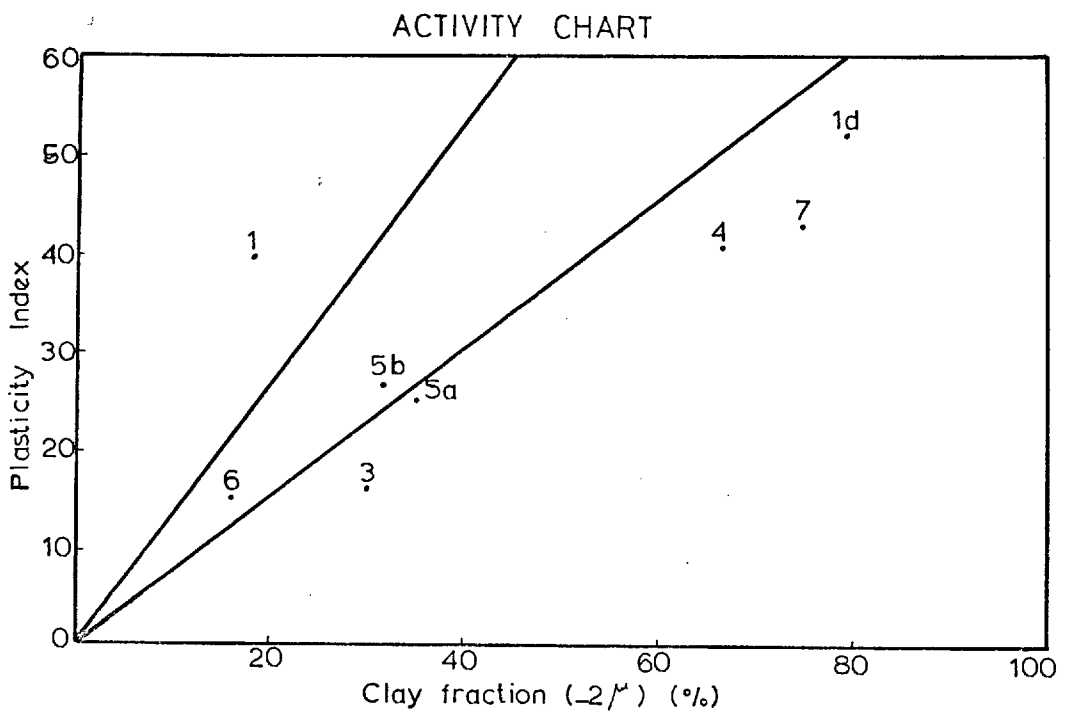
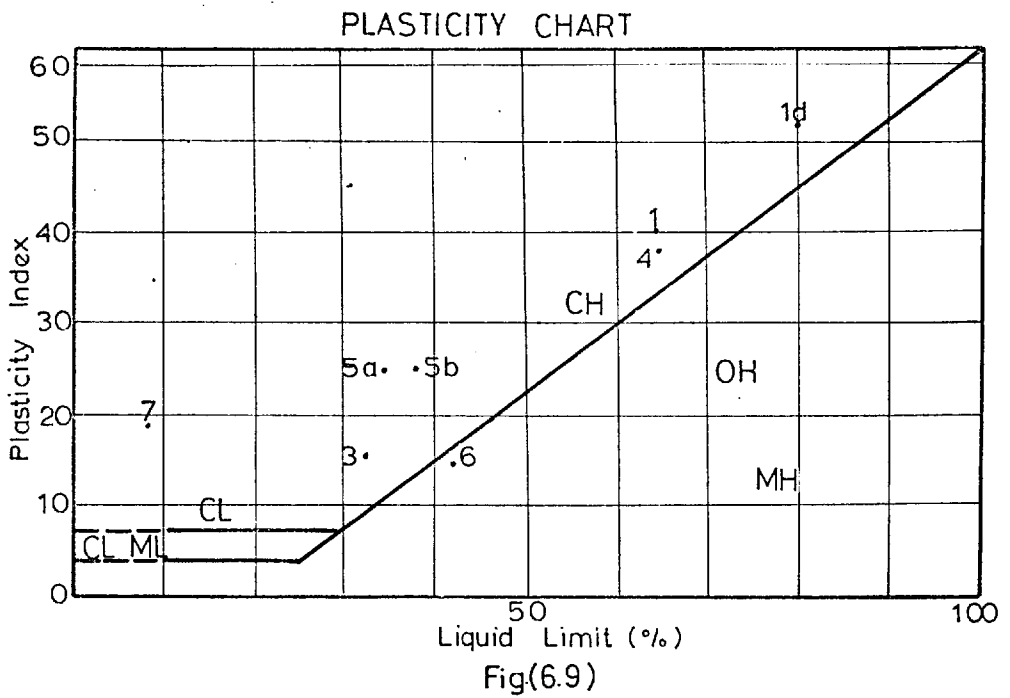
1. Impervious when compacted.
2. Poor shearing strength and high compressibility when compacted and saturated.

3. Poor workability as a construction material.
4. Suspect as to the erosion resistance and should not be used as surfacing in the roadways.
5. Poor as a fill and foundation material.

The second type of CL, inorganic silty clay of medium plasticity, has the following properties:-

1. Impervious when compacted.
2. Fair shearing strength and medium compressibility when compacted and saturated.
3. Good workability as a construction material.
4. It is not recommended for use as surfacing in the roadways whenever suitable material is available.
5. It may be used as fill material when it is the only source of borrow area.

Undoubtedly it is the first type of material (CH) which is potentially the most dangerous. The activity values show that one of the groups is an inactive to normal clay where the other is an active clay (Figure 6.10). This suggests a predominantly Illitic, Montmorillonitic clay (Skempton 1953).



PLASTICITY AND ACTIVITY CHARTS SHOWING POSITIONS OF
SAMPLES REPRESENTATIVE OF THE MATERIAL ALONG THE
PROPOSED ALIGNMENT

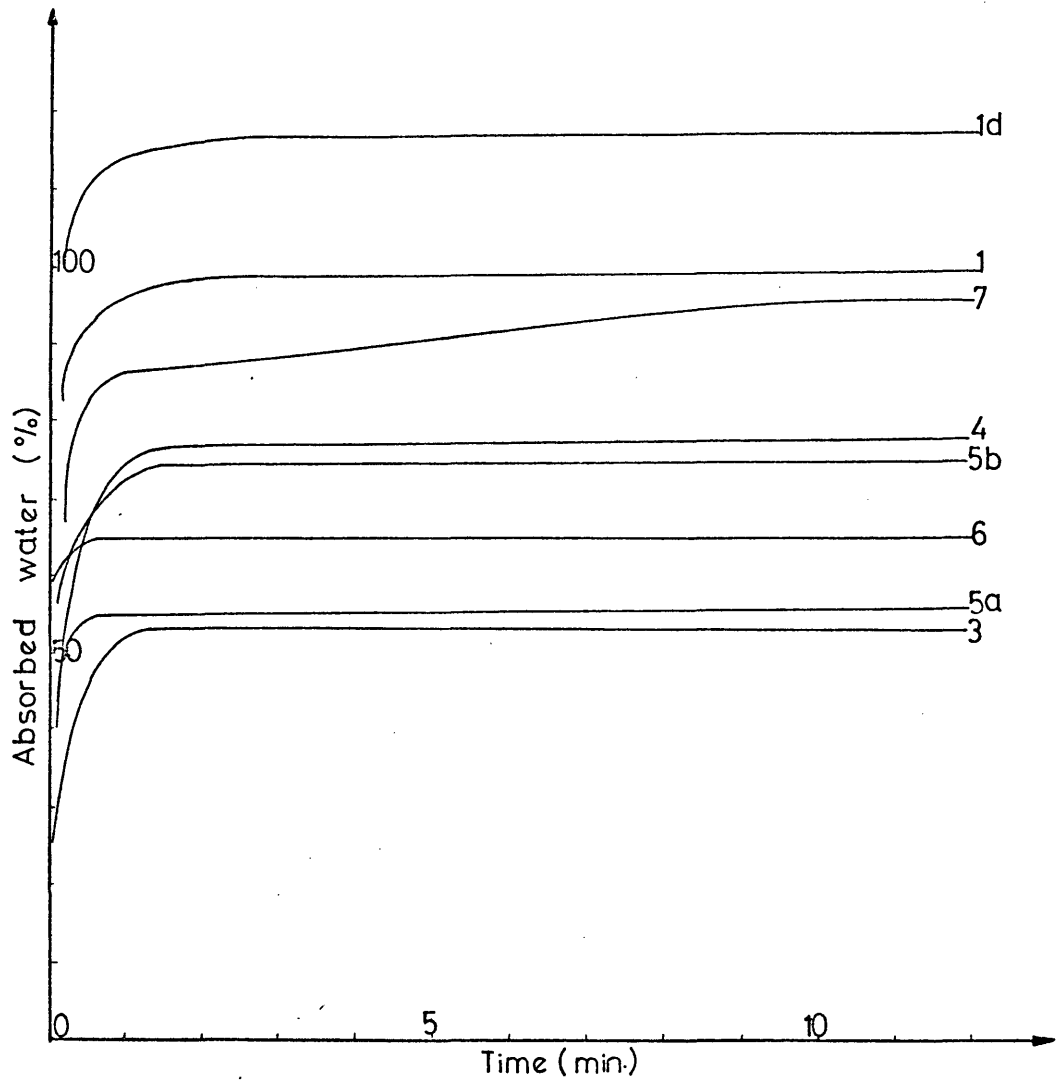
Fig(6.10)

The maximum water absorption tests on the samples gave medium to high values which were directly related to the percentage and type of the clay minerals present (Figure 6.11). The liquidity index suggests that this clay could be classified as stiff clay (Terzaghi 1936). The natural water content is above the plastic limit; this type of clay is over-consolidated in the present time. The gradation analyses show that the materials are sandy silty clays (Figure 6.12). The Proctor Compaction test results show maximum dry density in the ranges 1.2 g/cm^3 to 1.78 g/cm^3 with optimum moisture contents in the range of 15% - 36% (Figure 6.13). The C.B.R. Test values range between 1.5 - 14% for 2.5 mm penetration, and 1 - 5% swelling.

Shear strength parameters in terms of effective stresses were determined by carrying out consolidated-undrained triaxial compression tests with measurement of pore water pressures on three test specimens 3 x 1.5 in in diameter, taken from the same sample. The following results were obtained:

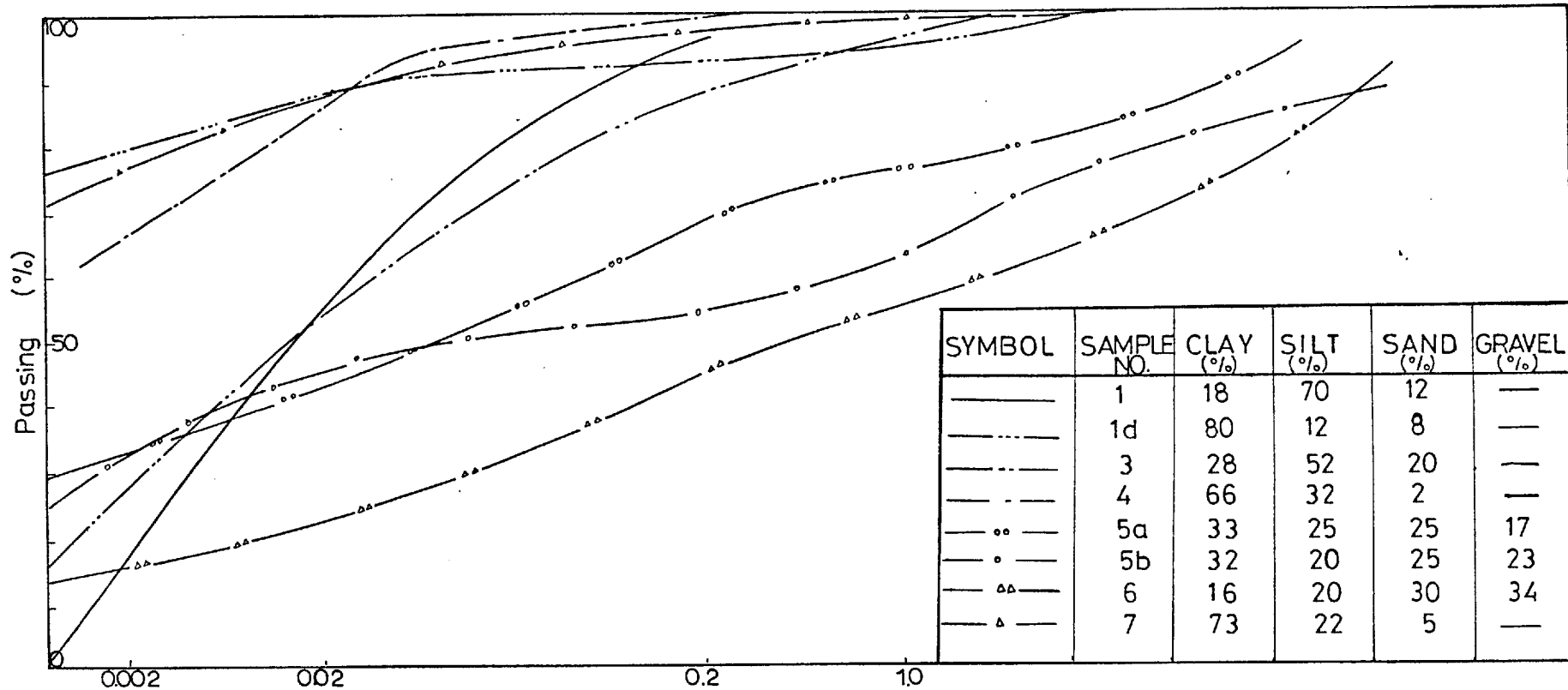
$$c'_p = 0.40 \text{ Kgf/cm}^2 \quad \phi'_p = 12^\circ$$

Undoubtedly this result is not representative of all the materials along the proposed road, but it is more or less representative of the clay materials of the lower part of the Ajlun group (marl-clay unit). The unconfined compressive



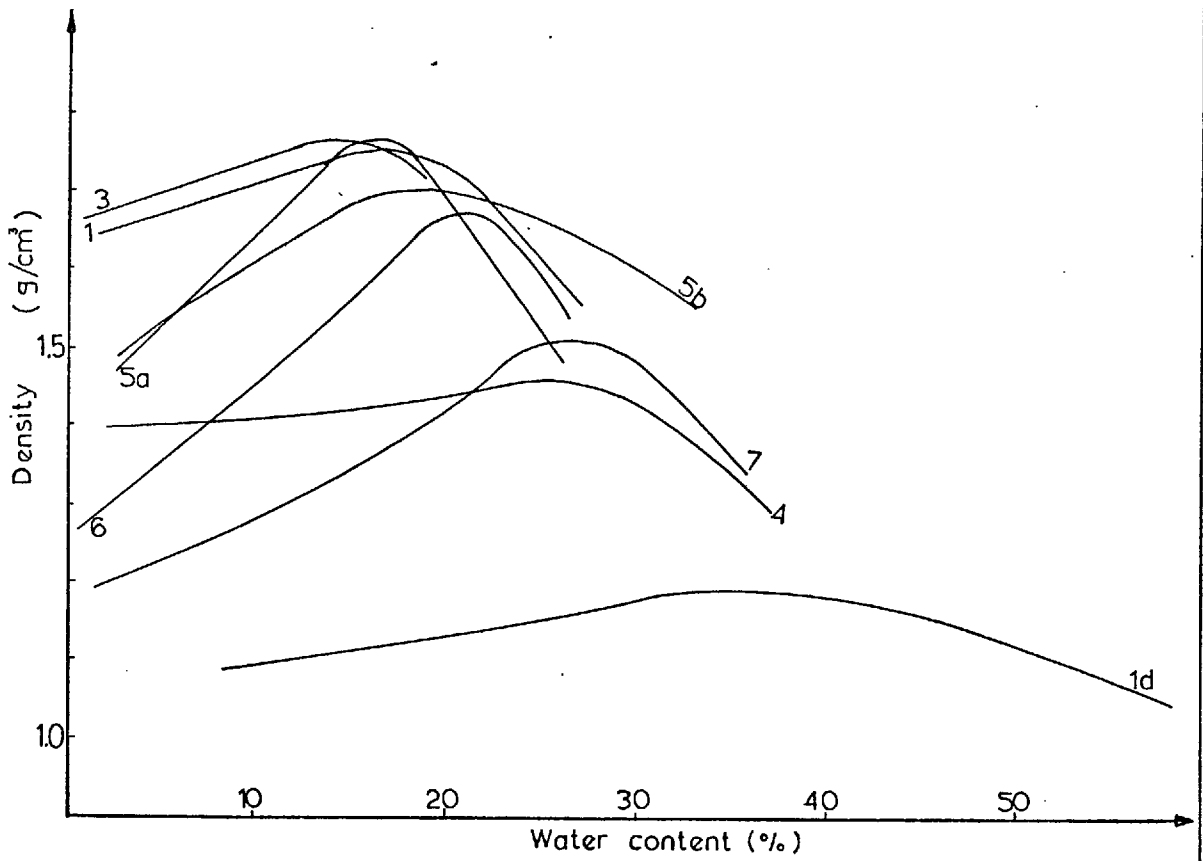
MAXIMUM WATER ABSORPTION OF THE SAMPLES REPRESENTATIVE OF THE MATERIALS ALONG THE PROPOSED ALIGNMENT

Fig.(6.11)



TYPICAL GRADING CURVES OF SAMPLES REPRESENTATIVE OF THE MATERIALS ALONG THE PROPOSED ALIGNMENT

Fig(6.12)



SAMPLE NO.	1	1d	4	5a	3	5b	6	7
MAXIMUM DRY DENSITY	1.76	1.20	1.46	1.78	1.77	1.71	1.68	1.52
OPTIMUM WATER CONTENT (%)	18	36	27	16	15	17	21	26

PROCTOR COMPACTION TEST AND SUMMARY OF THE RESULTS

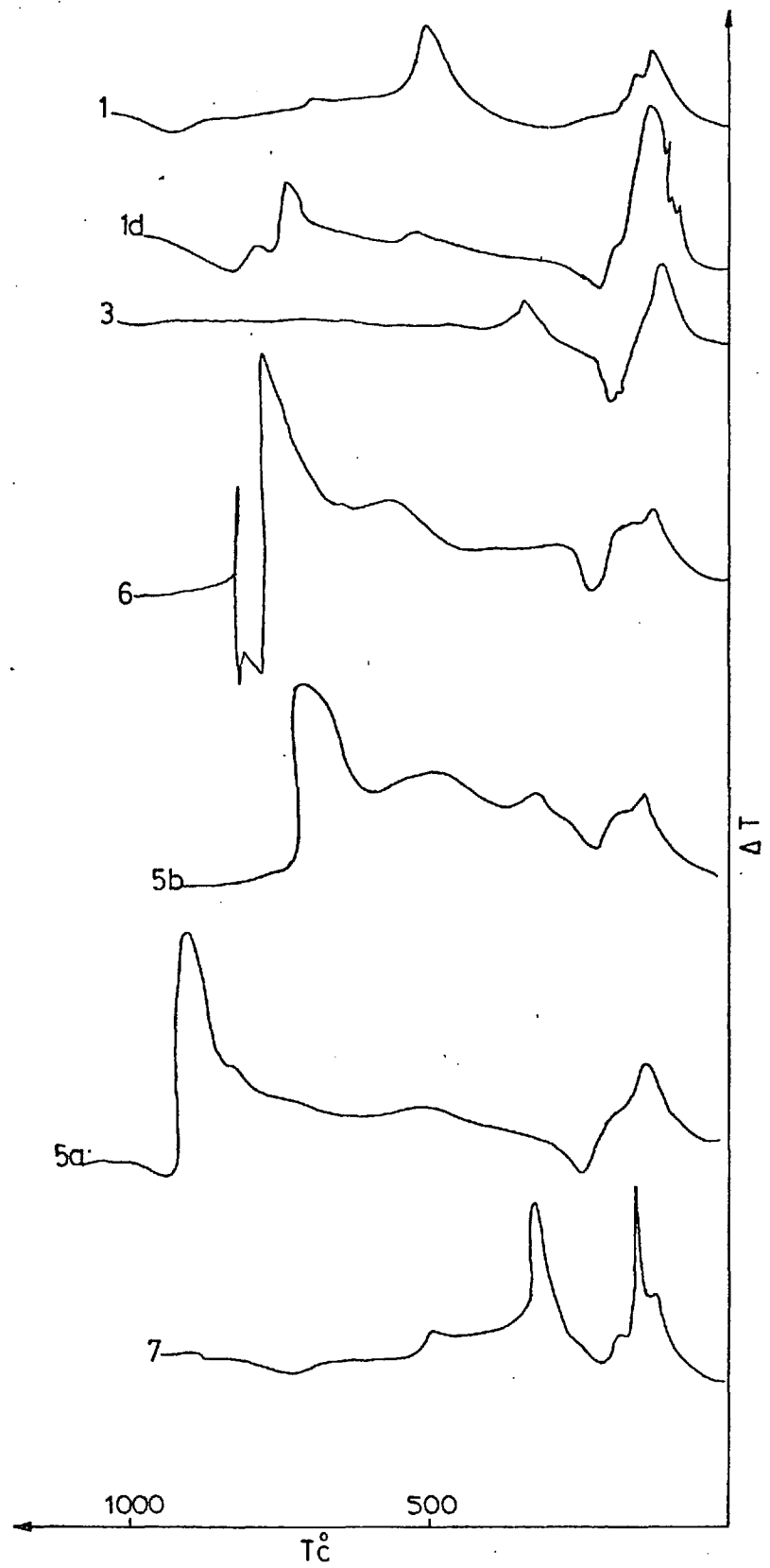
Fig.(6.13)

strengths for the same sample at its natural density and field moisture content were approximately 2.8 kg/cm^2 , which could be described as a very stiff clay. The quick triaxial tests* on remoulded samples of these soils at their natural density and moisture content are perhaps more indicative of the true strength of these soils at saturation, although even here, the results are higher than expected. The ϕ for these soils was found to vary between $9-12^\circ$, while their C' ranged between 0.60 and 1.34 kgf/cm^2 .

It should be mentioned here that a certain amount of disturbance has been unavoidable in obtaining tube samples from such clay owing to the amount of fissuring and structural disturbance.

The Differential Thermal Analyses of seven samples representing the different types of clays along the proposed alignment show that the dominant minerals are Halloysite, Illite mixed with carbonates and hydrated ferric oxide gel, Figure 6.14. (Detailed descriptions of these samples are compiled in Appendix B, Table 6.2B.) The complete chemical analysis of two representative samples shows the following results:-

* This test was performed in the American University of Beirut laboratory (AUB).



CORRELATION OF THE D.T.A. OF THE REPRESENTATIVE SAMPLES
ALONG THE PROPOSED ALIGNMENT

Fig(6.14)

Content	L.O. Ign.	Silica	CaO	MgO	Fe ₂ O ₃	TiO ₂	Al ₂ O ₃	Na ₂ O	K ₂ O	MnO	SO ₃	Total soil salts
Sample No. 4	8.96	54.21	2.0	2.10	5.80	1.08	20.97	3.80	2.90	0.03	1.20	3.48
Sample No. 3	22.0	4.97	21.33	2.54	3.60	0.56	7.14	1.41	1.13	0.04	n.d.	0.81

TABLE 6.4

6.7 SUMMARY AND CONCLUSIONS

As previously stated the materials crossed by the proposed alignment are heterogeneous, and it is difficult to estimate with any degree of accuracy the mass strength of these materials and to determine the allowable bearing pressure to be used in the design of the embankments, retaining walls and the associated structures.

The essentially geological characteristics of the Ajlun group are the main factors which govern all movements in the area. The marly sequence of this rock unit is known to be an aquiclude and the hard limy sequence (limestone, marly limestone) provides traps or reservoirs that store water during wet seasons. The weight and pressure of this trapped water besides many other factors contribute to the high shear stress imposed on this material and, also, the composition of the material, fissuring and jointing all contribute to a low shear strength.

Based on the field investigations, problems along the proposed alignment can be classified into two main categories:-

based on their nature and on the properties of the bedrock itself:-

- A. Engineering geological problems.
- B. Topographical and structural problems.

The essentially engineering geological problems are those related to tectonic and landslide movements. The tectonic movements in the study area are those which caused structural deformation in the strata, contributing to instability problems. Type "A" movements could be subdivided into two main groups:

- a. The first group which lies between observation points 1 and 6 could be described as old landslides and rockfalls. These types of movement are observed within the Upper Ajlun formation, where the proposed alignment lies within a sequence composed of thick hard layers of sandy, dolomitic, marly limestones intercalated with marl, and clay. The hard ledges of the bedrock within this group are influenced by different sets of joints contributing to the weakening of the strata. Some joint sets intersect the direction of the proposed alignment at an angle, while other joint sets are more or less parallel to the direction of the alignment; these parallel joints dip both into and out of the hillside. Due to the fact that these jointed ledges alternate with layers of soft marl and clay,

big blocks have slipped forward and fallen into the marl, Plates 6.7 and 6.8 . Slopes cut in this type of bedrock must take into consideration the effect and behaviour of sub-joint systems.

b. The second group can be described as landslides and creep movements which lie between observation points 6 and 20 (Figure 6.2.2). This type of movement is observed in the lower Ajlun group, where the proposed alignment crosses a sequence composed of marl and clay intercalated with ledges of nodular marly limestones. Many large and small scale landslides within zones of creep were observed within this formation (Plates 6.9 and 6.10 , and Figure 6.2.1). From a stability point of view, the section between observation points 6 and 12 is the most critical, where the alignment lies within the plastic clay of the Lower Ajlun group at the foot of the hanging blocks of the intensely jointed thick ledges of the Middle Ajlun group, therefore landslides, mass creep, rockfalls and toppling are expected (Plates 6.4 , 6.5 and 6.6).

The essentially topographic and structural problems were found within the Kurnub group where it is crossed by the proposed alignment between observation points 20 and 30; in this area this rock unit is composed of vari-coloured cross-bedded sandstone intercalated with thin bands of silt and clay.



Plate 6.7 Block flow within the Lower Ajlun Formation.



Plate 6.8 Block flow of the Middle Ajlun Formation underlain by the clay-marl unit of the Lower Ajlun Group.

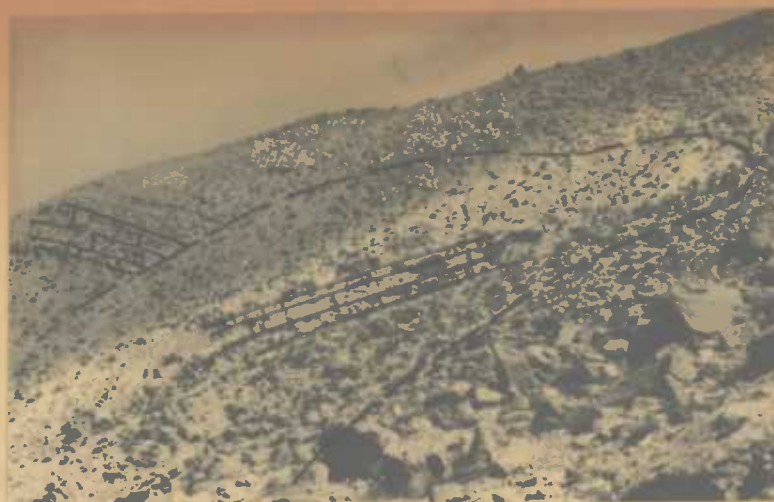


Plate 6.9 Creep of the hard ledges of bedrock into the underlying plastic clay of the marl-clay unit.



Plate 6.10 Old landslide within the marl-clay unit of the Lower Ajlun Group.

The surface of this unit is crossed by wide, steep vallies and gullies, needing large structures and bridging.

Stability problems are the most important consideration in the design of the highway in this particular area. The structural geology of the study area indicates the occurrence of old landslide movements including rockslips and creep. Special attention is necessary during the construction of the highway, any fill material at the crown of these landslides will indeed increase the driving forces and any cut at the toe will decrease the resisting forces thus triggering off the delicate balance of these old landslides.

Based upon regional observation and study, the following conclusions may be drawn:-

1. The stability of any cut or fill is suspect; careful stability analysis is necessary for each particular section.
2. From the stability point of view, the lower Ajlun formation is the most critical; but it is less troublesome in this area than in north Jordan owing to the presence of nodular limestone beds within this part; and the decreased thickness of the clays.
3. Slopes steeper than 14° are considered to be unstable.

4. Slopes between $10-14^{\circ}$ are in a delicate balance, and sensitive to any loading or fill at the crest of these slopes or undercutting of the lower part. Increases in groundwater pressure are also likely to accelerate movement.
5. Rockfall, rocksliding or toppling of the intensely jointed bedrock of the Middle and Upper Ajlun group may occur in cuttings.
6. The angle of shearing resistance of the clay materials within the lowermost part of the Ajlun group ranges between $\phi_p = 12 - 18^{\circ}$, while it is in the range of $18 - 24^{\circ}$ for the Middle and Upper Ajlun group.

However, the stability of the slopes in this particular area could be maintained by different kinds of treatment depending upon the nature of the material supporting the road, the side slopes and the cut slopes, the amount and orientation of the joints in the bedrock and the presence or absence of water.

The prevention of these stability problems could be attained by reduction of any activating forces and at the same time increasing the resisting forces, this in turn could be attained if the following factors were taken into consideration during the construction process along the alignment:-

1. It is important to have the minimum earth moving and the least interaction with the existing slopes where possible; that is, by shifting the alignment a few metres where necessary, if this would minimize the probability of the movement.

2. Proper slopes of cuts and fills; cut slopes are directly related to the geological characteristics of the bedrock. Slopes must be designed in such a way as will minimize sliding and increase stability. Cut slopes must be constructed with benches with longitudinal drainage grade along the inner edge of each bench.

Slopes and benches are based on three variables:-

- a) Angle of slope between benches.
- b) Maximum height of each cut.
- c) Width of the bench.

These are related to the type of material concerned, so it is necessary to carry out stability analyses, where deep cuts and fills can be constructed, to determine exactly the angle of slope and maximum heights of cuts and fills.

Concerning the benches, these should serve two purposes: to intercept and remove surface water from cut face, and to

prevent rock and debris from falling on to the highway.

Clear width of all benches is prepared to be six m.

3. Proper drainage: It is important to have a good drainage system along the alignment where necessary to minimize one of the major causes of the movements. Drainage methods could be classified into surface and subsurface.

Surface drainage is necessary to intercept runoff water. In the excavated areas along the inner edge of each bench and at the foot of every cut slope; there must be a longitudinal channel to remove surface water from the cut face. The bottom of the channels should be paved.

Subsurface drainage by means of horizontal drains, stabilization trenches and drainage blankets are one of the most effective measures. Horizontal drains are very effective to remove subsurface water whenever the ground water table is expected to be high. It is preferable to install these drains at the top of the impervious layers (marl and clay) where they are overlain by permeable fissured layers. Location, depth, number and spacing of these drains depend upon the type of material to be drained and the amount of water expected in the area.

Stabilization trenches are common methods to improve the stability. These deep trenches may be longitudinal or

transverse with reference to the centreline. They should be oriented in relation to the alignment. The bottoms of these trenches should be sufficiently deep below the strata of poor quality material. They should be filled with a 3-4 ft layer of permeable materials, an outlet usually on extension of the trench must be provided.

The use of drainage blankets is also one of the most effective and common methods of improving stability in the form of a layer of permeable material. Due to the poor permeability of partially saturated marl and clay, it can become saturated and weakened as the water content increases so causing creep or landsliding. In this case it is preferable to blanket the complete areas underlain by material such as the Lower Ajlun group and then construct the overlying embankments.

4. Due to the fact that the area mainly consists of materials of poor shear, so it is recommended that proper materials should be imported to be used in embankment fill.
5. Special attention is necessary in locating the retaining structures.

CHAPTER SEVEN

RECOMMENDATIONS AND CONCLUSIONS

RECOMMENDATIONS AND CONCLUSIONS

This thesis has presented the results of comprehensive engineering geological investigations of natural slopes along the major Jordanian highways. The study has included a detailed review of the theoretical slope stability analyses in addition to the essential field and laboratory investigations. The work has included an evaluation of the geology, and its relation to recorded slide history and different types of testing. The field work consisted essentially of topographic and geological mapping supplemented by exploratory drilling in the landslide area.

The purpose of this study has been to obtain information about slope stability along the Jordanian highways that will assist operation and maintenance of existing highways and supply information that will provide a basis for more reliable slope design for future highways.

The most significant conclusion arising from this study is that all of the instability problems of landslides on the Jordanian highways investigated occur within the same marl-clay sequence of the lower part of the Cenomanian clays (Lower Ajlun Group). These clays are found to consist of a mixture of montmorillonite, illite and kaolinite, in that order of abundance, and to have medium to high plasticities and low shear strength. Based on results of the studies, it appears that shear strength

parameters represented by $\phi'_p = 13 - 16^\circ$, $c'_p = 0.15 - 0.25 \text{ Kg/cm}^2$ would be conservative when applied to the Lower Ajlun Group of the marl-clay unit; while the strength parameters represented by $\phi'_p = 21 - 24^\circ$, $c'_p = 0.12 - 0.24 \text{ Kg/cm}^2$ are the most conservative to be used for natural slopes of the Upper Kurnub Group.

The low shear strength parameters are due to the presence of montmorillonite as the major clay mineral present in the clays, leaching of soluble salts and the general structural distortion of the strata. The fully softened strength parameters were considered to be the most realistic for use in the stability analyses for first-time slides. Since peak and residual strength parameters were found to consistently over and under estimate respectively, the factors of safety. Slopes steeper than 12° and 14° in such materials in northern and southern Jordan respectively can be considered to be potentially unstable. Areas where outcrops of the limestone-marl unit occur are considered to be stable due to the good drainage properties in all directions; while the flow of water within the marl-clay unit is mainly parallel to the strata and impervious in the perpendicular direction because of the relative impermeable clay beds. It was observed that slopes in the marl-clay units of southern Jordan are more stable than those in similar materials in northern Jordan. This is probably due to the presence of

nodular limestone ledges, thinning of the clay layers and decrease of precipitation in the areas of southern Jordan. Faulting is pronounced in the areas where landslides occur and this provides near vertical planes of weakness which allow softening of the clay materials to proceed more rapidly. Ground water tables in the landslide areas probably rise very rapidly during the short heavy rainstorms, but fall rapidly after the rain ceases; no permanent ground water table was observed in the study area. The rainfall for the period in which the landslides occurred was observed to be exceptionally high (e.g. for February, 1964 after a short period of heavy rainfall, landslide VI on Naur-Adasiye highway and the Fayadiye landslide in Beirut occurred, and in 1969 landslide V and a landslide in Galilee mountains occurred).

From the field studies and observations, it has been noted that the natural slopes which have been apparently stable for a long time do not always remain stable, particularly in the areas affected by tectonic movements or the man-made slopes of the highways within an old landslide area. In such a case there is a danger of softening and weakening of the materials and further landslides.

The stability analyses presented in this thesis clearly show that near surface water tables are necessary for

the development of instability. As no permanent near surface water table exists in the region, it is also clear that near surface perched water tables must develop in the marl-clay unit during short periods of heavy rainfall and it is at these times that slope failures have occurred. The extensive jointing and faulting in the limestone which overlies the marl-clay unit allows rainwater to penetrate into the clays where rapid softening occurs. The perched water table may be followed by exceptionally high rainstorm causing extra driving forces which would indeed trigger off the stability of the slopes.

With the main causes of the landslides established, the following recommendations for highway locations, design and construction can be given:-

1. Where possible, highways must be routed away from old landslide areas.
2. Highways should avoid these areas where the marl-clay units of the Lower Ajlun Group are particularly well developed, and minimum earth works within this unit are recommended.
3. Particular attention must be given to all drainage systems where highways cross marl-clay units.

4. Marl-clay unit should not be used as fill in embankments owing to the low shear strength and poor workability.
5. All the existing surface drainage canals along the highways should be paved to minimise leakage.
6. Instalation of permanent piezometers to observe changes in water level and hence to give information on the activating water table, over long periods, is necessary in areas where the stability is critical.
7. Removal of all gabions constructed near the crown of landslides, where the stability is delicate, and replacement by sheet piles if necessary.
8. As landslide VII is one of three major problems in Amman, sp detailed investigations of Juphah and Marikh mountains are also required.
9. Stability analysis of proposed reservoirs and those under construction.

The conclusions obtained from this study concerning the continuing problems of instability along the Jordanian highways should encourage the engineers in Jordan to be more critical in their selection of highway routes, especially with respect to engineering geological considerations.

A lack of any comprehensive regional engineering geological study in Jordan makes it essential to recommend that such a study should be made in order to help avoid any catastrophic failures in the future.

ACKNOWLEDGEMENTS

The present research work has been carried out under the supervision of Professor J.L. Knill, to whom I am deeply indebted with sincere gratitude for his guidance and advice in fruitful discussions which were of great value throughout the research programme and gave the author much reassurance at various times.

Sincere thanks are also expressed to Mr. R. Best for many stimulating discussions and his help during analysis of various problems and his reading of parts of the draft manuscript.

I am also very grateful to the staff of the Engineering Geology Division of the Imperial College, to the fellow research students and to my colleagues for their co-operation and encouragement.

To all those mentioned above I am deeply indebted.

Finally, I would like to acknowledge the British Council for their financial support, and Mr. M. Hawamdah, Vice-President of the Natural Resources Authority, and Mr. O. Dakhan for their encouragement which made this study possible.

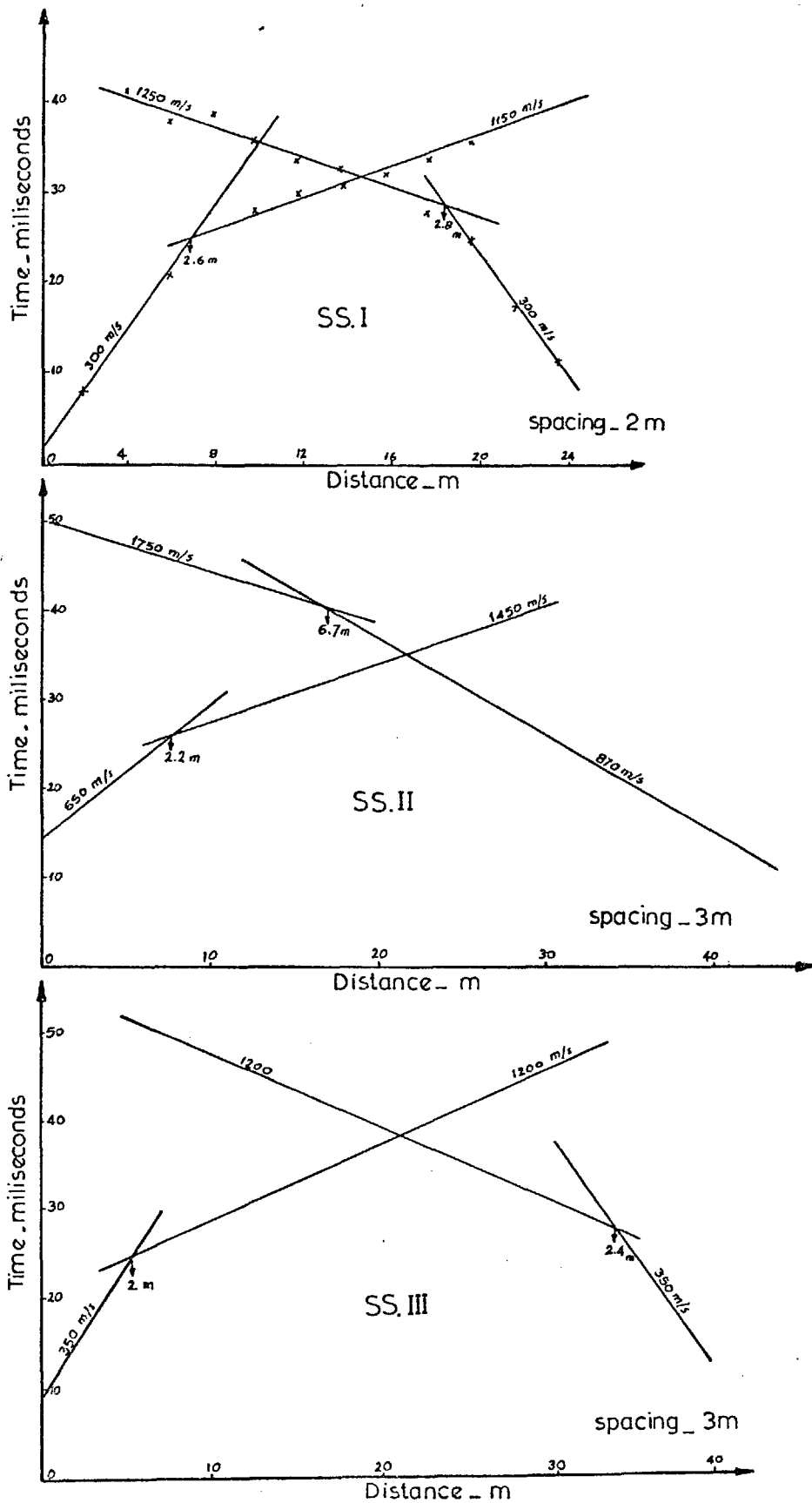
This thesis could not have been written without the forbearance and understanding of my wife, Anas.

APPENDIX

A, B & C

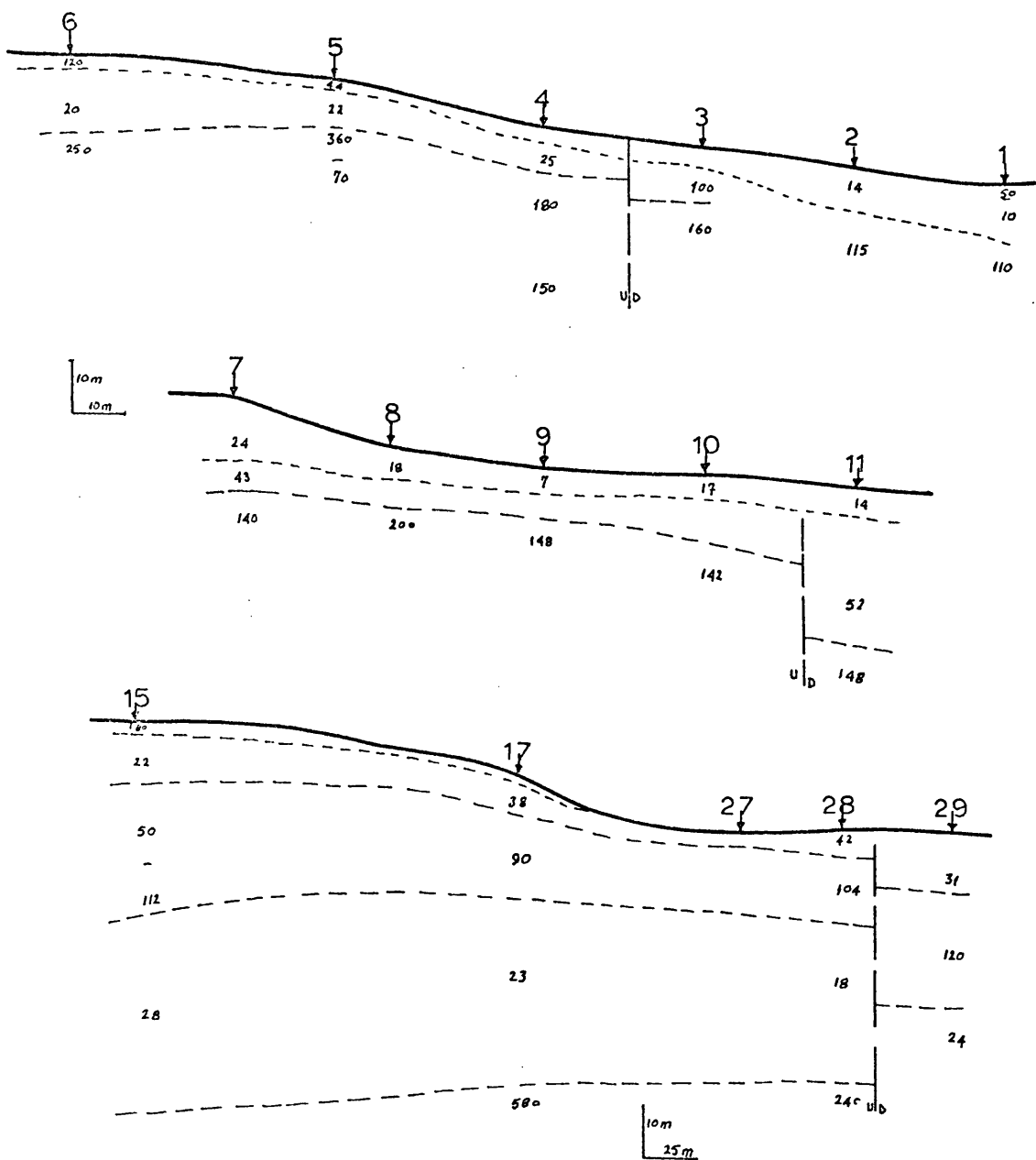
LANDSLIDE - V

SEISMIC REFRACTION PROFILES



Fig(4.1A)

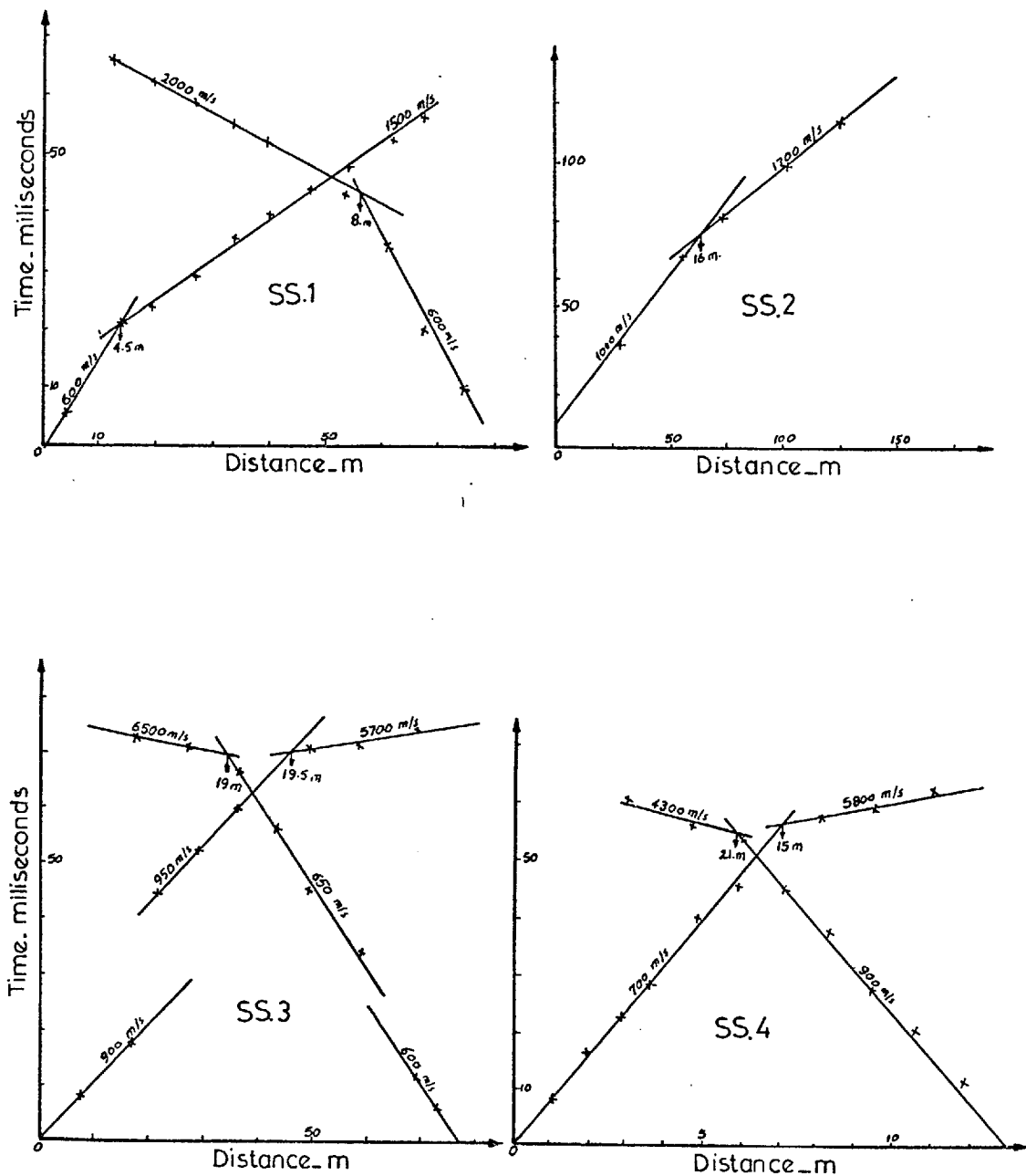
LANDSLIDE V RESISTIVITY SOUNDING PROFILES



Fig(4.2A)

LANDSLIDE - VI

SEISMIC REFRACTION PROFILES

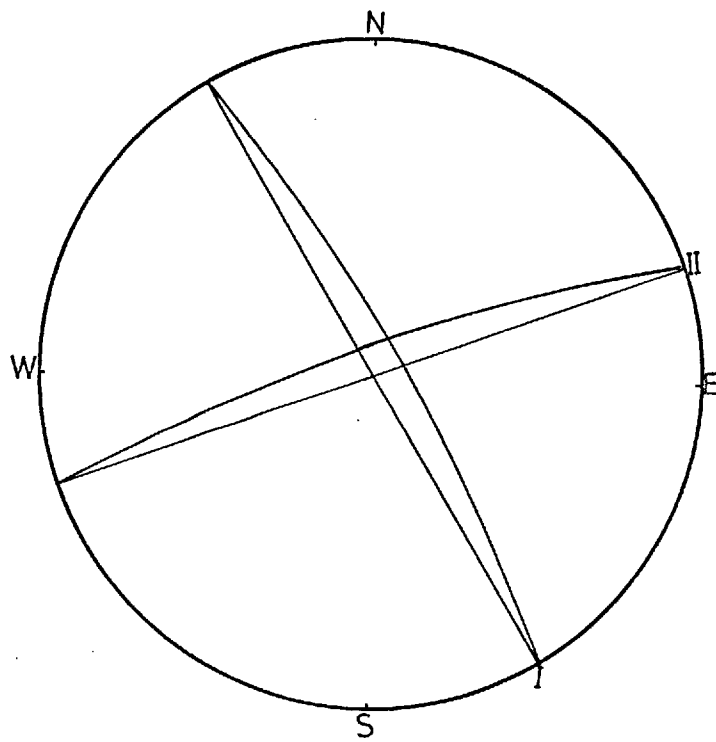
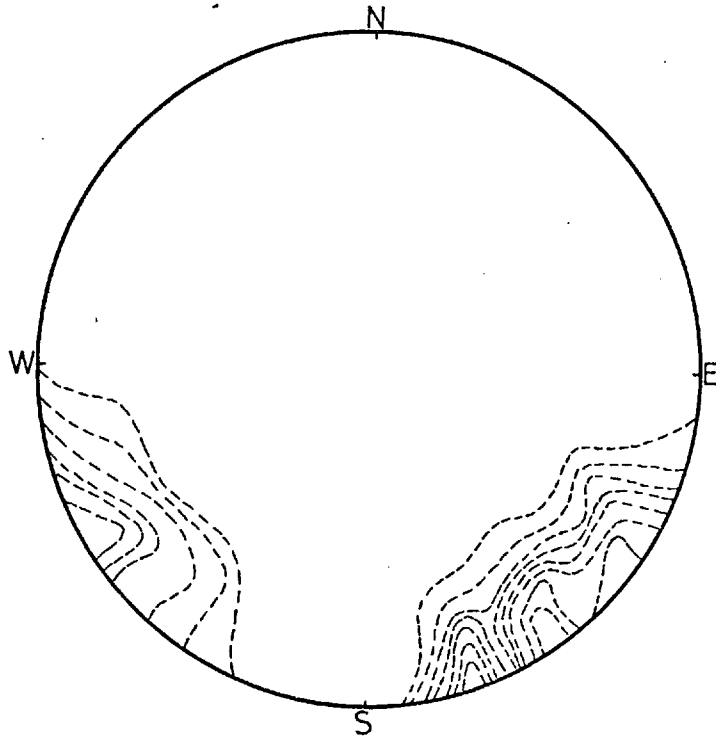


Fig(4.3 A)

FIGURE (5.1A)

For this figure, please refer to
the pocket at the end of the thesis.

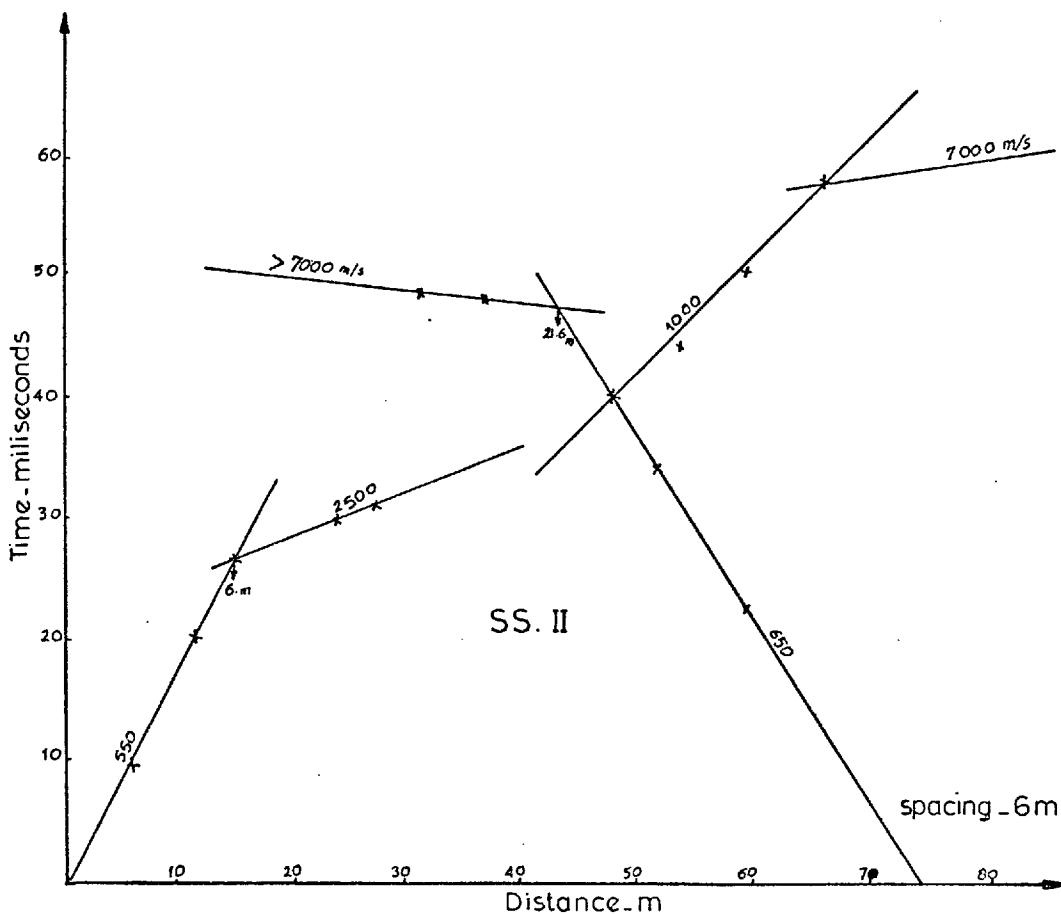
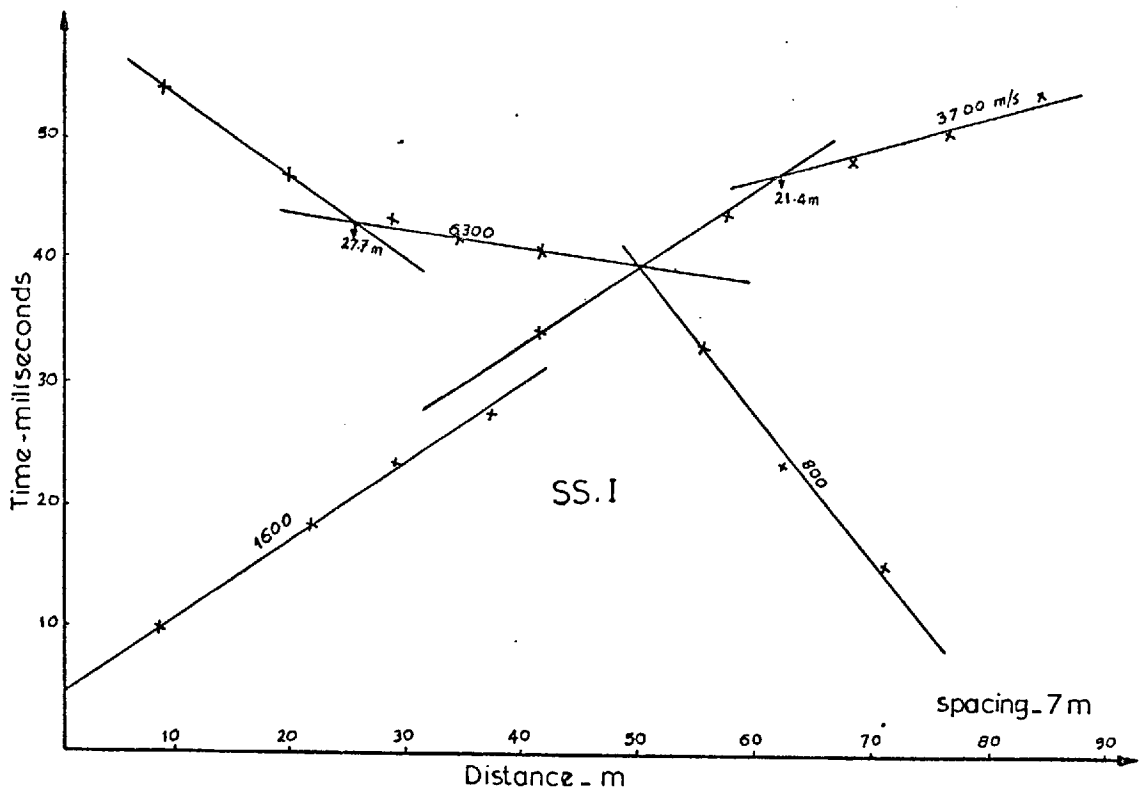
SWEILEH - JARASH ROAD
LANDSLIDE .III



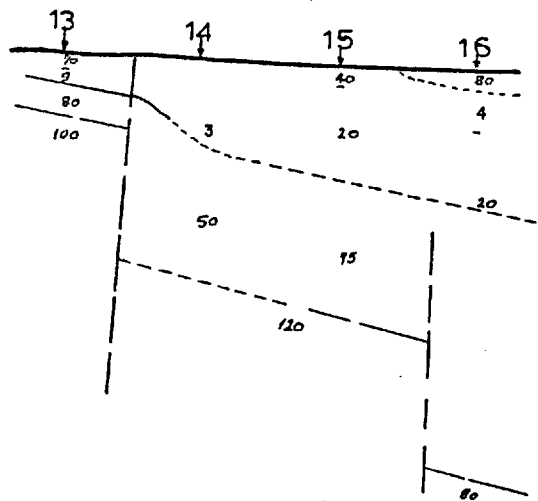
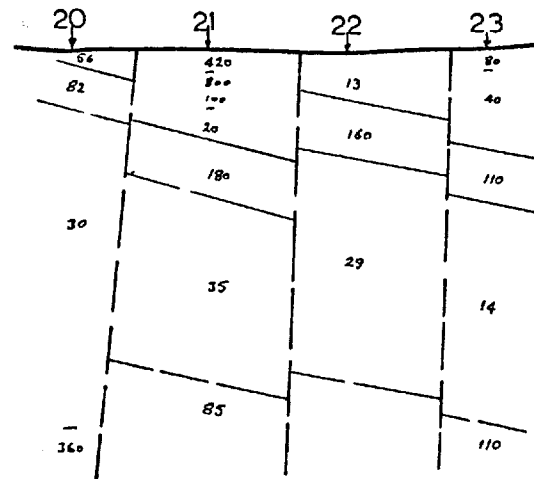
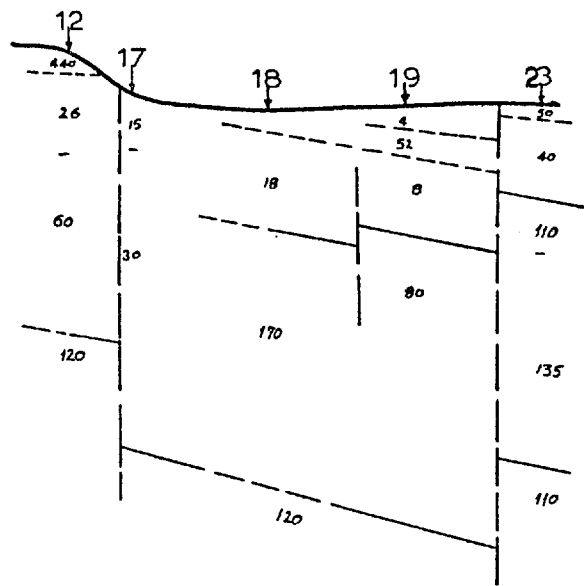
LOWER HEMISPHERIC PROJECTION - CONTOUR DIAGRAM
OF JOINTS (ABOVE) REPRESENTATIVE JOINT SETS (BELOW)

Fig(5.2A)

LANDSLIDE. III SEISMIC REFRACTION PROFILES



Fig(5.3A)

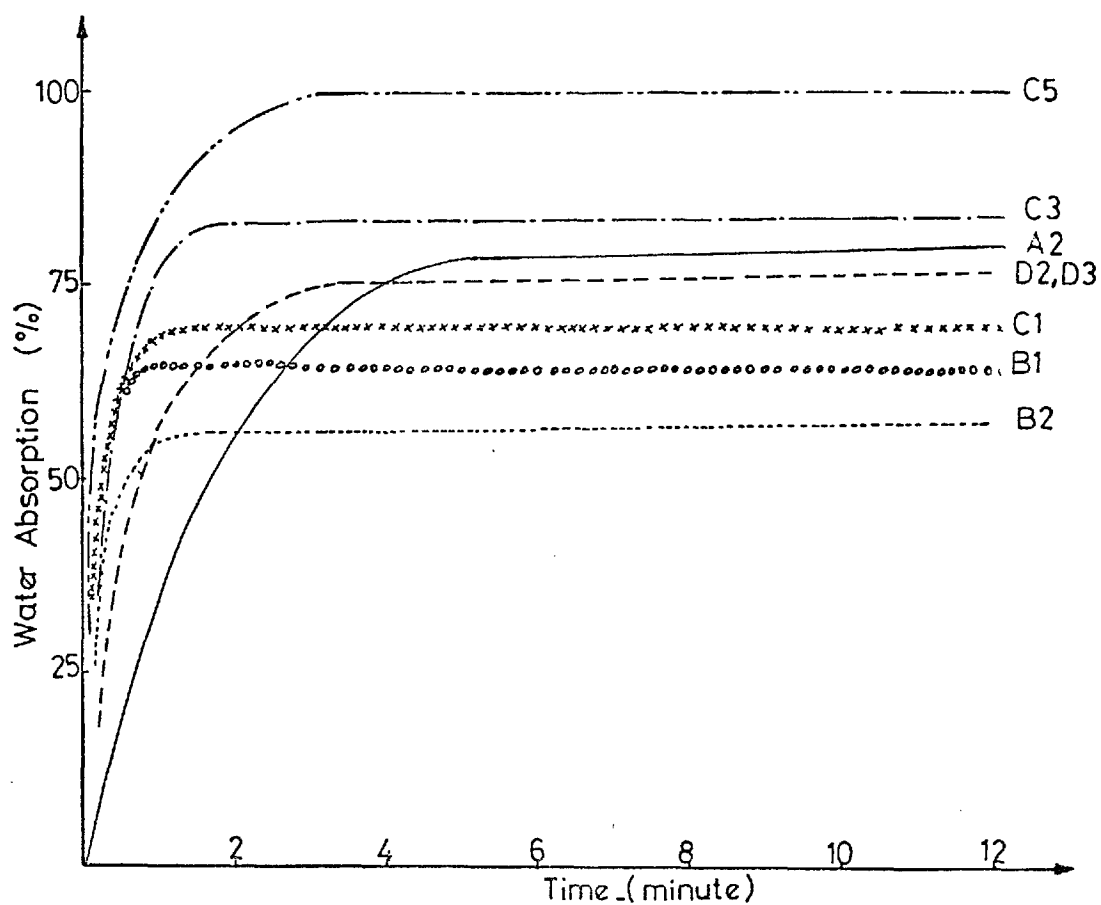


LANDSLIDE III
Resistivity Sounding Profiles

Scale
V - 1:2000
H - 1:1000

MAXIMUM WATER ABSORPTION

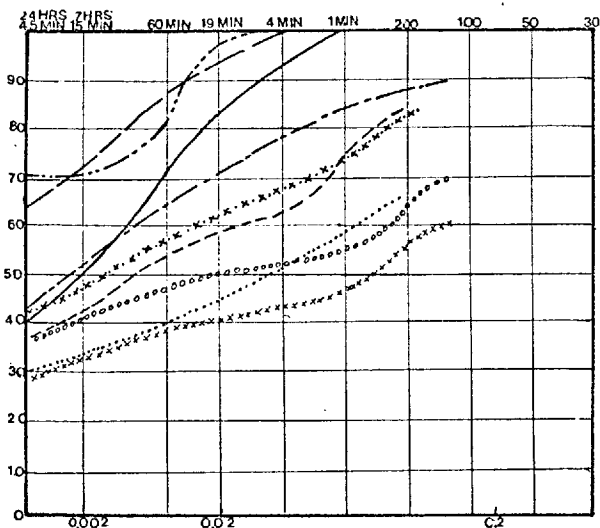
(Representative samples)



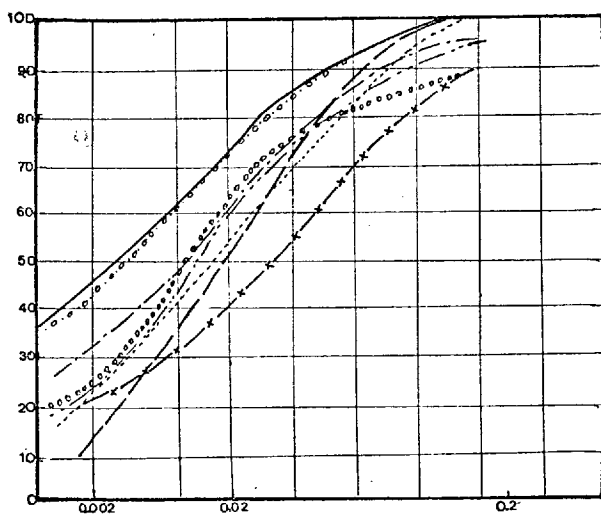
Maximum water absorption of representative samples along Sweileh-Jarash road

Fig(5.5A)

GRAINSIZE DISTRIBUTION OF REPRESENTATIVE SAMPLES FROM LANDSLIDES I, II, III & IV



Sample	Symbol	Clay	Silt	Sand
A1	————	47	53	—
A2	-----	72	28	—
A4	-----	73	27	—
A5	-----	42	43	15
B1	oooooooo	41	24	35
B2	xxxxxxxx	33	25	42
B3	34	34	32
B4	-----	51	37	12
B5	xxvxxx	48	35	17

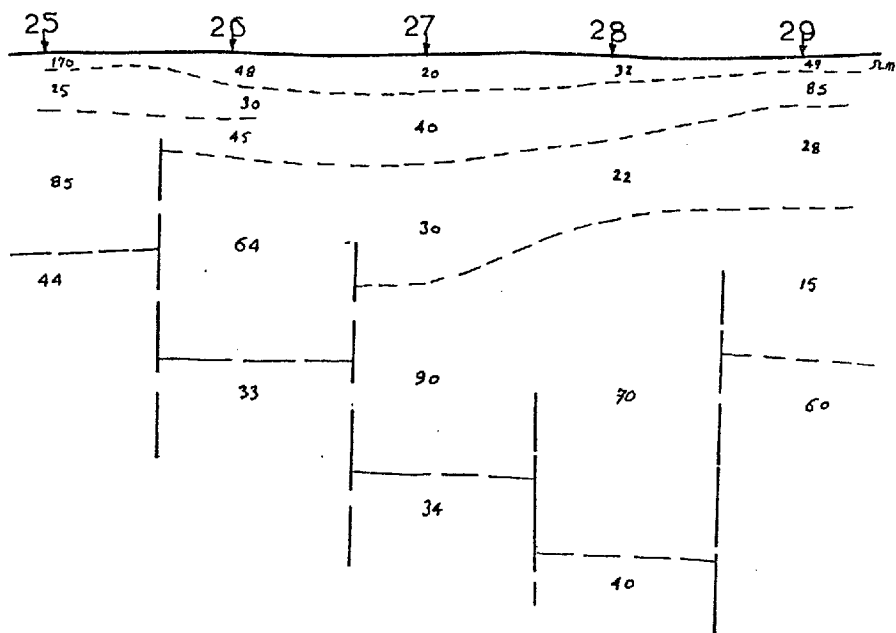
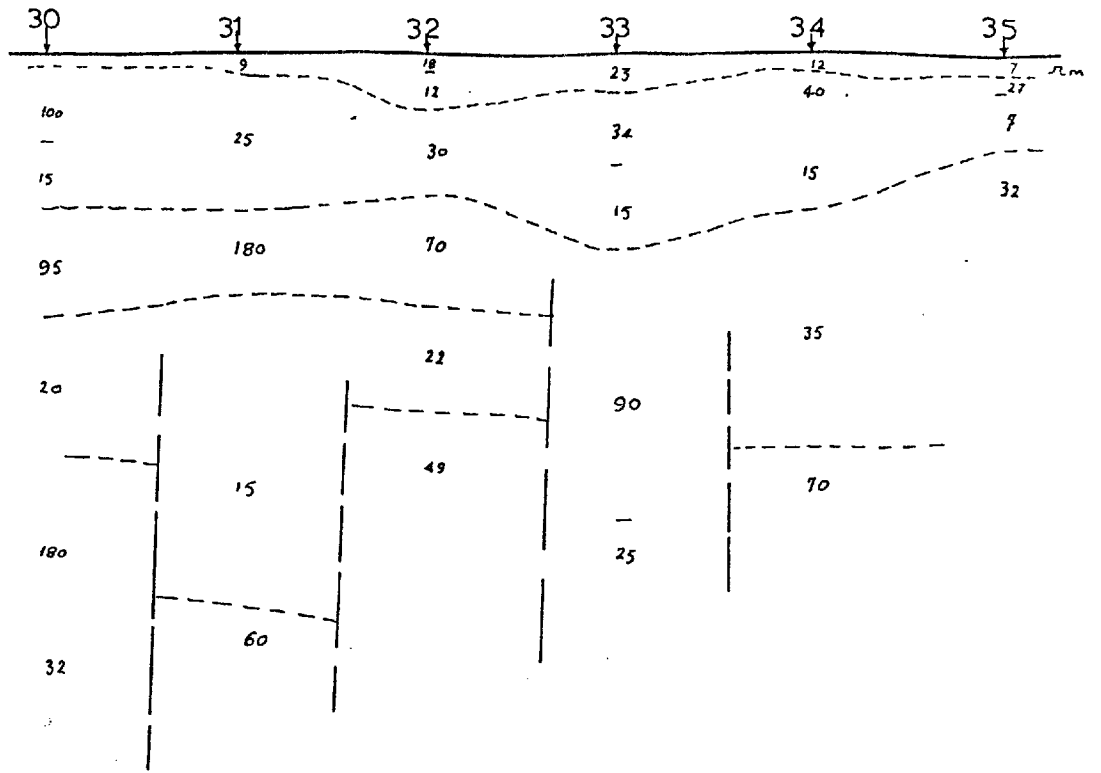


Sample	Symbol	Clay	Silt	Sand
C1	————	45	53	2
C2	o.o.o.o.o.o	32	63	5
C3	-----	44	54	2
C4	-----	23	74	3
C5	-----	13	85	2
D1	-----	23	70	7
D2	ooooooo	25	63	12
D3	—x—x—	20	65	15

A1,2... Landslide I
 B1,2... Landslide II
 C1,2... Landslide III
 D1,2... Landslide IV

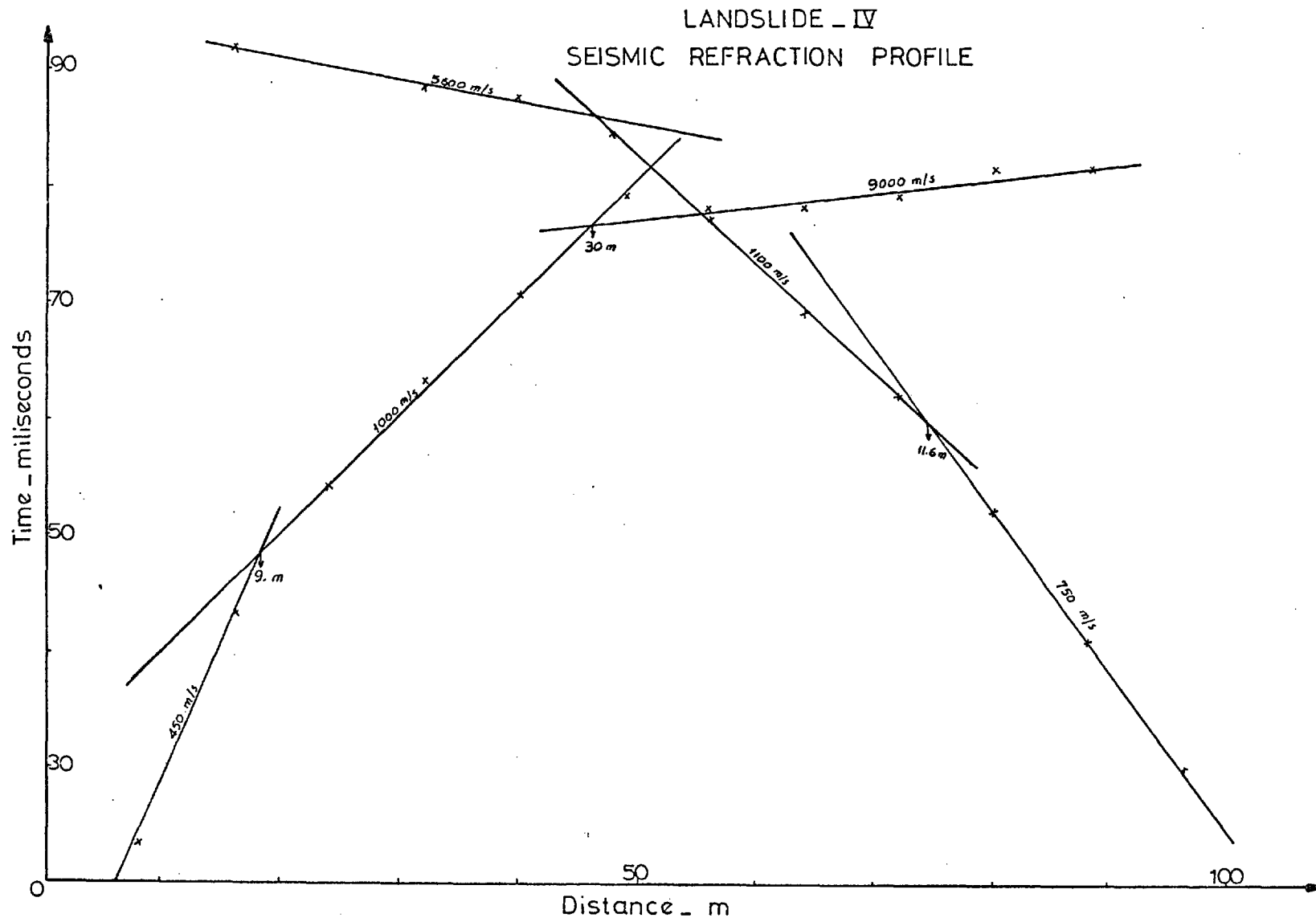
Fig(5.6A)

LANDSLIDE. IV RESISTIVITY SOUNDING PROFILES



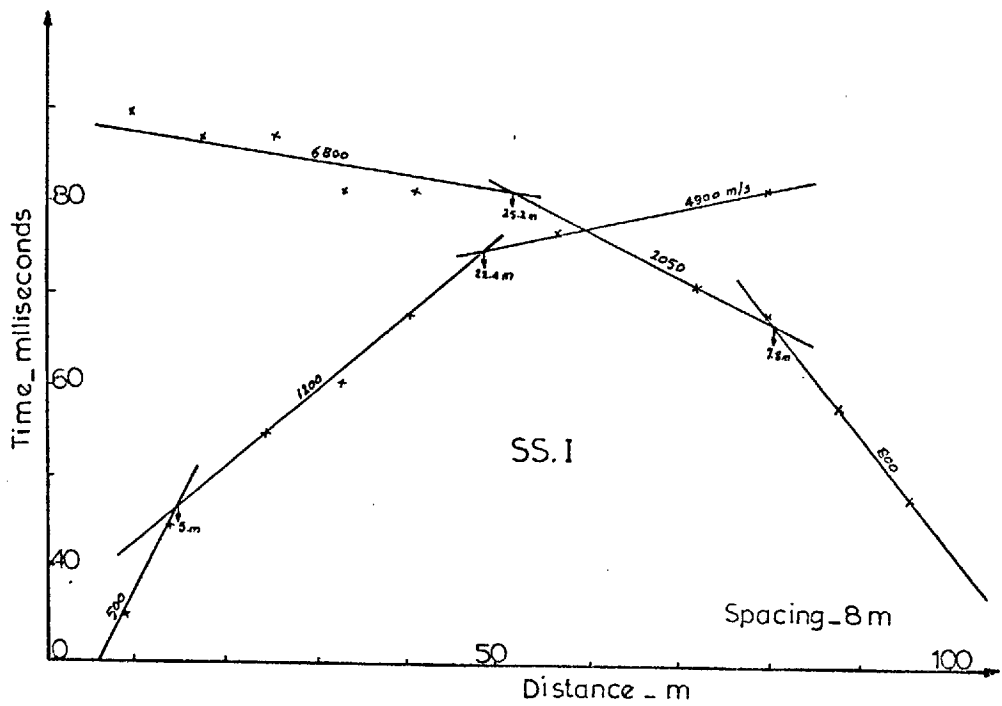
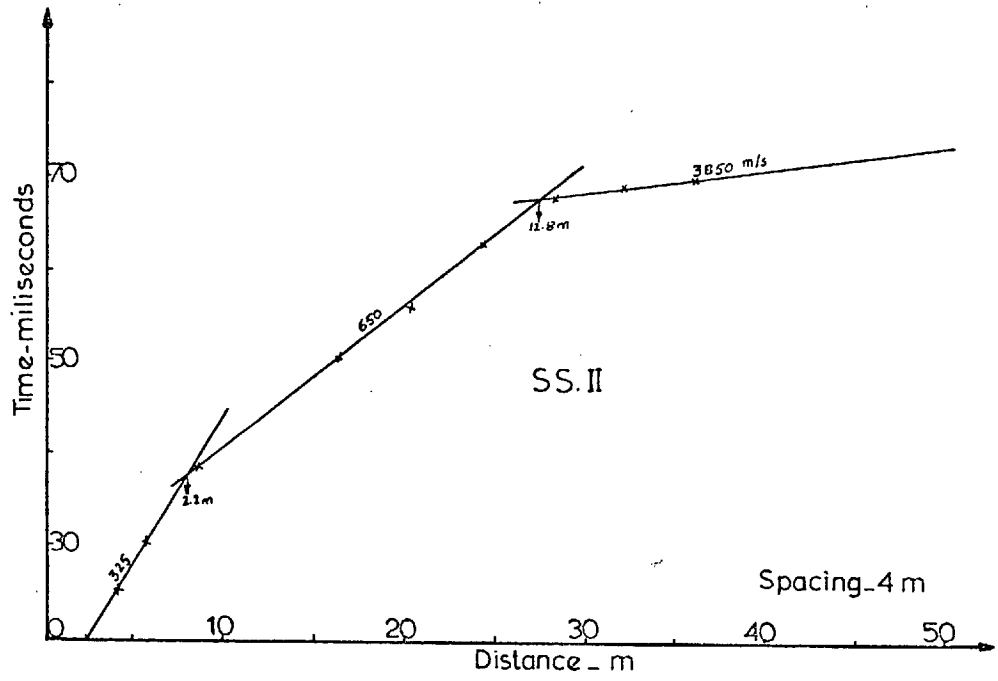
Scale
V - 1:2000
H - 1:1000

Fig(5.7A)



Fig(5.8A)

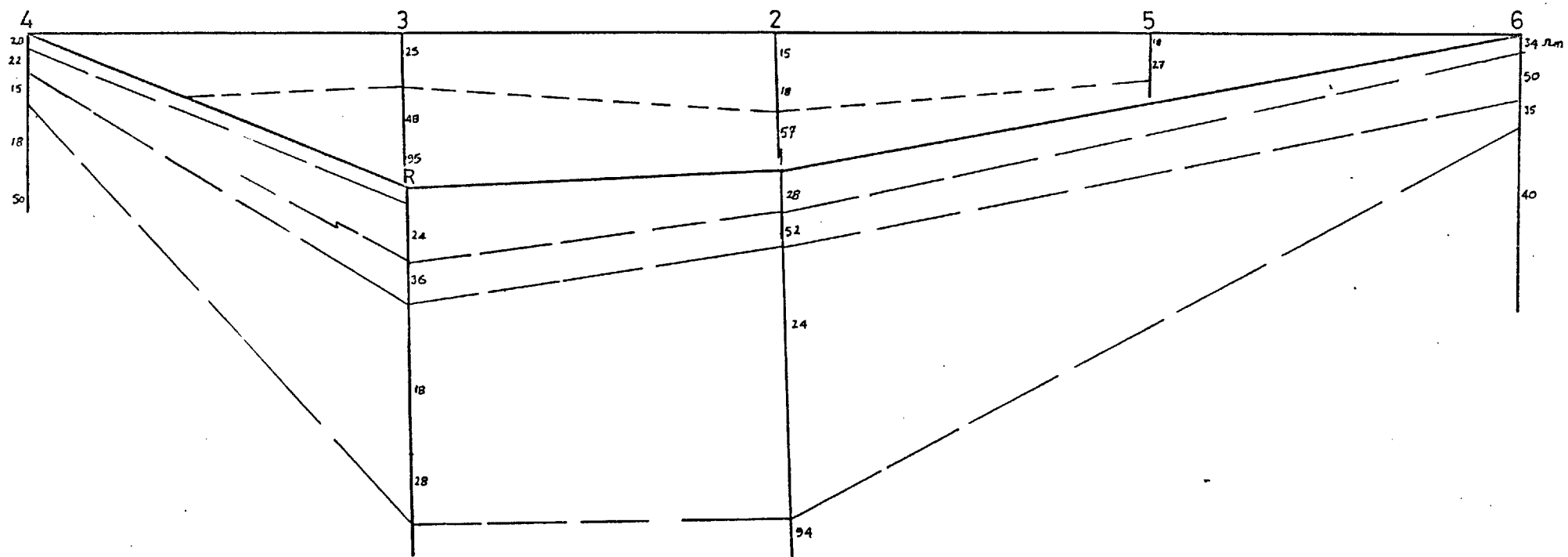
LANDSLIDE. II SEISMIC REFRACTION PROFILES



Fig(5.9A)

RESISTIVITY SOUNDING PROFILES

Fence diagram correlation



10 m.

Fig(5.10 A)

APPENDIX "B"

Year	Annual Precipitation (mm)	Year	Annual Precipitation (mm)
1942 - 43	547 mm	1958 - 59	430 mm
1943 - 44	315 mm	1959 - 60	254 mm
1944 - 45	862 mm	1960 - 61	516 mm
1945 - 46	529 mm	1961 - 62	445 mm
1946 - 47	308 mm	1962 - 63	132 mm
1947 - 48	571 mm	1963 - 64	610 mm
1948 - 49	748 mm	1964 - 65	56 mm
1949 - 50	604 mm	1965 - 66	381 mm
1950 - 51	179 mm	1966 - 67	803 mm
1951 - 52	573 mm	1967 - 68	441 mm
1952 - 53	416 mm	1968 - 69	599 mm
1953 - 54	636 mm	1969 - 70	407 mm
1954 - 55	313 mm	1970 - 71	577 mm
1955 - 56	639 mm	1971 - 72	590 mm
1956 - 57	621 mm	1972 - 73	352 mm
1957 - 58	326 mm		

TABLE 4.1.B

Sample No.	Sample		Density		Water Content %	Specific Gravity	% Porosity	Void Ratio	Max. Water Abs. %	Atterberg Limits			P.I.	Grain Size Analysis			Classification Symbol	Activity	Liquidity Index	Degree of Saturation	Total Soluble Solids
	Dis.	Uncl.	Wet g/cm ³	Dry g/cm ³						L.L.	P.L.	Sh.L.		Clay %	Silt %	Sand %					
LANDSLIDE V																					
1		u	1.93	1.49	32.5	2.64	43.7	0.77	11.45	89.35	27.2	14.0	62.15	82	18	-	CH	0.75	0.095	100	3.0
2		U	2.04	1.98	10.2	2.56	72.8	0.29	86.4	76.2	20.4	6.7	55.8	83.7	16.3	-	CH	0.66	-0.178	89.1	0.55
3		U	1.99	1.62	22.4	2.59	37.6	0.60	64.8	59.0	18.4	11.0	40.6	65	35	-	CH	0.61	0.098	96.9	0.37
4		U	1.83	1.47	26.25	2.60	43.6	0.77	76.4	62.9	19.58	13.8	43.3	84	16	-	CH	0.51	0.154	88.7	23.7
5	D				15.4	2.65			113.3	85.9	27.8	8.0	58.4	86	14	-	CH	0.67	-0.20		
6		U	1.90	1.50	24.29	2.72	45.0	0.81	103	80.23	23.7	3.4	56.43	76	24	-	CH	0.73	0.11	91.3	0.175
7		U	2.00	1.67	20.0	2.65	37.1	0.58	64.3	54.7	17.0	4.8	37.7	66.7	33.3	-	CH	0.56	0.079	90.3	0.10
LANDSLIDE VI																					
8		U	1.97	1.59	23.8	2.58	38.5	62.3	69.2	36.5	22.4	21	14.1	37.6	40.4	22	CL	0.36	0.099	98.6	0.10
9		U	2.03	1.69	19.8	2.68	37.1	58.6	69.2	57.25	19.17	12.8	37.55	76	24	-	CH	0.46	0.017	90.6	0.10
10		U	2.00	1.61	23.9	2.59	38.0	60.9	75	56.7	18.8	14.6	37.9	73	27	-	CH	0.52	0.134	100.0	0.29
11		U	1.91	1.65	15.7	2.70	39.0	63.6	52.7	29.27	13.3	10.4	15.94	39	44	1.7	CL	0.40	0.150	66.0	0.075
12	D				21.7	2.60			65.9	46.2	15.0	9.4	30.4	68	32	-	CH	0.44	0.19		
13	D				19.8	2.63			73.8	53.2	16.16	11.47	36.6	72	50	8	CH	0.88	0.10		0.10
14		U	1.89	1.58	19.4	2.61	39.6	65.2	84	61.4	16.5		44.9	55	33	-	CH	0.81	0.64	77.6	
15		U	2.02	1.50	34.6	2.63	48.1	75.3	74	56.6	17.5		38.1	60	38	2	CH	0.65	0.44	100.0	
16		U	2.00	1.51	32.0	2.60	42.1	72.2	70.4	53.6	14.6		34.0	60	32	8	CH	0.65	0.45	100.0	

TABLE 4.2B

Sample Number	Sample		Density		Water % Content	Specific Gravity	Porosity %	Void Ratio	Max. Water Abs. %	Atterberg Limits			P.I.	Grain Size Analysis			Classification Symbol	Activity	Liquidity Index	Degree of Saturation	Triaxial comp. test	
	Dis.	Uncl.	Wet g/cm ³	Dry g/cm ³						L.L.	P.L.	Sh.L.		Clay %	Silt %	Sand %					C _p	σ _v '
SLIDE I																						
A1		x	2.01	1.75	14.25	2.59	32	0.47	74.9	61.5	19.3	10.1	42.2	47	53	-	CH	0.89	-0.12	77		
A2		x	1.99	1.54	28.9	2.56	40	0.66	79.8	75.8	21.4	9.0	54.4	72	28	-	CH	0.76	-0.15	100		
A3		x	1.86	1.65	12.9	2.53	35	0.53	75.9	63.4	21.5	5.3	41.9	74	26	-	CH	0.56	-0.19	62		
A4		x	1.78	1.54	16.2	2.55	40	0.65	83.2	58.9	21.3	9.8	37.6	73	27	-	CH	0.52	-0.13	63		
A5		x	1.84	1.60	15.1	2.65	40	0.66	77.7	43.8	19.05	2.3	24.75	42	43	15	CH	0.59	-0.16	60		
SLIDE II																						
B1		x	2.00	1.75	14.4	2.61	34	49	65.8	28.3	13.0	10.1	15.25	41	24	35	CL	0.35	0.06	80	0.21	25
B2		x	2.00	1.80	11.5	2.57	30	43	57.3	17.5	13.05		4.45	33	25	42	CL-ML	0.15	-0.20	69	0.19	25
B3		x	1.79	1.50	19.3	2.61	43	74	57.9	30.4	15.15	11.6	15.23	34	34	32	CL	0.45	0.26	67	0.15	24
B4		x	1.89	1.49	27.5	2.63	44	76	70.2	42.2	20.3	11.8	21.9	51	37	12	CL-CH	0.43	0.31	95	0.16	26
B5		x	1.96	1.60	22.0	2.65	40	66	100	48.8	19.95		30.85	48	35	17	CH	0.64	0.10	88	0.18	24

TABLE 5.1B

Sample Number	Sample		Density		Water % Content	Specific Gravity	Porosity %	Void Ratio	Max. Water Abs. %	Atterberg Limits			P.I.	Grain Size Analysis			Classification Symbol	Activity	Liquidity Index	Degree of Saturation	Triaxial comp. test	
	Dis.	Uncl.	Wet g/cm ³	Dry g/cm ³						L.L.	P.L.	Sh.L.		Clay %	Silt %	Sand %					C _v	σ _v
SLIDE III																						
C1		x	1.87	1.34	40	2.65	49.4	98	69	77	18.0	11.2	59.0	45	53	2	CH	1.33	0.37	100	0.12	12
C2		x	2.08	1.78	17.2	2.65	33	49	52	50	14.4	10.1	35.6	32	63	5	CH	1.10	0.08	92	0.17	11
C3		x	1.47	1.52	30	2.60	43	74	82	88	19.6	12.2	67.6	44	54	2	CH	1.52	0.14	100	0.08	14
C4		x	1.83	1.40	31	2.66	47	89	76	66	18.6	10.6	47.4	23	74	3	CH	1.20	0.27	43	0.20	13
C5		x	1.89	1.49	27	2.65	43	78	99	78	17.3	9.8	60.7	13	85	2	CH	4.70	0.16	92	0.18	16
SLIDE IV																						
D1		x	1.87	1.54	21	2.66	42	72	94	71	20.0	10.1	51.0	23	70	7	CH	2.20	0.02	77	0.21	17
D2		x	1.76	1.39	27	2.65	48	91	74	45	15.7	10.4	29.3	25	63	12	CH	1.10	0.40	79	0.18	16
D3		x	1.89	1.55	22	2.66	42	72	74	70	20.5	11.1	49.5	20	65	15	CH	2.45	0.04	81	0.29	16.5
D4		x	2.01	1.61	24	2.66	40	65	90	62	19.8	9.7	42.0				CH		0.09	98	0.32	18.5
D5		x	1.97	1.57	25	2.65	41	69	91	58	16.4	10.4	42.0				CH		0.12	96	0.23	15.5
D6		x	1.99	1.60	24	2.65	40	66	86	68	17.4	10.3	50.6				CH		0.14	96	0.20	18

TABLE 5.2B

Sample Number	Sample		Wet Bulk Density ³ g/cm ³	% Water Content	Specific Gravity	% Porosity	Void Ratio	Max. Water % Absorption	Atterberg Limits			Plasticity Index	Standard Proctor Test		C.B.R.		Grain Size Analysis			Classification Symbol	Activity	Liquidity Index
	Disturbed	Undisturbed							Liquid Limit	Plastic Limit	Shrinkage Limit		Max. dry density	Optimum Moisture Content	2.5 m.m. pent.	5 m.m. pent.	% Clay	% Silt	% Sand			
1	+			26.0				100	65.0	25.1	15.7	39.9	1.76	78	14	10	18	70	12	CH	2.2	0.02
1D	+	+	1.47	57.3	2.75	55	12.2	117	80.5	27.4	9.6	53.1	1.2	36	1.75	1.6	80	12	8	CL	0.66	0.7
3	+				2.65	27	35	54	32.3	18.3	15.0	14.0	1.77	15	10	85	28	52	20	CL	0.5	
4	+	+	1.74	24.8		42	71	78	64.7	26.8	13.0	37.9	1.46	27	2.0	3.0	66	32	2	CH	0.57	-0.05
5A	+			26.6	2.77	32	47	56	34.3	10.2	10.1	24.1	1.78	16	2.5	3.5	33	25	25 + 17% gravel	CH	0.72	0.7
5B	+		1.8	13.0	2.57	33	48	75	38.4	13.3	23.0	24.7	1.71	17	2.5	3.0	32	20	25 + 23% gravel	CH	0.79	-0.04
6	+				2.56	34	44	65	41.7	28.2	24.1	13.6	1.68	21	4.3	5.5	16	20	30 + 34% gravel	OL	0.89	
7	+	+	1.85	22.5	2.70	40	66	96	63.0	21.0	13.9	42.0	1.52	26	1.5	2.0	73	22	5	OH	0.57	0.02

TABLE 6.1B

D.T.A. ANALYSIS

Sample No.	Expected Minerals
1	Halloysite or Illite and traces of organic matter.
3	Hydrated allophanes and hydrated ferric oxide gel. The 600°C peak does not appear, which means that the material is amorphous, but not well crystalline clay.
1D	Halloysite, mixed with carbonates and hydrated ferric oxide gel.
5A	Illite or meta-halloysite mixed with carbonates and hydrated ferric oxide gel.
5B	Illite or meta-halloysite mixed with hydrated ferric oxide gel, and dolomitic carbonates.
6	Illite or meta-halloysite mixed with much carbonate and hydrated ferric oxide gel.
7	Halloysite mixed with hydrated ferric oxide gel.

TABLE 6.2.B

APPENDIX 'C'

DIFFERENTIAL THERMAL ANALYSIS OF THE
REPRESENTATIVE SAMPLES

SAMPLE ONE:-

<u>The type of peak and approximate temp in °C</u>	<u>Explanation</u>
Endotherm 140	Evolution of absorbed H ₂ O.
Endotherm 188	Gypsum.
Exotherm 330	Burning of carbonaceous materials.
Endotherm 563	Evolution of Hydroxyl H ₂ O.
Endotherm 783	Evolution of last traces of H ₂ O (may be due to carbonates?).
Exotherm 921	Formation of new phases (M.I.).

Expected materials: poorly crystallised kaolinite with traces of organic materials. If the 783°C endotherm peak was due to the evolution of CO₂, then carbonates are present, gypsum.

SAMPLE TWO:-

<u>The type of peak and approximate temp in °C</u>	<u>Explanation</u>
Endotherm 152	Evolution of absorbed H ₂ O.
Endotherm 195	
Exotherm 331	Burning of carbonaceous materials.
Endotherm 571	Evolution of hydroxyl H ₂ O.
Endotherm 590	α - β quartz inversion.
Endotherm 765	Evolution of last traces of H ₂ O (may be evolution of CO ₂).
Exotherm 916	Formation of new phases.

Expected materials: poorly crystallised kaolinite with quartz and traces of organic materials (if the 765 peak was due to CO₂, then the carbonate is present).

SAMPLE THREE:-

<u>The type of peak and approximate temp in °C</u>		<u>Explanation</u>
Endotherm	149	Evolution of absorbed H ₂ O.
Endotherm	184	Water or gypsum.
Exotherm	351	Carbonaceous materials.
Endotherm	567	Evolution of hydroxyl H ₂ O.
Endotherm	788	Last traces of H ₂ O.
Endotherm	895	Evolution of CO ₂ .

Expected materials: poorly crystallised kaolinite with calcite and traces of organic materials and gypsum.

N.B. The 1000°C peak did not appear.

SAMPLE FOUR:-

<u>Type of peak and approximate temp °C</u>		<u>Explanation</u>
Endotherm	153	Water absorbed.
Endotherm	(180 (200	Water of gypsum.
Exotherm	340	Carbonaceous materials.
Endotherm	575	Hydroxyl H ₂ O.
Endotherm	588	α - β quartz inversion.
Endotherm	790	Last traces of H _s O.
Endotherm	930	New phases of CO ₂ ?

Expected materials: poorly crystallised kaolinite with gypsum and traces or organic material. If the 790 peak was due to CO₂, then calcite is present.

SAMPLE FIVE:-

<u>The type of peak and approximate temp in °C</u>		<u>Explanation</u>
Endotherm	163	Absorbed H ₂ O.
Exotherm	358	Carbonaceous materials.
Endotherm	567	Hydroxyl water.
Endotherm	812	Evolution of CO ₂ .
Exotherm	924	New phases.

Expected materials: poorly crystallised kaolinite, calcite and traces of organic materials.

SAMPLE SIX:-

<u>The type of peak and approximate temp in °C</u>		<u>Explanation</u>
Endotherm	161	Absorbed H ₂ O.
Exotherm	372	Carbonaceous materials.
Endotherm	576	Hydroxyl H ₂ O.
Endotherm	830	Evolution of CO ₂ .
Exotherm	870	?
Exotherm	925	Formation of new phases.

Expected materials: poorly crystallised kaolinite and montmorillonite with calcite and traces of organic materials.

SAMPLE SEVEN:-

<u>The type of peak and approximate temp in °C</u>		<u>Explanation</u>
Endotherm	151	Absorbed H ₂ O.
Exotherm	300	Carbonaceous materials.
Endotherm	570	Hydroxyl H ₂ O.
Endotherm	770	?
Endotherm	908	Evolution of CO ₂ .

SAMPLE SEVEN (continued)

Expected materials: poorly crystallised kaolinite and calcite and traces of organic materials. The 1000°C peak did not appear.

SAMPLE EIGHT:-

<u>The type of peak and approximate temp in °C</u>	<u>Explanation</u>
Endotherm 130	Evolution of absorbed H ₂ O.
Exotherm 330	Burning of carbonaceous materials.
Endotherm 552	Evolution of hydroxyl H ₂ O.
Endotherm 920	Evolution of CO ₂ .

Expected materials: poorly crystallised kaolinite with calcite and traces of organic materials.

SAMPLE NINE:-

<u>The type of peak and approximate temp in °C</u>	<u>Explanation</u>
Endotherm 148	Evolution of absorbed H ₂ O.
Exotherm 351	Burning of carbonaceous materials.
Endotherm 560	Evolution of hydroxyl H ₂ O.
Endotherm 890	Evolution of CO ₂ .

Expected materials: poorly crystallised kaolinite with calcite and traces of organic materials.

N.B. The 1000°C peak did not appear.

SAMPLE TEN:-

<u>The type of peak and approximate temp in °C</u>	<u>Explanation</u>
Endotherm 147	Evolution of absorbed H ₂ O.
Exotherm 367	Burning of carbonaceous materials.

SAMPLE TEN (continued)

<u>The type of peak and approximate temp in °C</u>	<u>Explanation</u>
Endotherm 572	Evolution of hydroxyl H ₂ O.
Endotherm 788	Loss of traces of H ₂ O.
Endotherm 893	Evolution of CO ₂ .

Expected materials: poorly crystallised kaolinite with calcite and traces of organic materials.

N.B. The 1000°C peak did not appear.

SAMPLE ELEVEN:-

<u>The type of peak and approximate temp in °C</u>	<u>Explanation</u>
Endotherm 143	Evolution of absorbed H ₂ O.
Exotherm 336	Carbonaceous material.
Endotherm 557	Hydroxyl H ₂ O.
Endotherm 588	α - β quartz inversion.
Endotherm 768	Last traces of H ₂ O.
Endotherm 918	Evolution of CO ₂ .

Expected materials: poorly crystallised kaolinite with calcite and traces of organic materials.

N.B. The 1000°C peak did not appear.

SAMPLE TWELVE:-

<u>The type of peak and approximate temp in °C</u>	<u>Explanation</u>
Endotherm 156	Evolution of absorbed H ₂ O.
Exotherm 345	Carbonaceous materials.
Endotherm 576	Evolution of hydroxyl H ₂ O.

SAMPLE TWELVE (continued)

<u>The type of peak and approximate temp in °C</u>		<u>Explanation</u>
Endotherm	576	Evolution of hydroxyl H ₂ O.
Endotherm	741	
Endotherm	910	Evolution of CO ₂ .

Expected materials: poorly crystallised kaolinite with calcite and traces of organic materials.

SAMPLE THIRTEEN:-

<u>The type of peak and approximate temp in °C</u>		<u>Explanation</u>
Endotherm	146	Absorbed H ₂ O.
Exotherm	360	Carbonaceous materials.
Endotherm	565	Hydroxyl H ₂ O.
Endotherm	590	- quartz inversion.
Endotherm	760	?
Endotherm	850	Evolution of CO ₂ .

Expected materials: poorly crystallised kaolinite with quartz and calcite and traces of organic materials.

APPENDIX C.2

DETAILED DESCRIPTION OF THE PROPOSED
REALIGNMENT OF RAS-EN-NAQAB ESCARPMENT

Observation Point

1 - 2

Near and around Km 41, thickly bedded, highly jointed, massive limestone and green-yellow soft marl over which some limestone blocks have been dragged. Reactivation of slope movements is expected.

2 - 3

Marl and rubble, no rock units are exposed. The lower part is an old landslide. Activation of this part is expected by loading the crown part with the embankment fill.

3 - 4

The same as above. An old landslide (100 m length) was observed.

4 - 5

An old landslide followed by rock falls. A fault plane was observed along the valley from which a spring is issuing.

5 - 6

Thickly bedded, highly jointed, dolomitic limestone, intercalated with yellow marl and marly limestone. Small scale landslides were observed. The upper part is unstable and movement is expected. Special attention is necessary.

6 - 7

Same features as above. Movement was observed above the marl in the form of landslides and rockfalls.

Observation Point

- 7 - 8 Small scale (50 m length) landslide was observed within the same material which is composed of marl and soft yellow green clay.
- 8 - 9 Green, yellow marl and soft clay intercalated with limestone.
- 9 - 10 The same features as before. Small scale landslide was observed within the marl and soft clay.
- 10 - 11 Many small scale movements were observed.
- 11 - 13 The alignment between observation points 6 and 13 lies within an old landsliding area, composed of marl and soft clay.
- 13 - 14 Soft yellow-green clay and marl.
- 14 - 15 Exposed bedrock as dolomitic limestone which is a good sub-grade stable area.
- 15 - 16 Marl intercalated with limestone ledges. This area needs major fill materials; no engineering geological problems were encountered.
- 16 - 17 Marl and thin bands of limestone. The bedrock is exposed at the bottom of the valley.
- 17 - 18 The same as before. Intercalation of thick and thin bedded dolomitic limestone and nodular marly limestone. The alignment between 13 and 17 requires many large cuts and fills.

Observation Point

- | | |
|---------|---|
| 18 - 21 | Weathered rock composed of transported limestone huge blocks. The bedrock is exposed at the bottom of wide steep valleys and gullies. |
| 21 - 23 | Steep hillside, transported materials of Kurnub sandstone. |
| 23 - 24 | Gap, wide large steep valley with the Kurnub sandstone formation. |
| 24 - 25 | As before, transported boulders. |
| 25 - 26 | Gap. A wide steep valley within the Kurnub sandstone formation. |
| 26 - 27 | Gap. A wide steep valley within the Kurnub sandstone formation. |
| 27 - 28 | End of the Kurnub sandstone formation and start of the Disi Formation which is composed of hard white sandstone. |

DETAILED DESCRIPTION OF THE MEASURED COLUMNAR
SECTION ON FIG. 6.3

Formation	Lithologic Description	Thickness (m)
B2	Chert and silicified limestone	-
B1	Green-yellow marl	10
Sand-marl unit	Brownish, hard, sandy limestone	1
	Brown-yellow silty marl	1
	Brownish, calcareous sandstone with lenses of deep brown crystal- line quartzite. The lower half metre is yellow sandy marl	2
	Yellow-brown marl	5
	Brown, whitish, cross-bedded sandstone	1
	Intercalation of green-brownish marl and thin-bedded white-yellow sandy limestone	6
	Yellow calcareous sandstone with concretions of quartzite	1
	Brownish-yellow marl	3
	Yellowish calcareous sandstone with concretions of quartzite	1
	Greenish, yellow silty marl	10
Upper Ajlun "limestone- marl unit"	Yellowish, whitish sandy limestone	2
	Brownish, yellow thin and cross- bedded calcareous sandstone with lenses of deep brown hard crystalline quartzite	2
	Brownish-yellow sandy limestone	0.2
	Intercalation of yellow, greenish marl and white marly limestone	3

Formation	Lithologic Description	Thickness (m)
	Yellowish-white, shaly, sandy limestone with thin lenses of crystalline quartzite	0.5
	Weathered, whitish limestone	1
	White loose sand	1
	Yellow marl	1
	Yellow, calcareous hard sandstone	1
	Yellow soft marl	1.5
	Yellow calcareous sandstone	0.5
	Weathered thick-bedded, vertically jointed calcareous sandstone	1
	Yellowish-green marl	3
	White-yellowish limestone	1
	Marl and marly sandstone	3
	Whitish sandy dolomitic limestone	1
	Yellowish silty limestone	0.5
	Marl	0.5
	Yellow, whitish hard vertically jointed thick-bedded marly limestone	6
	Calcareous sandstone	0.5
	Violet-reddish and yellowish soft friable calcareous clayey sand	5.5
	Green, brownish silty clay with thin bands of clayey dolomitic sandstone	3.5
	Thin-bedded, vertically jointed, fine crystalline limestone, sandy in some parts and dolomitic in the upper part	5
	Hard sandy, dolomitic, massive, thick-bedded vertically jointed limestone. In the upper part there is a horizon of concretionary chert	7.5

Formation	Lithologic Description	Thickness (m)
	White yellow, soft marl	0.5
	White brown shelly, highly jointed thin-bedded calcareous limestone, soft to medium marly in some parts	2
	White, brownish, massive limestone vertically jointed and sandy in some parts	2
	White yellowish, thin-bedded sandy limestone	1
	Whitish thin-bedded jointed, fine crystalline, sandy, dolomitic limestone brownish when weathered	1
	Greenish, yellow, soft marl	0.5
	Brownish to greyish, thin-bedded crystalline limestone	0.5
	Yellowish thin-bedded sandy dolomitic limestone, and calcareous sandstone, intercalated with thin bands of soft sand, marl, the upper part is massive and jointed	3
	Brownish, yellow, thick-bedded jointed calcareous sandstone with some quartzite concretions and yellowish sandy and marly limestone intercalated with thin bands of soft sandy marl. The upper part is massive and jointed	4
	Greenish, yellow soft marl	0.5
	Brown-reddish, silty clay	2
	Violet to blue, soft, friable, clayey, sandy silt intercalated with layers of violet soft marl (clay). The upper one metre is violet to blue marl (silty clay)	4
	Yellowish, hard to medium, thin-bedded, sandy, dolomitic marly limestone, intercalated with thin bands of silt of the same colour, the upper 0.5 metre is sandstone	2

Formation	Lithologic Description	Thickness (m)
	Light, brown, sandy, clayey silt, intercalated with violet thin bands of clay; the upper one metre is violet and brownish yellow marl	3
	Blue and red, soft silty clayey marl	3
	Whitish, thin-bedded massive limestone intercalated with thin bands of nodular yellow marly limestone. The upper part is jointed hard and dolomitic	3
	Nodular marly limestone	0.5
	Yellowish, white, thick to medium bedded, massive hard limestone.	4
	Whitish, light brown, thin-bedded massive to fine crystalline limestone slightly fossiliferous and oolitic	1.5
	White, brown limestone. The lower part is nodular.	0.5
	Thick-bedded, massive, jointed dolomitic limestone. The lower one metre is nodular and marly limestone	3
Lower Ajlun		
"marl-clay unit"		
	Yellowish, fossiliferous marly limestone	1
	Medium-bedded fossiliferous hard jointed, dolomitic limestone	1.5
	Yellow soft marl	2
	Intercalation of yellowish, silty sandy clay and brownish green soft marl	6
	White soft friable sand overlain with green, bluish and brownish reddish marl and silty marl	1.5

Formation	Lithologic Description	Thickness (m)
	Green, bluish and reddish-violet soft marl and silty marl	3
	Soft green, yellowish silty clay. The upper part is white-brownish hard and sandy.	2
	Yellowish, white, thin-bedded nodular limestone forming hog-backs intercalated with fossiliferous marl of the same colour	12
	White, yellowish fossiliferous nodular limestone	2
	Green, yellowish, thin-bedded soft to medium silty clay. The upper part is sandy	1
	Thin-bedded, nodular limestone forming hog-backs intercalated with fossiliferous marly nodular limestone and marl	10
	Greenish, grey (black shale) marl and clayey marl intercalated with yellow whitish fossiliferous marl with hypsum. Intercalated with thin bands of modular marly limestone	15
	White, massive, jointed thin-bedded chalky limestone intercalated with thin bands of soft white marly limestone	5
	Whitish, brown, thin-bedded, hard, dolomitic, sandy limestone which shows local undulation and cross bedding	1
	White nodular marly limestone	2
	White, brownish massive limestone, thick-bedded with thin bands of concretionary chert in the upper part. It shows vertical joints of N 70 W and N 25 W directions forming steep walls. The top is thin bedded	15

Formation	Lithologic Description	Thickness (m)
Kurnub Sandstone Unit	Yellowish white nodular fossiliferous limestone	6

APPENDIX C.4DETAILED DESCRIPTION OF THE BOREHOLES ALONG
THE PROPOSED REALIGNMENT OF RAS-EN-NAQAB ESCARPMENT

Borehole 1 E = 194.680 N = 937.040

The total depth of this borehole is 10.50 metres.

0.00- 2.00 m	weathered zone composed of marl, clay and rock fragments
2.00- 4.00 m	rock fragments of dolomite, ranging in size between 1 cm ³ - 5 cm ³ , intercalated with marly soil (rubble)
4.00- 5.75 m	brown yellow marly soil intercalated with rock fragments of dolomite
5.75- 6.90 m	dolomite intercalated with white cream marly soil
6.90- 7.50 m	yellow brownish marly clayey soil, with dolomite fragments. Moisture content is about 36% (rubble)
7.50- 9.90 m	white creamish dolomite, very hard with jointing surfaces broken as small fragments range in size between 1 cm ³ - 24 cm ³
9.90-10.30 m	brown yellow clayey marl soil intermixed with small fragments of dolomite. Moisture content is about 38%
10.30-10.50 m	Yellow marl, moisture content is about 16%

Borehole 2 E = 195.200 N = 936.300

0.00- 2.00 m	weathered zone composed of 90% carbonaceous sandy silty, clayey soil
2.00- 3.50 m	rock fragments of cream white dolomitic limestone ranging in size between 1 cm ³ - 18 cm ³
3.50- 4.00 m	rock fragments of dolomitic limestone and dolomite intercalated with cream whitish marl (80% marl)
4.00- 5.00 m	rock fragments of soft marl and dolomitic limestone (marl is about 90%)
5.00- 6.00 m	rock fragments of creamish yellow dolomite, 10 cm sandstone in the bottom. Jointing surfaces are observed.

Borehole 2 (continued)

6.00- 7.00 m	whitish cream dolomite, intercalated with marl, jointing surfaces dipping about 45°.
7.00- 7.80 m	rock fragments of creamish white dolomite and marl with jointing surfaces
7.80- 8.40 m	no core. Drilling is very easy and fast
8.40- 8.70 m	rock fragments of white cream dolomitic limestone with jointing surfaces
8.70- 9.90 m	white cream dolomitic limestone to dolomite, slightly sandy, very hard, with jointing surface, broken as small fragments, ranging in size between 1 cm ³ - 16 cm ³
9.90-10.00 m	very hard dolomite
10.00-11.00 m	rock fragments of creamish dolomite
11.00-13.50 m	dolomitic limestone to dolomite, broken as small fragments ranging in size between 0.5 cm ³ - 18 cm ³
13.50-13.80 m	dolomite and marl as small fragments
13.80-14.90 m	cream white dolomite and marl, broken as small fragments ranging in size between 1 cm ³ - 3 cm ³
14.90-15.50 m	no core; very fast drilling, loose material
15.50-17.25 m	yellow white dolomite as small fragments ranging in size between 0.5 cm ³ - 3 cm ³ , fast drilling, loose material
17.25-18.00 m	cavity (drop about 10 cm); rock fragments, limestone 5 cm dolomite in the bottom
18.00-18.90 m	rock fragments of yellow brown dolomite, very hard
18.90-19.90 m	no core, fast drilling and loose material
19.90-20.00 m	fresh soft, yellow, wet marl

Borehole 3

E = 195.830

N = 234.440

0.00- 3.00 m	weathered zone composed of clayey marly soil; the moisture content ranges between 9% at a depth of 0.99 m - 2.40 m, and 10.8% at a depth of 3.00 m
3.00-10.00 m	yellow cream, very hard dolomite, intensely jointed with jointing surfaces; at a depth of 8.70 - 8.85 m there was no core recovered and complete air loss

Borehole 3 (continued)

10.00-10.60 m	cream yellow dolomite, very hard, intensely jointed with polished surfaces
10.60-11.20 m	rock fragments of sandy marlstone, 10 cm dolomite at the bottom
11.20-12.60 m	white cream dolomite as small fragments ranging in size between 1 cm ³ - 3 cm ³ ; during the drilling, there was a 15 cm drop due to cavity
12.60-12.90 m	rock fragments of yellow cream dolomite
12.90-13.00 m	yellow, wet marl

APPENDIX C.5

DESCRIPTION OF TRIAL PITS ALONG THE PROPOSED
REALIGNMENT OF THE RAS-EN-NAQAB ESCARPMENT

Seven pits were dug along the proposed alignment.

Their locations are shown on Fig.6.2.2 and described as follows:-

Pit No. 1 The top 20 cm is composed of light brown clayey soil with rock fragments. The bedrock below is highly disturbed and weathered and composed of white chalky marly limestone and yellow green marl. This feature indicates an old landslide movement, which shows shearing and disturbance.

Pit No. 2 The material is composed of alternations of yellow, blue and red marl, brownish reddish and white sand covered with a thin mantle of surface soil.

Pit No. 3 Light brown, clayey, silty soil and rock fragments.

Pit No. 4 Greenish, yellowish marl and clay moistured.

Pit No. 5 Light brown clayey soil with rock fragments and boulders.

Pit No. 6 As Pits Nos. 5 and 6. The bedrock is composed of light green-yellow marl with gypsum exposed at the bottom of the pit.

BIBLIOGRAPHY

- Akroyd, T.N.W. Laboratory Testing in Soil Engineering. Soil Mechanics Ltd. - London.
- Arnold, M. Slope Stability Analysis by a new Graphical Method. M. ASCE - 1961.
- Aune, Q.A. Quick Clays and Californian Clays no quick Solution. The Resources Agency, Dept. of Conservation, Division of Mines and Geol. Special Reports 86, 87 - California, 1966.
- Baker, R.F. Criteria for Compacted Fills. Association of Engineering Geologists National Meeting, 1966.
- Baker & Harza Eng. Co. Yarmouk-Jordan Valley Project, Master Plan Report, Vol. 1-13.
- Bender, F. Geologie von Jordanien.
- Best, R. & Fookes, P.G. Some geotechnical and sedimentary aspects of ball clays from Devon. Q.J.E.G. Vol.3, No.4, 1970.
- Bishop, A.W. The use of slip circles in the stability of slopes. Geotechnique V, 1955.
- Bishop, A.W. & Bjerrum, L. The relevance of the triaxial test to the solution of stability problems. Norwegian Geot. Inst. Oslo, 1960.
- Bishop, A.W. & Morgenstern, N. Stability coefficient for earth slopes. Geotechnique X, No. 4, 1960.
- Bishop, A.W. & Henkel, D.J. The measurement of soil properties in the Triaxial Test. Edward Arnold Ltd., London 1962.
- Bishop, A.W. Progressive failure, with special reference to the mechanisms causing it. Proc. Geot. Conf. Oslo, Vol. 2, 1967.
- Bishop, A.W. The influence of progressive failure on the choice of the method of stability analysis. Geot. 21, No. 2, 1971.

- Bjerrum, L. Stability of natural slopes in quick clays. Geot. V, 1955.
- Bjerrum, L. Progressive failure in slopes of over-consolidated plastic clays and clay shales. (A.S.C.E. Struct. Eng. Conf. Miami, 1966) Journal Soil Mech. Fdn. Div. Am. Soc. Civil Eng. 93, SM5, 1967.
- Bjorn, K. & Simons, N. Stability investigations of the north bank of the Drammen river. Geot. 12.
- Brown, G. The X-ray identification and crystal structures of clay minerals (Handbook). Min. Soc. 1961.
- Burdon, D.J. Ground water in the Hashemite Kingdom of Jordan Xth Congress U.G.G.I. Rome 1953.
- Burdon, D.J. Handbook of the Geology of Jordan, 1959. Colches
- Chandler, R.J. A shallow slab slide in the Lias clay near Uppingham, Rutland. Geot. 20, No. 3, 1970.
- Chaudhry, A.H. Study of Fayadiya landslide. M.Sc. Thesis, 1964. (American Univ. of Beirut).
- Cole, D.C.H & Lewis, J.G. Progress report on the effect of soluble salts on stability of compacted soils. Proc. 3rd Australia-New Zealand Conf. Soil Mech. and Foundation 1960.
- De Lory, F.A. Long-term stability of slopes in over consolidated clays. Ph.D. Thesis, University of London, 1957.
- Dishaw, H.E. Massive landslides. R.C. Thurber and Assoc. Ltd., Victoria, British Columbia, Canada.

- Evans, D.A. Pre-construction design against landslides. American Assoc. of Eng. Geologists. National meeting, 1966.
- Fellenius Calculation of the stability of Earth Dams. 2nd Cong. on large dams - Washington D.C. 1936.
- Gilbert, G.D. The basic shear strength properties of Weald clay. Ph.D. Thesis.
- Golder, H.G. & Palmer, D.J. Investigation of a bank failure at Scarpsgate, Isle of Sheppey, Kent, Geot. V, 1955
- Grim, R.E. Mineralogical composition in relation to the properties of certain soils. Geot. I, 1948.
- Hanna, W. Soil mechanics and soil conditions in Egypt. Geot. I, 1948.
- Heiland, C.A. Geophysical exploration.
- Henkel, D.J. Discussions on earth movements affecting the LTE railway in deep cutting east of Uxbridge. Proc. Inst. Civil Eng., 5 part 2, 1956.
- Henkel, D.J. Investigations of two long-term failures in London clay slopes at Wood Green and Northolt. Proc. 4th Int. Conf. on Soil Mech., Vol. 2, 1957
- Hock, E. & Bray, J.W. Rock slope Engineering. The Inst. of Mining and Metallurgy, London, 1974.
- Hood, R.G. Role of Engineering Geologist Investigation. Assoc. of Engineering Geologists National Meeting, 1966.
- Hull, E. Memoirs on the geology and geography of Palestine - Survey of Western Palestine, 1886.
- Hunting Technical Services Ltd. Report on the range classification survey of the Hashemite Kingdom of Jordan, 1956. London.

- Hutchinson, J.N. Stability of cliffs composed of soft rocks with particular reference to the coast of South-East England. Ph.D. Dissertation.
- Hutchinson, J.N. Mass-Movement. Encyclopedia of geomorphology, Reinhold. 1968.
- Hutchinson, J.N. A reconsideration of the coasted landslides of Folkestone Warren, Kent. Geot. XIX, 1969.
- Janbu, Applications of composite slip surfaces for stability analysis. Prof. European Conf. Stability of Earth Slopes, Stockholm, 1957.
- Jones, F.O. Landslides along Columbia river valley. U.S.G.S., 1961.
- Kenney, T.C. An examination of the methods of calculation of the stability of slopes. M.Sc. thesis, 1956.
- Kenney, T.C. The influence of mineral composition on the residual strength of natural soils. Proc. Geot. Conf. (Oslo), Vol. 1.
- Kerr, P.F. Quick Clays. Dept. of Conservation, Div. of Mines and Geology. Special reports 86, 87, California 1966.
- Klaus, K.A. & Weinert, H.H. Soluble salts in road foundations. Proc. 4th Regional Conf. for Africal and Soil Mech. and Foundation, 1967.
- Klaus, W.J. Graphical stability analysis of slopes in jointed rock. A.S.C.E., Vol. 94. SM2-1968.
- Knill, J.L. & Price, D.G. The engineering geology of Édinburgh Castle Rock. Geol. 17, 1967.
- Knill, J.L. & Fookes, P.G. The application of Engineering Geology in the regional development of northern and central Iran. I.C., Dept. of Geology, 1968.

- Knill, J.L. & Price, D.G. Seismic evaluation of rock masses.
24th Int. Geol. Congress.
- Knill, J.L. Slope instability in British Columbia.
Royal School of Mines Journal, 1973.
- Lacey, W.C. Quantitizing geological parameters for the
prediction of stable slopes. Soc. of Mining
Engineers of AIME, 1963.
- Lambe, T.W. & Whiteman, R.V. Soil Mechanics, 1969.
John Wiley & Sons, Inc.
- Lartret, L. La geologie de la Palestine.
Ann. Sc. Geol. Paris 1, Part 1, 1969.
- Leighton, F.B. Origin and control of landslides in the urban
environment of California.
24th Int. Geol. Cong. Section 13.
- Liebling, R.S. & Kerr, F.P. Observations on quick clays.
Geol. Soc. of America Bulletin V, 76, 1965.
- Little, A.L. & Price, V.E. The use of an electronic computer for
slope stability analysis. Geotechnique, Vol.8,
No. 3.
- Lloyd, J.W. Investigation of the sandstone aquifers of east
Jordan - the hydrology of the southern desert
of Jordan, 1969. U.N. Development Programme.
LA:ST/JOR9. Technical Report 1.
- Londe, P., Vigier, G. & Vormeringer, R. The stability of rock
slopes. J.S.M.F.O. ASCE, Vol. 95, No. 5M1, 1969
- MacDonald, Sir. M. & Partners (1965a). East Bank Water Resources.
Vols. 1-6.
Central Water Authority - Jordan, 1965.

- Meyerhof, C.G. The mechanism of flow studies in cohesive soils. Geotechnique Vol. 7, No. 1, 1957.
- Miller, A.A. Three new climatic maps. Trans. Inst. Brit. Geog. No. 17, 1951.
- Ministry of Public Works, Amman. Ramtha-Jerusalem highway, 1972 (Geophysics Report).
Araby Consulting Eng. Office & Partners.
- Morgenstern, N.R. Stability charts for earth slopes during rapid draw down. Geot. 13, 1963.
- National Academy of Sciences, National Research Council.
Landslides and Engineering Practice Highway Research Board, Special Report, 29, 1958.
- Nikola, P.P. & Magleby, D.C. Land subsidence in Pleasant Valley area, Fresno County, California. Journal American Water Works Assoc., Vol. 60, No. 4, 1968, U.S.A.
- Oliverina, R. An example of the influence of lithology on slope stability, 24th Int. Geol. Cong., Sec. 13
- Olsen, R.E. The shear strength properties of calcium illite Geot. 12, 1962.
- Parker, D.H. The hydrogeology of the Mesozoic-Cainozoic aquifers of the western highlands and plateau of East Jordan, 1969. U.N.D.P. FAO.
AGL:SF/JOR.9 Technical Report No. 2.
- Papadopolous, D.N. Stability of clay slopes in cuts and embankment M.Sc. Thesis, 1969. London University.
- Petterson, K.E. & Hultin, S. Kajraseti Goteborg des 5re Mars 1916. Teknisk Tidskrift, Vol. 46, 1916.

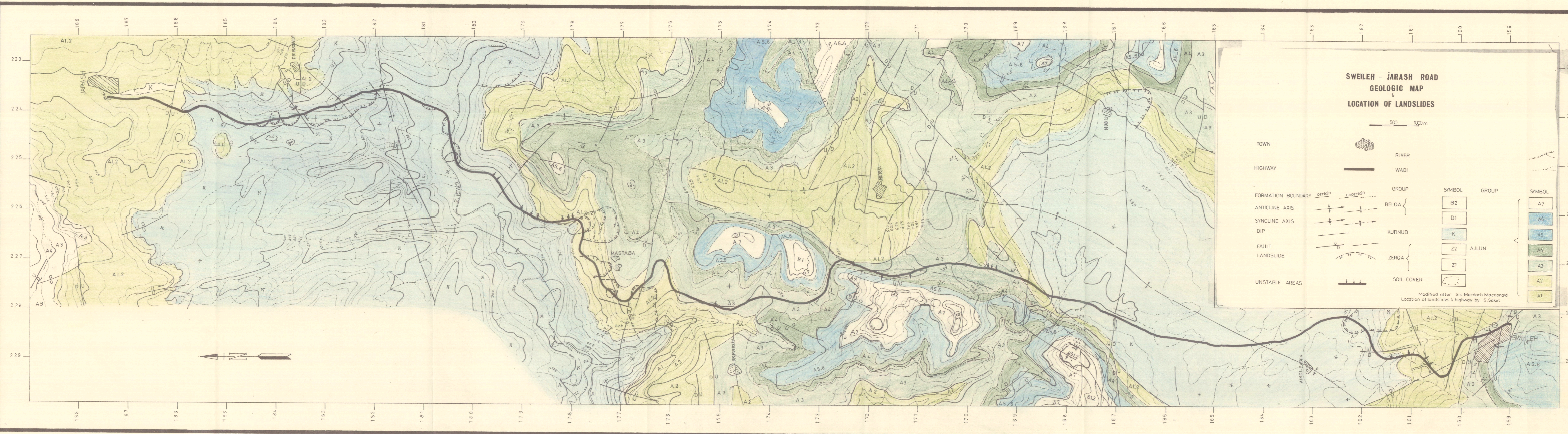
- Quennell, A.M. Geological map of Jordan 1:250,000, 1951.
- Quennell, A.M. The structural and geomorphological evaluation of the Dead Sea Rift. Read before the Geological Soc.; London, 1956.
- Quennell, A.M. Tectonics of the Dead Sea Rift. Int. Geol. Cong. in Mexico, 1959.
- Quennell, A.M. Geology of Jordan, 1959.
- Roberts, D.V. Geologic and other hazards in desert areas. American Assoc. of Engineering Geologists, National Meeting, 1966.
- Rosenqvist, I.TH. Consideration of the sensitivity of Norwegian quick clays. Geot. 3, 1952-53.
- Ruef, M. Report on the Geology of the landslides at Km. 20.800 of Amman-Jerusalem Highway, 1964.
- Saket, S.K. Marikh landslide - Amman. N.R.A. Eng. Geol. Div., 1966.
- Saket, S.K. Sweileh-Jarash road - landslides at Km. 39-40 and 44-45. N.R.A. Eng. Geol. Div. 1969-70. Amman.
- Saket, S.K. Naur landslide at Km. 25. N.R.A. Eng. Geol. Div. 1970.
- Saket, S.K. Ras Al-Ain slide. N.R.A. Eng. Geol. 1970, Amman.
- Saket, S.K. & Tal, A.B. Shabsough road slide. N.R.A. Eng. Geol. Div. 1970, Amman.
- Saket, S.K. & Tal, A.B. Study of Azraq-Saudi Arabian border highway. N.R.A. Eng. Geol. Div., 1970, Amman.
- Saket, S.K., Tal, A.B. & Sabbah, A.S. Ma'an-Aqaba Highway. N.R.A. Eng. Geol. Div., 1971, Amman.

- Saket, S.K. & Toakan, Z.R. Ajlun hospital site investigations.
N.R.A. Eng. Geol. Div., 1972, Amman.
- Saket, S.K. & others. Comments on Ramtha-Jerusalem highway study.
Ministry of Public Works, Amman, 1972.
- Schultz, L.G. Analytical methods in geochemical investigation
of the pierre shale. Quantitative interpretation
of mineralogical composition from X-ray and
chemical data for the pierre shale. U.S. Geol.
Soc. Prof. Paper 391, C-1-39, 1964.
- Scott, Wilson, Kirkpatrick. Ma'an Aqaba Road Preliminary Report,
1968, Amman.
- Sewardson, R.A. The slide at Lodalen. Geot. VI, No. 4, 1956.
- Sharp, G.F.S. Landslides and related phenomena: a study of
mass movements of soil and rock. New York,
California University Press.
- Shaw, H.F. The clay mineralogy of recent sediments in the
Wash, Eastern England. Ph.D. Thesis, 1971.
- Shaw, H.F. Clay mineralogy of Quaternary sediments in the
Wash embankment, Eastern embankment.
Mar. Geol. 14, 29-45, 1972.
- Skempton, A.W. Rate of softening in stiff fissures clays, with
special reference to London clays. Proc. 2nd
Int. Conf. Soil Mech., Rotterdam, Vol. 2, 1948.
- Skempton, A.W. & Northey, R.D. The sensitivity of clays. Geot. 3,
1952-53.
- Skempton, A.W. The colloidal activity of clays.
Skempton collected papers III, 1953-55.
- Skempton, A.W. & Bishop, A.W. Soils. Skempton collected papers
III, 1953-55.
- Skempton, A.W. & Henkel, D.J. Landslide at Jackfield in an o/c clay
Geot. V, 1953 and Skempton collected papers II
1953-55.

- Skempton, A.W. & Delory, F.A. Stability of natural slopes in London clay. Proc. 4th Int. Conf. Soil Mech., Vol. 2, 1957.
- Skempton, A.W. & Early, A.W. Investigations of the landslide at Waltón's Wood, Staffordshire. 1972.
- Skempton, A.W. Discussion on Earth Dams, Slopes and open excavations. Proc. 5th Int. Conf. on Soil Mech., Paris, Vol. 3.
- Skempton, A.W. & Brown, J.D. A landslide in boulder clay at Selset Yorkshire. Geot. II, 1961-62.
- Skempton, A.W. Long-term stability of clay slopes. Geot. 14, 1964 (4th Rankine Lecture), 1964.
- Skempton, A.W. & Rouchelle, La. The Bradwell slip, a short-term failure in London clay. Geot. 15, No.3, 1965.
- Skempton, A.W. Some observations on tectonic shear zones. Proc. 1st Int. Conf. on Rock Mech., Lisbon.
- Skempton, A.W. & Petley, D.J. The strength along structural discontinuities in stiff clays. Proc. Geol. Conf., Oslo, Vol. 2, 1967.
- Skempton, A.W. & Hutchinson, J. Stability of natural slopes and embankment foundation state of the Art Report, Vol. 7, 1969.
- Skempton, A.W. First time slides in o/c clays. Geot. 20, No. 3, 1970.
- Smith, T.W. Repair of landslides. American Assoc. of Eng. Geologists National Meeting, 1966.
- Snow, D.T. Landslide of Cerro Condor-Seneca. Dept. of Ayacucho, Peru.
- Spencer, E. A method of analysis of the stability of embankments assuming parallel inter-slice forces. Geot. 17-1967.

- Strieble, X., Tal, A.B. & Sabbah, A.S. Mastaba landslide.
N.R.A. Eng. Geol. Div., 1969.
- Stimpson, B. Slope stability in the proposed Butterwell
open cast site. I.C. Rock Mech. Project.
- Terzaghi, C. The mechanics of shear failures on clay slopes
and the creep of retaining walls. U.S.B. of
Public Roads Research Consultant. Vol. 10,
No. 10, 1929.
- Terzaghi, K. Stability of slopes of natural clay.
Proc. 1st Int. Conf. Soil Mech., Harvard, 1936.
- Terzaghi, K. Mechanism of landslides. The Geological Soc.
of America - Eng. Geology (Berkeley), 1950.
- Terzaghi, K. Principles of Soil Mech. II Compressive Strength
of Clays. Eng. News Record, Vol. 95, 1925.
- Terzaghi, K. & Peck. Soil mechanics in engineering practice,
1967.
- Terzaghi, R.D. A realistic approach to the hazards associated
with rock defects. American Association of
Eng. Geologists, National Meeting, 1966.
- Underwood, L.B. Classification and identification of shales.
Soil Mech. Div. Proc. ASCE.SM6, 1967.
- Vroman, A.J. Strike-slip movements, their associated
features and their occurrence in Israel.
Int. Geol. Cong. Mexico, 1957.
- Weinert, Hill & Klaus, K.A. Soluble salts in road foundations.
Proc. 4th Regional Conf. for African and
Soil Mech. and Foundations.

- Wetzel, R. & Morton, D.M. Contribution a la geologie de la Trans-Jordanie - Note et Memoirs sur le Moyen-Orient, 1959.
- Whitman, R.V. & Moore, P.J. Thought concerning the mechanics of slope stability. 2nd Pan-Am. Conf. on Soil Mech. & Found. Eng., 1963.
- Wiesemann, G. The geological and hydrogeological survey in the area between Ma'an and Ras-en-Naqab and El-Jasr-Mashaysh Kibid, 1966.
- Wilson, G.R. & Morton, D.M. Chemical quality of water occurring in the Jordan valley area. Xth Congress U.S. G.I., Rome, 1954.
- Zaruba, Q. & Menet, V. Landslides and their Control, 1969. Czechoslovak Academy of Sciences, Prague.



**SWEILEH - JARASH ROAD
GEOLOGIC MAP
&
LOCATION OF LANDSLIDES**

500 1000m

TOWN		RIVER									
HIGHWAY		WADI									
FORMATION BOUNDARY		GROUP									
ANTICLINE AXIS		BELQA	<table border="0"> <tr> <td>SYMBOL</td> <td>GROUP</td> <td>SYMBOL</td> </tr> <tr> <td></td> <td rowspan="2">AJLUN</td> <td></td> </tr> <tr> <td></td> <td></td> </tr> </table>	SYMBOL	GROUP	SYMBOL		AJLUN			
SYMBOL	GROUP	SYMBOL									
	AJLUN										
SYNCLINE AXIS		KURNUB									
DIP		ZERQA									
FAULT											
LANDSLIDE		SOIL COVER									
UNSTABLE AREAS											

Modified after Sir Murdoch Macdonald
Location of landslides & highway by S.Saket